NASA
National Aeronautics and
Space Administration

George C. Marshall Space Flight Center
Marshall Space Flight Center, Alabama 35812

Atomization and Mixing Study Interim Report

Contract NAS8-34504
July 27, 1983
Contractor Report No. RI/RD83-170

Prepared By:
Rocketdyne Division
Rockwell International

Rockwell International

Rocketdyne Division
6633 Canoga Avenue
Canoga Park, California 91304

RI/RD83-170

ATOMIZATION AND MIXING STUDY
INTERIM REPORT

27 July 1983

Contract NAS8-34504

PREPARED BY

A. Ferrenberg
V. Jaqua
Advanced Combustion Devices

APPROVED BY

F. Kirby
Program Manager
Advanced Booster Propulsion Programs

PREPARED FOR:

NASA/George C. Marshall Space Flight Center
Marshall Space Flight Center, Alabama 35812

FOREWORD

This is an interim report describing the work performed during the period February 1982 through June 1983 under NASA Contract NAS8-34504, "Atomization and Mixing Study." The Rocketdyne project engineer for this program is Dr. Allan Ferrenberg, who also is responsible for the technical quality and guidance of the atomization work. Vance Jaqua provides technical expertise for the mixing work. Frank Kirby is the Rocketdyne Program Manager. Other Rocketdyne personnel supporting this program are Stan Pinkowski, Ed Bechtel, and Tony Exposito. This program was performed under the technical direction of Fred Braam of the NASA Marshall Space Flight Center.

CONTENTS

ILLUSTRATIONS

TABLES

SUMMARY

This report describes the results, findings, and conclusions obtained to date as a result of work performed under NASA Contract NAS8-34504, "Atomization and Mixing Study," during the period February 1982 through May 1983. This report contains the results of literature surveys and studies of the atomization and mixing characteristics of liquid rocket injectors (especially triplets, pentads, and coaxial injectors that may be applicable to LOX/hydrocarbon propellants), the correlating parameters and other means by which such data is organized and reported, and the methods by which this data is obtained. Also, the results of the propellant mixing tests performed under this contract are reported herein.

The major findings and conclusions of this report are summarized in the following:

1. In general, very little data exists regarding the atomization and mixing characteristics of triplet, pentad, and coaxial elements, especially for impinging gas/liquid elements. Also, practically no effort has been expended in these areas since 1975.

2. In general, the mixing correlating parameters provide gross estimates of optimum mixing efficiency, although the validity of these correlating parameters (and/or the validity of their reported optimum values) is questionable for some elements and test conditions.

3. Perhaps the most critical parameter affecting droplet size is the local combustion gas velocity field. This appears to be especially true for impinging elements. This is unfortunate since the actual velocity field in a rocket combustor and in atomization experiments is unknown.

4. Atomization and mixing correlations and data for injector types of interest are presented, assessed, and summarized.

5. The state of the art in the areas of atomization and mixing is generally quite poor. The physics is poorly and only qualitatively understood. No quantitative theories exist. The available data and correlations generally are of questionable validity and/or utility. Many of the most critical parameters are unknown (e.g., combustion gas velocity field,

multiple element effects) and/or are not simulated in tests (e.g., gas densities, real propellant fluid properties, combustion gas motion). In addition, the measurement techniques used generally employ questionable assumptions.

6. The mixing characteristics of seven liquid/liquid and gas/liquid triplet, pentad and coaxial, single-element injectors, representative of various LOX/hydrocarbon designs, have been established at various flow conditions.

7. The more general objective of the mixing tests is to establish the existence of, and define the optimum values of, mixing correlating design parameters. The test results obtained to date are insufficient to accomplish this. Additional testing is planned.

INTRODUCTION

The two major effects that reduce the performance of liquid rocket engines, especially larger, long-burn duration engines, are propellant mixing and evaporation. Droplet evaporation rates and chamber length requirements are highly dependent on the initial sizes of the droplets produced by the injectors. Hence, the atomization and mixing of propellants is a major concern in the design of rocket engines, and especially in the design of injectors. In addition, the potentially most powerful tools for rocket engine design are the complex computer codes that evaluate the combined effects of all the physical processes occurring in order to predict performance, stability, spacecraft contamination, heat loads, et. al. In order that these codes may work properly, it is necessary that the important physical process be quantitatively known (i.e., can be described mathematically). Unfortunately, this is not the case generally, and the atomization and mixing processes are especially poorly known. Thus a need exists for a quantitative understanding, and/or extensive data, defining the atomization and mixing processes as a function of injector type, propellant properties, and operating conditions. This data consists of the mass flux distributions of the propellants and the characteristics of the droplets formed. Such information is of great importance in determining critical combustion effects. Mixing efficiency is greatly dependent upon the initial mass flux distribution, and vaporization efficiency is highly dependent upon initial droplet size (and perhaps to a lesser extent on the initial drop velocity). Therefore, performance prediction codes require detailed and accurate data regarding mass flux and droplet size distributions. Also, an assessment of mixing is important in evaluating "streaking" and hot spots on turbine components.

This report describes the state of the art in atomization and mixing for triplet, pentad, and coaxial injectors. Injectors that are applicable to LOX/hydrocarbon propellants and main chamber and fuel rich preburner/gas generator mixture ratios are of special interest. The various applicable correlating equations and parameters, and test data found in the literature searches are presented herein. The validity, utility, and important aspects of these data and correlations are discussed. The measurement techniques employed also are presented and evaluated.

In addition, the propellant mixing tests performed to date under this program are described and summarized, results are reported, and tentative conclusions are presented. Additional atomization and mixing tests are planned.

Much of the work discussed in this literature review is over 10 years old. The more recent atomization and mixing work has been performed as a part of injector or engine development programs. The primary intent of such efforts is the evaluation of specific injectors operated at their design conditions, and not a determination of the effects of the various geometric and operational variables on atomization or mixing. Such a "try this and see what happens" type of approach may be the simplest way to develop an injector, and perhaps the quality of the atomization and mixing data obtained with past measuring techniques did not warrant a detailed scientific study. However, new measuring techniques are being developed, and our future understanding of atomization and mixing processes requires a detailed, scientific study. The "try this and see what happens" approach is not the best, or the most cost effective, in the long run.

ATOMIZATION

This section describes the state of the art in the area of liquid rocket injector atomization. The need for this information, the parameters of importance, the manners in which the data are correlated and reported, the droplet size measure ment techniques employed, and the specific correlations and data pertaining to rocket engine injectors (triplets, pentads, coaxial, and some doublet data), are described, discussed, and assessed. In the study of the atomization literature, emphasis was placed on experimental programs and empirical results directly related to liquid rocket injectors. The more theoretical or basic research efforts are to be studied in a subsequent phase of this program. A bibliography of the atomization reports reviewed to prepare this assessment is included in the list of references at the end of this section.

In liquid rocket engines, the combustion process generally is considered to be evaporation limited, i.e., the evaporation of the propellants is the slowest step in the combustion process and, therefore, very important to model correctly. Droplet evaporation rate is a strong function of droplet size and velocity rela tive to the gas phase. Some computer codes calculate drop velocity and motion. This is important in properly assessing evaporation, stability, spacecraft con tamination by ejected propellant droplets, performance, and wall effects (e.g., wall film buildup, heat transfer). Droplet acceleration is due to an imbalance between droplet inertial forces (a function of drop diameter cubed) and drag forces (generally a function of drop diameter squared). Thus, the droplet size is an important parameter in the assessment of droplet evaporation rate and motion.

It is possible to write the equations governing the motion and evaporation of a droplet. The forms of these equations and most of the parameters are known fairly well over many operating regimes of interest. The equations are ordinary differential equations that can be solved readily. However, as with all differ ential equations, any such solution requires knowledge of the initial or boundary conditions. And this is the problem--these initial conditions are not known well enough. These conditions are the droplet size and velocity distributions at the

locations where the droplets are formed. Given these initial conditions, the governing equations can be solved, and this is precisely what the combustor codes do. However, errors in the initial conditions produce corresponding errors in the predictions.

This problem has long been recognized and a number of experimental programs have been performed to establish these initial conditions. Due to the complexity of the physical processes occurring during atomization, these initial droplet conditions generally are characterized by empirical correlations. Some of these correlations and experiments are described later. Both mixing and atomization experiments often are performed with propellant simulants. This introduces a set of corrections that must be employed to extrapolate to the actual propellants of interest. Another set of corrections generally must be applied to extrapolate the test data to the operating conditions (pressures, temperatures, etc.) of interest. Thus, the establishment of these critical initial conditions depends entirely upon a relatively small quantity of empirical data, relating the effects of a few of the many parameters affecting these complex physical processes, and several sets of corrections to this data.

The utilization of such atomization data and correlations in the combustor analysis codes is a major source of difficulty and error. This has been demonstrated repeatedly in code development programs at Rocketdyne. The three major performance codes in use at Rocketdyne (TPP, CICM, and SDER) all attempt to use such correlations. In all three cases, it has been found to be necessary to modify the experimental correlations to force the codes into agreement with large-scale, rocket engine performance tests. Such "calibration" of computer models with the actual hardware they attempt to model is a standard procedure when dealing with complex unknown phenomena, although it is obviously a technique of last resort. Codes that are calibrated in such a manner can be relied upon to produce good results as long as they are applied to designs and conditions not significantly different from those that they were calibrated against. However, the accuracy of the codes becomes increasingly questionable as they are applied to situations and problems significantly different from the calibration points.

The poor performance of these drop size correlations indicates that something is wrong with the measurement techniques, the correlations developed from the measurements, and/or the manner in which they are applied. The assessment of the state of the art, as described in the remainder of this section, provides reason to suspect all of these.

PARAMETERS AFFECTING ATOMIZATION

The physical processes occurring during atomization cannot be reduced currently to sets of equations derived from basic physical principles. The most common case of the break up of a single jet of liquid has been theoretically studied for over 100 years, and these theoretical studies have been unable to predict, to an adequate degree, the characteristics of the droplets produced. Impinging streams and other fan-forming injectors also have been investigated theoretically. These studies and experimental efforts, combined with the strictly empirical investigations of others, provide an indication of the parameters of importance in the atomization process. However, there is considerable disagreement regarding the relative importance of specific variables.

The properties of a liquid propellant that are considered of importance are the surface tension, viscosity, and density. For a propellant injected as a gas, the only thermodynamic property generally considered of importance is the gas density. The geometric variables of importance for impinging-type injectors are the orifice diameter, orifice length, orifice entrance conditions, number of orifices (triplet or pentad), free jet distance (i.e., distance from the orifice to the impingement point), and impingement angle. Flow variables to be considered are the velocities of the liquid streams and the existence of turbulence in these streams.

For coaxial injectors, the geometric variables of potential importance are the propellant flow areas, the inner tube (LOX post) wall thickness, and the recess of the LOX post. The flow variables of greatest concern are the liquid velocity and the relative gas to liquid velocity.

Another parameter that has been shown to be of very great importance is the velocity of the combustion gases relative to the injected fluids. This parameter affects the aerodynamic breakup of the large droplets and ligaments after they have separated from the spray fan. This is often referred to as secondary atomization and many basic research efforts have been performed to evaluate this. Separation of atomization into primary and secondary atomization processes is certainly an oversimplification, but it has been employed. The importance of the combustion gas velocity is unfortunate, since the actual velocity field in the combustor cannot be determined adequately. The combustion gas velocity field depends entirely upon the droplet evaporation rate and distribution, which in turn is highly dependent on initial droplet size, which in its turn is greatly affected by the combustion gas velocity field. Thus, all of these phenomena are interrelated highly and must be considered together. Even in cold flow tests, the local gas velocity field in unknown. There is no such thing as "spraying into still air," as the spray itself transfers momentum to the gas and sets it in motion.

Another important parameter that is difficult to quantify is the liquid velocity. Generally, this is assumed to be the average velocity at the orifice exit assuming the orifice is flowing full. But this is not the velocity of the liquid in the fan, or of the ligaments, which is probably the velocity of greater concern.

The effects of combustion on atomization are unknown. Matching the density and velocity field of the combustion gases in a cold flow atomization test may not be sufficient. Burning droplets may break up differently (secondary atomization) than nonburning droplets due to the effect of the burning gas envelope about them.

Our knolwedge of many of the parameters affecting rocket engine atomization comes primarily from the study of doublets. Details of many of these studies are included later in this report where the relative importance of the parameters affecting atomization are discussed in greater detail.

ATOMIZATION CORRELATING EQUATIONS

The objective of atomization studies is to develop quantitative relationships defining the effects of the various governing parameters on the characteristics of the spray. The characteristics generally most desired are a representative droplet size (a mean or average value) characterizing the spray, and a droplet distribution defining how the number of droplets in the spray varies with droplet size. Other parameters of interest are the distribution of droplets in space, and the velocities of the droplets.

The data generally most desired is the number of drops of each size in a given spray. Often the data is obtained in the form of numbers of droplets counted, n, in each of many uniform size ranges (e.g., 5 to 10μ, 15 to 20μ, etc.) as shown in Fig. 1a. However, this discrete form of data presentation has the undesirable characteristic that as the width, ΔD, of the size ranges is varied the count will change. In order to quantify the data in the form of a continuous mathematical expression, the data is often converted to the form of Fig. 1b. Here, the number of droplets per unit size range (e.g., per micron) is plotted. This continuous function is called a distribution function f, and is determined by evaluating $\frac{n(D)}{\Delta D}$ as ΔD approaches zero. n(D) is the number of droplets having diameters between $D - \frac{\Delta D}{2}$ and $D + \frac{\Delta D}{2}$. This distribution function is the mathematical expression that best defines the size distribution of the droplets. All the other forms and techniques for expressing droplet size distributions can be derived mathematically from this distribution function, f, where

$$f = \lim_{\Delta D \to 0} \frac{n}{\Delta D}$$

Another useful function is the fraction of droplets in the spray at diameter D, which is

$$f/n_t = \lim_{\Delta D \to 0} \frac{n/n_t}{\Delta D} \quad \text{where } n_t = \text{total droplet count}$$

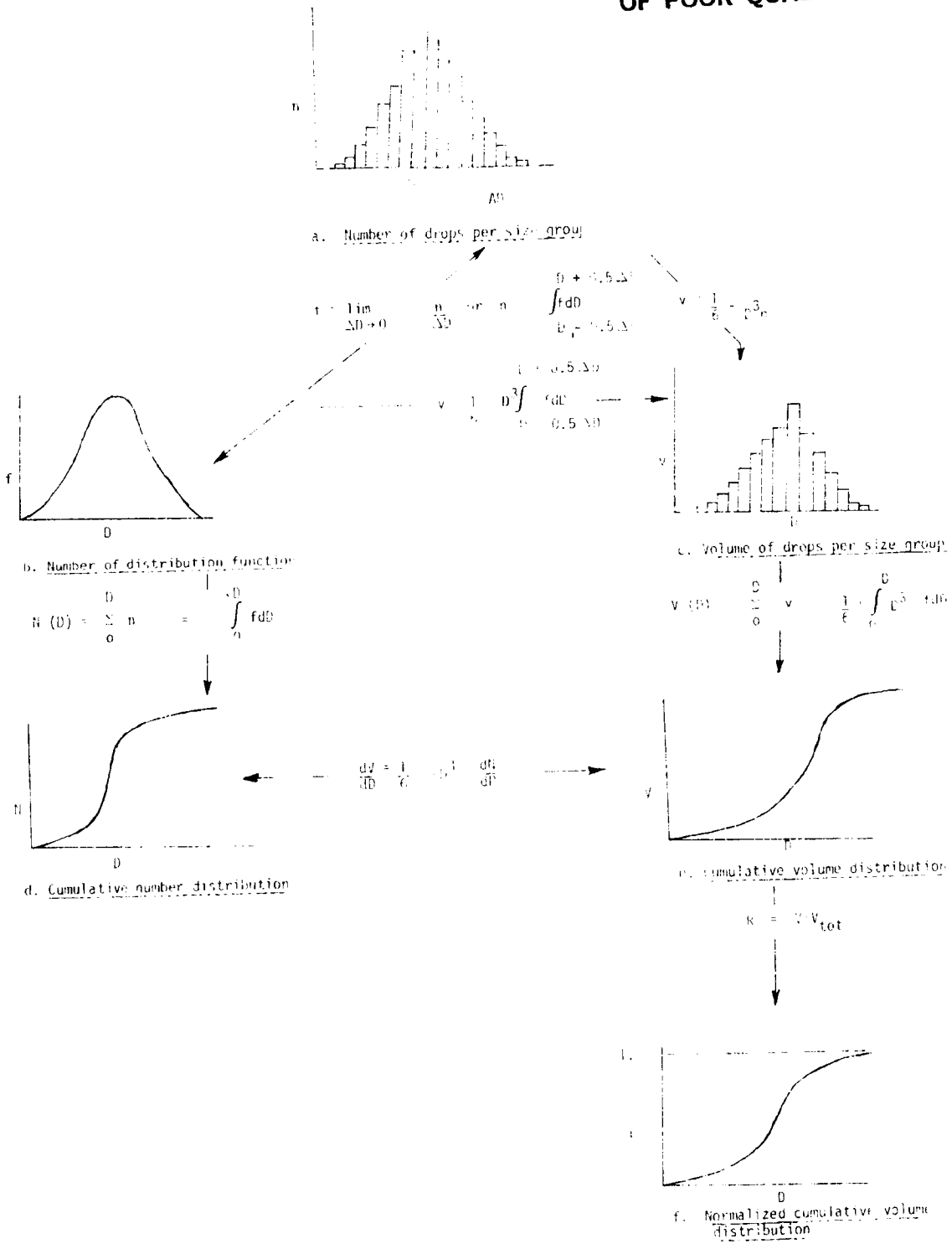

Figure 1. Droplet Size Distributions and Relationships

In some applications, the volume of liquid in the spray as a function of drop diameter is of interest. Multiplying the number of drops in each diameter range by the volume of a drop of that diameter converts the number distribution to a volume distribution (Fig. 1c). It is also possible to construct a volume distribution function (not shown in Fig. 1) analagous to the size distribution function. Another useful representation is a cumulative distribution. The cumulative number, N, of droplets at any diameter D is the sum of the number of all droplets having diameters less than D (Fig. 1d).

$$N(D) = \sum_{0}^{D} n = \int_{0}^{D} f\, dD \qquad \text{or} \qquad \left(\frac{dN}{dD}\right)_{D} = f(D)$$

Similarly, the cumulative volume distribution, V, of the droplets at any diameter D is the sum of the volumes of all drops in the spray having diameters less than D (Fig. 1e).

$$V(D) = \sum_{0}^{D} v = \int_{0}^{D} \left(\lim_{\Delta D \to 0} \frac{V}{\Delta D}\right) dD \qquad \text{or} \qquad \left(\frac{dV}{dD}\right)_{D} = \frac{1}{6}\pi D^3 f$$

The normalized cumulative volume distribution, R, (Fig. 1f) is the volume distribution divided by the total volume of all the droplets measured, i.e.,

$$R = \frac{V}{V_{tot}}$$

The cumulative volume distribution (often normalized) is the most commonly utilized manner for graphically presenting the data.

The mathematical expressions defining the drop size distribution that are encountered most commonly are

$$\frac{dV}{dD} = AD^5 \exp(-BD^n) \qquad \text{Nukiyama - Tanasawa}$$

$$\frac{dV}{dD} = BnD^{n-1} \exp(-BD^n) \qquad \text{Rosin - Rammler}$$

$$\frac{dV}{dY} = \delta\, \pi^{-1/2} \exp(-\delta^2 Y^2) \qquad \text{Log probability}$$

where $Y = \ln(D/\bar{D})$

and A, B, n, and δ are the adjustable constants. Many other distribution functions have been utilized and a more complete list and description of these is contained in Ref. 11. Since:

$$\frac{dV}{dD} = \frac{1}{6} \pi D^3 \quad \frac{dN}{dD} = \frac{1}{6} \pi D^3 f$$

these distributions actually define the desired distribution function, f. Given the distribution function, f, the cumulative volume (or number) distribution can be obtained by integrating the distribution function, f, over various size ranges.

More often, the data is plotted in terms of the cumulative volume, or normalized cumulative volume, versus drop diameter. For some droplet measurement techniques, particularly the frozen wax technique, it is this cumulative volume (or mass) distribution which is measured directly. Evaluation of the slope of this distribution then can be performed to define the droplet number distribution or distribution function. Cumulative distributions tend to "smooth" the data, mask inaccuracies due to too few droplet measurements, and reduce the apparent differences between different distributions. Usually, only the cumulative volume distribution is reported, so this problem is overlooked often. One very comprehensively reported investigation (Ref. 66), which presented all of the data and plots of V and $\frac{dV}{dD}$ versus D, demonstrates this problem. Figure 2 is a cumulative volume plot of the data from one set of droplet size measurements as presented in that report. The data appear to be in good agreement with the integral of the particular distribution function chosen. However, the plot of the actual volume distribution, $\frac{dV}{dD}$, and the data (Fig. 3) demonstrate that this apparent agreement between the distribution function and the data is misleading.

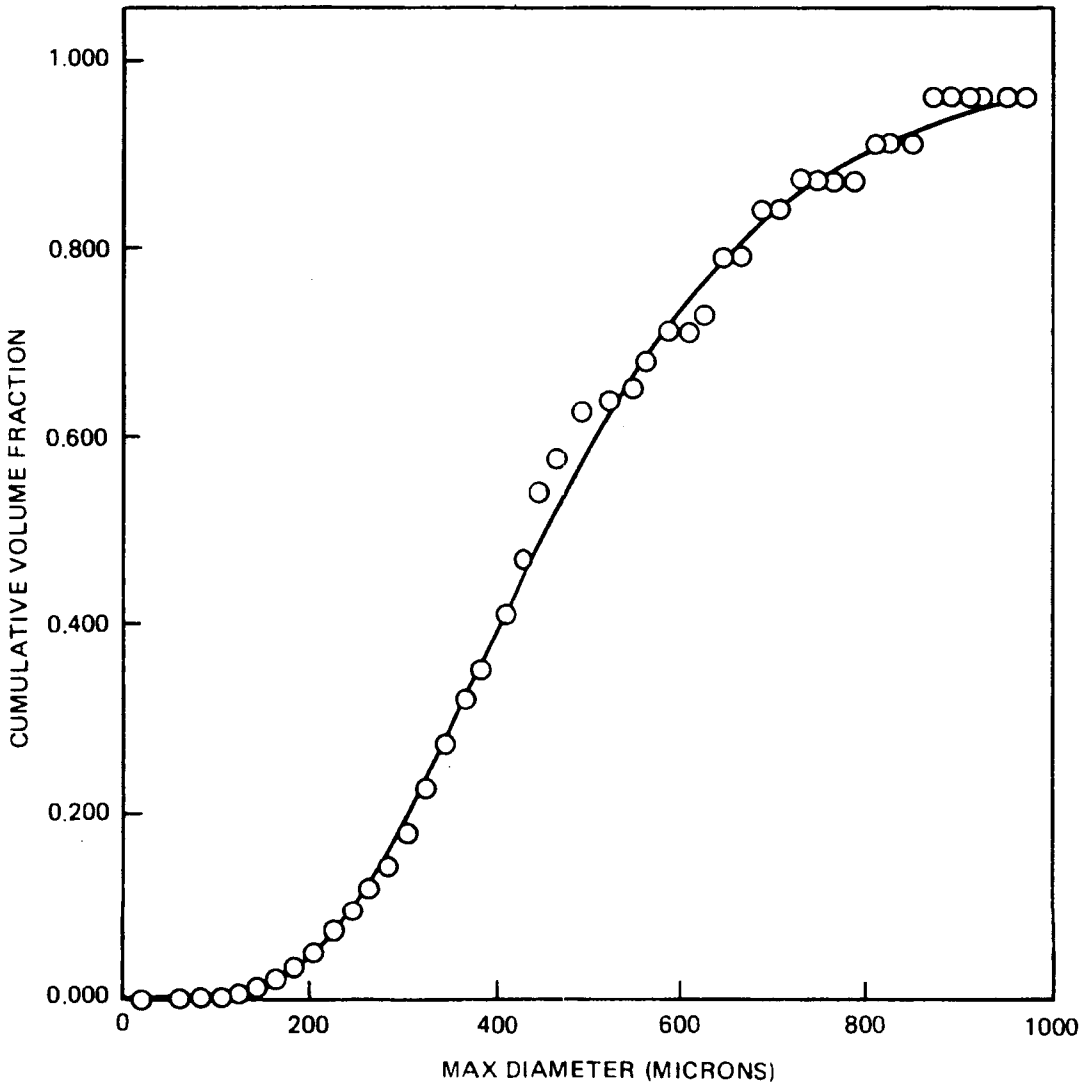

Figure 2. Droplet Cumulative Volume Distribution and Equation (Ref. 66)

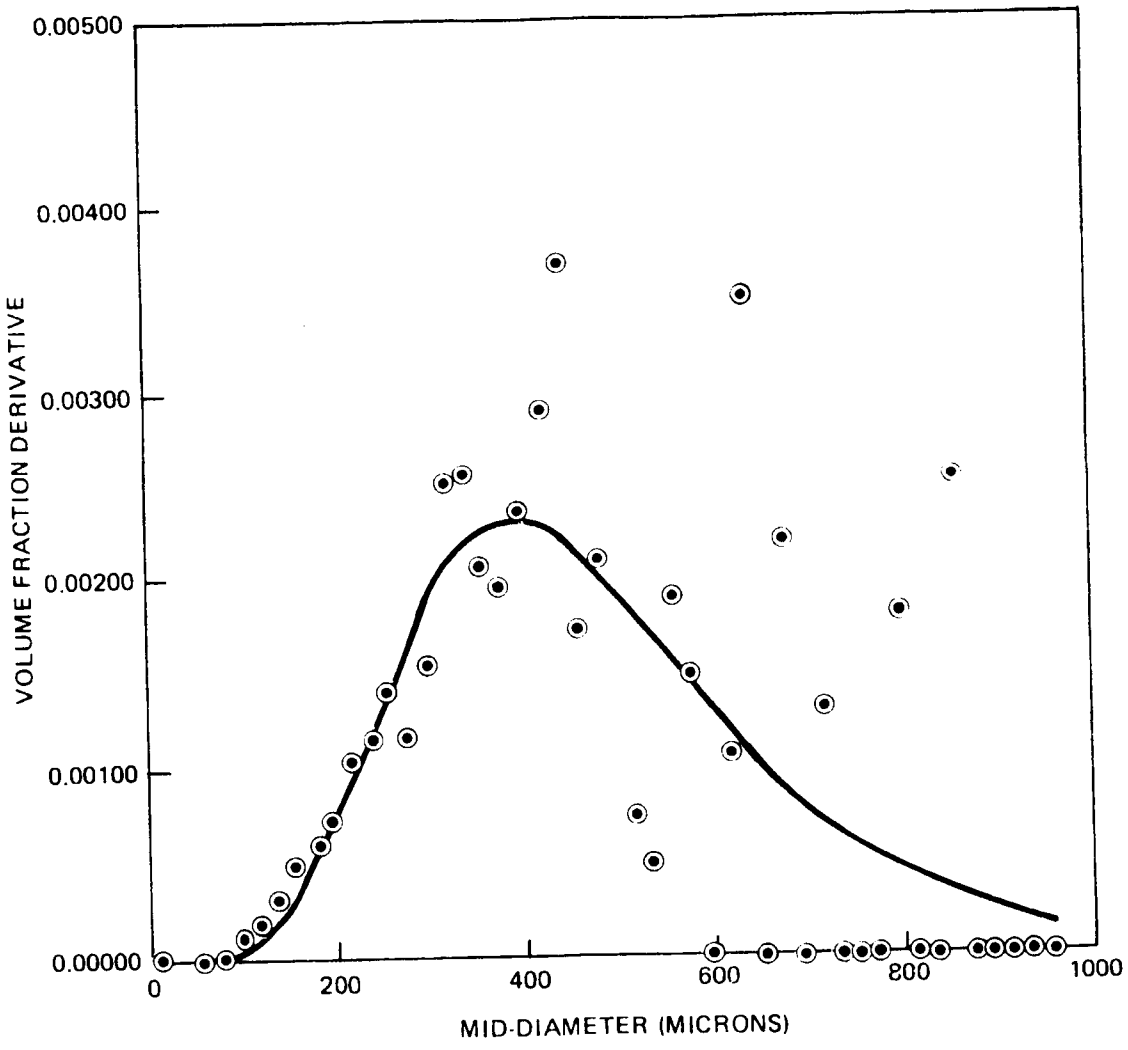

Figure 3. Derivatives of Droplet Cumulative Volume Distribution Data and Equation (Ref. 66)

Often the drop distribution is characterized by a single value- a representative drop diameter. Some such common representative diameters are the mean or average drop diameter, volume mean diameter, Sauter mean diameter, or mass median diameter. The mean or average diameters are defined according to the following general relationship:

$$D_{pq} = \left[\frac{\Sigma n_i D_i^p}{\Sigma n_i D_i^q} \right]^{\frac{1}{p-q}}$$

where i denotes size range considered.

n_i = number of droplets in size range i
D_i = middle diameter of size range i

Thus, D_{10} is the linear average diameter of all the droplets measured, D_{30} is the diameter of the droplet having the average volume of all the droplets measured, and D_{32} is the diameter of the droplet whose volume to surface area ratio is the average of all the droplets in the spray (referred to as the Sauter mean diameter). The mass median droplet diameter is the droplet whose size is such that one half of the mass (or volume) of the spray is contained in droplets having a larger diameter. On a plot of R versus D (Fig. 1f), the mass median diameter is the diameter occurring at a value of R = 0.5. All of these representative diameters can be calculated from the distribution function, f.

Most of the correlations developed to define the effect of various geometric and operational variables on droplet size define this effect in terms of the influence these parameters have on one of these representative diameters. These usually take a form:

$$\text{Representative diameter} = A\, X_1^{\,m}\, X_2^{\,p}\, X_3^{\,q} \ldots\ldots$$

where the X terms are the variables, or collections of variables, of interest, and A, m, p, q, ... are the adjustable constants by which the relationship is made to fit the data. In some instances, sums of terms, each similar in form to the right-hand side of the above equations, are employed. It must be recognized that such relationships as this do not completely characterize the spray, and that two sprays with the same mass median or Sauter mean diameter are not the same. It is often the smallest drop size and/or the largest drop size that are of greatest importance (e.g., in assessing stability and performance respectively). The mean or median droplet size does not provide this information. Thus, it is important to also characterize the droplet size distribution--i.e., to establish the correlating equation defining the distribution function, f.

DROPLET MEASUREMENT TECHNIQUES

A variety of techniques have been employed to measure droplet sizes. All of these techniques are subject to inaccuracies and questions associated with the basic assumptions employed, their manner of use, and/or the quantities of data usually obtained. Details of these techniques can be found in the literature, including some of the references contained in the bibliography. The discussion here is limited to the three primary techniques previously employed to obtain atomization data for rocket engine injectors. The findings obtained regarding rocket engine injection atomization utilizing these techniques is discussed subsequently.

Imaging Techniques

These include photography and holography and have been the most extensively employed methods for droplet sizing. They generally require a fairly dilute spray and offer the advantage of actually "seeing" the droplets as they exist at the point and time where knowledge of their size is desired. Although multiple exposure techniques can be employed to obtain droplet velocity data, none of the experimental programs discussed herein did so. As will be discussed shortly, velocity information is essential to the determination of accurate droplet size distributions when imaging techniques are employed. Imaging techniques have been employed to measure droplet sizes in reacting flows. This is an important and valuable feature that apparently has only been employed for the case of a rocket engine combustor in the investigations reported in Ref. 26, 72, 73, and 76.

A major problem with the use of imaging techniques has been the need for human analysis of the images. Although computerized techniques have been developed recently for analysis of photographic images, all of the rocket injector atomization work described herein employed at least some degree of human involvement in the analysis of the droplet images. It is necessary for someone to determine which droplets are to be counted (i.e., which droplets are in focus), and in most cases, to manually measure the droplet sizes. This causes errors in two ways human judgment and insufficient droplet counts to define the spray.

Another problem associated with imaging techniques is the time (i.e., cost) required to manually identify, count, and measure the droplets. This often prevents the counting of a sufficient number of droplets to assure an accurate distribution. A large number of droplets must be counted. The number of small drops may be over 1000 times as great as the number of large ones, and yet these large drops are often the most important to include. In Ref. 5, it is calculated that it is necessary to count 5500 droplets to be 95% confident that the Sauter mean diameter is correct to within 5%. Rarely are so many droplets counted per sample with imaging techniques.

Perhaps the most important problem associated with imaging techniques is that these techniques only measure the concentration of droplets in a given volume of space (i.e., spatial distribution) rather than the true droplet distribution, the temporal distribution. This problem is recognized in the older literature (Ref. 11), but appears to have been neglected by many others. The nature of this problem is discussed in detail in the following.

In a steady-state flow of droplets, the number of droplets, and the number of droplets of each size entering a particular region in space per unit time must be constant. It is possible to write a droplet number conservation equation (analagous to a mass conservation equation) as follows:

$$\dot{N}_i = \rho_i A V_i$$

where $\dot{N}_i$ = number of droplets of size group i entering a region or control volume (drops/sec)

ρ_i = local concentration of droplets of size i (drops/cm^3)

A = cross sectional area of region perpendicular to the direction of flow (cm^2)

V_i = velocity of the droplets of size group i (assuming all drops in size group i are travelling at the same velocity) (cm/sec)

Now, the temporal distribution of droplets produced by an injector can be obtained by counting the droplets per second of each size group i crossing A, that is, by measuring the values of the $\dot{N}_i$ terms. As long as the droplets are moving in one direction (i.e., the spray is not spreading), measurements of the $\dot{N}_i$ values at any location in the spray will not change. However, the imaging techniques measure the droplet concentrations, i.e., the ρ_i terms. As long as the droplet velocities remain constant as the spray moves downstream, these ρ_i terms also will remain constant. However, if the droplet velocities change in such a way that the smaller drops are no longer moving at the same speed as the larger drops, then the ρ_i terms also change. The $\dot{N}_i$ values must remain constant for this is a steady flow situation. Thus, an imaging technique measures the ρ_i terms, and the ratios of the ρ_i terms is not the ratios of the actual number of droplets of each size group in the spray. The only time that the imaging techniques produce true drop size distributions is when all the droplets move at the same velocity. This condition rarely, if ever, occurs in nature or in experiments.

One particularly noteworthy effort that appears to demonstrate this effect is the work of George (Ref. 72. 73. 76). In these experiments, measurements were made at several axial locations downstream of the injector utilizing an imaging technique (holography). In all these tests, the gas velocity exceeded the liquid injection velocity. In such a case, the small droplets would be accelerated more rapidly than the larger droplets. This would cause the spatial concentrations of smaller drops to decrease faster than for the larger drops as we move downstream from the injector face. Thus, we should expect to see more larger drops than smaller drops in the holograms as we move downstream. This effect was observed (Ref. 73) and was quite significant. The value of D_{30} was found to increase by 50 microns or more over a 2 inch change in axial distance. Also, a simple computer simulation of droplet dynamics in a constant velocity gas flow (Ref. 84) demonstrates significant differences (40% or more variation in representative droplet sizes) between temporal and spatial measurements.

This problem of spatial versus temporal distributions places some doubt on the utility of the results obtained with imaging techniques. Not only are the distributions measured not the true distributions, but the distributions will vary at different locations due to differences in velocities of the various size droplets. This may account for much of the disagreement between various investigators. The only situation in which the temporal and spatial distributions are the same is when the velocities of the droplets are not a function of droplet size. Spraying into "still" air will never produce this condition; and spraying into flowing air only will approximate this condition beyond some unknown distance downstream from the injector (where the droplets and gas velocities are equal). It is the temporal distribution that is needed for the combustor models.

Liquid Droplet Capture Technique

This technique involves the capture of a sample of the spray on a solid surface (e.g., a glass slide) or in another liquid. The droplets captured are measured under a microscope or photographed for later analysis. Most of the work utilizing this type of technique was performed before 1960 and the technique seems to have been supplanted, to a large extent, by photographic and other methods. In many cases the captured droplets are no longer spherical (e.g., droplets captured on a surface) and corrections to account for this must be applied.

This type of measuring technique requires the use of highly nonvolatile liquids and, when the droplets are captured in another liquid (e.g., a heavy oil or glycerine), further requires that the droplet liquid be immiscible in the capturing liquid. This limits the choice of liquids that can be utilized. Also, the droplets must be captured gently so as to prevent droplet shattering.

In many applications of this technique, it is obviously the temporal distribution of droplets that is obtained. For some sampling methods, however, there is some question as to whether it is the spatial or temporal distributions that are measured. Such questionable methods include the slide "waving" technique, where a glass slide is passed rapidly through a spray.

Like the imaging technique, the liquid droplet capture technique requires considerable manpower to count and size the droplets. Thus, the size of the sample counted may be a serious source of error. Also, this technique requires the spray to be diluted sufficiently to prevent a significant amount of coalescense of the droplets in the sample. In order to accommodate this requirement, one technique often employed is a spray splitter. The spray impinges on a plate containing a hole or slit through which only a portion of the spray may pass. Only this small portion is allowed to fall on the collection surface. This same procedure also is used occassionally with imaging techniques to dilute the spray. One aspect of this spray splitting procedure that occassionally is overlooked is the effect and probability of droplets colliding with the edge of the splitter plate. Such collisions can shatter droplets thereby causing the sampled spray to have a droplet distribution different from that of the main spray. This problem is analyzed in some detail by Dickerson (Ref. 47).

Droplet Freezing Technique

This technique has been applied extensively in the study of rocket engine injectors. Much of this work that is related directly to rocket engine injectors was performed at Rocketdyne during the period 1967 through 1975, and utilized wax as the injected liquid. Fluids other than wax have been used and droplet capture and freezing in liquid nitrogen also has been performed. All of the work described herein utilizing this technique was done with wax.

The frozen wax technique offers several advantages over other methods. The liquid wax is injected into the atmosphere or a large pressure vessel where the droplets rapidly cool and solidify, and then are collected and sampled. The sample then is subjected to a sieving operation where the wax droplets are separated into size groups. Each size group then is weighed and a plot of droplet mass (volume) versus size is constucted. Thus, the cumulative volume, volume distribution, and mass median diameter are measured directly, without the great time and manpower associated with the sizing and counting of individual droplets. Also, the true or temporal distribution of droplets is measured, since all the droplets produced by the spray over a long period of time (several seconds) are collected. And finally, the number of frozen wax droplets included in the sample is on the order of millions. This technique does not suffer from a lack of a sufficient sample size to be statistically accurate.

One serious disadvantageous feature of the hot-wax technique is the limited choice of materials that can be applied conveniently. Since the properties of the actual propellants are different from the simulants, it is necessary to establish the effects of these properties (surface tension, density, and viscosity) on the atomization process. Thus, the capability to perform tests with different fluids having widely varying properties is important. Another feature of the wax technique that merits consideration is the density increase upon freezing. Because of this, some earlier investigators have corrected the wax droplet sizes by multiplying the measured droplets' volumes by the ratio of the solid to liquid densities. However, the physics of the freezing phenomena indicates that the droplets should freeze on the outside first. If this is correct, then the frozen drops should be hollow and no density change drop size correction is required. Dickerson (Ref. 47) has discovered that the droplets indeed are hollow, and that the volume of the central void is approximately equal to the size change due to freezing- at least for the larger drops.

One of the most serious criticisms of most of the hot-wax investigations involves the problem of defining the temperature (and hence the properties) of the liquid wax during atomization. In most investigations, the hot liquid wax is injected into a relatively cold gas (e.g., the atmosphere). For these cases, it is necessary to question whether the wax has cooled significantly prior to the completion of atomization. Zajac (Ref. 58) presents data showing that the surface tension and viscosity of the particular wax utilized (shell 270) increase by 12% and 83%, respectively, between 93 C (the nominal injection temperature) and 66 C (slightly above the wax fusion temperature). Certainly, the surfaces of the wax ligaments and droplets must be cooler than the bulk wax injection temperature. Thus, the wax properties at the injection temperature may not be the same as those existing during atomization. Longwell (Ref. 1) presents results suggesting the wax technique erroneously may give large droplets due to viscosity increases as the liquid cools during atomization. However, Hasson and Mizrahi (Ref. 23) present extensive data demonstrating that the wax technique produces significantly and erroneously <u>small</u> droplets (they corrected for an assumed shrinkage of the droplets upon freezing, but this correction is not great enough to account for the observed difference). Several investigators (Ref. 29, 70, 71, 78) performed hot-wax experiments in which the wax was injected into hot gas and subsequently

cooled after atomization was complete. In these investigations the potential problem of wax cooling during atomization should have been eliminated or minimized.

DROPLET SIZE MEASUREMENT RESULTS AND CORRELATIONS FOR ROCKET ENGINE INJECTORS

This section presents all the pertinent atomization results that were found relating to triplet, pentad, and coaxial injectors. Since very little data pertaining to these injector types has been found, and since most of our knowledge of atomization comes from the study of like doublets, a discussion of like doublets also is included.

The expressions relating representative droplet diameter to injector geometry, operating conditions, and environment vary with each investigator. The most common representative diameters utilized are the Sauter mean (D_{32}), volume or mass mean (D_{30}), and mass median ($\bar{D}$). Conversion between these diameters requires that the droplet size distribution be known, and a generalized conversion requires that the distribution function be known and integrable. Generally, such information is not available, so a direct comparison between these representative diameter equations cannot be accomplished (one exception to this is described later). However, inspection of the exponents of some of the more important variables (e.g., liquid velocity, V_L, and orifice diameter, d_j), indicates considerable disagreement between these equations. This may be due to the previously discussed questions and problems regarding the measurement techniques, testing over different ranges and conditions, the use of different fluids, unmeasured and/or uncontrolled variables (the most important being the local gas velocity, V_g), and/or other unknown causes. In a few cases, these drop size equations contain variables that are not varied significantly during the testing. In many cases (all cases for the triplet, coaxial, and pentad injectors), all of the potentially significant variables have not been tested. The equations developed from such data are incomplete. All of the droplet size equations described herein are strictly empirical or are based only in part on very limited theoretical considerations.

Like Doublet Correlations

The most extensively studied rocket engine type injector is the like doublet. Much can be learned through a review of these doublet studies about atomization processes and measurements in general that is relevant and important to the study of triplets, pentads, and even coaxial injectors. Table 1 is a list of selected impinging doublet injector atomization studies showing the droplet size correlations derived and the conditions of the experiments.

One of the earliest studies of impinging element injectors was the work of Tanasawa, et. al. (Ref. 9). This study employed totally opposed impinging streams to develop the equation presented in Table 1, and also indicated that liquid viscosity is of little importance. Although it is not clear, it appears that other properties were varied with viscosity. Subsequent studies indicated that viscosity effects cannot be neglected.

Prof. Dombrowski of Imperial College performed a number of investigations (Ref. 32, 33, 34, 35, 40, 45) of atomization of impinging streams utilizing photography. Many of these experiments were performed in a pressurizable vessel with a weak gas flow to prevent droplet recirculation. Some of these results (Ref. 33) show the surprising result that increasing chamber gas density first causes a decrease in droplet size, but at higher chamber pressures (>1 mPa) the effect of gas density is to increase droplet size. In order to cover both these regions, two droplet size equations were fit to the data as shown in Table 1. Reference 33 also presents data showing the effect of chamber gas density on ligament and droplet velocity. Dombrowski (Ref. 40) also demonstrates the differences in the spray fans and the droplets formed by laminar and turbulent streams. Turbulent stream droplet size correlations did not fit laminar stream data. Measurements of the liquid velocities in fans were performed and show that these liquid velocities can exceed the average stream velocity if the streams are flowing laminar. An explanation of this phenomena is presented. This difference

m^3	J ΔP = 25 - 100 psi	μ_L = 1 - 5 cP $V_g \sim 0$	
^{3}			
	V_L = 7.3 - 19.5 m/s α = 50 - 140°		TURBULENT FLOW ONLY LAMINAR DATA DID NOT FIT
$\overline{V_L - V_g}$	d_j = .074 - .226 cm V_L = 9.15 - 30.5 m/s V_g = 19.8 - 91.4 m/s	α = 90° μ_L = .386 cP ρ_L = 680 kg/m^3 σ = .020 Nt/m	$\Delta V \neq V_L$ $D_{30} \propto \left(\frac{\mu_L \sigma}{\rho_L}\right)^{.25}$ (INGEBO 1957)
	d_j = .066 - .206 cm V_L = 15.5 - 45.3 m/s α = 60° V_g = 0	WAX PROPERTIES (?) μ_L = 3.0 cP ρ_L = 764 kg/m^3 σ = .017 Nt/m	ADJACENT FANS (WATER) HAD NO EFFECT ON $\bar{D}$, BUT DID AFFECT DISTRIBUTION
52 LAMINAR JETS α = 60° .1 TURBULENT JETS α = 60°	d_j = .152 - .206 cm V_L = 9.14 - 67.0 m/s α = 45-90° V_g = 0 $\frac{P_c}{P_j}$ = RATIO OF CENTERLINE TO AVERAGE DYNAMIC PRESSURE (A MEASURE OF VELOCITY PROFILE)	WAX PROPERTIES	ORIFICE ENTRANCE CONDITIONS, MISIMPINGEMENT, JET DISINTEGRATION, TURBULENT VS LAMINAR, VELOCITY PROFILE, L/d (ORIFICE), L/D (FREE STREAM), ET. AL., INVESTIGATED.

FOLDOUT FRAME 2

TABLE 1. (Concluded)

REFERENCE	MEASUREMENT TECHNIQUE	CORRELATION
GEORGE (1973)	HOLOGRAPHY N_2H_4 DROPS BURNING IN N_2O_4 H_2O DROPS IN N_2 1" TO 4" FROM INJECTOR	$D_{30} = A_o + A_1 V_L + A_2 \ln \rho_L + A_3 \frac{\rho_g V_g^2 d_j}{12\sigma}$ COLD FLOW $D_{30} = \frac{d_j}{B_1 + B_2 d_j + B_3 W_L}$ HOT FLOW d_j = .15 - .244 cm V_L = 18.6 - 38.7 m/s α = 60° V_g = 75.6 - 114 m/s
ZAJAC (1973)	HOT WAX INJECTED INTO WARM, FLOWING N_2 IN A VARIABLE AREA DUCT	$\bar{D} = \tau \bar{D}_c \left\{ 1 - 1.77 \times 10^{-3} \bar{D}_c \left(\frac{V_{gm} - V_L}{V_L} \right) \text{EXP} \left[-.24 \frac{V_{gm} - V_L}{V_L} \left\lvert \frac{V_{gm} - V_L}{V_L} \right\rvert \right] \right\}$ FOR $-1 \leq \frac{V_{gm} - V_L}{V_L} \leq 1.25$ $\bar{D} = \tau \left\{ \bar{D}_c \left(1 - 1.52 \times 10^{-3} \bar{D}_c \right) - 12 \ln \left(\frac{V_{gm} - V_L}{V_L} \right) \right\}$ FOR $\frac{V_{gm} - V_L}{V_L} > 1.25$ WHERE $\bar{D}_c = 2.01 \times 10^5 d_j^{.375} / V_L^{.75} = 10.9 \bar{D}_o^{.66} / V_L^{.09}$ $\tau = \left[1 + 5.8 \times 10^{-6} \frac{\bar{D}_c V_L}{L} \left(\frac{V_L}{V_{gm}} \right)^{.5} \right]^{.41}$ $L \geq 5$ cm

ALL D VALUES IN MICRONS, ALL OTHER VALUES IN THE EQUATION SHOULD BE INPUT IN CGS UNITS

were performed at NASA-Lewis (Ref. 12, 13, 15, 21, 25, 26, 39, 49). These include studies of the effects of various parameters on impinging stream fans, single stream crosscurrent injection, and photographic measurements of droplet sizes produced by impinging streams. One of the most often quoted references of these is the work of Ingebo (Ref. 15). He performed experiments utilizing like doublets injecting heptane into a low-velocity gas stream. The heptane was injected in the direction of the gas flow (cocurrently) and the droplets were photographed and counted throughout the spray at a distance of 6 inches from the injector. The heptane streams were flowing in the turbulent regime. One of the most unique and important features of this work was the use of the flowing gas stream to simulate the combustion gas motion in a rocket combustor. Unfortunately, one of the greatest problems then (and now) is that we are unable to adequately define the actual combustion gas velocity field in a rocket combustor. And Ingebo's work demonstrates the great importance of this effect. The droplet size correlating equation developed from this data (Table 1) contains a term $(V_L - V_g)$, which accounts for this gas velocity effect on droplet size. Ingebo also utilized the data to evaluate the constants in a Nukiyama - Tanasawa general droplet size distribution equation to obtain:

$$\frac{dR}{dD} = \left(\frac{3.915}{D_{30}}\right)^6 \quad \frac{D^5}{120} \quad \exp \quad \left(-3.915\ D/D_{30}\right)$$

Furthermore, in an earlier investigation (Ref. 13), Ingebo established a relationship for the effect of injected liquid properties on droplet size as:

$$D_{30} \propto \left(\frac{\mu_L \sigma}{\rho_L}\right)^{.25}$$

However, this relationship was determined in experiments involving crosscurrent injection of single streams into flowing gases. Its applicability to cocurrent injection may be questionable, yet, it is often utilized.

In a subsequent study (Ref. 26), Ingebo utilized a moving camera to photograph burning ethanol droplets and measured their velocities. At a distance of 0.1 m from the injector, the drops were observed to be traveling at a higher velocity than their injection velocity. Most importantly, the small droplets were observed to have been accelerated much more than the larger droplets. 35 micron droplets had undergone a velocity increase 9 times as great as 344 micron droplets. Again, this would indicate that the spatial concentration of each size of droplets would be rapidly and differently varying with distance from the injector. The effect this would have on the measured spatial droplet size distribution apparently was not considered.

In 1964, several studies (Ref. 36 through 38) were reported by investigators at Aerojet General. Brown (Ref. 38) captured droplets on glass slides that were produced by the injection of a stream of liquid into flowing cold and hot (up to nearly 1300 K) gas. One of the important features of this work was the recognition that the spray affects the gas velocity. An attempt was made to quantify this effect in a droplet size relationship with a term containing the mass flow-rate ratio of liquid to gas. In another of these investigations, Wolfe and Anderson (Ref. 37) performed experiments and developed a relationship for the breakup of large droplets (i.e., secondary atomization) based upon the earlier work of Weiss and Worsham (Ref. 29). This relationship includes a liquid properties effect of the form,

$$D_{30} \propto \sigma^{1/2} \quad \mu_L^{1/3} \quad \rho_L^{-1/6}$$

In the early 1970s, photography and the new technique of holography were utilized at AFRPL to measure droplet sizes (Ref. 54, 66, 72, 73, 76). Kuykendal (Ref. 54) investigated the effects of liquid velocity, orifice diameter, impingement angle, stream alignment, orifice length, and surface finish for like doublets flowing water. Droplet size equations were developed to define these effects, but the average drop sizes were based upon a relatively small drop count (occasionally less than 100), and these equations appear to disagree greatly with most other similar studies. George (Ref. 72, 73, 76) utilized holography to measure droplet sizes in both hot flow (hydrazine drops burning in nitrogen tetroxide) and cold flow (water in N_2). The form of the droplet size correlations developed in that effort are presented in Table 1.

During the late 1960s and early 1970s, a very elaborate hot-wax capability was developed at Rocketdyne and many atomization investigations were performed (Ref. 47, 48, 50, 51, 52, 55, 56, 58, 60, 61, 63, 64, 65, 67-71, 74, 78). Two of the most comprehensive of these investigations are those of Dickerson, et. al. (Ref. 47) and Zajac (Ref. 58). Their correlations for like doublets are presented in Table 1. Both of these efforts were performed by spraying wax into "still" air. Dickerson's droplet size correlations, as reported in Ref. 47, are not in agreement with his subsequent paper (Ref. 52). Discussions with Dickerson revealed that the earlier liquid velocity data was incorrect, and the correlations of his latter paper include the correction. Dickerson evaluated the atomization characteristics of a variety of impinging injectors, with great emphasis on doublets. Experiments were performed with impinging fans from unlike pairs of like doublets utilizing water as the other fluid. These tests indicate that impinging fans tend to broaden the droplet size distribution but have little effect on D. Droplet size distributions for several of the injectors tested are presented in Fig. 4. Note that both axes have been normalized in such a way that all distributions must pass through the point (1.0, 0.5). Also, as previously discussed, it is the slope of these cumulative volume distributions that truly defines the spray. Thus, the apparently small differences in the plots of Fig. 4.are, in fact, large differences of great importance.

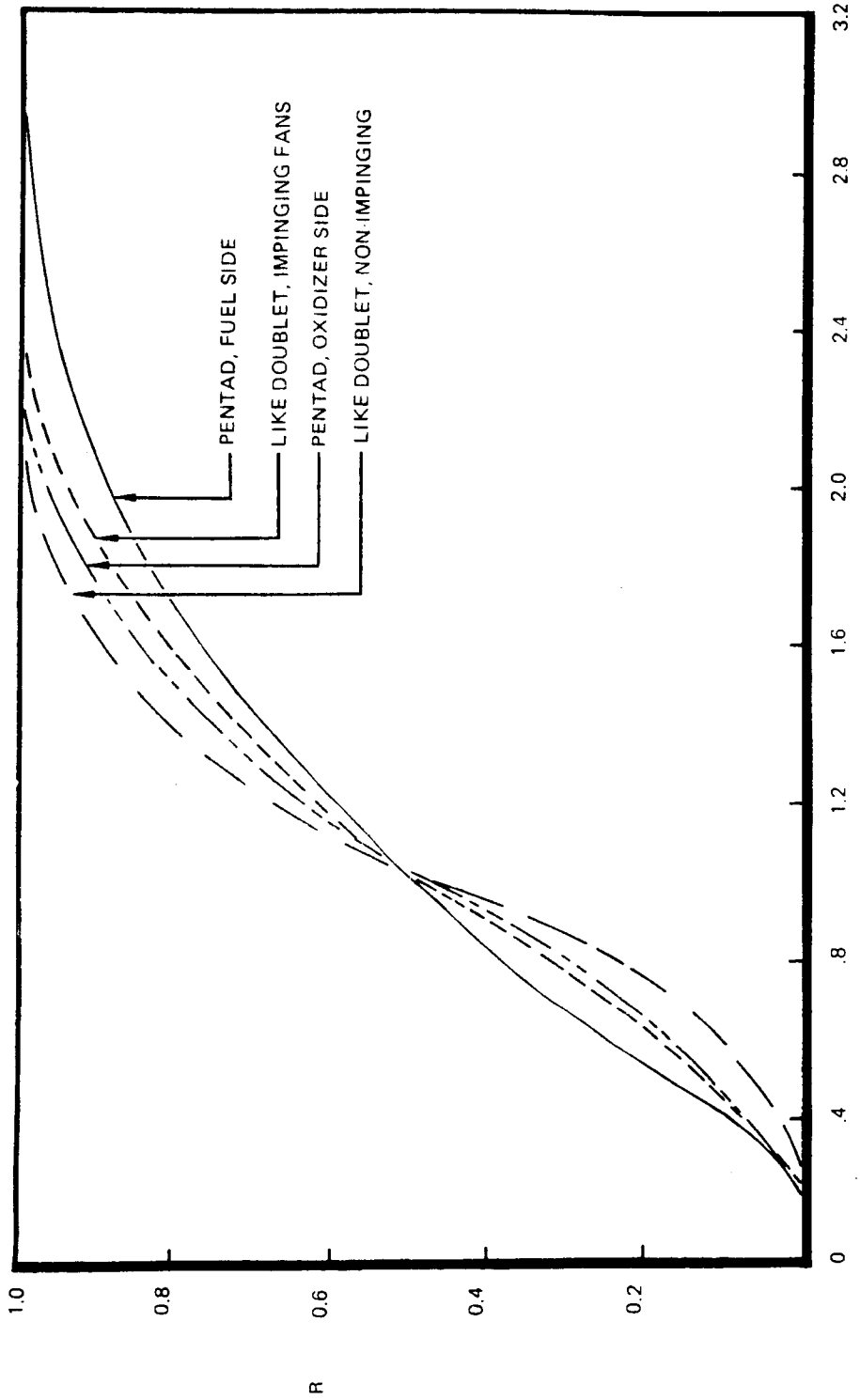

Figure 4. Normalized Droplet Size Distributions for Selected Injectors (Ref. 52)

The single most comprehensive study of atomization of rocket engine-type injectors is the work of Zajac (Ref. 58). Zajac examined the effects of liquid velocity, orifice diameter, velocity and diameter ratios, orifice length, free jet length (distance from orifice to impingement point), angle of impingement, orifice entrance conditions (geometric and flow conditions), misimpingement, and propellant miscibility for like and unlike doublets are well as triplets and pentads. In addition, he measured transient pressure distributions within the free streams (a measure of velocity profile and turbulence). Zajac found that streams flowing turbulent acted considerably different than laminar streams with regard to atomization (Dickerson had neglected this, but earlier investigators, e.g., Dombrowski (Ref. 40), already had indicated this). Thus, it was necessary to establish two droplet representative diameter equations, one for turbulent and one for laminar. Velocity profile also was found to be important, but only in laminar flow. Free stream breakup prior to impingement was shown to be important and can occur at a free stream length of from 5 to 10 orifice diameters in turbulent streams. The much higher gas densities in a real combustor could cause breakup in shorter lengths.

The state of the art circa 1971 was that the wax technique yielded sufficient quantity and apparent quality of data to define droplet sizes and size distributions of hot wax droplets sprayed from like doublets into still air. Several problems remained, as follows:

1. How valid is the hot-wax technique? Does wax significantly change properties before atomization is complete?
2. How can hot-wax results be correlated to that of real propellant?
3. What is the effect of the actual rocket combustor environment (hot, high-density combustion gases moving at high velocity) on the atomization process?

In an attempt to solve some of these problems, tests were performed with combinations of waxes to examine viscosity effects (Ref. 69) and a large pressure tank was utilized to simulate high-density gases (Ref. 64, 69, 74, et. al.). In addition, several attempts (Ref. 65, 68, 74, et. al.) were made to validate these

droplet size correlations by utilizing them in computer models of rocket engines and comparing the results of these models with the actual hot-fire tests the models were attempting to simulate. In one program (Ref. 65), a test engine operating on wax and liquid oxygen was utilized. Although all of these efforts reported some degree of success, these three basic questions still remain essentially unanswered.

One of the most unknown aspects of this problem was (and is) the effect of the combustion gas velocity on droplet size. The actual velocity field existing in and around the spray in cold-flow experiments is never measured. The actual velocity field existing in and around the spray in an operating engine also is unknown. And finally, the effect of a known flowfield on the formation and breakup of a spray fan or stream (primary atomization) is essentially unknown. There is, however, a considerable body of work performed to evaluate the effects of gas flowfields on the deformation and breakup of individual droplets (secondary atomization). Such efforts demonstrate the great complexity of this latter process.

In an effort to establish the effect of gas velocity on the size of droplets produced by impinging liquid streams, experiments have been performed in low pressure wind tunnels. In such experiments, the gas velocity is defined as the velocity that existed prior to the introduction of the spray. The effect of the spray on the gas velocity, although often recognized, is not taken into account-very crudely included by Brown (Ref. 38), and is not measured. Similarly, the liquid velocity in the gas is assumed to be the average liquid velocity at the injector orifice exit, and not the actual liquid velocity in the spray fan. Thus, in attempting to correlate this very important effect of relative gas velocity (gas velocity relative to liquid velocity), the velocities used are incorrect and are, at best, only representative of the true velocities. Despite this, these experiments do provide an indication of the importance of the relative gas velocity. Probably the most extensive of these efforts for impinging like doublets are the work of Ingebo (Ref. 15) and George (Ref. 76), as previously discussed, and the latter investigations of Zajac (Ref. 70 and 71).

Zajac utilized a doublet injecting hot wax cocurrently into a ducted hot (~ 60 C) nitrogen stream. He separated the atomization process into two parts (i.e., primary and secondary) and studied these separately. In the primary atomization study, the effect of constant velocity and accelerating gas streams on the sizes of droplets initially formed was investigated. In the secondary atomization study, known droplet size distribution sprays were subjected to accelerations to observe droplet breaking. The rate and degree of acceleration was controlled by varying the length and area of the duct downstream of the injection location.

Zajac found that many of the parameters investigated in his previous work were of little importance compared to the effect of relative gas velocity. Much of his data was plotted in the form of Fig. 5, showing droplet size versus a nondimensionalized relative gas velocity. Note that all of the investigations in which the liquid was injected into "still" air would be plotted at the -1 value of the nondimensionalized velocity. Shown in Fig. 5 are volume mean diameter data from Ingebo showing the effect of gas velocity on droplets produced by two different injectors, mass median diameter data from Zajac, and the calculated droplet size based upon tests with $V_g = 0$. The data from Zajac presented here was obtained with a constant gas velocity (i.e., duct area remained constant). Figure 5 demonstrates the great efect of gas velocity on droplet size.

Based upon his experiments with accelerated and constant velocity flows, Zajac constructed the droplet size correlation equations shown in Table 1. These equations compute the mass median droplet size based upon the gas and liquid velocities, the droplet size, $\overline{D}_c$ occurring when the maximum gas velocity equals the injected liquid velocity (i.e., $V_g - V_L / V_L = 0$), and a parameter , which includes the distance over which the gas is accelerated (at V_g = constant, L = infinity). The parameter $\overline{D}_c$ is computed from the liquid velocity and orifice diameter. A study of the derivation of these equations indicates they are applicable to turbulent flow only.

The correlation of Zajac is, to some extent, supported by the earlier work of Ingebo, and the very important effect of relative gas velocity is demonstrated. Unfortunately, the application of such results to real combustors is difficult since the combustion gas velocity cannot be defined adequately.

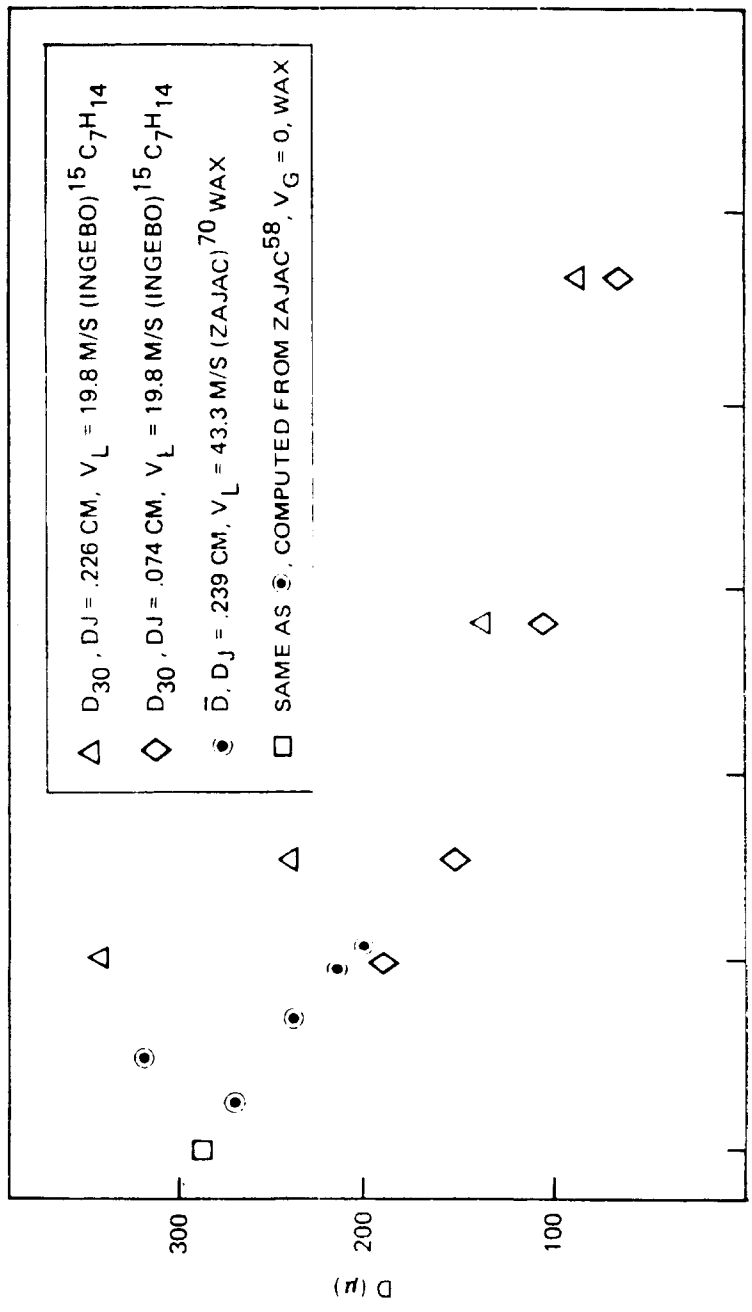

Figure 5. Effect of Gas Velocity on Droplet Size

Since about 1975, there has been very little atomization work directly relateable to rocket engine like doublet injectors. This is certainly not because the problem has been considered solved. Despite all the earlier efforts to define the initial droplet sizes produced by like doublets in combustors, our knowledge in this area is very crude and/or qualitative. All of the droplet size data to date is of questionable accuracy and/or validity due to real or possible droplet size measurement technique problems as previously discussed. The droplet size correlations and distributions developed from this data are generally, strictly empirical. They are mere curve fits of the test data and, as such, may be neglecting important untested variables and are certainly not of the proper form. These correlations are based upon data that demonstrated poor or usually unknown repeatability, considerable spread, and often a relatively low quantity of droplet counts. To some extent, these features of the data are masked by the extensive use of semilogarithmic plots of the data and cumulative droplet size distribution plots.

Perhaps the greatest problems involve the application or utility of the atomization data. Extrapolation of the cold-flow data using wax or other liquids to the actual propellants and to the conditions existing in a rocket combustor requires many questionable assumptions and estimates. One of the most important and, unfortunately, most questionable of these extrapolations involves the combustion gas velocity, as previously discussed. Also, since the correlations developed are empirical, extrapolation to any conditions outside the ranges tested is dangerous. And finally, the attempts to utilize the correlations in rocket combustor codes have not been successful. All of the major rocket combustor codes in use at Rocketdyne (i.e., TPP, SDER, CICM) have arbitrary multipliers of the initial droplet sizes, either as a part of the code or as an input, in order to force agreement between the codes and hot-fire engine test data.

Properties Correlations for Like Doublets

In addition to all the like doublet "lessons learned" discussed above that are applicable in general to rocket engine-type injectors, these studies provide the only known corrections or correlations by which we may relate real propellant atomization to that of the simulants used in atomization experiments. Although

many of the droplet size correlating equations contain liquid properties effects, probably the two properties correlations quoted most generally are

$$D_{30} \propto \left(\frac{\mu \sigma}{\rho_L}\right)^{.25} \qquad \text{Ingebo (Ref. 13)}$$

and

$$D_{30} \propto \mu_L^{.333}\ \sigma^{.5}\ \rho_L^{-.167} \qquad \text{Wolfe and Anderson (Ref. 37)}$$

Ingebo's correlation comes from a droplet size correlation equation defining the droplet sizes produced by the breakup of a single stream injected transversely into an airstream. Wolfe's and Anderson's correlation is based on the breakup of already formed droplets in gas streams (i.e., secondary atomization). The applicability of either of these relationships to like doublets can be questioned. In addition, no attempts to establish the effect of liquid properties on droplet size distributions were found in the literature. Also, properties correlations for unlike doublets, triplets, pentads, or coaxial injectors, or any gas/liquid injector apparently do not exist.

Another aspect of the liquid properties correlations problem that often is overlooked is the actual values of the properties of the real propellants and the simulants at their injection conditions. Since liquids are generally, relatively incompressible, since viscosity usually is not considered to be a function of pressure, and since density, viscosity and surface tension data for many propellants and test fluids is readily available only at room temperature and one atmosphere or at the liquid's normal boiling point (for cryogenics), these room temperature and one atmosphere or NBP properties data often are utilized. This can cause considerable error. Liquid oxygen is a propellant of considerable interest which serves as a good example. For LOX at 134 K (the SSME preburner LOX injection temperature) the density increases by 11% and the viscosity increases by 52% between 17 and 340 atm (data from NBS Table TN 384). LOX properties are, of course, a fairly strong function of temperature, and choosing the wrong temperature (e.g., using NBP data) also can cause great errors.

Surface tension is a particularly difficult property for which to find nonroom temperature and one atmosphere or non-NBP data. Surface tension is a strong function of temperature and techniques are available to compute the effect of temperature. For LOX, the surface tension changes from 13.2 dynes/cm at its NBP of 90 K to 6.4 dynes/cm at its SSME injection temperature of 134 K. As part of an attempt to determine the effect of pressure on surface tension, papers were found that indicated a very strong effect (e.g., O.K. Rice, "The Effect of Pressure on Surface Tension,: Journal of Chem. Physics, Volume 15, #5, May 1947). However, based upon discussions with Prof. A. Adamson and Dr. R. Massoudi of the University of Southern California's Chemistry Department, this effect apparently is not due to pressure, but rather to the absorption of gases into the liquid. The effect of pressure alone on surface tension should be on the order of a 1% increase per 100 atm pressure. This absorption of gases also probably would have a great effect on other properties. Since the time available for absorption, i.e., the time between injection and atomization is so short, very little absorption would be expected. If this is the case, the effect of pressure on surface tension should be of little concern.

Triplet Correlations

Very little data was found regarding the atomization characteristics for triplets. This data is synopsized in Table 2. All these investigations were performed at Rocketdyne utilizing the hot-wax technique. In all these tests, the wax was injected into "still" air at ambient pressure.

As a small part of Zajac's earlier investigation (Ref. 58), a particular liquid/liquid triplet having all three holes the same size was subjected to atomization testing. In order to separately evaluate the droplet size produced by the inner and outer streams, wax and hot water were employed. The wax was injected through the inner orifice and the water through the outer orifice, and the liquids then were reversed on a subsequent test. The only variables investigated were the liquids' velocities, and these were varied in such a way as to maintain a constant mixture ratio. Most of these tests were performed under laminar flow conditions. At high velocity (turbulent flow), the data begins to markedly deviate from the correlating equation presented in Table 2.

TABLE 2. DROPLET SIZE CORRELATIONS FOR TRIPLETS

REFERENCE	MEASUREMENT TECHNIQUE	CORRELATION	
ZAJAC (1971)	WAX AND WATER	$\bar{D}_c$ & $\bar{D}_o \propto 3.03 \times 10^4 \, V_L^{-.575}$ V_L (cm/s) IS VELOCITY OF LIQUID IN ORIFICE OF INTEREST (CENTER OR OUTER)	$\alpha = 30°$ $V_L = 9.14 - 45.7$ m/s $d_c = d_o = .17$ cm $\rho_g = 1.1$ kg/m^3
McHALE AND NURICK (1974)	WAX AND WATER	PLOTS NEW DATA AND ZAJAC's VS $W_e \cdot (L/d)$ $W_e = \frac{\rho_L V_L^2 d}{\sigma}$ L = ORIFICE LENGTH	d_c OR $d_o = .051 - .17$ cm $\frac{d_o}{d_c} = .522 - 1.0$ L = ORIFICE LENGTH = 7-50d $\rho_g = 1.1$ kg/m^3 (P_c = ATMOSPHERI
MEHEGAN, ET. AL. (1970)	WAX AND HOT GAS (N_2) CENTER ORIFICE GAS	2 DATA POINTS	$d_c = 1.48$ cm $d_o = .52$ cm $\rho_g = 1.1$ kg/m^3

SUBSCRIPT:

C - CENTER
O - OUTER

fully developed the velocity profile has become. This effect is included in Zajac's correlation for doublets in the P_c/P_j term (Table 1).

The data of Fig. 6 confirms Zajac's earlier work regarding the lack of difference in drop size when by the central and outer streams are of the same size. Note that the ordinate is normalized by the orifice diameter. Also, Fig. 6 is a logarithmic plot. As previously mentioned, such plots tend to minimize significant differences and scatter in the data. At low Weber numbers, which Zajac did not investigate, the normalized mass median drop size for the center and outer streams was no longer the same.

Figure 6 contains all the known droplet size data for liquid/liquid triplets (except for a few higher velocity tests of Zajac). All of the data in Fig. 6 is from laminar flowing orifices, while most future triplet designs would be flowing turbulent. All of the data was obtained with wax and hot water, so there is no way to evaluate liquid properties effects and, hence, to extrapolate this data to actual propellants. And finally, none of this data includes the very important effects of combustor gas velocity.

The only data available regarding gas/liquid impinging elements was obtained by Mehegan, et. al. (Ref. 55). Two tests were performed with triplets utilizing two wax streams impinging on a central hot, gaseous nitrogen stream. These test conditions also are presented in Table 2.

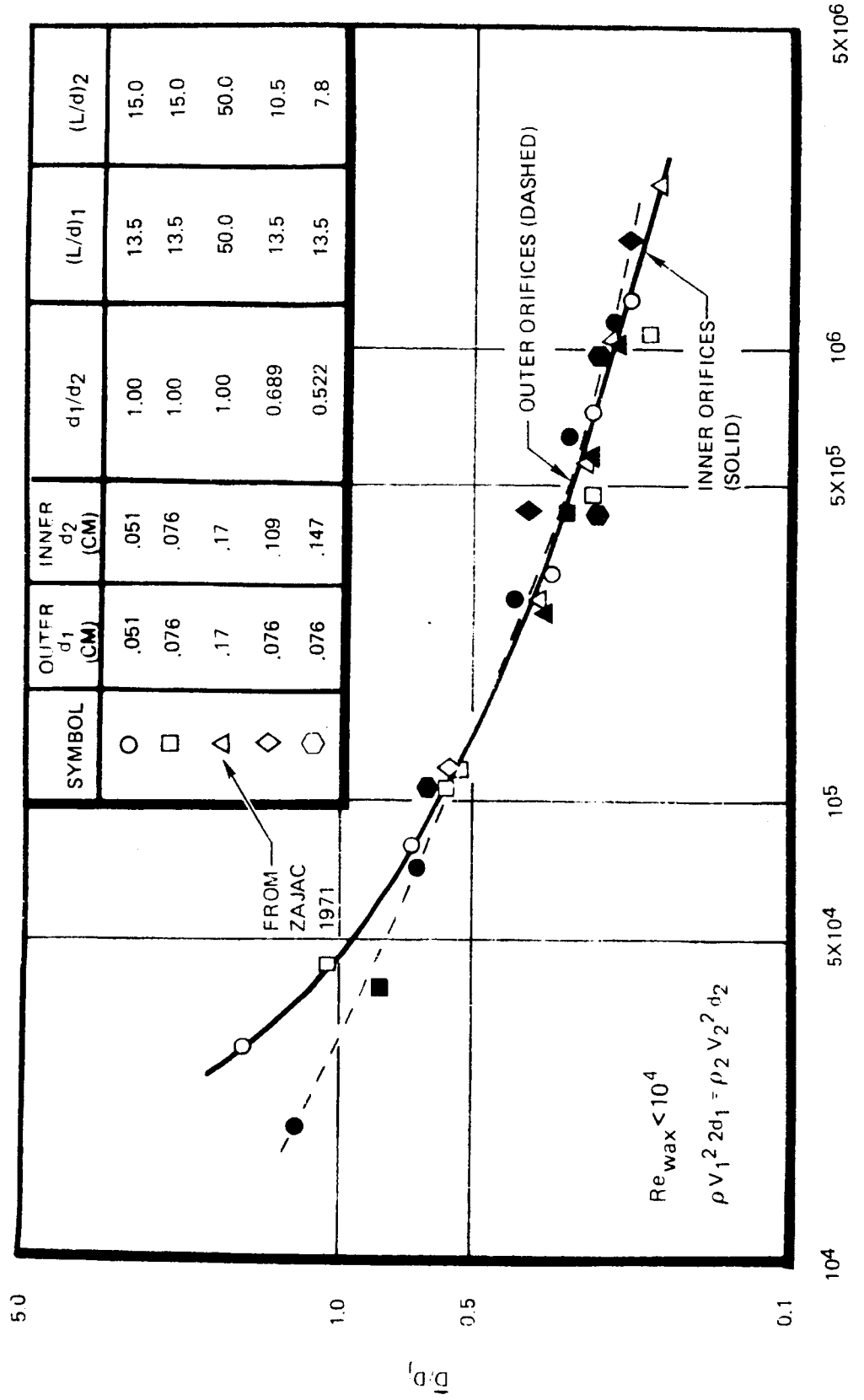

Figure 6. Correlation of Relative Droplet Diameter with Weber Number and Orifice L/d for Triplets (Ref. 74)

Pentad Correlations

The state of the art for pentad atomization knowledge is essentially the same as for triplets. What little data is available was obtained from Rocketdyne wax tests. All of these tests were performed by injection of the propellant simulants into "still" air. The data is synopsized in Table 3.

As a part of Dickerson's (Ref. 47) investigation of injector atomization characteristics, a number of tests were performed on a set of pentad injectors. Droplet size correlating equations were developed relating the mass median drop size to the orifice diameters and injection velocities. Separate equations were obtained for the inner and outer orifices. Wax and hot water were used as the test liquids in a manner similar to the previously discussed triplet tests. In addition, droplet size distribution data were obtained. Normalized volume distribution plots from this work were presented earlier (Fig. 4), and show the different distributions obtained for the center and outer orifices. In addition, the droplet size distribution equations for this data are presented in Ref. 52. As previously discussed, the droplet size correlating and distribution equations presented in Ref. 47 are incorrect, and the equations in this latter paper (Ref. 52) are correct. Dickerson also notes that the quality of the wax spheres was poorer than usual for these pentad tests.

Zajac (Ref. 58) performed a few similar tests and found that the very few higher velocity tests were in crude agreement with the correlations of Dickerson. Most of Zajac's tests were at lower velocities and were in great disagreement with Dickerson's correlating equation (Dickerson did not perform tests at these lower velocities). The deviation at the low velocities is speculated to be due to velocity profile and/or laminar flow effects. Zajac speculates that the flow regime of the outer streams is more important than that of the inner stream.

As a part of the investigation of Mehegan, et. al. (Ref. 55) of gas/liquid injectors, atomization characteristics were determined for a set of pentads. These experiments employed wax and hot gas, with the central orifice always flowing the gas. These tests were performed at atmospheric pressure with variations in gas and liquid velocity and orifice sizes. No correlating equations were developed.

TABLE 3. DROPLET SIZE CORRELATIONS FOR PENTADS

REFERENCE	MEASUREMENT TECHNIQUE	CORRELATION	
DICKERSON (1969)	WAX AND WATER	$\bar{D}_c = 8.26 \times 10^5 \frac{d_c^{.1} d_o^{.12}}{V_c^{.086} V_o^{.89}}$ $\bar{D}_o = 5.66 \times 10^6 \frac{d_o^{.68}}{V_o^{.56} V_c^{.57} d_c^{.35}}$	$\alpha = 30°$ (ANGLE BETWEEN CENTER $\rho_g = 1.1$ kg/m^3 d_o AND d_c = .0635 - .218 cm WAX AND H_2O PROPERTIES
ZAJAC (1971)	WAX AND WATER	AGREES WITH DICKERSON EXCEPT AT LOW V_L (SEPARATE EQUATIONS SHOULD BE DERIVED FOR LAMINAR)	$\rho_g = 1.1$ kg/m^3 $\alpha = 30°$ d_o AND d_c = .16 - .218 cm V_L = 9.14 - 18.3 m/s
MEHEGAN, ET. AL. (1970)	WAX AND N_2 (OR H_e) CENTRAL ORIFICE GAS GAS HEATED >140 F	$\bar{D} \propto (\rho_g V_g^2)^{-\frac{1}{4}}$ $\bar{D} \propto d_o/d_c$ $\bar{D} \propto \frac{X_p}{d_c}$ FOR $\frac{X_p}{d_c} > .8$, OTHERWISE INDEPENDENT MR NOT IMPORTANT LARGER DROPLETS FOR PENTADS THAN TRIPLETS	$\alpha = 45°$ d_c = .66 - 2.1 cm d_o = .17 - .52 cm V_c (GAS) = 183-914 m/s WAX PROPERTIES

SUBSCRIPT:

c = CENTER STREAM
o = OUTER STREAM

ALL d VALUES IN cm
ALL v VALUES IN cm/s

slightly better than that of triplets. At present, there is no way to extrapolate to the actual propellants. Also, there is no data by which to assess the effects of combustion gas motion.

Coaxial Correlations

The standard coaxial injector (gas flowing through the annulus about a central liquid stream) has been studied more extensively than gas/liquid triplets and pentads. Again, all of this work was performed at Rocketdyne utilizing the hot-wax technique. These efforts are synopsized in Table 4.

As a part of the investigation of gas/liquid injectors by Mehegan, et. al. (Ref. 55), a number of tests of the effects of inner tube recess, gas and liquid velocities, and mixture ratio on mass median droplet size were performed. These tests were performed with a large coaxial element. The results of these tests are presented graphically in Fig. 7. Since it is generally believed that the liquid stream breakup is dependent strongly on aerodynamic forces, the velocity difference between the gas and liquid is often of great concern. The effect of inner tube recess also is shown to be of great importance in Fig. 7. A smaller element also was tested, which indicated little effect of recess, but this data was considered questionable. Also, the sizes of the droplets produced by this large injector were quite large.

TABLE 4. DROPLET SIZE CORRELATIONS FOR COAXIAL INJ

REFERENCE	MEASUREMENT TECHNIQUE	CORRELATION		
MEHEGAN, ET. AL. (1970)	WAX AND HOT N_2 SPRAYED INTO ATMOSPHERE	$\bar{D} \propto \frac{1}{R}$ $\bar{D} \propto \frac{1}{V_g V_L}$ $\bar{D} \propto \frac{\dot{W}_L}{\dot{W}_g}$ R = RECESS IN UNITS OF d_L	d_L = CENTER TUBE ID = .704 cm Y = ANNULUS GAP = .259 cm $\frac{\dot{W}_L}{\dot{W}_g}$ = 5.7 - 13.8 V_L = 1.6 - 12.5 m/s	V_g R
BURICK (1972)	WAX AND HOT N_2 SPRAYED INTO PRESSURIZED TANK	INCREASE V_g (BY DECREASING Y AT CONSTANT $\dot{W}_g$) DECREASES $\bar{D}$ GREATLY FOR SMALLER Y INCREASE V_L (BY DECREASING d_L AT CONSTANT $\dot{W}_L$) DECREASES $\bar{D}$	d_L = .177, .274, .345 cm Y = .013, .046, .104 cm $\frac{\dot{W}_L}{\dot{W}_g}$ = 3 - 7.5 V_L = 12.2 - 42.7 m/s	R ρ_g
McHALE AND NURICK (1974)	WAX AND HOT N_2 SPRAYED INTO PRESSURIZED TANK	D/Y DECREASES AS $\rho_g V_g^2$ INCREASES BUT THE EFFECT IS LESS AT HIGHER V_L	ρ_g = .9 - 4.3 kg/m^3 V_L = 1.2 - 16.8 m/s V_g = 91.4 - 305 m/s $\frac{\dot{W}_L}{\dot{W}_g}$ = 6	R d_L Y
FALK (1975)	WAX AND HOT N_2 SPRAYED INTO FLOWING GAS	$\bar{D} \propto V_L$ (CONSTANT d_L) SMALL EFFECT $\bar{D} \propto 1/V_g$ (ESPECIALLY WHEN $V_{CG} = 0$) $\bar{D} \propto \dot{W}_L/\dot{W}_g$ (ESPECIALLY WHEN $V_{CG} = 0$) $\bar{D} \propto 1/L$ (NEGLIGIBLE EFFECT EXCEPT AT LARGE D_o D_o = DROP SIZE WHEN $V_{CG} = 0$	d_L = .14 - .41 cm Y = .25 - 1.45 cm V_g = ANNULUS GAS VELOCITY = 61-305 m/s V_L = 23 - 76 m/s V_{cg} = SIMULATED COMBUSTION GAS MAX VELOCITY = 61-244 m/s L = LENGTH OVER WHICH GAS WAS ACCELERATED = 5-20 cm	$\frac{\dot{W}_L}{\dot{W}_g}$

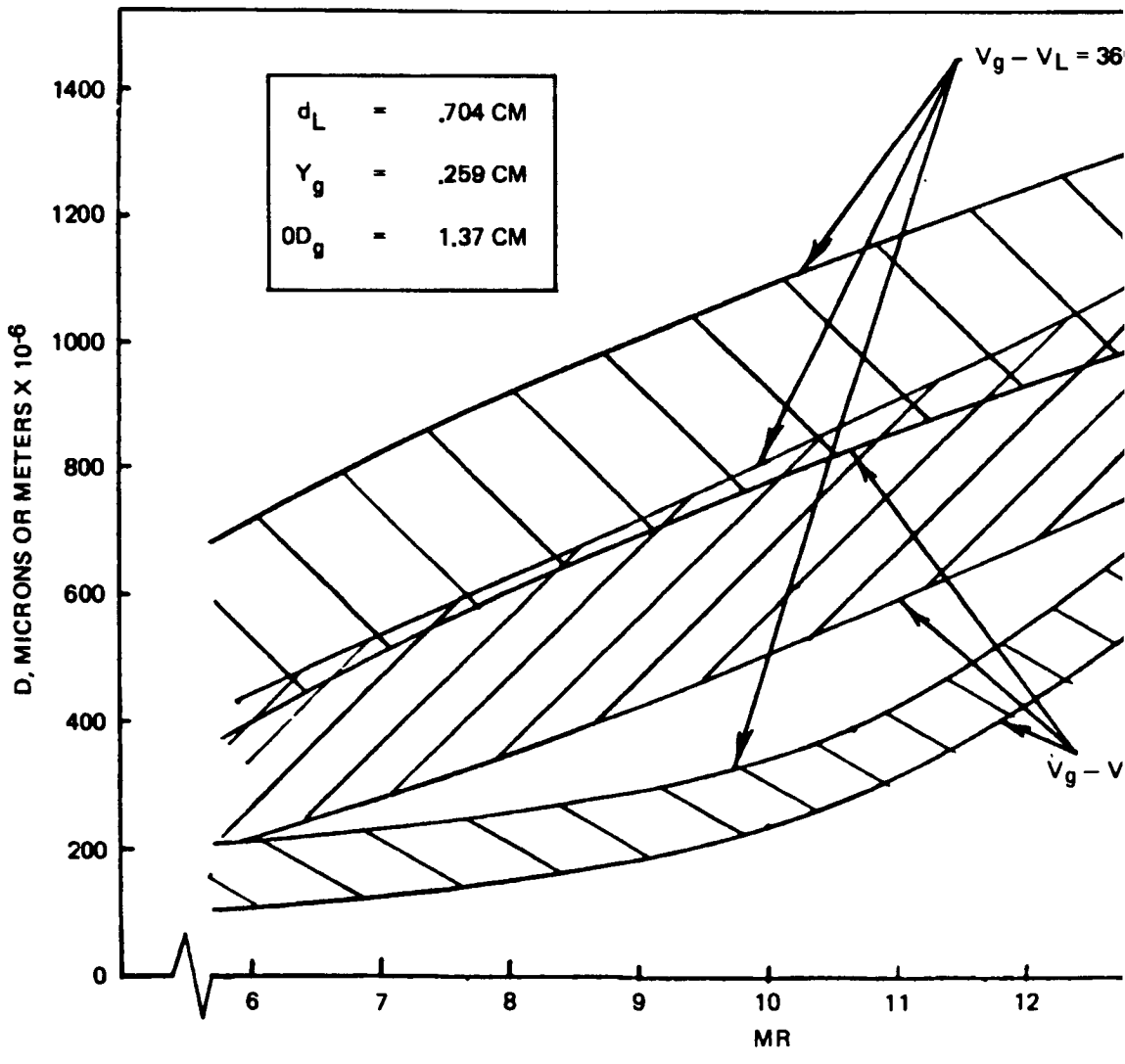

Figure 7. Mixture Ratio Influence on Dropsize for Coaxial Injectors

Investigations by Burick (Ref. 64 and 67) and McHale and Nurick (Ref. 74) utilized hot wax and nitrogen injected into a pressurized chamber to examine coaxial element atomization. The combined work of these two studies, along with the previously discussed work of Mehegan, indicate that recess only reduces D at low pressures and/or for large elements. Burick correlated his data as shown in Fig. 8. Again, the normalization and logarithmic plotting of the data masks the "spread" of the data. Although McHale and Nurick were investigating primarily the atomization characteristics of noncircular orifices, they did perform limited tests on circular orifices. Their data indicates that increased annulus gas dynamic pressure ($\rho_g V_g^2$) reduces droplet size, especially at low liquid velocity. References 67 and 74 present droplet size distribution plots. Although McHale and Nurick state that recess is a major factor influencing droplet size, this conclusion is based upon tests of all of their injectors, which are primarily noncircular. The limited testing performed with circular coaxial elements indicates a 10 to 20% reduction in drop size as recess is increased to $R = d_L$. Even the noncircular elements do not show an effect of recess anywhere near as significant as that found by Mehegan, et. al.

Falk (Ref. 78) investigated the atomization characteristics of coaxial elements injecting wax and hot nitrogen cocurrently (i.e., axially) into a duct flowing hot nitrogen. This work utilized the same test apparatus and techniques as the analagous work of Zajac (Ref. 70 and 71) on like doublets. One potentially very important finding of this work was that the droplet size distribution of these coaxial injectors could be described by the distribution function defined by Zajac for like doublets. Also, the mass median droplet sizes observed in both of these investigations were essentially the same at high relative gas velocity. This would seem to indicate that the manner in which the liquid is broken up (i.e., the type of injector) has no effect on the ultimate droplet size in the presence of a sufficiently accelerating combustion gas. If this is truly the case, it is a most important discovery that will direct the course of future studies of rocket engine injectors.

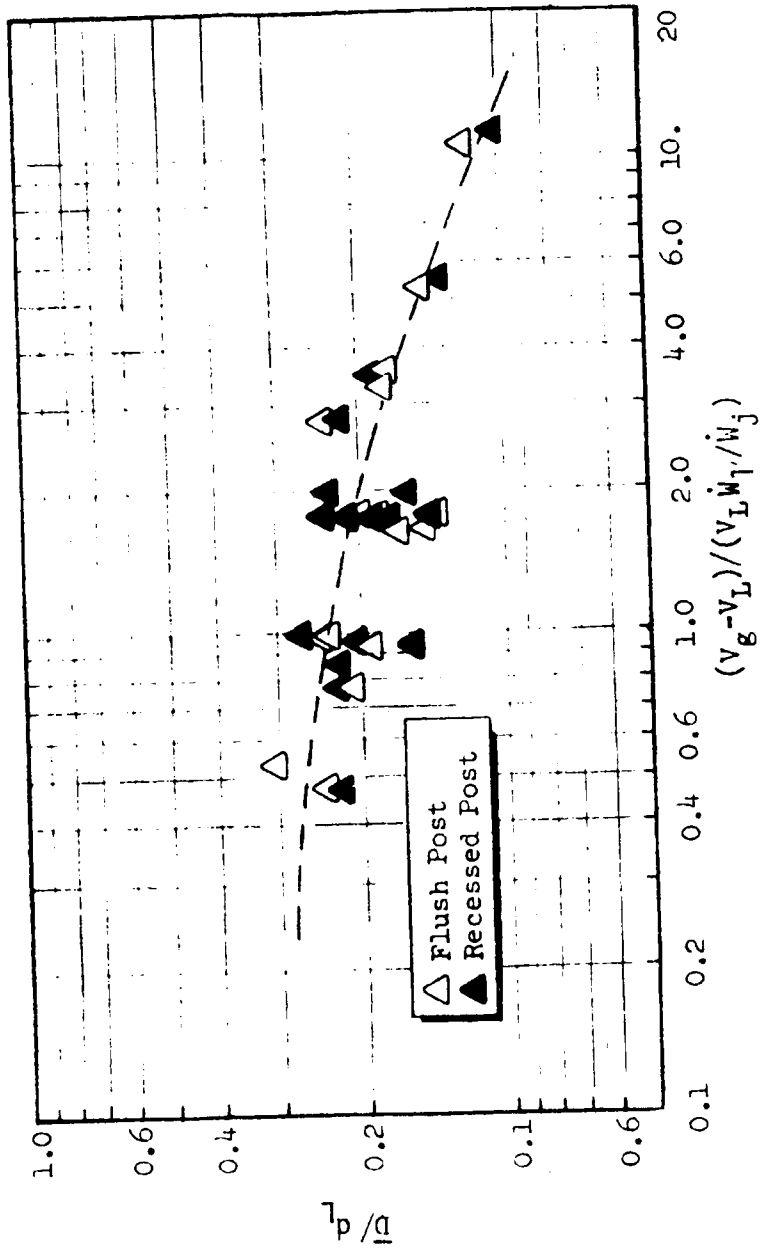

Figure 8. Correlation of Cold-Flow Atomization for Coaxial Injectors (Ref. 67)

Some of Falk's results, showing the effect of simulated combustion velocity on droplet size, are presented in Fig. 9. This data indicates that injectors, which form larger droplets when no combustion gas motion is simulated (i.e., when $V_{cg} = 0$), show more effect of this gas motion than injectors producing smaller droplets. Recognizing this important influence of the relative combustion gas velocity on the droplet size, Falk correlated the data in a manner shown in Fig. 10. This correlation is based only upon the relative, simulated, combustion gas velocity and $\overline{D}_o$, the mass median droplet size produced by an injector in the absence of this gas flow.

ATOMIZATION SURVEY - FINDINGS, CONCLUSIONS, AND RECOMMENDATIONS

The state of the art regarding our knowledge of atomization processes is generally quite poor. The physics is poorly and, at best, only qualitatively understood. Only very rudimentary quantitative theories exist. The available data and correlations are generally of questionable validity and/or utility. Many of the most critical parameters are unknown (e.g., combustion gas velocity field, multiple element effects) and/or are not simulated in tests (e.g., gas densities, real propellant fluid properties, combustion gas motion). This sad state of affairs appears to be attributable to two primary causes: the great complexity of atomization processes, and the inaccuracies, errors, and limitations associated with droplet size measurement techniques. Nevertheless, the available data does provide information regarding the importance and relative effects of a number of variables on droplet size.

Probably the most critical of these parameters affecting droplet size is the combustion gas velocity field. This is unfortunate since the actual velocity field in a rocket combustor, and in atomization experiments, is unknown. Combustion gas velocity also is the one parameter that greatly increases the complexity of the atomization assessment problem. This is due to the fact that atomization is highly dependent on the combustion gas velocity field, and in turn, the combustion gas velocity field is established by the rate of combustion, which is determined by the rate of propellant evaporation, which is highly dependent on how well the propellants are atomized (i.e., initial droplet sizes) and mixed. Thus, all of these problems are coupled and the solution of any one requires at least an approximate solution of each of them.

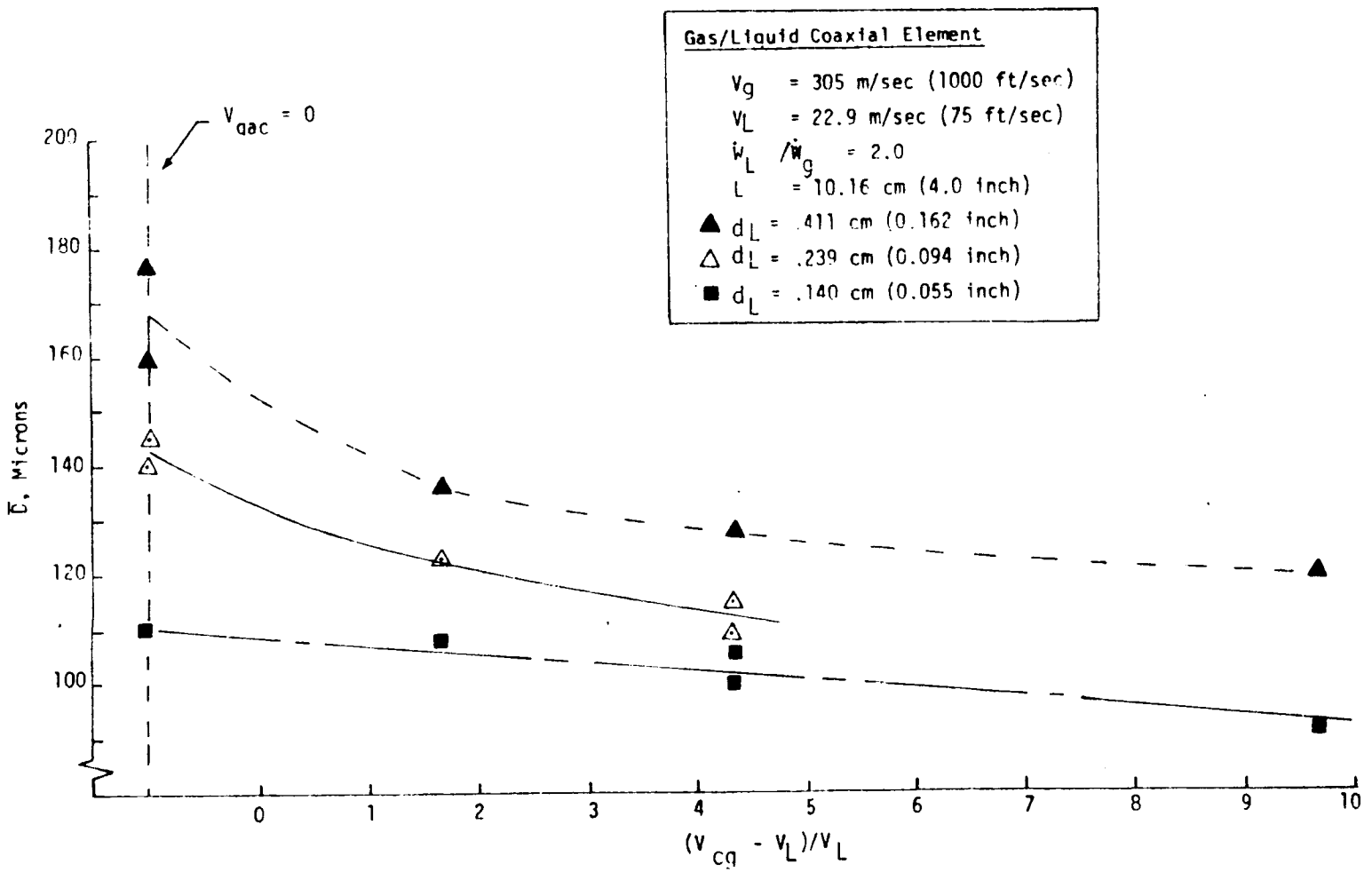

Figure 9. Influence of Combustion Gas Simulant Velocity on Mass Median Dropsize - Coaxial Injectors (Ref. 78)

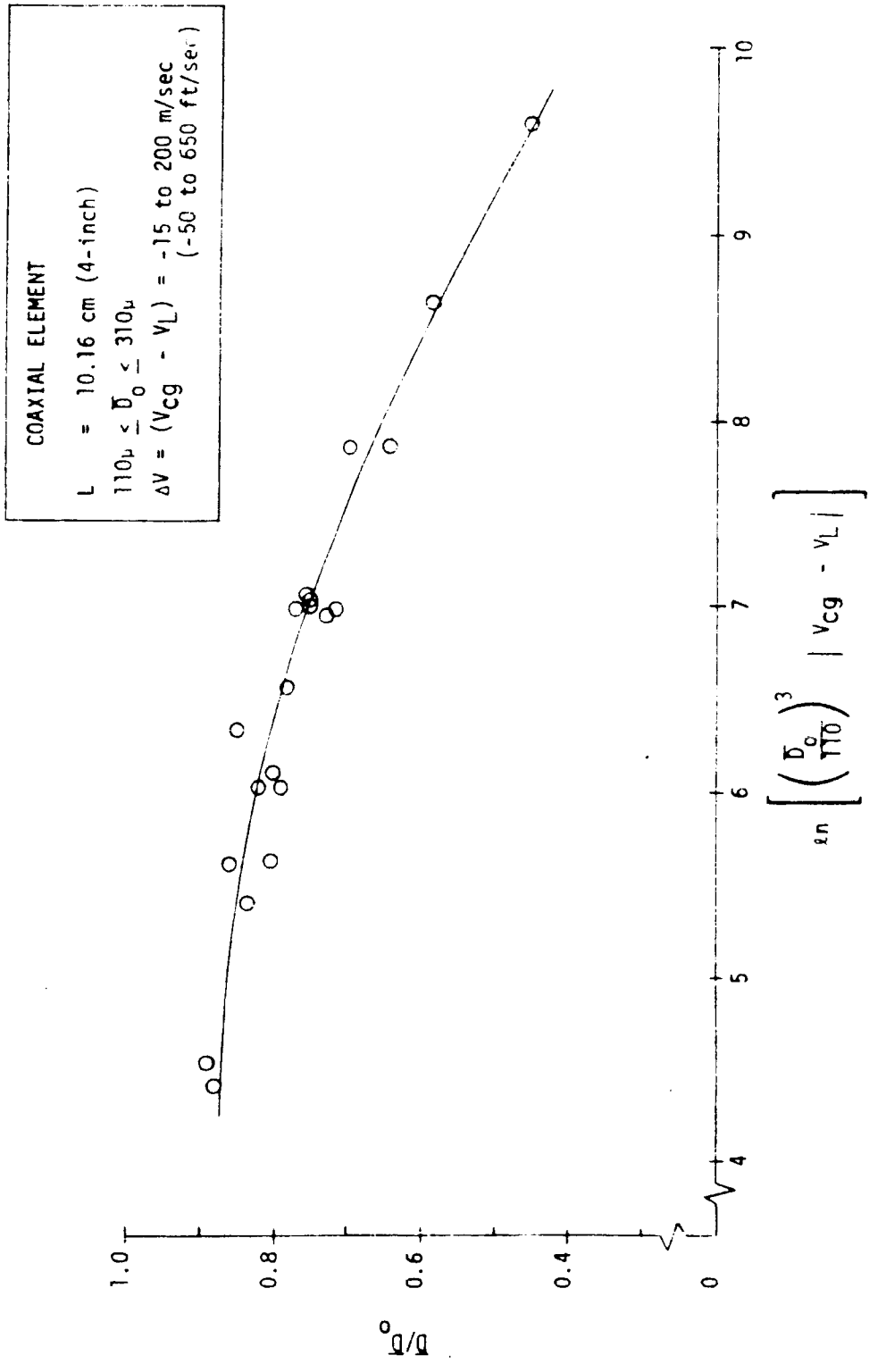

Figure 10. Correlation of Droplet Breakup (Atomization) Data - Coaxial Injectors (Ref. 78)

All of the droplet size measurement techniques applied to atomization studies have serious limitations and potential and/or known sources of error. Imaging techniques measure the spatial concentrations of the various size droplets. Such spatial concentrations can be utilized only rarely to define the actual droplet size distribution or representative droplet size characterizing all of the droplets produced by a given spray (temporal distribution). Spatial and temporal distributions are often quite different. Thus, the photographic techniques and the droplet freezing (i.e., hot wax) technique do not measure the same thing.

In order to utilize cold-flow atomization data, it is necessary to be able to account for the effects of the different liquids' properties on the droplet sizes. The only data available for this purpose applies to like doublets, is of questionable validity and applicability, and differs from one investigation to another. No methods have been proposed to accomplish this properties effects correlation for any gas/liquid injector or for any liquid/liquid injector except like doublets. No attempts have been amde to assess injected fluids properties effects on droplet size distributions.

Very little information could be found regarding the atomization characteristics of triplet, pentad, and coaxial injectors. Such data, as is available, is presented along with a representative sampling of the data for like doublets.

The following actions are recommended for the purpose of (1) improving our knowledge of atomization processes, (2) developing the droplet size data required by the combustor analysis codes, and (3) utilizing the data in such codes. These actions are divided into near and long-term approaches.

Near term: For the most immediate future, it is recommended that droplet size data for combustor analysis be determined in the following manner. First, the existing data can be utilized (it should be verified first, however) and/or tests can be performed to better define $\bar{D}_o$, the droplet size produced in the absence of any simulated combustion gas motion. This can be considered primary atomization. Then the data and correlations of Falk (Ref. 78) and Zajac (Ref. 70 and 71) can be employed to estimate the effect of gas velocity on droplet size. In order to do this it is, of course, necessary to estimate the combustion gas

velocity where the injector is to be employed. This can be accomplished through the use of combustor performance computer codes that generally compute the axial velocity of the gas. Thus, at least the major (hopefully) gas phase velocity component will be estimated. Since the computed axial gas phase velocity will depend on initial droplet sizes, a few iterations of this process may be necessary. That is, the codes can be used to predict V_g, which then can be used to estimate $\bar{D}$, which will be input to the codes to predict a new V_g, etc.

Another problem in the use of cold flow droplet size data is that it is necessary to convert from the test fluids to the real propellants. With great reservation, and only because no better information is available, the properties effects correlations of Ingebo (Ref. 13) or Wolfe and Anderson (Ref. 37) are recommended for this purpose, when liquid, like impinging elements, are being considered.

The method described above provides a rudimentary technique for estimating a representative droplet size. Drop size distributions in general, and representative droplet size information for gas/liquid injectors, cannot be estimated via this technique due to the lack of data regarding combustion gas velocity effects and fluid properties' effects on atomization. Even when applied to the case of like doublets, which have been most extensively studied, this technique may be little better than a consistent guessing method.

In order to better utilize this technique and improve its accuracy the following are recommended:

1. Experiments to investigate gas velocity effects on droplet sizes
2. Additional tests to better define $\bar{D}_o$ for the injectors of greatest interest, especially gas/liquid injectors. Most of the geometric and operational variables have not been tested
3. Experiments to establish fluid properties effects for all types of injectors, like and unlike liquid and gas/liquid injectors, and separate effects for primary and secondary atomization

Such studies and experiments will provide the basis for improvements to atomization assessment methods and will establish the nature, feasibility, and desireability of pursuing the long-term approach.

Long term: As previously discussed, due to the importance of the combustion gas motion on atomization, the problem becomes coupled with those of droplet evaporation, combustion, and three-dimensional fluid mechanics with momentum and mass sources and sinks. Unless some simplifying assumptions are identified earlier, the only available solution would consist of a coupling and solution of all the equations governing these processes. This would probably involve a long-term effort consisting of a number of programs to model (probably with a computer code) various parts of the problem, experimentally verify these models, and combine them in one comprehensive model. Such an approach offers the greatest potential for a comprehensive, accurate, proven solution to the problem of spray definition for rocket engine injectors. If a satisfactory measurement technique exists, experiments with operating, small-scale rocket combustors should be performed to validate the atomization model. In its ultimate form, such a model would include multiple element effects and would predict mixing efficiencies.

NOMENCLATURE

Some atomization nomenclature is defined in text.

A	area (cm^2)
d	injector orifice diameter (cm)
D	droplet diameter (microns)
$\overline{D}$	mass median diameter
$\overline{D}_o$	droplet mass median diameter observed when $V_g = 0$
D_c	droplet mass median diameter observed when $V_g = V_L$
f	droplet distribution function, (drops/micron)

$$f = \lim_{\Delta D \to o} \frac{n}{\Delta D}$$

L	length over which gas is accelerated in atomization studies in accelerating gas flows (cm)
n	number of droplets counted in a given size range
n_t	total number of droplets counted
N	cumulative number distribution,

$$N(D) = \sum_{O}^{D} n$$

$\dot{N}_i$	flowrate of droplets of size group i
ΔP	injector orifice pressure drop (Pascals)
R	normalized cumulative volume distribution, $R = V/V_{tot}$
$\dot{W}$	mass rate of flow (kg/s)
V	velocity (m/s)
V_{gm}	maximum gas velocity
V	cumulative volume distribution,

$$V(D) = \sum_{O}^{D} v$$

v	volume of all drops in a given size range (cm^3)
V_{tot}	total volume of all droplets counted
V_i	velocity of drops of size group i

V_{cg} simulated combustion gas maximum velocity (gas/liquid injectors only)

Y annulus gap for coaxial injectors (cm)

Z axial spatial coordinate

α impingement angle

μ viscosity (cP)

ρ density

ρ_i concentration of drops of size group i (drops/cm^3)

σ surface tension (dynes/cm)

Subscripts

g gas (either local chamber gas or injected gas)

i size group of droplets

j jet or orifice

L large drops

L liquid

s small drops

REFERENCES

1. Longwell, J.P.: "Fuel Oil Atomization," D. Sc. Thesis, MIT, 1943.

2. Hinze, J.: "Critical Speeds and Sizes of Liquid Globules," Appl. Sci. Res., 1948, Vol A1.

3. Lane, W.: "Shattering of Drops in Streams of Air," Industrial & Engineering Chemistry, Chemical Defense Experimental Establishment, England, June 1951, Vol. 43, No. 6.

4. Mugele, R. and H. Evans: "Droplet Size Distributions in Sprays," Industrial & Engineering Chemistry, Chemical Defense Experimental Establishment, England, June 1951, Vol. 43, No. 6.

5. Bowen, I. and G. Davies: "Particle Size Distribution and Estimation of Sauter Mean Diameter," Shell Petroleum Co. (London), October 1951, Report No. I.C.T. 28.

6. Heidmann, M. and J. Humphrey: "Fluctuations in a Spray Formed by Two Impinging Jets," ARS Journal, May-June 1952, Vol. 22, No. 3.

7. Moore, B. and A. Hussman: "Fuel Injection Studies with Impinging Jet Nozzles", Penn State University, October 1955, ONR Contract 656(07), AD 119844.

8. Fraser, R. and P. Eisenklam: "Liquid Atomization and the Drop Size of Sprays," Trans. Instn. Chem. Engrs., 1956, Vol. 34.

9. Tanasawa, Y., S. Sasaki, and N. Nagai: "The Atomization of Liquids by Means of Flat Impingement," Technology Reports of the Tohoku University, 1957, Vol. 22, No. 73.

10. Graves, C. and D. Bahr: "Atomization and Evaporation of Liquid Fuels," Basic Considerations in the Combustion of Hydrocarbon Fuels with Air, NACA Report 1300, Chapter 1, 1957.

11. Putnam, A., et. al.: Injection and Combustion of Liquid Fuels, Battelle Memorial Institute, March 1957, WADC-TR-56-344, AD 118142.

12. Heidmann, M.F., R.J. Priem, and J.C. Humphrey: "A Study of Sprays Formed by Two Impinging Jets," March 1957, NACA TN 3835.

13. Ingebo, R. and H. Foster: "Drop Size Distributins for Crosscurrent Breakup of Liquid Jets in Airstreams," October 1957, NACA TN 4087.

14. Fuhs, A.: "Spray Formation and Breakup and Spray Combustion," February 1958, AFOSR-TN-58-414, AD 158217.

15. Ingebo, R.: "Drop Size Distributions for Impinging Jet Breakup in Airstreams Simulating the Velocity Conditions in Rocket Combustors," March 1958, NACA TN 4222.

16. Weiss M.A. and C.H. Worsham: "Atomization in High-Velocity Airstream," ARS Journal, April 1959.

17. Rossman, T.: "A High-Speed and High-Resolution Photographic Technique for the Observation of Propellants Injected into a Firing Chamber," May 1959, AFOSR-TN-59-8 (2 parts).

18. Benson, G., M.E. Walil, P. Myers, and O. Uyehara: "Fluorescent Technique for Determining the Cross Sectional Drop Size Distributions of Liquid Sprays," ARS Journal, May 1960, Vol. 30, No. 5.

19. Rossman, T.: "Observation of Propellants Injected into a Firing Rocket Chamber," July 1960, AFOSR-TR-60-98.

20. Dykema, O.: "A Study of Injector Geometry by Spray Analysis," Rocketdyne Report 60-19, August 1960.

21. Heidmann, M.: "Photography & Analysis of Time Variation in Drop Size Distribution of a Liquid Spray," Fifth International Congress on High-Speed Photography, Paper N-7, Washington, D.C., October 1960.

22. Taylor, G.: "The Dynamics of Thin Sheets of Fluid," Proceedings of the Royal Society of London, November 1970, Vol. 259 A.

23. Hasson, D and J. Mizrahi: "The Drop Size of Fan Spray Nozzles: Measurements by the Solidifying Wax Method Compared With Those Obtained by Other Sizing Techniques," Trans. Instn. Chem. Engs., Chemical Engineering Department, Technion, Haifa, Israel, 1961, Vol. 39.

24. Ungureanu, C.: "Some Results Concerning the Distribution of Drops of Fuel Atomized Through Low-Pressure Injectors," Rumanian periodical Energetica, 1961, Vol. 4, No. 3, (FTD-TT-63-29/1+2+3+4).

25. Heidmann, M.F. and H. Foster: "Effect of Impingement Angle on Drop Size Distributions and the Spray Pattern of Two Impinging Water Jets," July 1961, NASA TN D-872.

26. Ingebo, R.: "Size Distribution and Velocity of Ethanol Drops in a Rocket Combustor Burning Ethanol and Liquid Oxygen," ARS Journal, April 1961, (also see NASA-TN-D-290, June 1960).

27. Popov, M.: "Model Experiments on the Atomization of Liquids," NASA TT-F-65, July 1961.

28. Fraser, R.: "Liquid Atomization," Journal of Royal Aeronautical Society, Imperial College, London, November 1961, Vol. 65.

29. Weiss, M. and C. Worsham: "Nozzle Sprays in Air Streams," Chemical Engineering Science, Esso Research & Engineering Co., New Jersey, December 1961, Vol. 16, No. 1 and 2.

30. Lewis, J.: "Studies of Atomization and Injection Processes in the Liquid Propellant Rocket Engine," Rocket Propulsion Establishment TM No. 241, Westcott, Great Britain, December 1961.

31. Lambris, S., L. Combs, and R. Levine: "Stable Combustion Processes in Liquid Propellant Rocket Engines," 5th Colloquim of the Combustion and Propulsion Panel, 1962, NATO, AD 283525.

32. Dombrowski, N. and P. Hooper: "The Effect of Ambient Density on Drop Formation in Sprays," Chemical Engineering Science, Imperial College, London, 1962, Vol. 17.

33. Dombrowski, N. and P. Hooper: "The Performance of Characteristics of an Impinging Jet Atomizer in Atmospheres of High Ambient Density," Fuel, 1962, Vol. 41.

34. Fraser, R., P. Eisenklam, N. Dombrowski and D. Hasson: "Drop Formation from Rapidly Moving Liquid Sheets," A. I. Ch. E. Journal, Imperial College, London, November 1962, Vol. 8, No. 5.

35. Dombrowski, N. and P. Johns: "The Aerodynamic Instability and Disintegration of Viscous Liquid Sheets," Chemical Engineering Science, Imperial College, London, 1963, Vol. 18.

36. Brown, R. and K. Leonard: "Methods of Describing Droplet Size Distributions from Atomized Solutions," Aerojet Report 0395-04(15) SP, AD 434106, March 1964.

37. Wolfe, H. and W. Anderson: "Kinetics, Mechanism, and Resultant Droplet Sizes of the Aerodynamic Breakup of Liquid Drops," Aerojet General Report 0394-09(18)SP, AD 437340, April 1964.

38. Brown, R.E.: "The Atomization of a Solution of 2, 4 - Dihydrobenzophenone in Bis (2 Ethylhexyl) Hydrogen Phosphate," Aerojet General Report 0395-04(20)SP, AD601462, May 1964.

39. Clark, R.: "Breakup of a Liquid Jet in a Transverse Flow of a Gas," August 1964, NASA TN D-2424.

40. Dombrowski, N. and P. Hooper: "A Study of the Sprays Formed by Impinging Jets in Laminar and Turbulent Flow," Journal of Fluid Mechanics, 1964, Vol. 18, Part 3.

41. Lewis, J.: "Some Basic Studies of Liquid Propellant Injection Processes,: Journal of the Royal Aeronautical Society, Rocket Propulsion Establishment, England, November 1964, Vol. 68.

42. Lapple, C., J. Henry and D. Blake: "Atomization - A Survey and Critique of the Literature," Stanford Research Inst., Report No. 6, April 1967, AD 821314.

43. Luna, R. and W. Klikoff: "On Aerodynamic Breakup of Liquid Drops," Sandia Laboratories Research Report SC-RR-66-2716, June 1967.

44. Hiroyasu, H.: "Mathematical Expressions for Drop Size Distribution in Sprays," NASA-CR-72272, November 1967.

45. Dombrowski, N. and G. Munday: "Spray Drying," Biochemical and Biological Engineering Science, Academic Press, 1968, Chapter 16.

46. Adelberg, M.: "Mean Drop Size Resulting From the Injection of a Liquid Jet into a High-Speed Gas," AIAA Journal, June 1968, Vol. 6, No. 6.

47. Dickerson, R., K. Tate, and N. Barsic: "Correlation of Spray Injector Parameters with Rocket Engine Performance," Rocketdyne Report R-7499, AFRPL-TR-68-147, June 1968.

48. Sloat, T.: "Dropsize Measurements with Large Thrust Coaxial and Triplet Elements," Rocketdyne Internal Letter IC69-344 24, June 1969.

49. Ingebo, R.: "Maximum Drop Diameters for the Atomization of Liquid Jets Injected Cocurrently Into Accelerating or Decelerating Gas Streams," NASA-TN-D-4640, July 1968.

50. Knight and Nurick: "Interim Report, Correlation of Spray Dropsize Distribution and Injector Variables," Rocketdyne Report R-7995, September 1969.

51. Sloat, T. and D. Campbell: "Atomization Characteristics of Gas/Liquid Injectors," 6th Liquid Propellant Combustion Instability Conference, Chicago, September 1969.

52. Dickerson, R.: "Like and Unlike Impinging Injection Element Droplet Sizes," J. Spacecraft, November 1969, Vol. 6, No. 11.

53. Walkden, A. and R. Kell: "Characteristics of High-Flux Sprays From Colliding Water Jets," Trans. Instn. Chem. Engrs., General Electric Co., Wimbly, Middlesex, England, 1969, Vol. 49.

54. Kuykendal, W.: "The Effect of Injector Design Variables on Average Drop Size for Impinging Jets," AFRPL-TR-70-53, May 1970.

55. Mehegan, P., D. Campbell, and C. Scheuerman: "Investigation of Gas Augmented Injectors," Rocketdyne Report R-8361, NASA-CR-72703, September 1970.

56. Nurick, W. and R. McHale: "Noncircular Orifice Holes and Advanced Fabrication Techniques for Liquid Rocket Injectors," Rocketdyne Report R-8224, NASA-CR-108570, September 1970.

57. Huang, J.: "The Breakup of Axisymmetric Liquid Sheets," J. Fluid Mech, 1970, Vol. 43, Part 2.

58. Zajac, L.: "Correlation of Spray Dropsize Distribution and Injector Variables," Rocketdyne Report R-8455, Contract NAS7-726, February 1971.

59. Kim, K. and W. Marshall: "Drop Size Distributions From Pneumatic Atomizers," A. I. Ch. E. Journal, University of Wisconsin, May 1971, Vol. 17, No. 3.

60. Nurick, W.: "Analysis of Sprays From Rocket Engine Injectors," Journal of Spacecraft and Rockets, Rocketdyne, July 1971, Vol. 8, No. 7.

61. Zajac, L. and W. Nurick: "Correlation of Spray Dropsize and Injector Variables," 8th JANNAF Instability Conference, October 1971.

62. Simpkins, P. and E. Bales: "Water Drop Response to Sudden Accelerations,: Journal of Fluid Mech., Bell Labs & Stevens Inst. Tech., 1972, Vol. 55, Part 4.

63. Combs, L.: "Catalog of Injector Spray Correlations," Rocketdyne, NASA Contract NAS7-746, 1972.

64. Burick, R.: "Atomization and Mixing Characteristics of Gas/Liquid Coaxial Injector Elements," Journal of Spacecraft, May 1972, Vol. 9, No. 5.

65. Nurick, W.: "Study of Spray Disintegration in Accelerating Flow Fluids," Rocketdyne Report R-9017, NASA-CR-114479, June 1972.

66. George, D. and F. Spaid: "Holography As Applied to Jet Breakup & An Analytical Method for Reducing Holographic Droplet Data," AFRPL-TR-72-72, September 1972.

67. Burick, R.: "Space Storable Propellant Performance Program Coaxial Injector Characterization," Rocketdyne Report R-8973-2, NASA-CR-120936, October 1972.

68. Falk, A.: "Space Storable Propellant Performance Gas/Liquid Like Doublet Injector Characterization," Rocketdyne Report R-8973-1, NASA-CR-120935, October 1972.

69. Nurick, W.: "Physical Property Effects on Spray Atomization," Rocketdyne IR&D Report ITR-73-014-C, September 1973.

70. Zajac, L.: "Droplet Breakup in Accelerating Gas Flow, (Primary Atomization)," Part 1, Rocketdyne Report R-9337-1, NASA-CR-134478, October 1973.

71. Zajac, L.: "Droplet Breakup in Accelerating Gas Flows (Secondary Atomization)," Part 2, Rocketdyne Report R-9337-2, NASA-CR-134479, October 1973.

72. George, D.: "Rocket Injector Hot-Firing and Cold-Flow Spray Fields," AIAA/SAE 9th Propulsion Conference, Las Vegas, November 1973.

73. George, D.: "Rocket Injector Hot-Firing and Cold-Flow Spray Fields," 10th JANNAF Combustion Meet, December 1973, CPIA No. 243, Vol. 3.

74. McHale, R. and W. Nurick: "Noncircular Orifice Holes and Advanced Fabrication Techniques for Liquid Rocket Injectors (Phases I, II, III, & IV)," Rocketdyne NASA CR-R-9271, May 1974.

75. Buschulte, W.: "Liquid Propellant Atomization by Injector Elements and Its Effects on Combustion Chamber Efficiency," Israel Journal of Technology, 1974, Vol. 12.

76. George, D.: "Droplet Size Distribution Functions For Rocket Combustor Spray Fields," 11th JANNAF Combustion Meet, December 1974, CPIA No. 261.

77. Anon: "Analysis of Rocket Engine Injection/Combustion Processes," Rocketdyne Report R-9668P-1, March 1975.

78. Falk, A.: "Coaxial Spray Atomization in Accelerating Gas Stream, Final Report," Rocketdyne Report R-9753, NASA-CR-134825, June 1975.

79. Rizkalla, A. and A. Lefebvre: "The Influence of Air and Liquid Properties on Airblast Atomization," Journal of Fluids Engineering, Cranfield Inst. Tech., Trans ASME, September 1975.

80. Rao, K. and A. Lefebvre: "Fuel Atomization in a Flowing Airstream," AIAA Journal, October 1975, Vol. 13, No. 10.

81. Farmer, W.: "BRL Particle Sizing Interferometer," University of Tennessee Space Institute, Tullahoma, Tenn., circa 1980.

82. Lefebvre, A.: "Airblast Atomization," Prog. Energy Combustion Science, Purdue University, 1980.

83. Elkotb, M.: "Fuel Atomization for Spray Modeling," Progress in Energy & Combustion Science, Cairo University, 1982, Vol. 8, No. 1.

84. Ferrenberg, A.: "Liquid Rocket Injector Atomization Research," Proceedings of ASTM Symposium on Liquid Particle Size Measurement Techniques, Kansas City, June 1983.

Cold flow mixing tests frequently have proven to be a significant aid in predicting potential performance, or diagnosing problems with rocket engine injector components. Cold flow tests are not sufficiently reliable so as to serve as a replacement for hot-fire testing, but should be considered as complementary to hot-fire tests, aiding in minimizing the number of hot-fire tests required to obtain an optimum configuration. In almost every case, an injector or element that performs poorly in cold flow testing will not perform well in hot-fire testing. However, the counter side of this statement cannot be applied universally. An element can be excellent in cold flow mixing, but the combustion reaction may override the hydromechnical mixing provided by the injection streams. This effect is most notable with storable hypergolic propellants, where a phenomena of reactive demixing "blowapart" is frequently a significant factor in combustion performance. There have been other reports of combustion systems suffering from reactive demixing, but none have been as well documented as the hypergolic reaction systems.

Aerodynamic forces in the combustion zone also are factors that cannot be simulated in cold flow mixing tests. Gas forces in recirculation can be strong factors influencing mixing and atomization. There are, however, useful correlations between cold flow mixing and combustion results, and the relative cost factor between cold flow and hot-fire tests generally is a rational reason for utilizing cold flow tests as an injector design and development tool.

The key objective, to establish correlations between cold flow mixing data and hot-fire results, requires a large empirical data base as well as a consistent assessment of the data and an applied scientific evaluation of the resultant correlating parameters. Therefore, an assessment criteria was established, which allowed compilation of existing cold flow experimental data acquired within the industry on element types suitable for LOX/hydrocarbon injector advancement.

The triplet, pentad, and coaxial element injection devices were selected for study based on available hotfire and cold flow experience with LOX/hydrocarbon

propellants. The cold flow correlating parameters used for these devices were identified and an extensive literature survey conducted to obtain related cold flow data. Data from the literature search was compiled into a displayable format. The information then was plotted by the appropriate correlating parameter(s) against mixing efficiency, a standard measure of cold flow performance.

In addition to the literature survey, five impinging triplet elements, one pentad element, and three coaxial elements were fabricated for cold flow testing. The sizing of these elements encompassed designs for both preburner (gas generator) and main injector mixture ratios at high chamber pressure. The propellant combinations were LOX/methane (gas/liquid), LOX/RP-1 (liquid/liquid), and LOX/propane (liquid/liquid and gas/liquid). The low-pressure cold flow mixing test program was conducted with these elements at several flow conditions. Measures of mixing efficiency were established and plotted as a function of mixing parameters. Maps depicting mixture ratio-normalized mass distribution were constructed from the cold flow tests to provide a good visual indication of relative mass and mixture ratio concentrations for the different element types.

INJECTOR MIXING CORRELATING PARAMETERS

Mixing correlation parameters are mathematical expressions based upon injector element geometry and flow conditions. Their utility as injector design criteria depends upon (1) their ability to be related to mixing efficiency and (2) the existence of optimum values of these correlation parameters at which mixing will be maximized.

Numerous correlating parameters have been proposed for different injector configurations, propellant conditions, and hot fire related operating conditions. The scientific basis for the parameters generally has been derived from momentum and stream diameter relationships of the injection element. A survey of available literature showed that of these relationships, most correlating parameters were derived for liquid/liquid impinging-type injectors. Many of the experimenters have established formulas to plot data from numerous test conditions on a single curve, or at least, within a family of curves.

The correlating parameters used in the literature survey data reduction and in the subsequent low-pressure mixing tests are presented in Table 5. A description of these important parameters is discussed below. Illustrations of the three element types studied under this program (coaxial concentric tube, triplet, and pentad) are presented in Fig. 11 through 12, with the appropriate terminology and physical parameters identified.

Rupe Factor/Rupe Number

The best example of an injector correlating parameter for mixing criteria is the Rupe Factor, or Rupe Number, developed for use on unlike impinging doublets elements. This basic expression (Eq. 2) primarily was developed in the '50s by its namesake, Jack Rupe of Jet Propulsion Lab (JPL). He ran a great number of cold flow mixing tests and conducted related hot fire experiments. Applying stream momentum and diameter ratios, he developed an expression, since referred to as the "Rupe Factor," which indicated the best mixing when it equalled unity. This parameter also can be expressed as the diameter ratio over the momentum ratio. Since this expression is a ratio, the mathematical range of this factor from zero to one is the same as from one to infinity, which is difficult to interpret. For this reason, the expression has been revised to the "Rupe Number" (Eq. 3), which has a total range from zero to one and an optimum value of 0.5.

This expression has been utilized widely for sizing of unlike doublets and has demonstrated good correlation over a wide range of conditions. This does not mean that a Rupe number of 0.58 reflects a certain quantitative level of mixing efficiency, but that in sizing an element for a given design, mixing, for most cases, optimizes very near the 0.5 value.

Momentum Ratio

Other element types have been analyzed in a similar manner as the Rupe Number, and modified momentum/diameter relationship expressions have been derived for triplet and pentad impinging element patterns. These parameters are based on more limited cold flow data and virtually no hot fire data, and should be used more cautiously in universal application than the doublet expressions.

TABLE 5. INJECTOR ELEMENT CORRELATING PARAMETERS

PARAMETER	COMMON APPLICATION	EXPRESSION	OPTIMUM VALUE
• MOMENTUM RATIO	IMPINGING ELEMENTS	$\frac{\rho_{FU} A_{FU}}{\rho_{ox} A_{ox}} \left(\frac{\dot{m}_{ox}}{\dot{m}_{fu}}\right)^2$ (1)	NONE
• RUPE FACTOR	UNLIKE IMPINGING DOUBLET ELEMENTS, LIQUID/LIQUID	$\frac{\dot{m}_{FU} V_{FU} D_{ox}}{\dot{m}_{ox} V_{ox} D_{FU}}$ (2)	1
• RUPE NUMBER		$\frac{1}{1 + \text{RUPE FACTOR}}$ (3)	0.5
• [illegible] - MOREY CRITERIA	IMPINGING TRIPLET ELEMENTS, LIQUID/LIQUID	$\left(\frac{\dot{m}_{out}}{\dot{m}_{in}}\right)^2 \left(\frac{\dot{m}_{in}}{\dot{m}_{out}}\right) \left(\frac{A_{in}}{A_{out}}\right)^{1.75}$ (4)	0.66
	IMPINGING PENTAD ELEMENTS, LIQUID/LIQUID	$\left(\frac{\dot{m}_{out}}{\dot{m}_{in}}\right)^2 \left(\frac{\dot{m}_{in}}{\dot{m}_{out}}\right) \left(\frac{A_{in}}{A_{out}}\right)^{1.25}$ (5)	1.22
• [illegible]	IMPINGING ELEMENTS, GAS/ LIQUID, CENTRAL GAS STREAM	[illegible] $\left(\frac{\dot{m}_{out}}{\dot{m}_{in}}\right) \left(\frac{\dot{m}_{in}}{\dot{m}_{out}}\right)^5 \left(\frac{D_{in}}{D_{out}}\right)^3$ (6)	0.5
• VELOCITY HEAD RATIO	GAS/LIQUID, LIQUID/LIQUID IMPINGING AND COAXIAL ELEMENTS	$\frac{\rho_{FU}}{\rho_{ox}} \left(\frac{A_{FU} \dot{m}_{ox}}{A_{ox} \dot{m}_{FU}}\right)^2$ (7)	1
• COAX PARAMETER	COAXIAL CONCENTRIC TUBE ELEMENTS, GAS/LIQUID	$\frac{(\rho_g V_g)^2}{MR\ V_l}$ (8)	?

LEGEND

VARIABLES

$\dot{m}$ = MASS FLOW RATE, Kg/SEC

V = VELOCITY, M/SEC

A = ELEMENT DISCH FLOW AREA, M^2

D = ELEMENT HOLE DIA, M

ρ = PROPELLANT DENSITY, Kg/M^3

MR = MASS MIXTURE RATIO, OXID/FUEL

θ = VERTICAL ANGLE BETWEEN INNER AND OUTER STREAMS, DEGREES

SUBSCRIPTS

ox = OXIDIZER

FU = FUEL

g = GAS

L = LIQUID

in = INSIDE OR CENTRAL ORIFICE

out = OUTER ORIFICES

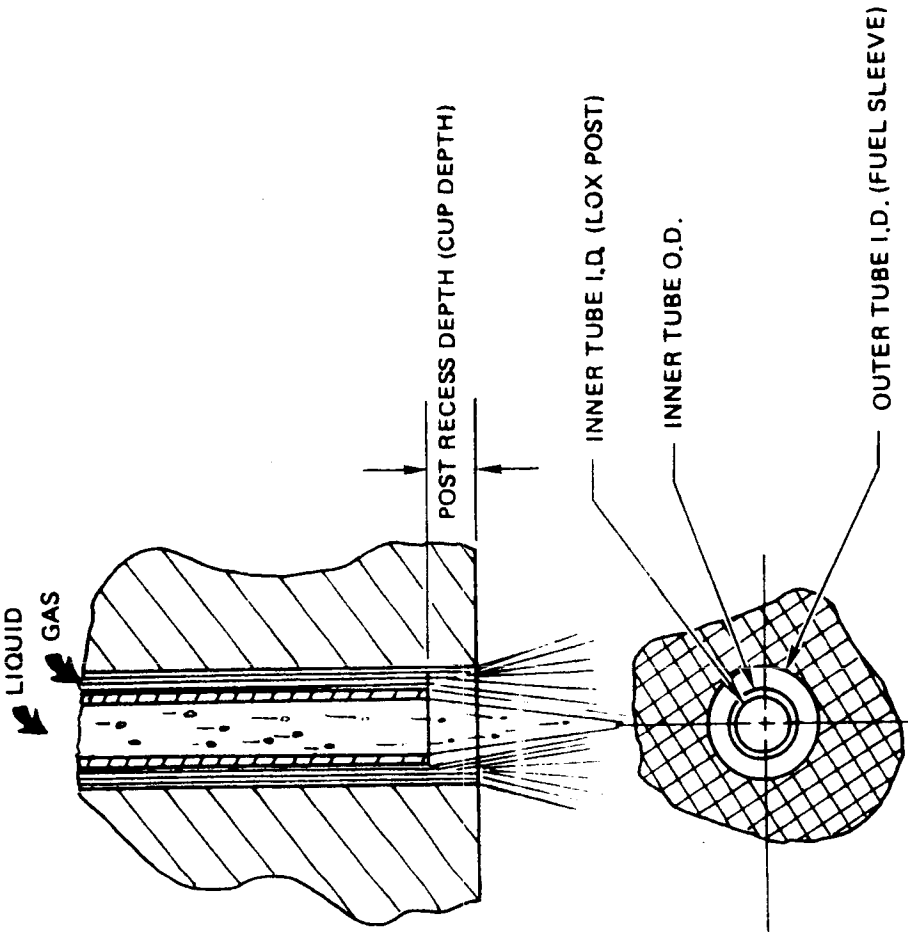

Figure 11. Coaxial Concentric Element

Figure 12. Impinging Triplet and Pentad Elements

As previously mentioned, the primary root for almost all impinging element mixing parameters is the momentum ratio. As a general rule, the momentum ratio always is expressed as the oxidizer total momentum over the fuel total momentum regardless of the number or placement of oxidizer streams relative to fuel streams within the element. Relating this ratio to the values available to the designer, we have the form of momentum ratio as shown in Table 5, (Eq. 1). There is no design optimum for this parameter and, again, this is a ratio with theoretical values from zero to infinity, where values over one indicate that the oxidizer has higher momentum than the fuel.

Elverum-Morey Factor

The equivalent of the Rupe Factor for triplet and pentad elements was developed by Rupe's colleages, Elverum and Morey, and is based also on momentum/diameter (area) relationships as shown in Table 5, (Eq. 4). For the triplet element, with two outer angled streams and a central axial stream, the relationships are set as inner and outer streams rather than oxidizer and fuel streams, since both fuel-oxidizer-fuel and oxidizer-fuel-oxidizer triplets are in general use.

For liquid/liquid triplets, within the range of study by Elverum and Morey, the optimum value for this expression was 0.66. Triplet injectors have been used most commonly for hypergolic storable propellants, and use of the Elverum-Morey Factor has been successful under these conditions. For the nominal mixture ratio of liquid oxygen and liquid hydrocarbons*, very little data has been available. A modified Elverum-Morey expression, Table 5 (Eq. 5), was designed for pentads and has a purported optimum value of 2.75.

*The typical mixture ratio for storable propellant combinations, such as NTO/MMH or UDMH/IRFNA, is between 1.5 and 2.5 ox/fu for main injector operation. The mixture ratio for liquid/liquid LOX/hydrocarbon propellants, i.e., RP-1/LOX, is optimum near 2.8 ox/fu for main injector maximum Isp, and near 0.4 ox/fu for fuel-rich preburner (turbine drive combustor) applications.

Penetration Factor

This parameter has been developed for gas/liquid triplet injectors where two liquid streams impinge on a central gas stream. It relates the predicted penetration of the liquid streams to the central gas flow. Optimum mixing is predicted if the liquids barely penetrate to the center, with liquid droplets being sheared off and entrained by the gas flow on the way. The penetration factor is presented in Table 5, (Eq. 6).

A value of 0.5 is the theoretical optimum. Lower numbers infer that the liquid is being deflected away by the gas or is not fully penetrating the gas stream. Over penetration, on the other hand, produces a liquid fan within the gas flow, which also reduces the uniformity of gas/liquid mixing. This factor was created from a combination of analysis and cold flow experiments, and hot fire data appears to support the basic premise. Pentads and other impinging patterns with liquid streams impinging on a central gas core also would be expected to correlate with some form of the penetration parameter. However, data is limited for these applications.

The use of this factor for the reverse case of gas streams impinging on a central liquid, or any other extremes in the density relationships, is questionable. Triplets with the gaseous reactant in the outer streams have been used in numerous cases, but there is little data on any correlating parameters. Some limited information suggests that high levels of gas to liquid momentum ratio are beneficial to the mixing process in impinging element injectors.

Velocity Head Ratio

Another parameter that does not have a stated optimum value is the velocity head ratio shown in Table 5 (Eq. 7). This roughly relates to the very practical

consideration of "Delta P" ratio, or pressure drop ratio. The usual starting point in an injector design is based on the desired level of pressure drop at the design flowrates. Isolation between feed system and chamber pressure disturbances generally dictates a desire for a high level of injection orifice pressure drop, and system pressure limitations would like a low pressure drop. A compromise solution usually results in an injector delta P of about 15 to 20% of chamber pressure, and an initial starting point would be for both oxidizer and fuel systems to be roughly the same value. Therefore, an injector design that has velocity head ratios significantly distant from 1 would require some compensation in design approach (i.e., supplementary orifices, etc.).

As mentioned previously, there is no theoretical optimum for the velocity head ratio, but the values close to 1 are desirable for system integration. Many times, sizing the injection orifices to optimize one of the other parameters will result in an unacceptable level of velocity head ratio. For this reason, the velocity head ratio should be computed at the same time as the other parameters, and evaluated and adjusted concurrently.

Coaxial Parameter

The gas/liquid coaxial concentric tube injector element has had wide, successful usage for hydrogen/oxygen combustion. Cold flow and hot fire experience with this element still has not provided a good correlating parameter. In this element, typical design practice has been to provide a low-velocity central liquid stream (liquid oxygen) sheathed by a high-velocity gas flow (gaseous hydrogen or fuel-rich preburner gases) as shown in Fig. 11. Mixing and atomization are provided primarily by the shear forces between gas and liquid and by the momentum of the expanding gases.

Recessing the liquid stream upstream of the exit plane of the outer (gas) stream is popularly held to increase both atomization and mixing. Cold flow testing has not established a strong correlation with this practice, although hot fire results generally reflect a performance increase that usually is accompanied by an increase in face heating.

Increasing the gas velocity (relative to the liquid velocity) generally improves mixing. This design approach should not be employed blindly, since some references suggest that mixing can be impacted adversely by velocity ratios that are too high. This would tend to suggest that some correlating parameter for optimization may be possible. Very high gas velocity apparently can reverse the gas liquid relationship, "blowing out" the center of the spray and dispersing excess liquid to the outside of the spray cone.

A review of existing data, as a part of this effort, indicates trends that may be useful for providing a general optimizing expression for the coax element. Falk and Nurick of Rocketdyne (NASA CR-72703 R-8361) have suggested the coaxial parameter presented in Table 5, (Eq. 8). However, no optimum value of this parameter has been established. One of the objectives of the remainder of this program is the establishment of a coaxial element mixing parameter.

MIXING TEST METHODS

Liquid/Liquid Mixing Test Methods

The liquid/liquid testing for mixing efficiency is relatively easy and low cost, if facilities are available. The procedure for liquid/liquid mixing utilizes a grid-like sample device, which ducts the individual position captured liquid into an appropriate sample container (Fig. 13a). This technique utilizes two immiscible liquids as propellant simulants, typically water and a high-density, low-vapor pressure solvent such as 1,1,1-trichloroethane. The fluids collected in the sample tubes separate by the variation of density and their quantities in each tube are measured (Fig. 13b). Typically, the sample grid represents hundreds of data points, and a computer data reduction process is required to provide meaningful quantitative data.

Different fluid combinations have been employed for liquid/liquid mixing in an effort to better match injected reactant conditions, while addressing concerns for toxicity, flammability, and general questions of safety, convenience, and cost. Other solvents used for these purposes have included many of the lower

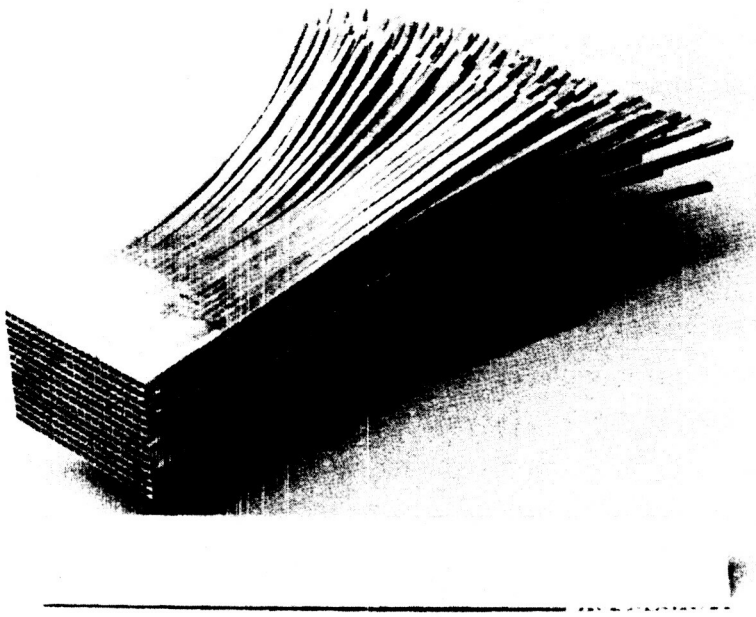

a. Square Tube Assembly

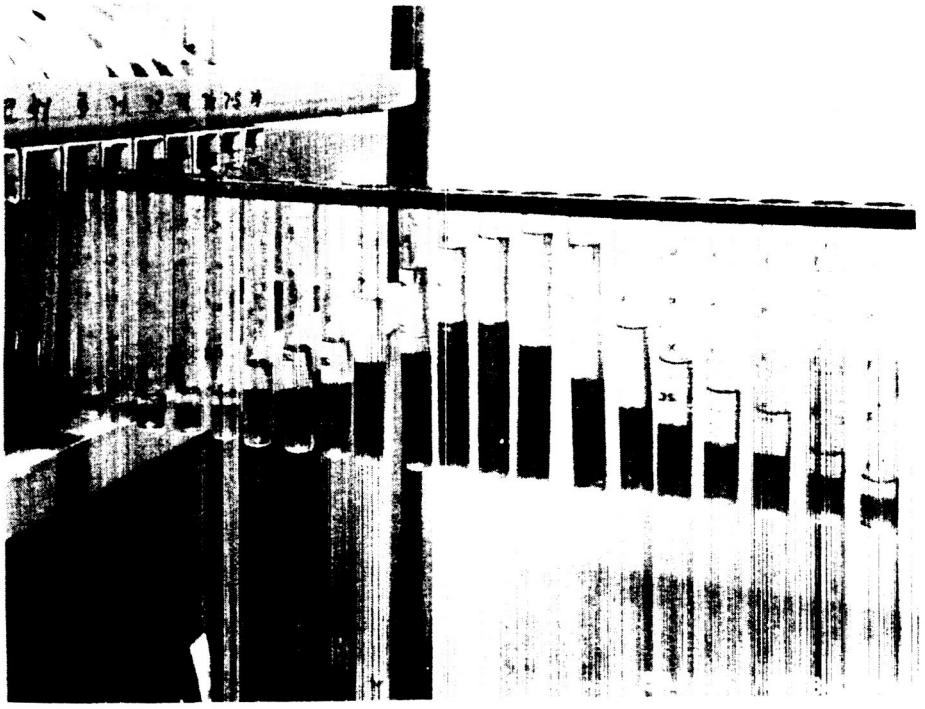

b. Test Sample

Figure 13. Liquid/Liquid Mixing

vapor pressure "freon" compounds, perchlorethylene (a dry-cleaning solvent), as well as fuel-type hydrocarbon liquids. At least one past program at Rocketdyne utilized a water/brine system, with the mixture ratio of the sample determined by an electric salinity meter. Data acquisition using this method was significantly slower than the immiscible fluid method, and accuracy was poor in the low mass flow outer zones.

Gas-Liquid Mixing Test Methods

Gas-Liquid mixing tests are significantly more time consuming than the liquid-liquid mixing, which probably is the reason that gas-liquid data is more limited. A gas-liquid mixing measurement system has been utilized extensively at Rocketdyne for hydrogen/liquid oxygen concentric elements (with the gas annulus surrounding the liquid core). The schematic of the process is shown in Fig. 14. The sample element is installed at the "head end" of a transparent, pressurized chamber, with a traversable probe mounted at the desired sampling plane. Water typically is used for the liquid oxygen simulant and a nonreactive gas simulates the hydrogen fuel (or hydrogen-rich hot gas in a staged combustion cycle). Typically, the gas used is nitrogen, sometimes diluted with helium to provide a desired density. Gas density is controlled by tank back pressure, and the mixture of gases supplied. A "base bleed" gas usually is supplied through the face around the injection element to minimize recirculation from the injected flow, and to simulate partially the axial gas flow present in a combustion chamber. A tracer gas (frequently oxygen) is included in this base bleed flow to allow this local gas flow to be measured and extracted mathematically from the measured element gas flow in each sample.

The sample is extracted from the gas-liquid element flowfield by the use of a sharp edge probe that can be positioned in the desired sample area. The liquid spray in the sample zone is collected physically by the opening in this probe, and accumulated in a sample container over a measured time period. The gas flow flux in the sample zone is determined from the relationship between total and static pressure (corrected for the liquid in the two-phase flow). The gas measurement may require a second correction for the entrained "base bleed" flow, and the data for this correction is obtained from an "on-line" gas analysis technique.

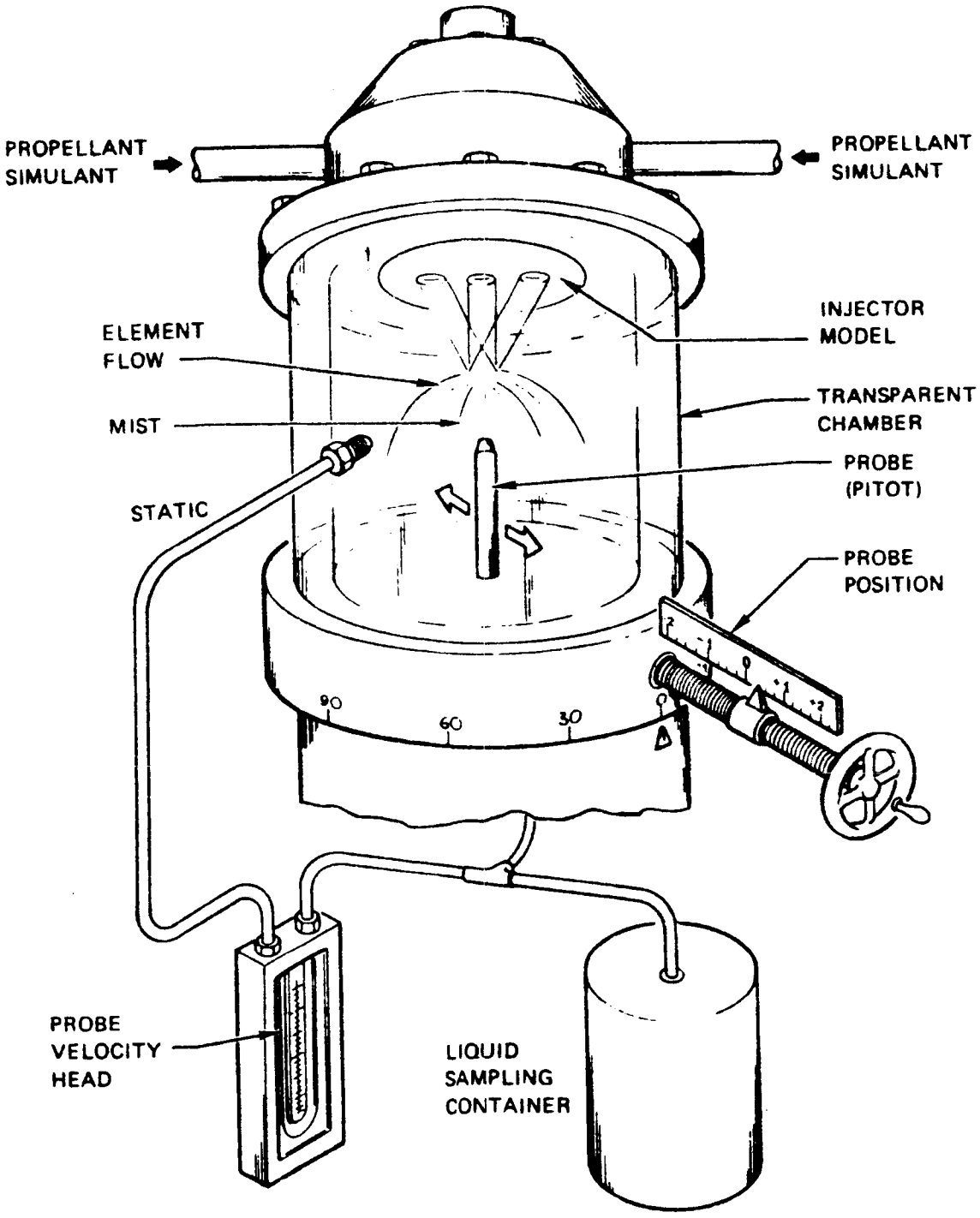

Figure 14. Cold Flow Gas/Liquid Mixing Measurement System

As might be deducted from the preceding description, each sample requires a sufficient time to stabilize the required readings and collect the liquid. When compared to the hundreds of sample points simultaneously obtained in the liquid-liquid testing, the increase in test time for gas-liquid testing is readily apparent. Testing with concentric elements permits a reasonable assumption of circular symmetry, allowing a reduced number of required sample measurements. However, the more complex "fan" shapes of gas-liquid triplets and pentads require careful study of the sample locations, and require more sample points than for a co-ax test. Previous work with triplets and pentads in a gas/fluidized solid system, Ref. 30, and triplets in a gas-gas system have indicated the shape of expected mass distribution, and show that numerous sample points are required to characterize these element types.

COLD FLOW MIXING DATA REDUCTION

The data reduction procedures for the liquid-liquid and the gas-liquid cold flow mixing tests are very similar. As in the testing itself, the data reduction for the liquid-liquid testing is a bit more straight forward. The total sample grid usually encompasses all the injected flow, and the grid openings usually have no open spaces between them. Therefore, the collected totals should equal the injected totals, thus providing a good cross-check on the data. This is the first factor computed in gas/liquid mixing tests, and is referred to as the "collection efficiency."

Collection Efficiency

To calculate the collection efficiency of the test system, fluid input values are compared with fluid collected values. The input values of mass flow rate W is frequently calculated theoretically by the Injector Pressure Drop Equation (9), based on previous cold flow resistance calibration of the test model:

$$\dot{W}_{input} = \frac{\pi}{4} N D^2 C_d (2\rho \Delta P)^{1/2} \qquad (9)$$

where

$\dot{W}$ = mass flowrate

N = total number of oxidizer or fuel holes

D = diameter of orifice

Cd = dimensionless discharge coefficient as determined from the calibration flow test

ρ = density of simulant

ΔP = injector pressure drop

If direct flow measurement capability exists in the cold flow mixing facility, the values from these measurements are used.

The collected values of mass flowrates are calculated from the test data; summing all of the individual sample measurements:

$$\dot{W}\ \text{collected} = \frac{\rho\, Q}{t} \tag{10}$$

where:

ρ = density

Q = local corrected sample volume

t = collection time in seconds

Collection efficiency of the system is calculated then by:

$$\eta_{col} = \frac{\dot{W}\ \text{collected}}{\dot{W}\ \text{input}} \tag{11}$$

where a value of "1" represents perfect collection efficiency. Large deviations in the collection efficiency would indicate problems in the system or the data for the testing. Unfortunately, collection efficiency rarely is included in reports of mixing tests and in some cases may not even be calculated. Liquid/liquid mixing testing is relatively simple and collection efficiency generally

is not needed or obtained. However, the much greater complexity of gas/liquid testing requires the "check" on test methods and procedures that collection efficiency provides.

Mixing Efficiency

The most meaningful expression for assessing mixing efficiency is the E_m (E-sub m) value proposed several years ago by Jack Rupe at JPL. This is an expression for the mass mixture ratio distribution of the samples based purely on the relationship of the samples to the overall mixture ratio with no regard to such factors as theoretical stoichiometry, etc.

This value is computed as a mass weighted summation of the mixing errors in all the samples. In practice, it is computed as a summation of decrements based on how far the mixture ratio of each sample deviates from the overall mixture ratio, and weighted by the mass fraction of each of these samples. The range of this expression is from zero to 100%, with 100% indicating all samples are the same mixture ratio, and zero indicating the samples are all one component or the other.

The nominal form for computation of E_m is expressed by:

$$E_m = 100 \left[1 - \Sigma MF_{sb} \frac{R-R_{sb}}{R} + \Sigma MF_{sa} \frac{R-R_{sa}}{R-1} \right. \quad (12)$$

where

E_m = mixing efficiency from 0 to 100%

R = overall mixture ratio as expressed by weight flow oxidizer/weight flow total

R_{sb} = mixture ratio of sample below overall mixture ratio

MF_{sb} = mass fraction of sample below overall mixture ratio

MF_{sa} = mass fraction of sample above overall mixture ratio

R_{sa} = mixture ratio of sample above overall mixture ratio

Each local sample that is not at the overall mixture ratio thus provides a mixing efficiency decrement proportional to how far it is from the nominal mixture ratio, and what mass fraction of the total flow it represents. For example, if a sample representing 50% of the total mass has a mixture ratio fraction of 0.35 when the overall is 0.70, the total mixing loss from this sample is

$$100\ (0.5\ \frac{0.70 - 0.35}{0.70}) \quad = \quad 25\% \text{ loss in mixing efficiency}$$

This factor is much more sensitive to mixing deficiencies than combustion efficiency-related factors, which are "rounded off" by theoretical curves and the relationship between test mixture ratio and stoichiometric mixture ratio.

Mixing Limited C-Star

A frequently used parameter to describe mixing test results is mixing limited C-star or c^* mix (ETA C-star mix). This can be applied only to tests for a specific reactant combination, and actually only for an assumed chamber pressure. It is a prediction of the expected hot fire C-star efficiency (assuming total vaporization). The product of vaporization efficiency and mixing limited C-star efficiency is the predicted combustion efficiency.

At Rocketdyne, the mixing limited C-star is computed by a single stream tube performance model technique. The computer program is provided with a theoretical C-star function and the theoretical C-star value (M/sec) is calculated for each sample mixture ratio. Each sample collected mass is multiplied by the sample C-star, and these products are summed for the entire sample. This answer is divided by the total mass collected to provide the mixing limited C-star.

$$\text{Mixing Limited C-star} \quad = \quad \frac{C^*_1 \times \text{Mass}_1 + C^*_2 \times \text{Mass}_2 \ \ldots\ . + C^*_N \times \text{Mass}_N}{\text{Total Sample Mass}} \qquad (13)$$

The mixing limited C-star efficiency then is determined by comparing this value to the theoretical C-star for the overall mixture ratio:

$$\eta_{c^*} = \frac{\text{mixing limited } C^*}{\text{theoretical } C^*} \tag{14}$$

A C-star efficiency of one indicates that at uniform mixture ratio, $E_m = 1$, mixing limited C-star is equal to theoretical C-star. This parameter is used to make a rough estimate of performance potential for given operating conditions of certain mixture ratio and mixing efficiency.

REVIEW OF EXISTING DATA

An extensive literature search was conducted on past experience in determining and evaluating mixing efficiency for triplet, pentad, and coaxial elements. Numerous document references were accessed and reviewed, and a bibliography of the pertinent reports reviewed is presented herein. The intent of this search primarily was to find reports containing quantitative cold flow mixing test data for these injectors.

The literature search yielded fewer reports than had been anticipated, although several valuable references were encountered. The abundance of data involved liquid/liquid impinging doublets followed by liquid/liquid triplets and pentads. Gas/liquid reports were almost entirely limited to coaxial elements and presented little data regarding gas/liquid triplets or pentads.

The data from each report was re-reduced in order to provide a uniform basis for comparison. In each instance, the objective was to obtain as close to raw data as possible from the information in the report. Using a computer program designed for this task, a table of injection parameters relating to measured performance was constructed. Information from each report thus was computed in the same consistent fashion for best comparison of results.

As expected, many important test conditions typically were omitted from the reports, such as the distance from the injector face to the sample plane, the

relative size of the sample grid, and the number of sample points in the test plane. For gas/liquid coaxial element data there had been controversy on the use of averaged data for sample grid points, and the reports typically did not elaborate on data reduction methods. With these limitations and constraints in mind, the data was analyzed and reviewed for some generalized conclusions.

The data was extracted from all the reports that had usable mixing data and has been prepared in summary chart form (Table 6). The data has been organized by element types and propellant condition (i.e., gas-liquid triplet, liquid-liquid pentad, etc.). All of the normally used injector sizing and operating parameters are displayed (if they were available or calculable from the report information). Where a report provided information on more than one element type or propellant condition combination, it has been listed in appropriate multiple locations in the charts, with cross-reference to the other elements. These charts are intended as a summary reference source, rather than a quick graphic comparison, and a review of data comparing similar configurations can be accomplished with minimum confusion. Most of the data also is presented elsewhere in this report in graphic form, with mixing efficiency plotted against the common injection parameters.

Triplet - Liquid/Liquid

Two documents for liquid/liquid triplets, were found each containing significant single element data on several configurations (Ref. 5 and 7). The data was relatively consistent and indicated a reasonable correlation with the Elverum Morey Factor (Fig. 15 and 16). These plots depict the Elverum Morey Factor on a logarithmic scale since this factor is computed as a ratio. In both references, it can be stated generally that maximum mixing efficiency occurs near the 0.66 value for the factor. Elements with near the same orifice diameters appear to provide the highest maximum mixing efficiency, and multiple elements reflect interelement mixing with higher average values and reduced sensitivity to the

	F-O-F 1.71 · 2.87 1.88 · 2.71 2.57 · 3.67 O-F-O 2.78 · 3.45 MULTI F-O-F 2.06 · 3.83	F-O-F 1.32 · 2.21 1.57 · 2.34 1.36 · 2.84 O-F-O 2.37 · 3.66 MULTI F-O-F 1.34 · 4.22	F-O-F 0.77 · 1.20 0.58 · 0.86 0.53 · 0.74 O-F-O 0.85 · 1.06 MULTI F-O-F 0.86 · 1.16	F-O-F 0.85 · 2.05 0.58 · 1.06 0.40 · 0.77 O-F-O 1.03 · 1.89 MULTI F-O-F 0.81 · 1.81	F-O-F 3.43 · 1.06 0.77 · 1.83 0.95 · 1.84 O-F-O 1.27 · 1.96 MULTI F-O-F 0.43 · 1.36	F-O-F 0.49 · 0.77 0.58 · 0.84 0.84 · 0.76 O-F-O 1.36 · 6.70 MULTI F-O-F 0.43 · 0.76		F-O-F 0.82 · 0.93 0.76 · 0.93 0.78 · 0.91 O-F-O 0.87 · 0.94 MULTI 0.87 · 0.95	F-O-F 0.91 · 0.96 0.86 · 0.97 0.79 · 0.83 O-F-O 0.87 · 0.96 MULTI 0.93 · 0.97		COLD FLOW STUDY FOR LOX/RP TYPE OPERATION WITH UNLIKE IMPINGING TRIPLETS. QUASI 3-D PLOTS OF MASS DISTRIBUTION SHOW TRIPLET UNBALANCE EFFECTS
O — F .044 - 0.0138 2 ELEMENTS) .087 - 0.0287 ELEMENTS) .063 - 0.0280 ELEMENTS)	1.48 · 1.82 0.98 · 1.98	0.73 · 0.76 0.46 · 1.73						0.77 · 0.83 0.83 · 0.88	0.93 · 0.96 0.94 · 0.99		COLD FLOW MIXING TESTS TO OBTAIN CALIBRATION AND CHARACTERIZATION DATA PRIOR TO HOT FIRE TRIPLET MIXED DOUBLET AND UNLIKE DOUBLET TESTED FOR LEM ASCENT ENGINE. UNLIKE DOUBLET CHOSEN AS FINAL DESIGN PRIMARY TEST VARIABLE WAS MIXTURE RATIO (1 TO 2). 10 COLD-FLOW MIXING TESTS CONDUCTED. 129 HOT FIRE TESTS. NO COLD-FLOW ATOMIZATION TESTS
d_s d_O .030 - 0.038 .030 - 0.043 .030 - 0.0575 .020 - 0.028	0.36 · 1.83 0.67 · 2.47 1.88 · 3.73 0.54 · 1.22	0.22 · 5.80 0.18 · 4.66 0.36 · 1.48 0.48 · 2.48	0.74 · 1.67 0.46 · 2.27 0.88 · 1.39 0.74 · 1.68	0.36 · 0.13 0.28 · 7.54 0.71 · 2.82 0.80 · 4.11	0.13 · 3.2 0.13 · 3.3 0.3 · 1.2 0.28 · 1.8	0.41 · 2.88 0.32 · 1.81 0.38 · 0.76 0.81 · 1.40	SINGLE INJECTOR ELEMENT WAS STUDIED. MIXING PROCESSES AND ATOMIZATION WERE INVESTIGATED INDEPENDENTLY FROM COLD FLOW. FROZEN WAX WAS USED.	0.46 · 0.93 0.28 · 0.88 0.78 · 0.82 0.71 · 0.92		EQUATION FOR OPTIMUM MIXXING OF CIRCULAR TRIPLET ELEMENTS WAS PRESENTED. LIST OF VARIABLES AFFECTING ATOMIZATION IS ALSO AVAILABLE.	INFLUENCE ON ELEMENT SHAPE UPON PERFORMANCE OF INJECTORS. DIFFERENT LIKE DOUBLET INJECTORS WERE DESIGNED COLD FLOW AND HOT FIRE TESTED. NON-CIRCULAR ORIFICES WERE INVESTIGATED. THE REPORT ALSO CONTAINS DESIGN CRITERIA FOR UNLIKE TRIPLET AND RECTANGULAR CONCENTRIC TUBE ELEMENTS
	2.3 · 7.8	0.08 · 0.50	0.03 · 0.084	0.47 · 2.92	0.30 · 1.88	0.26 · 0.62		0.89 · 0.89	0.82 · 0.96		FULL SCALE HOT FIRE TESTS. SINGLE ELEMENT MIXING AND ATOMIZATION TESTS
O MULTI .040 .080	7.18 · 3.2	3.84 · 0.39		16.8 · 0.08	1.10 · 0.12			0.888 · 0.974			COLD FLOW MASS AND MIXTURE RATIO DISTRIBUTION TEST PROGRAM TO EXPERIMENTALLY EVALUATE THE LS-14 INJECTOR ELEMENT CONTRIBUTION TO THE COMBUSTOR THERMAL GRADIENT AND SUBSEQUENT NOZZLE DEGRADATION PROBLEM.
AREA AREA	6.28 4.4 · 8.9 4.4 · 8.9 6.28 4.4 · 8.9 4.4 · 8.9		2.1 · 4.0				PERFORMANCE IS COMPROMISED FOR SMALLER IMPINGEMENT ANGLE. ELVERUM-MORSE CRITERIA WAS USED TO SIZE THE ELEMENTS $\left(\frac{w_F}{w_O}\right)^2\left(\frac{A_O}{A_F}\right)\left(\frac{A_O}{2AF}\right)^{1.75} = .86$	0.77 0.82 · 0.88 0.89 · 0.92 0.87 0.82 · 0.88 0.72 · 0.89	0.95 0.97 · 0.98 0.98 · 0.99 0.98 0.97 · 0.98 0.93 · 0.96	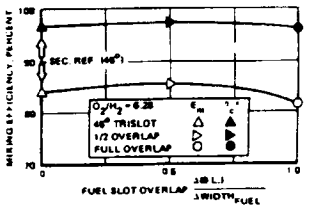	COMPREHENSIVE STUDY FOR HIGH PRESSURE INJECTOR CONCEPT. 4 INJECTORS WERE COLD FLOW TESTED. CONCENTRIC TRIPLET, DIFFUSE FACE AND TRISLOT 2 WERE SELECTED FOR HOT FIRE TESTS. CONCENTRIC AND TRISLOT "C" FROM HOT FIRE IS WITHIN 7% OF COLD FLOW. COLD FLOW SAMPLING AT 7" FROM FACE FUEL SLOT OVERLAP CONFIGURATION AND SMALLER IMPINGEMENT ANGLE WERE INVESTIGATED. GOOD CORRELATION BETWEEN COLD FLOW AND HOT-FIRE WAS OBTAINED. HOT-FIRE DATA SUMMARY IS AVAILABLE.
ET - O .002 .002	TRIPLET 2.4 · 5.5	TRIPLET 3.0 · 39.0			TRIPLETS 0.1 · 10.8			TRIPLETS 0.44 · 0.89			STUDY FOR PULVERIZED COAL/AIR TYPE OPERATION WITH UNLIKE TRIPLETS AND PENTAD ELEMENTS TESTED FOR MASS AND MR DISTRIBUTION

2 FOLDOUT FRAME

TABLE 6. (Continued)

PENTAD

DATE	REPORT I.D TITLE	PROPELLANTS SIMULATED	SIMULANTS	ELEMENT CONFIGURATION	OPERATING RANGE			INJECTION PARAMETERS (CALCULATED FROM INPUT)					
					INJECTION PATTERN	ELEMENT SIZE RANGE (DIA IN)	SIMULATED MR	MOMENTUM RATIO	VELOCITY RATIO	VELOCITY HEAD RATIO	ELVERUMMOREY FACTOR (TRIPLET, PENTAD)	PENETRATION FACTOR	
8/65	AFRPL TR-66-152 VOL I STUDY OF DROPLET EFFECTS ON STEADY-STATE COMBUSTION (ROCKETDYNE)	50/50 N_2O_4 / N_2H_4 CLF_3 / UDMH IRFNA	WATER/ TRICHLOROETHYLENE	PENTAD SINGLE & MULTI-ELEMENT LIQ/LIQ	REVERSE θ = 30°	SINGLE O - F 0.104 - 0.185 0.070 - 0.1285 MULTI O - F 0.041 - 0.072	1.72 - 2.47 1.87 - 2.47	1.88 - 3.32 1.88 - 3.32	0.83 - 1.34 1.01 - 1.36	1.27 - 2.82 1.51 - 2.83	1.61 - 3.13 1.78 - 2.22	1.58 - 2.38 1.72 - 2.38	
JUN 68	AFRPL TR-68-167 CORRELATION OF SPRAY INJECTOR PARAMETERS WITH ROCKET ENGINE PERFORMANCE (DICKERSON, TATE, BARSIC)	N_2O_4/ N_2H_4-UDMH (50-50)	WATER/ TRICHLOROETHYLENE	PENTAD LIQ/LIQ	OXIDIZER FUEL D_F D_{ox} 60° θ = 30° REVERSE	OX - FU 0.033 - 0.0686 0.070 - 0.129 0.221 - 0.469	0.83 - 1.21 0.82 - 2.11 0.89 - 2.83	0.48 - 1.78 0.48 - 2.80 0.81 - 4.86	0.52 - 1.00 0.54 - 1.23 0.89 - 1.95	0.39 - 1.46 0.42 - 2.20 0.89 - 5.88	0.43 - 1.80 0.48 - 2.50 0.80 - 5.00	0.87 - 1.67 0.88 - 2.01 0.96 - 2.78	
NOV 68	NASA CR-72487 R-7677 SPACE STORABLE PROPELLANT PERFORMANCE STUDY (FALK, CLAPP, HAGAN)	FLOX (80% O_2) & LPG (65% METHANE/ 45% ETHANE)	TRICHLOROETHYLENE & WATER	PENTAD LIKE DOUBLET LIQ/LIQ	PENTAD REVERSE θ = 30° 95 MULTI-ELEMENT	O - F 0.026 - 0.039 0.025 - 0.0282 [0.032 - 0.03721 [0.040 - 0.04681	2.72 - 5.83 2.38 - 5.18	1.27 - 5.82 1.19 - 6.27	0.47 - 1.00 0.53 - 1.21	0.32 - 1.48 0.41 - 2.14	0.89 - 4.12 0.91 - 4.78	1.41 - 3.02 1.36 - 3.13	
10/11/71	NASA CR 72827 R-8416 SPACE STORABLE THRUSTER INVES (McFARLAND/JAQUA)	FLOX/C_3H_8	WATER & PERCHLOROETHYLENE	UNLIKE PENTADS LIQ/LIQ	REVERSE θ = 30°	O - F 0.036 - 0.042	3.43 - 7.16	3.88 - 11.88	0.74 - 1.86	0.88 - 3.77	1.96 - 8.46	2.00 - 4.16	
					NORMAL θ = 30°	O - F 0.073 - 0.091	7.86 - 7.89	13.84 - 13.38	1.88 - 1.87	4.31 - 4.39	0.01 - 0.1	0.343 - 0.346	
8/30/67	NASA CR-72393 R-7189 TWO STATE BIPROPELLANT INJECTION SYSTEM STUDIES (MEHEGAN)	LOX/GH_2/ HOT GAS	WATER/GH_2/ H_2	PENTAD LIQ/GAS		PENTAD O - 0.813 IN^2 F - 1.88 IN^2 G - 3.00 IN^2	0.73 0.87 8.1	PENTAD HOT GAS 13.0 FUEL 5.3				0.80	
9/70	NASA CR 72760 R-8361 INVESTIGATION OF GAS-AUGMENTED INJECTORS (MEHEGAN, CAMPBELL AND SHEUERMAN)	LOX/GH_2 FLOX/CH_4 LF_2/GH_2	WATER/GN_2/H_2	PENTAD LIQ/GAS	REVERSE PENTAD J = 48° NORMAL PENTAD θ = 60°	PENTAD REVERSE O - F 0.249 - 0.81 0.436 - 0.334 - 0.135 - 0.209 - 0.81 0.084 - 0.277 0.185 - 0.82 NORMAL O - F 0.334 - 0.81	REVERSE 8.9 - 18.0 NORMAL 4.5 - 7.4	0.16 - 1.170 0.627 - 1.881	0.0136 - 0.088 0.139 - 0.228	0.136 - 5.831 14.745 - 39.177	0.161 - 1.842 0.288 - 0.774	0.700 - 1.220 1.388 - 2.232	
1/17/77	ITR-76-011-C COAL COMBUSTION FOR MHD COLD FLOW MIXING STUDIES (JAQUA/YU)	COAL/AIR	COAL/GN_2	UNLIKE PENTAD SOLID/GAS	PENTAD REVERSE	PENTAD O - 0.213 F - 0.139	PENTAD 4.9 - 8.6	PENTAD 9.0 - 16.0					

ASPECT RATIO X_1/Y_1 X_2 in .305 1.0 .460 0.67 Y_2 GAS AREA LIQUID AREA .305 .0416 .0201 .162 .0361 .0201	CIRCULAR 0.28 - 0.61 RECTANGULAR 0.9		CIRCULAR 0.76 211.0 RECTANGULAR 22.0 - 43.9				$.044 D_L < R < 1.5 D_L$ $.0043 < \frac{\rho_G}{\rho_L} < .0240$			TABLES OF PHYSICAL VARIABLES AND DIMENSIONLESS GROUP REQUIRED FOR THE DESCRIPTION OF GAS/LIQUID CONCENTRIC ELEMENT MIXING AND ATOMIZATION FROM DIMENSIONAL ANALYSIS[8]	COLD FLOW MIXING AND COLD FLOW ATOMIZATION WERE STUDIED. RECTANGULAR CONCENTRIC TUBE INJECTOR WAS HOT-FIRE TESTED TO EVALUATE THE EFFECT OF THE ELEMENT GEOMETRY UPON INJECTOR PERFORMANCE ANALYTICAL COMBUSTION MODEL WAS DEVELOPED TO CORRELATE ℓ_{mix} AND $\bar{D}$ INTO η_{c^*} MIX AND η_{c^*} VAP
	(a) FPB 0.5 - 1.14 OPB 0.4 - 1.22 (b) MAIN ELEMENT 0.4 - 0.8 BAFFLE ELEMENT 4.0 - 5.8		(a) FPB 5.7 - 24.9 OPB 4.8 - 24.9 (b) MAIN ELEMENT 14.0 - 23.3 BAFFLE ELEMENT 13.0 - 41.8					(a) FPB 0.899 - 0.931 OPB 0.89 - 0.936 (b) MAIN ELEMENT 0.771 - 0.880 BAFFLE ELEMENT 0.833 - 0.932	(a) FPB 0.9946 - 0.9993 OPB 0.999 - 1.000 (b) MAIN ELEMENT 0.853 - 0.987 BAFFLE ELEMENT 0.973 - 0.982		SPACE SHUTTLE ELEMENTS HAVE BEEN COLD-FLOW EVALUATED MIXING OVER PLANNED OPERATING RANGE. SINGLE-ELEMENT TESTS COULD POSSIBLY BE COMPARED WITH LATER HOT-FIRE RESULTS. SUPER-CRITICAL PROPELLANTS. EXCELLENT QUALITY COLD-FLOW DATA AVAILABLE.
	3 - 7.5		$100 < V_G < 630$ $5 < V_L < 100$				PHYSICAL PARAMETERS V_G, V_L, AND P_G INFLUENCE MIXING AND ATOMIZATION FOR GAS/LIQUID INJECTORS.	R = 0 0.80 - 0.85 R = 1 D_L 0.88 - 0.98		CORRELATION MADE BETWEEN MIXING DATA θ_{mix} AND THE PARAMETER $\rho_G V_G \theta^2 / 980 \cdot V_L L$	REPORT ON ATOMIZATION AND MIXING EFFECTS ON COAXIAL ELEMENTS WITH VARYING POST RECESS AND LIQUID AND GAS FLOW AREAS. PROGRAM WAS CONDUCTED TO CHARACTERIZE GAS/LIQUID COAXIAL INJECTOR IN ORDER TO OBTAIN HIGH η_{c^*} WITHOUT SACRIFICING HARDWARE DURABILITY. VARIOUS SINGLE ELEMENT GEOMETRIC CONFIGURATIONS WERE COLD FLOW AND HOT-FIRE TESTED. ALSO FULL SCALE INJECTOR WAS BUILT AND TESTED. η_{c^*} HOT-FIRE WAS WITHIN 2% OF η_{c^*} COLD FLOW.
	4.0 - 10.3		V_G/V_L 3.80 - 91.4				$\frac{\Delta P (V_G - V_L)}{283 - 943}$ POST RECESS/D_L 0.0 - 0.8	0.951 - 0.999			ANALYTICAL COLD FLOW HOT-FIRE PERFORMANCE CORRELATION TECHNIQUES DEVELOPED FOR INJECTOR DESIGNS FOR GAS/LIQUID INJECTORS. COLD FLOW TESTS DETERMINED DROPLET SIZES AND DISTRIBUTION AND THE MASS AND MIXTURE RATIO DISTRIBUTION FOR LARGE THRUST PER ELEMENT DESIGNS.
	G.F.O (F/S) 0.89-0.92 7:1 0.73-1.07 6.7	TRIAXIAL HOT GAS 40.0 FUEL 18.0 COAXIAL INJ'T HOT GAS 21.0 FUEL 11.0			0.85						COMPREHENSIVE STUDY FOR LARGE THRUST PER ELEMENT INJECTORS. TWENTY INJECTOR DESIGNS WERE REVIEWED INITIALLY AND FOUR WERE CHOSEN FOR COLD FLOW AND TWO FOR HOT-FIRE. LIQUID MASS DISTRIBUTION MAPS PRESENTED FOR SELECTED INJECTORS.
ID POST OD POST ID SLEEVE .141 .184 .308 .141 .184 .308 .141 .184 .308 .141 .184 .229 .100 .261 .288	4.4 - 8.9 4.2 - 9.4 4.2 - 9.4 4.4 - 8.9 4.4 - 8.9						LARGER η_{c^*} ANNULUS INCREASE η_{c^*} BY 3%	0.78 - 0.84 0.76 - 0.83 0.78 - 0.85 0.88 - 0.91 0.84 - 0.88	0.89 - 0.95 0.86 - 0.97 0.95 - 0.98 0.95 - 0.98 0.89 - 0.99	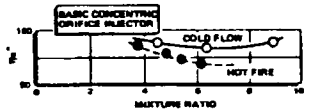 FIGURE 14. CORRELATION OF COLD-FLOW PERFORMANCE PREDICTION OF HOT-FIRE RESULTS	COMPREHENSIVE STUDY FOR HIGH PRESS. INJECTOR CONCEPT. 6 INJECTORS WERE COLD FLOW TESTED. CONCENTRIC TRIPLEY, DIP, PUNE FACE AND TRISLOT. 2 WERE SELECTED FOR HOT-FIRE TESTS. CONCENTRIC AND TRISLOT η_{c^*} FROM HOT-FIRE IS WITHIN 3% OF COLD FLOW. COLD FLOW SAMPLING AT .3" FROM FACE. FUEL SLOT OVERLAP CONFIGURATION AND SMALLER IMPINGEMENT ANGLE WERE INVESTIGATED. GOOD CORRELATION BETWEEN COLD FLOW AND HOT-FIRE WAS OBTAINED. HOT-FIRE DATA SUMMARY IS AVAILABLE.

C-2

2 FOLDOUT FRAME

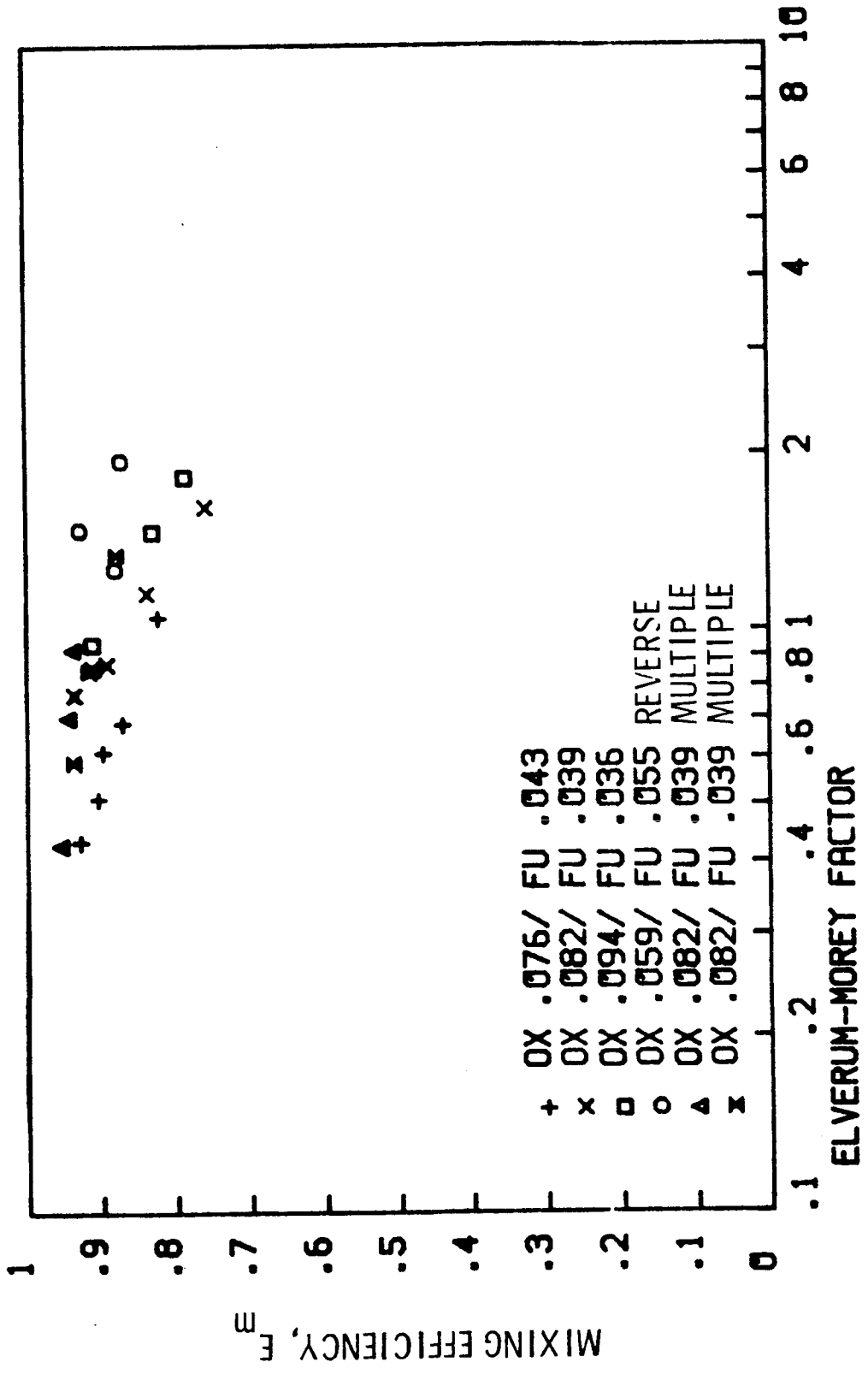

Figure 15. Mixing Efficiency of Liquid/Liquid Triplers (ITUR-80-9) Depicting Elverum-Morey Factor Influence

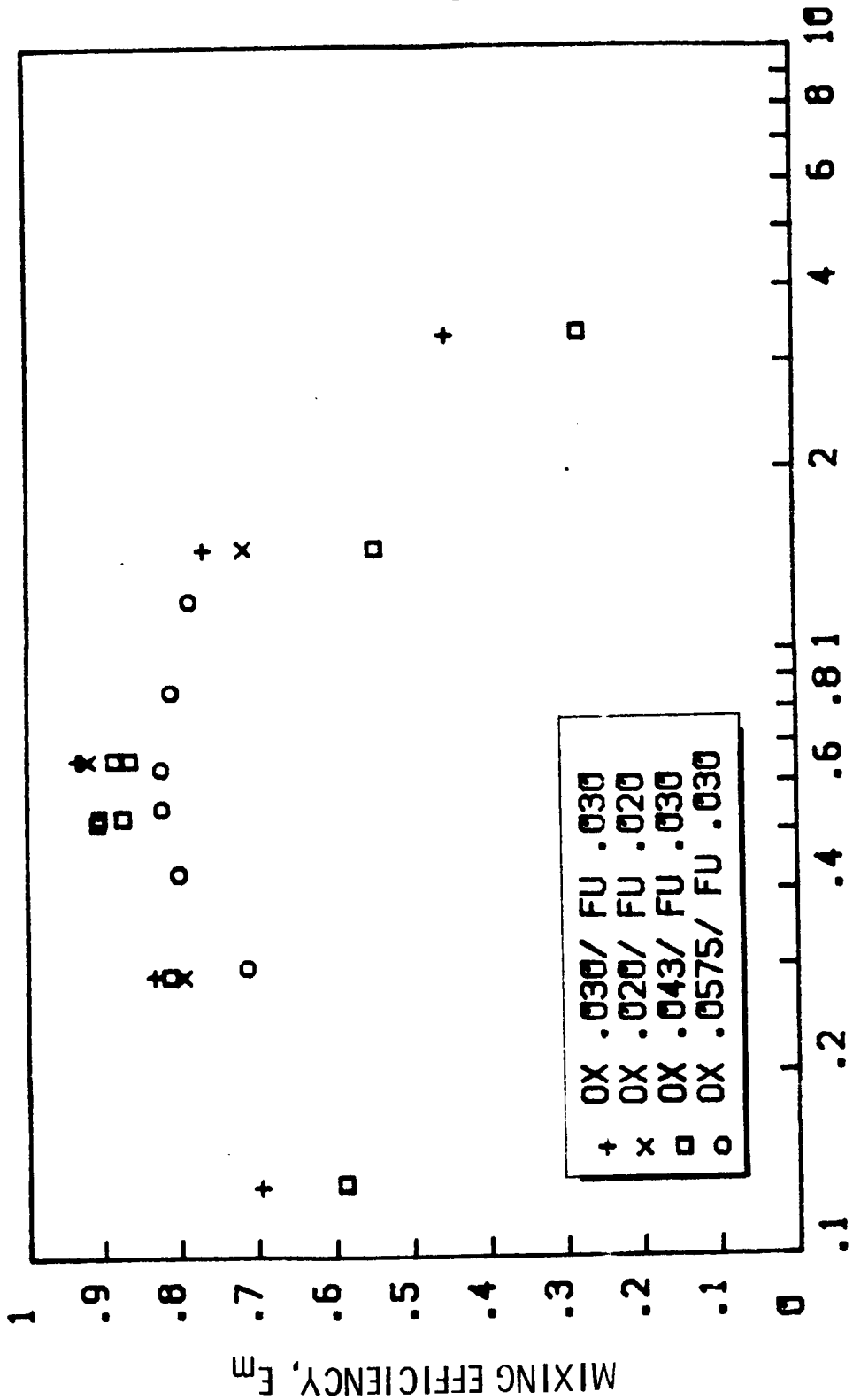

Figure 16. Mixing Efficiency of Liquid/Liquid Triplets (NASA CR-R-9270) Depicting Elverum-Morey Factor Influence

characteristics would appear to be warranted since liquid/liquid hydrocarbon mixtures favor a reverse triplet configuration at main chamber mixture ratios.

Triplet - Gas/Liquid

One report was found on LOX/hydrogen work (Ref. 34) which provided data on a liquid/gas/liquid configured element. Suprisingly, the penetration factor, designed for liquid/gas/liquid elements, did not produce the desired correlation of maximum mixing efficiency (E_m) at the 0.5 theoretical optimum value (Fig. 17). Visual aids from the report depict the gas/liquid normalized mass flux profiles for each of three cold flow tests. Figure 18 depicts representative samples of those three tests. The sample mixture ratio is equivalent to the overall inlet mixture ratio where the dashed lines (gas) intersect the solid lines (liquid). It can be inferred from the distribution plots that the balance of gas and liquid was optimum at the under-penetrated condition (penetration factor 0.4), which contributed to the maximum-measured mixing efficiency. At penetration factors greater than 0.4, the gas blowout produced by the impinging liquid jets was visible. This contributed to the poorer mixing efficiency noted.

The Elverum-Morey criteria for this element, shown in Fig. 19, did reflect a correlation between the 0.66 optimum value and the peak mixing efficiency. In this test, the oxidizer-to-fuel density ratio was over 600, markedly removed from the design application range of 1.7. These parameters bear additional testing since there are good designs for liquid/gas/liquid elements in LOX/ hydrocarbon gas generators and preburners.

Pentad - Liquid/Liquid

Documents obtained with mixing data for liquid/liquid pentad elements consisted primarily of reverse configuration* element studies (Ref. 3, 4, and 10). In these

* A reverse pentad generally is considered to have the denser liquid (oxidizer) in the outboard streams and the less dense liquid (fuel) as the centrally located stream.

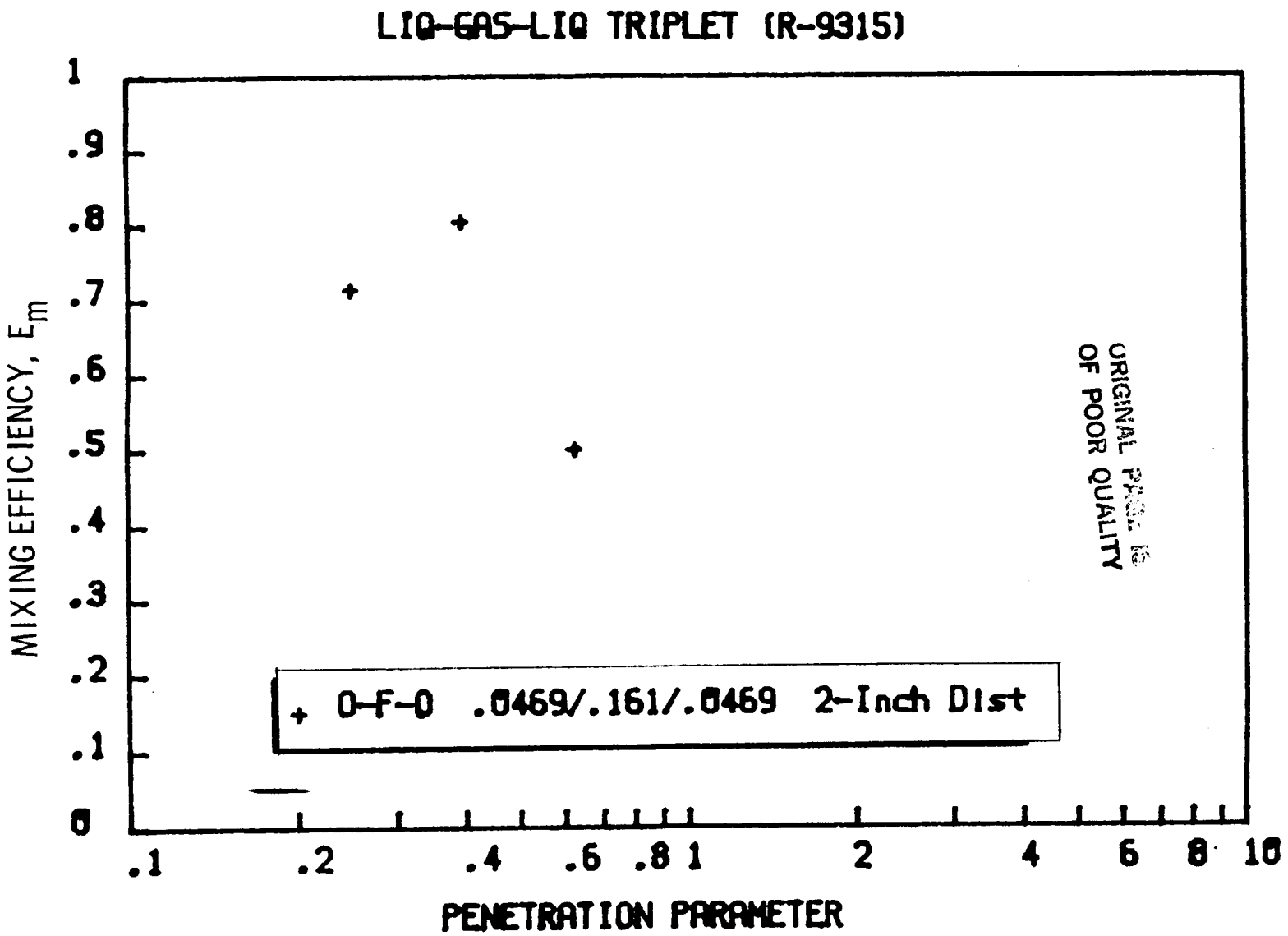

Figure 17. Mixing Efficiency of a Gas/Liquid Triplet (R-9315) Depicting Penetration Factor

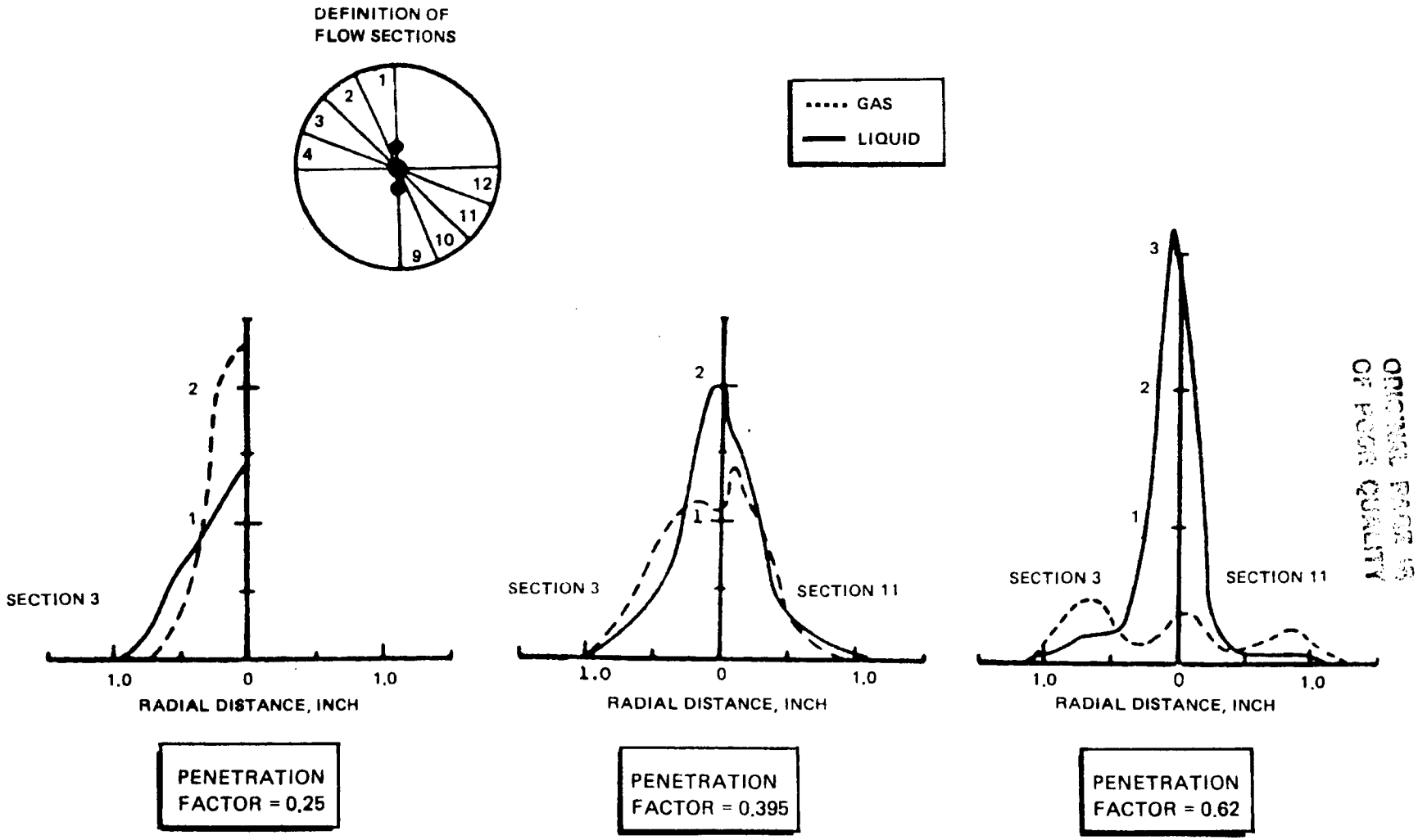

Figure 18. Normalized Cold Flow Mass Flux Profiles for FOX/CH_2, Liquid/Gas/Liquid Triplet, 2-inch Collection Tubes (Ref. 34)

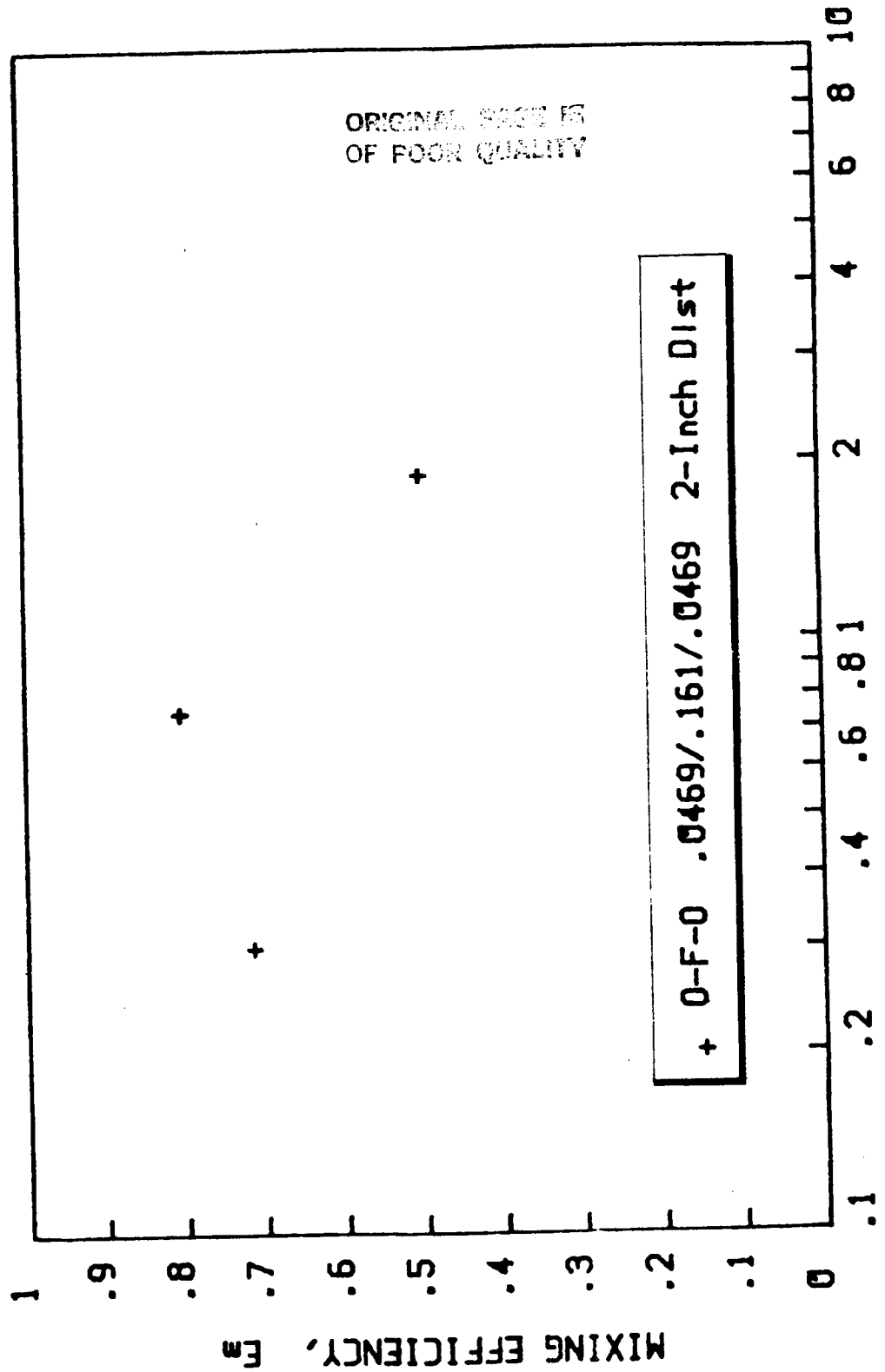

Figure 19. Mixing Efficiency of a Liquid/Gas/Liquid Triplet (R-9315) Depicting Elverum-Morey Factor Influence

studies, the overall level of mixing efficiency was generally good. Single element characteristics did not adhere to the Elverum-Morey theoretical optimum very well for the large element tests shown in Fig. 20 (Ref. 3), although the multi-element tests did show peak mixing efficiency near the 2.75 optimum value for the same experimentors. This is either a result of secondary mixing enhance ment from the multiple element configuration or is indicative of absolute size limitations in parameter application. Other data presented in Fig. 21 and 22 indicate some small degree of correlation with the 2.75 optimum parameter value.

Pentad - Gas/Liquid

The volumetric unbalance realized with gas/liquid propellant combinations frequently dictates the use of pentad (four on one) elements. With the gaseous reactant on the four outside elements, this bears some resemblance to an impinging concentric element.

With the gaseous component of the reaction system in the center stream, the case resembles an extension of the liquid-gas-liquid triplet where a form of the penetration factor becomes the most likely mixing parameter.

One document was located with gas/liquid pentad data (Ref. 31), which includes test data for both configurations, liquid-gas-liquid and gas-liquid-gas. This data was replotted against three different parameters, momentum ratio, Elverum Morey ratio, and penetration factor.

Both pentad configurations showed improved mixing characteristics with increased oxidizer (liquid) momentum (Fig. 23), regardless of the orientation of the oxidizer stream(s). This is not understood fully since prior experience on other programs, such as the gas/fluidized-solid program (Ref. 30), indicated contrary relationships, i.e., an increase in performance with a reduction in momentum of the central-fluidized stream with maximum performance occurring at a relatively high gas to liquid momentum ratio.

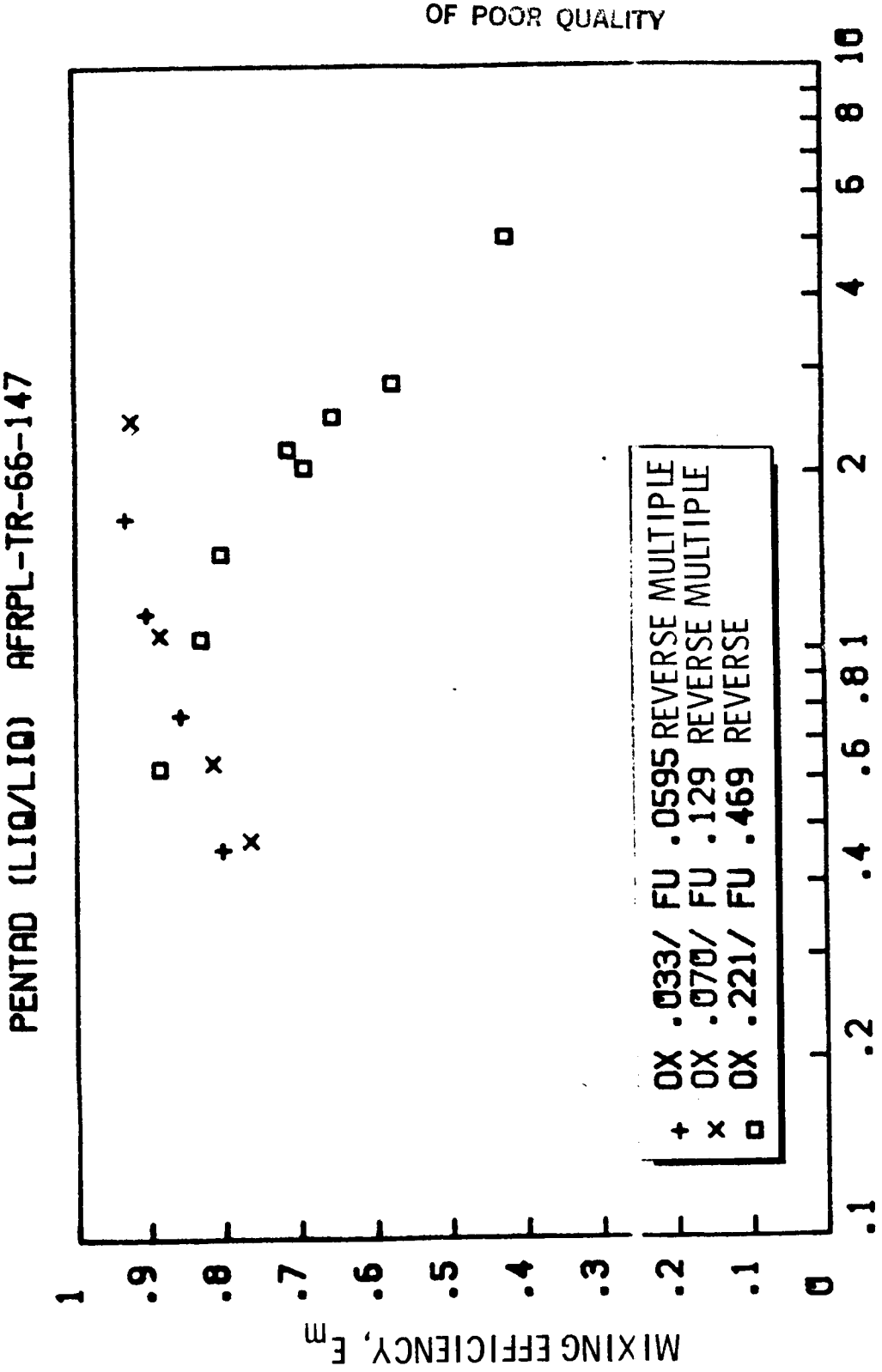

Figure 20. Mixing Efficiency for Liquid/Liquid Pentads (AFRPL-TR-66-147) Depicting Elverum-Morey Factor Influence

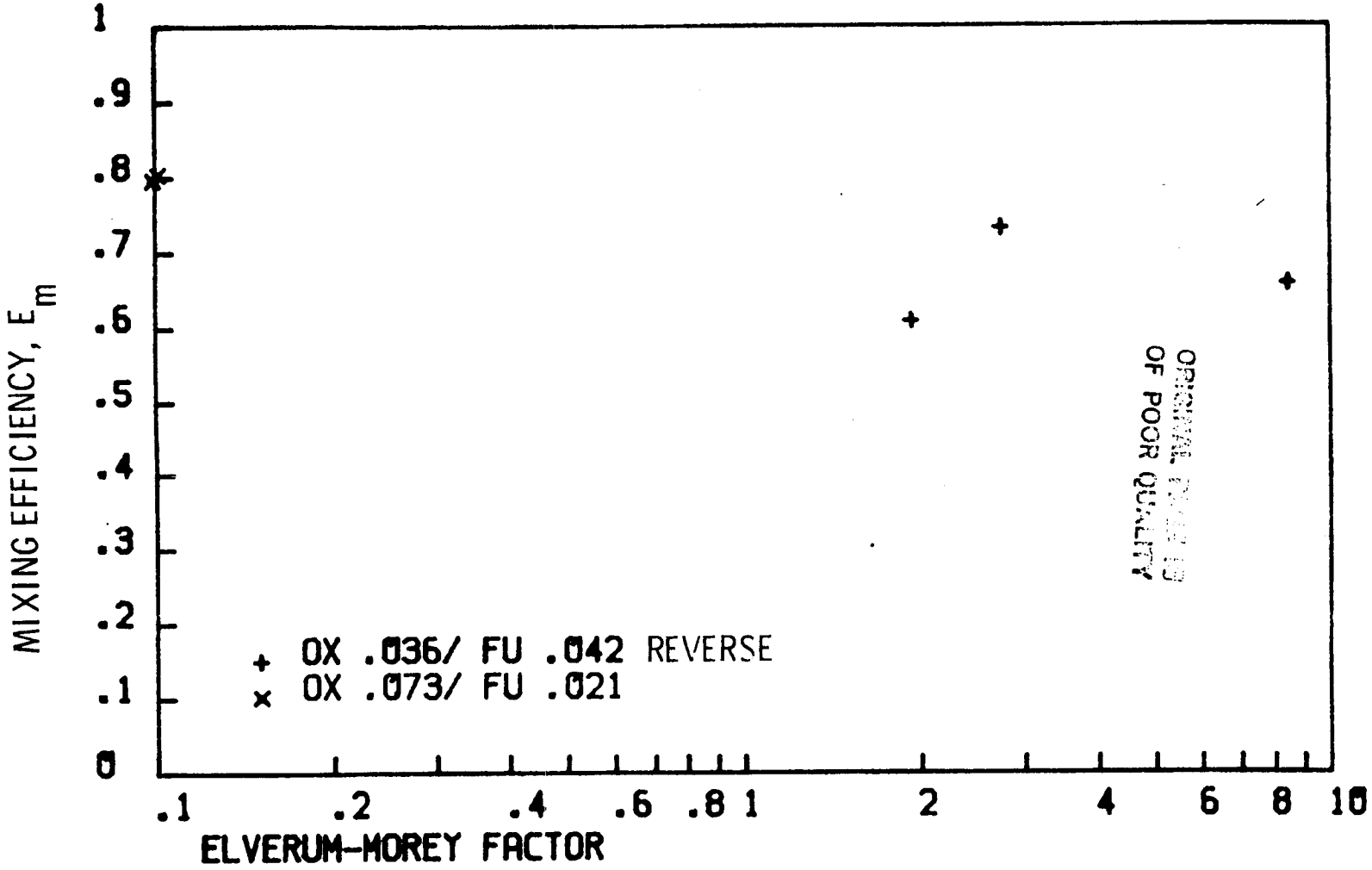

Figure 21. Mixing Efficiency for Liquid/Liquid Penteds (NASA CR-72827 R-8415) Depicting Elverum-Morey Factor Influence

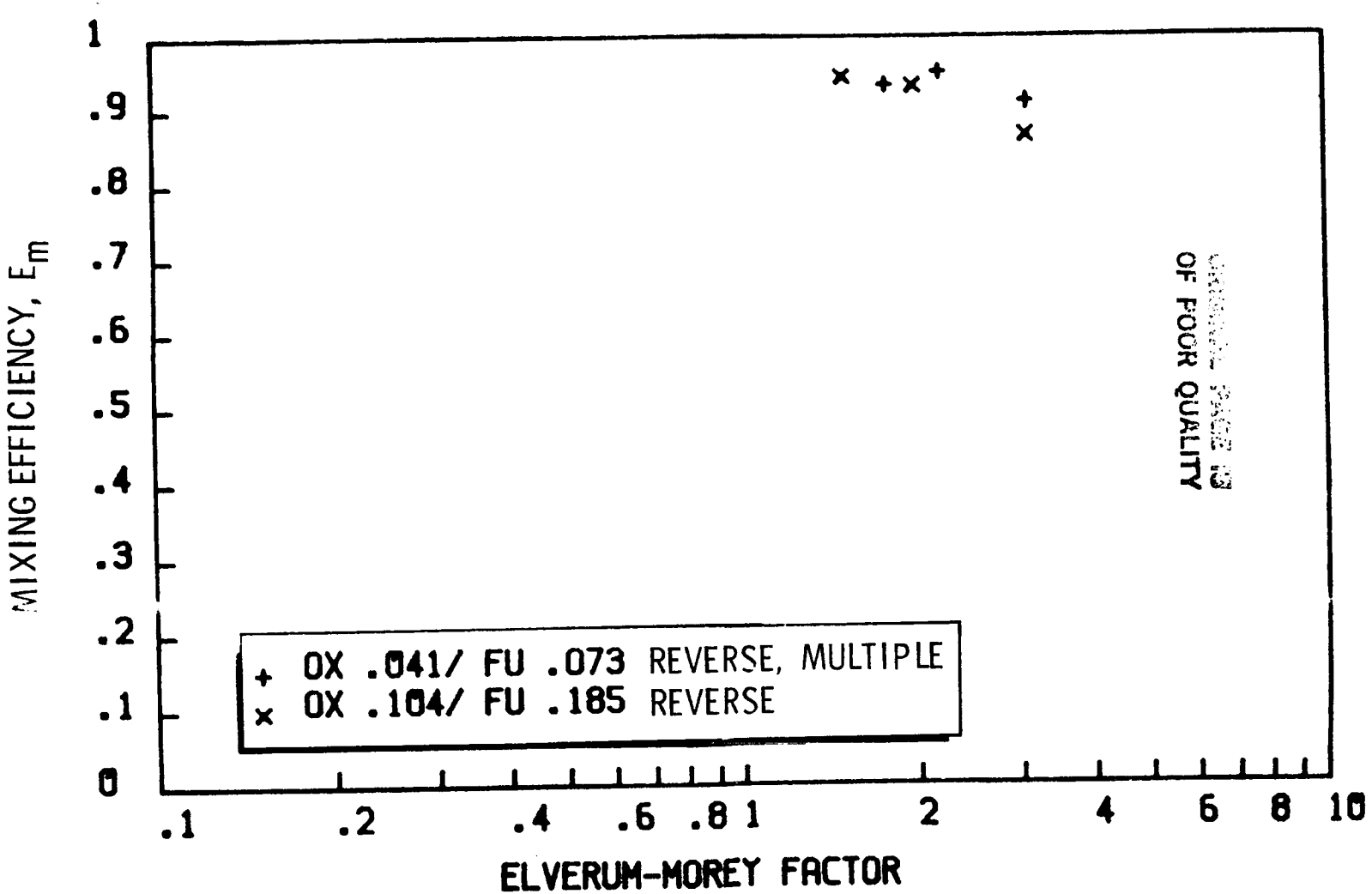

Figure 22. Mixing Efficiency for Liquid/Liquid Pentads (AFRPL-TR-66-152) Depicting Elverum-Morey Factor Influence

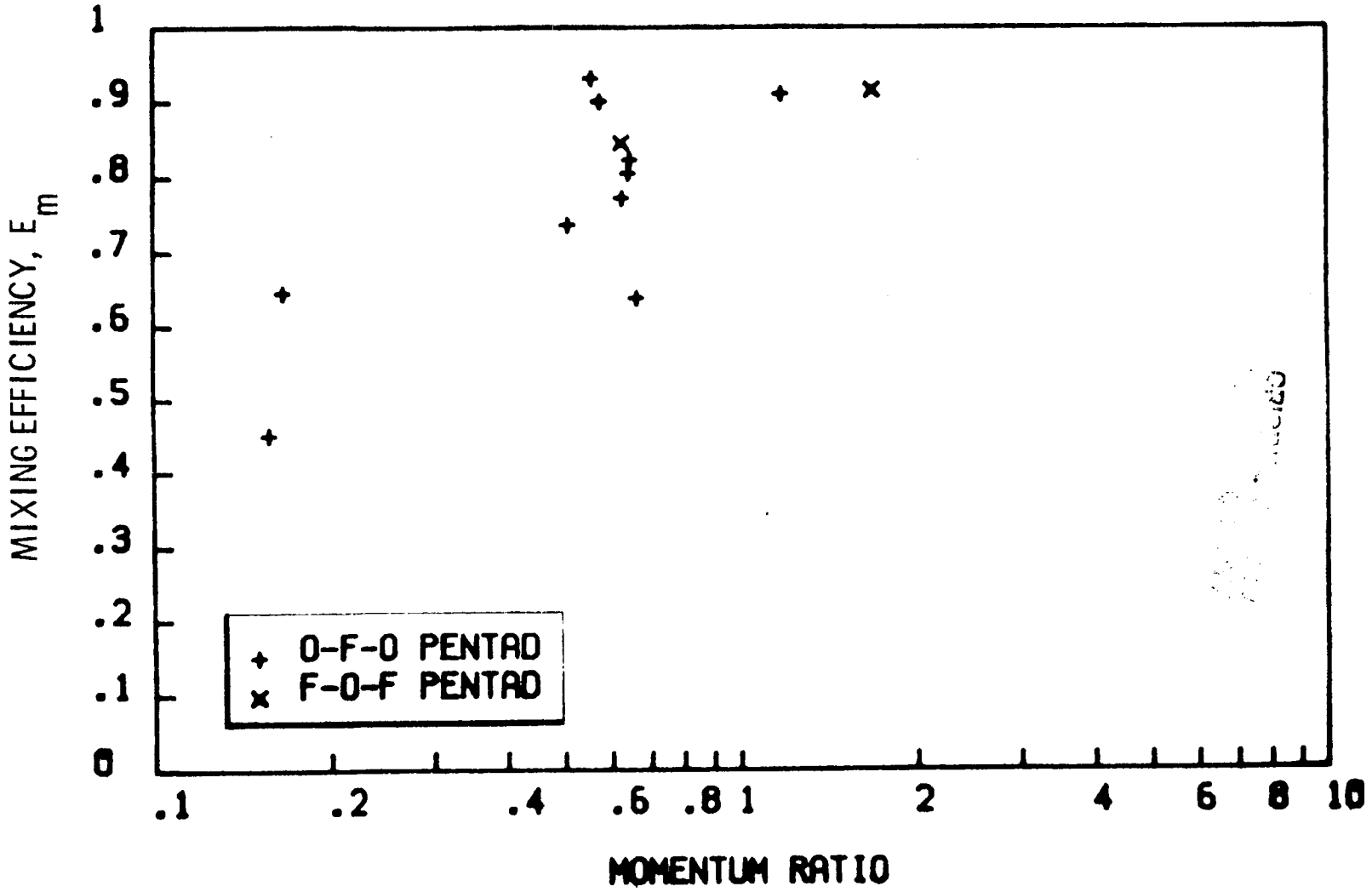

Figure 23. Mixing Efficiency for Gas/Liquid Pentads (NASA CR-72703 R-8361) Depicting Momentum Ratio Influence

Extrapolating the liquid-gas-liquid test data along the Elverum-Morey curve, Fig. 24 suggests a trend toward the 2.75 optimum value for pentads, whereas the gas liquid-gas data do not obey the parameter functions. Extrapolating the penetration factor data for the gas-liquid-gas element may indicate a trend toward the 0.5 optimum value (Fig. 25). The liquid-gas-liquid element apparently does not adhere to the penetration factor function.

Concentric Coaxial Element

Several report references were obtained in the literature search containing cold flow mixing data for coaxial elements. Some of these were from the Space Shuttle Main Engine (SSME) Program. The mixing data from these sources were plotted against the conventional parameters applicable to coaxial injectors, namely LOX post recess and velocity ratio.

In most concentric element configuration, relatively large improvements in mixing are anticipated as the central tube (oxidizer post) recess is increased to one liquid stream diameter. Data presented in Fig. 26 (Ref. 7) depict less effect than had been expected. The curve indicates poor overall mixing efficiency (E_m = 50 to 65%) with very little improvement obtained as recess is increased. However, Falk and Burick report in their studies (Ref. 19) that cup recess does improve mixing. This conflict needs to be resolved by additional testing, especially in the areas of hydrocarbon fuels.

The influence of gas-to-liquid velocity ratio on the level of mixing efficiency is presented in Fig. 27 and 28, depicting the characteristics of SSME LOX/ hydrogen preburner and main injector elements in cold flow test. In these figures, mixing efficiency is consistantly high. Propellant density matching was achieved for these tests, which also resulted in nominal matching of hot fire (design range) velocity and momentum ratios simultaneously.

Additional tests conducted by Rocketdyne (Ref. 31 and 7) are presented in Fig. 29 and 30, respectively, depicting the effects of velocity ratio on mixing efficiency. The latter figure shows the influence of gas-to-liquid density ratio

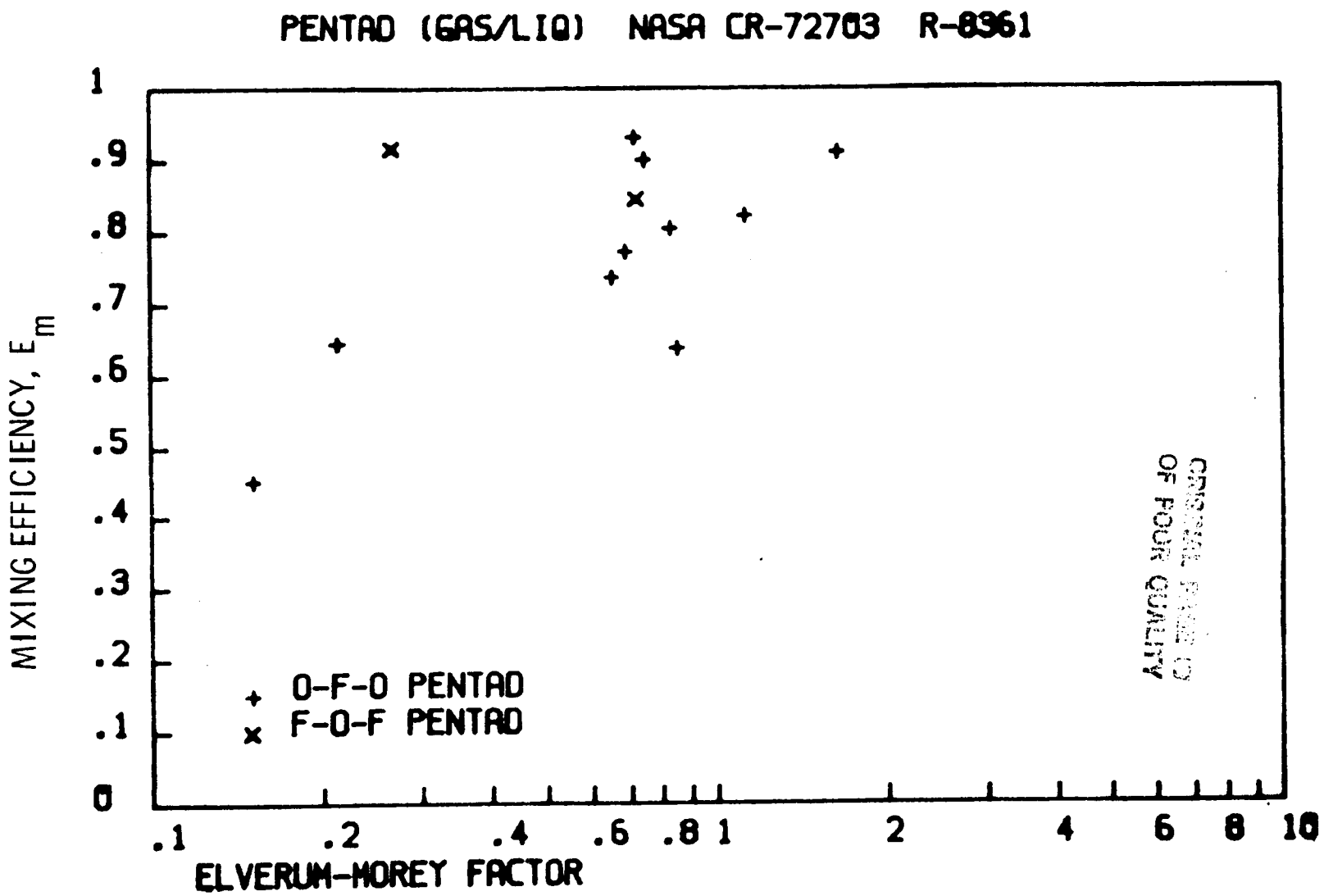

Figure 24. Mixing Efficiency for Gas/Liquid Pentads (NASA CR-72703 R-8361) Depicting Elverum-Morey Factor Influence

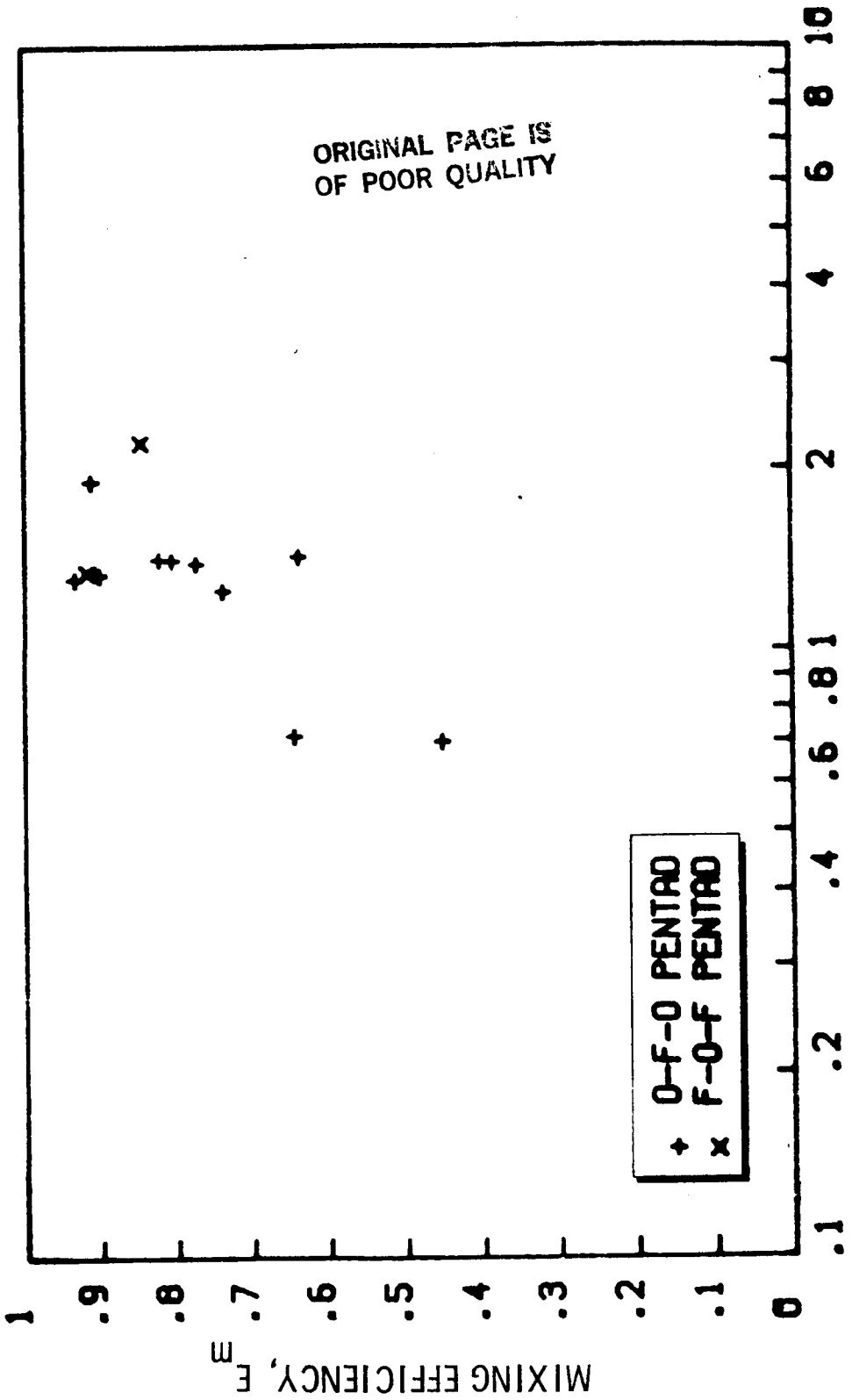

Figure 25. Mixing Efficiency for Gas/Liquid Pentads (NASA CR-72703 R-8361) Depicting Penetration Factor Influence

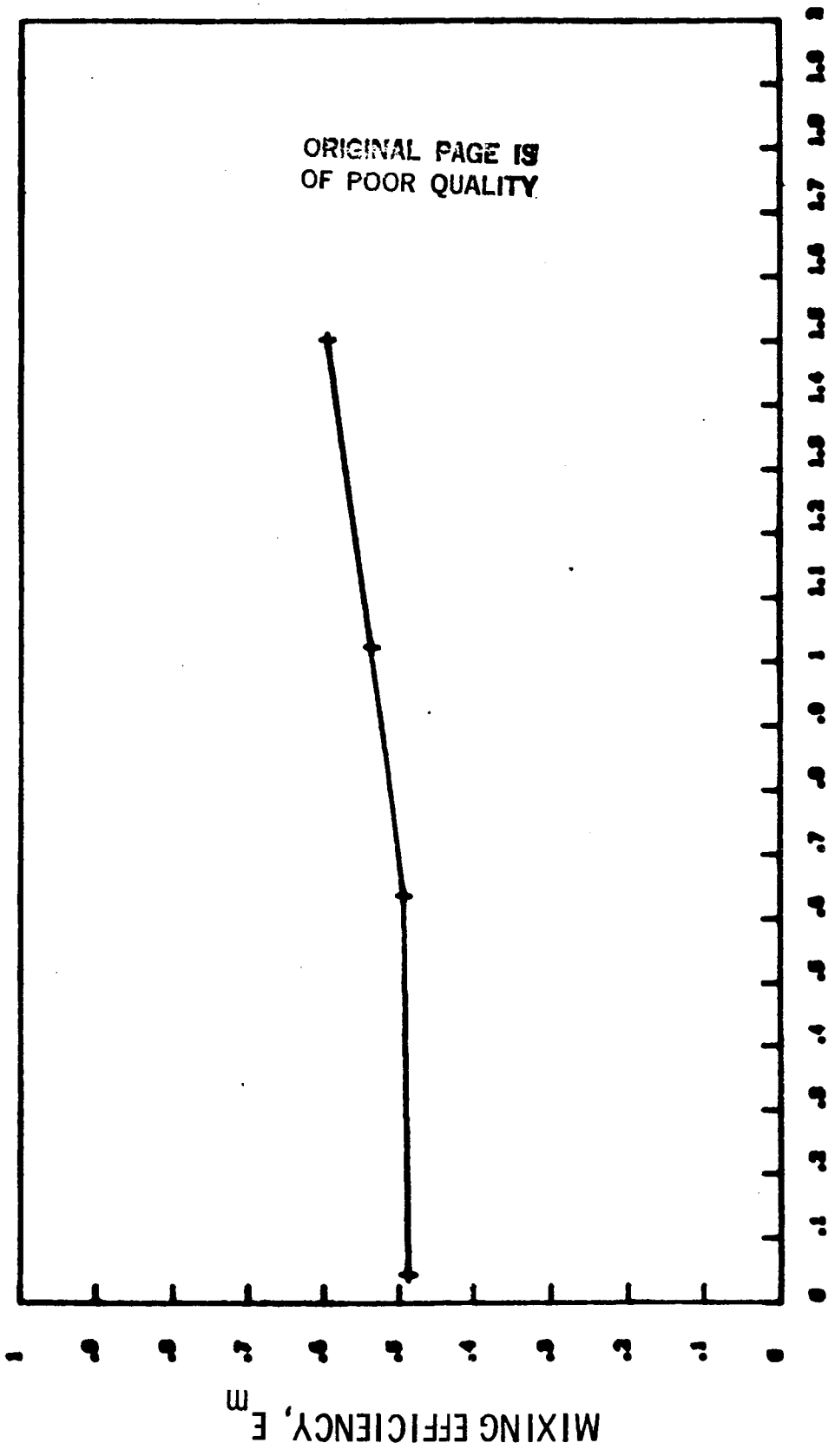

Figure 26. Mixing Efficiency for Coaxial Element (NASA CR-R-9270) Depicting LOX Post Recess Influence

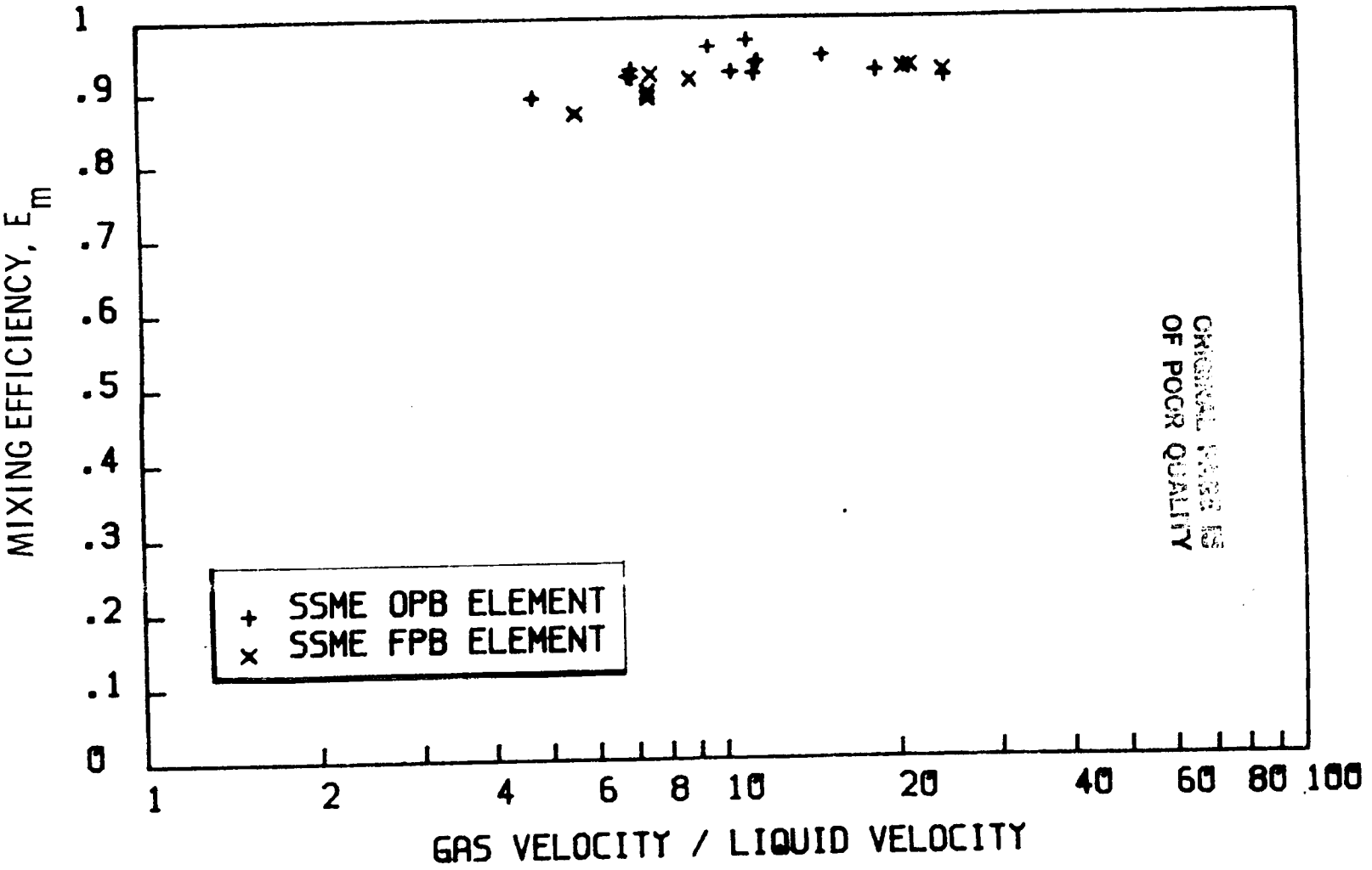

Figure 27. Mixing Efficiency for Coaxial Elements (IL PT 73-30) Depicting Velocity Ratio Influence

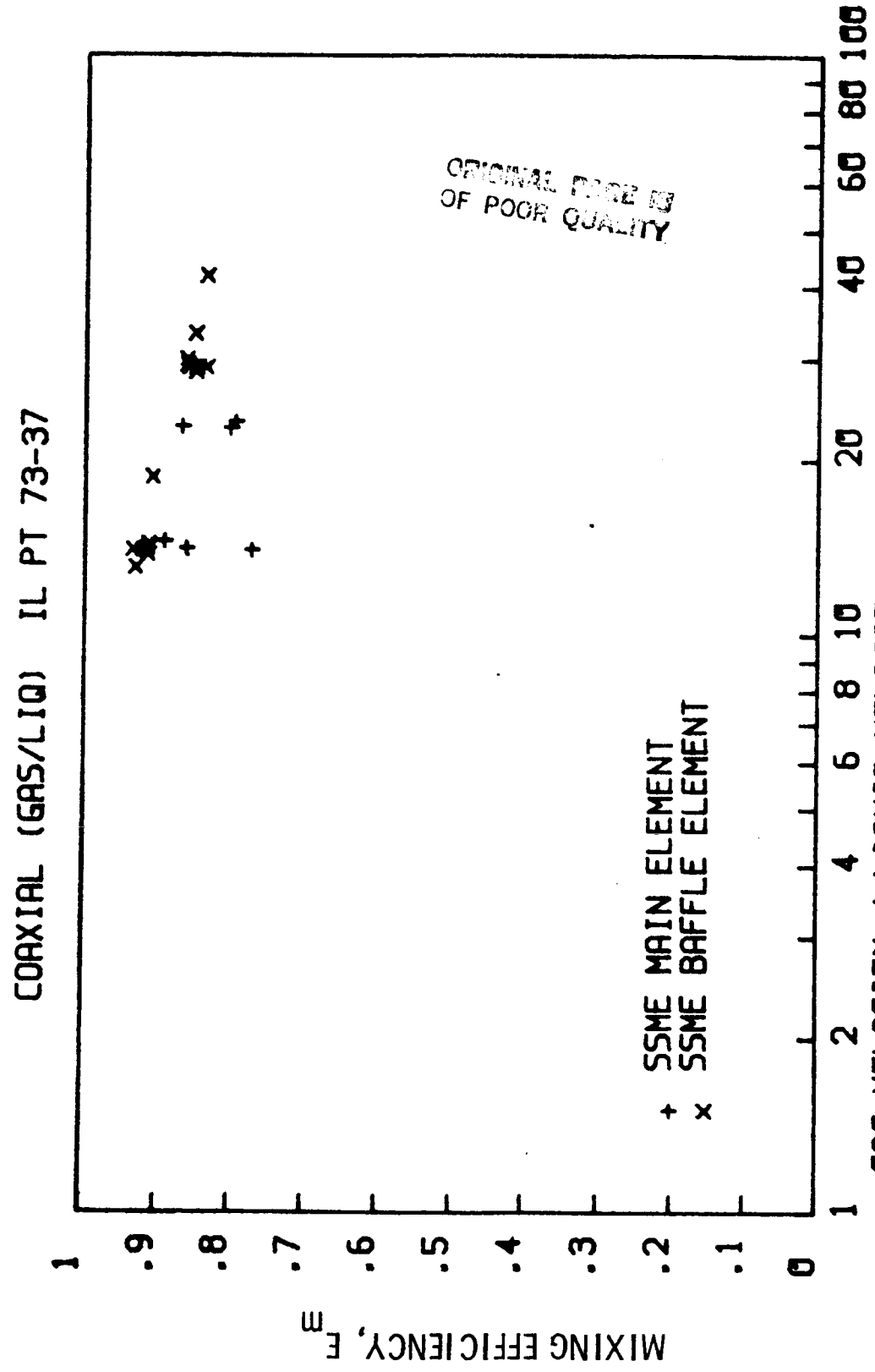

Figure 28. Mixing Efficiency for Coaxial Elements (IL PT 73-37) Depicting Velocity Ratio Influence

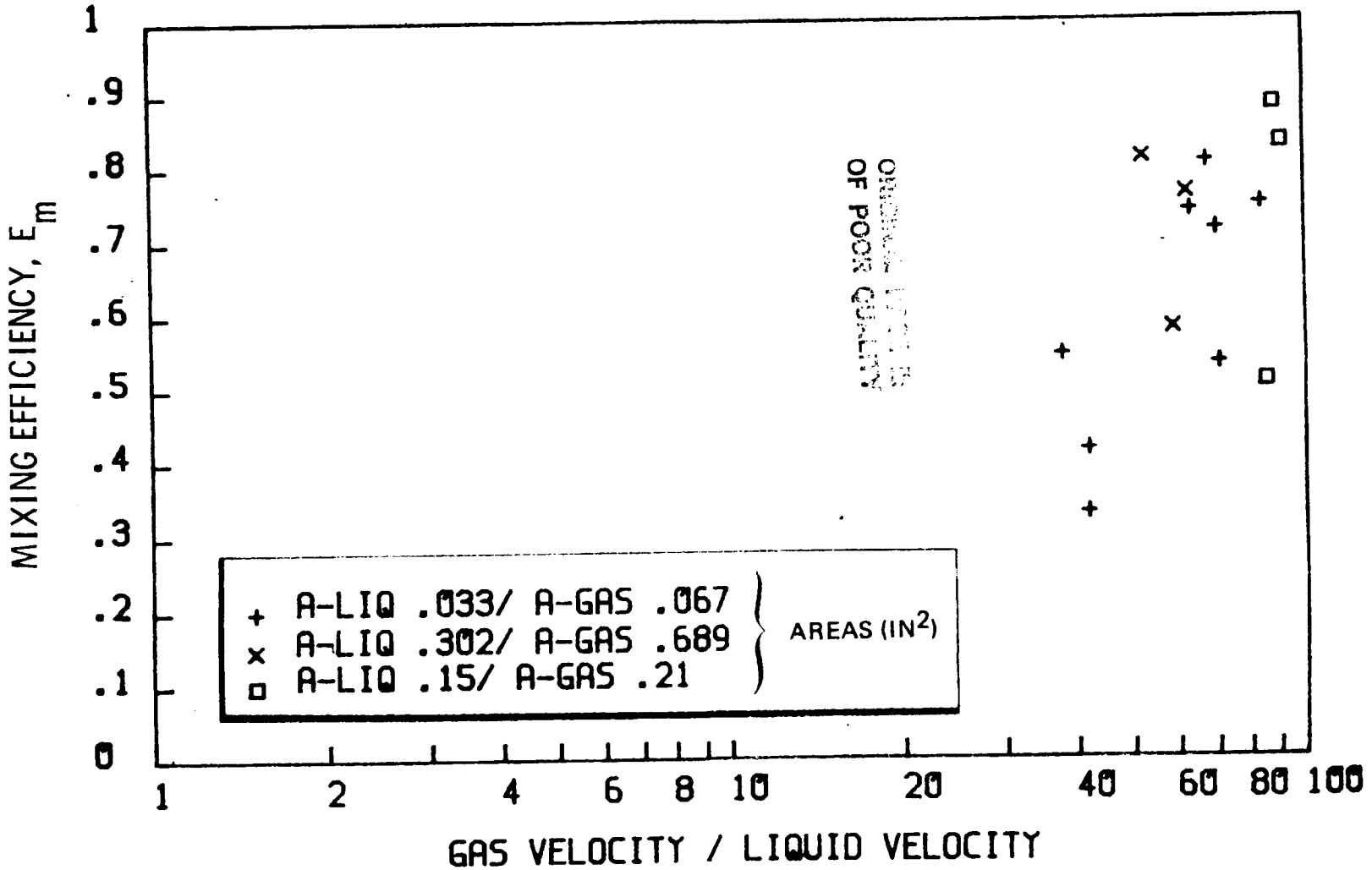

Figure 29. Mixing Efficiency for Coaxial Elements (NASA CR-72703 R-8361) Depicting Velocity Ratio Influence

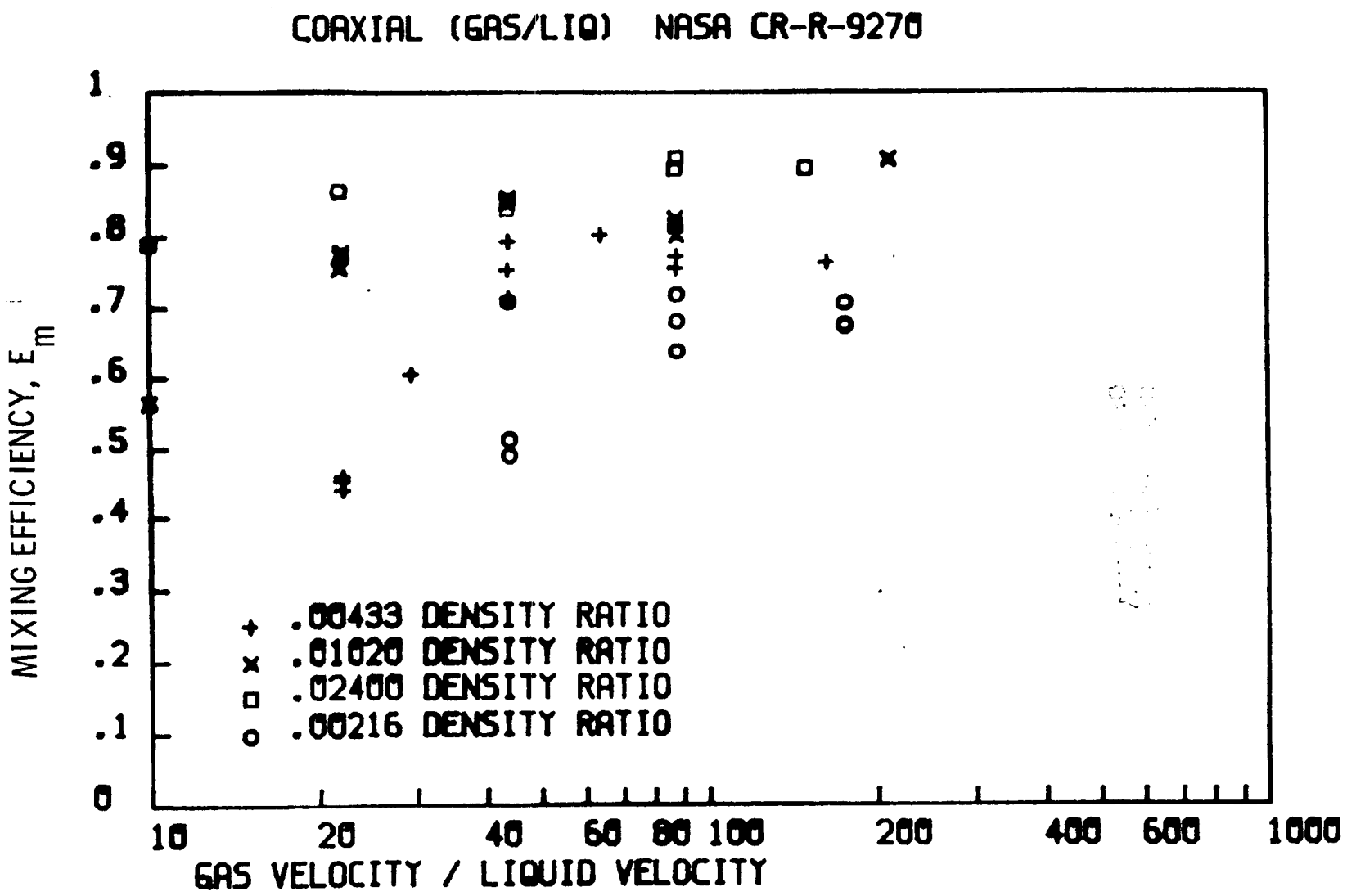

Figure 30. Mixing Efficiency for Coaxial Elements (NASA CR-R-9270) Depicting Velocity Ratio for Varying Density Ratios

as well, and clearly indicates that higher gas-to-fuel density ratios produce higher mixing efficiencies for a given velocity ratio. This relationship strongly suggests that a velocity-density product, such as momentum ratio, will not peak at an optimum value, but will approach ideal mixing as the gas momentum continuously increases. For this reason, an alternate parameter (Table 5. Eq. 8) has been considered in an effort to characterize the data with a single expression. The coax parameter (Ref. 19) was applied to the SSME preburner and main injector data as shown in Fig. 31 and 32). Because of the high overall mixing efficiency of that data, no predominant trends were evident.

LITERATURE SURVEY CONCLUSIONS AND RECOMMENDATIONS

As a result of the literature review and data examination, most of the initial impressions regarding the state of the cold flow data have been confirmed. Large discrepancies exist in test results noted between the various experimenters, and there does not appear to be any proven correlating parameters for coaxial element mixing efficiency. In general, the available data is insufficient to confidently confirm or establish the optimum value of the correlating parameters for impinging elements.

Although the gas/liquid triplet element has significant potential for future liquid-oxygen/gaseous-hydrocarbon propulsion systems, very little quantitative data exists to either support design calculations or provide correlating expressions for combustion modeling. Most hydrocarbons considered for advanced booster applications will be delivered to the injectors as warm or hot gas with densities relatively high as compared to hydrogen or combustion gases used in current concentric element injectors. This higher density favors impinging elements rather than the concentric element. The gas annulus gap required for the denser fuels in a coaxial element injector may approach small absolute values that ultimately result in poor concentricity and element contamination problems. Greater emphasis should be placed on obtaining mixing data on gas/liquid impinging (especially triplet) elements.

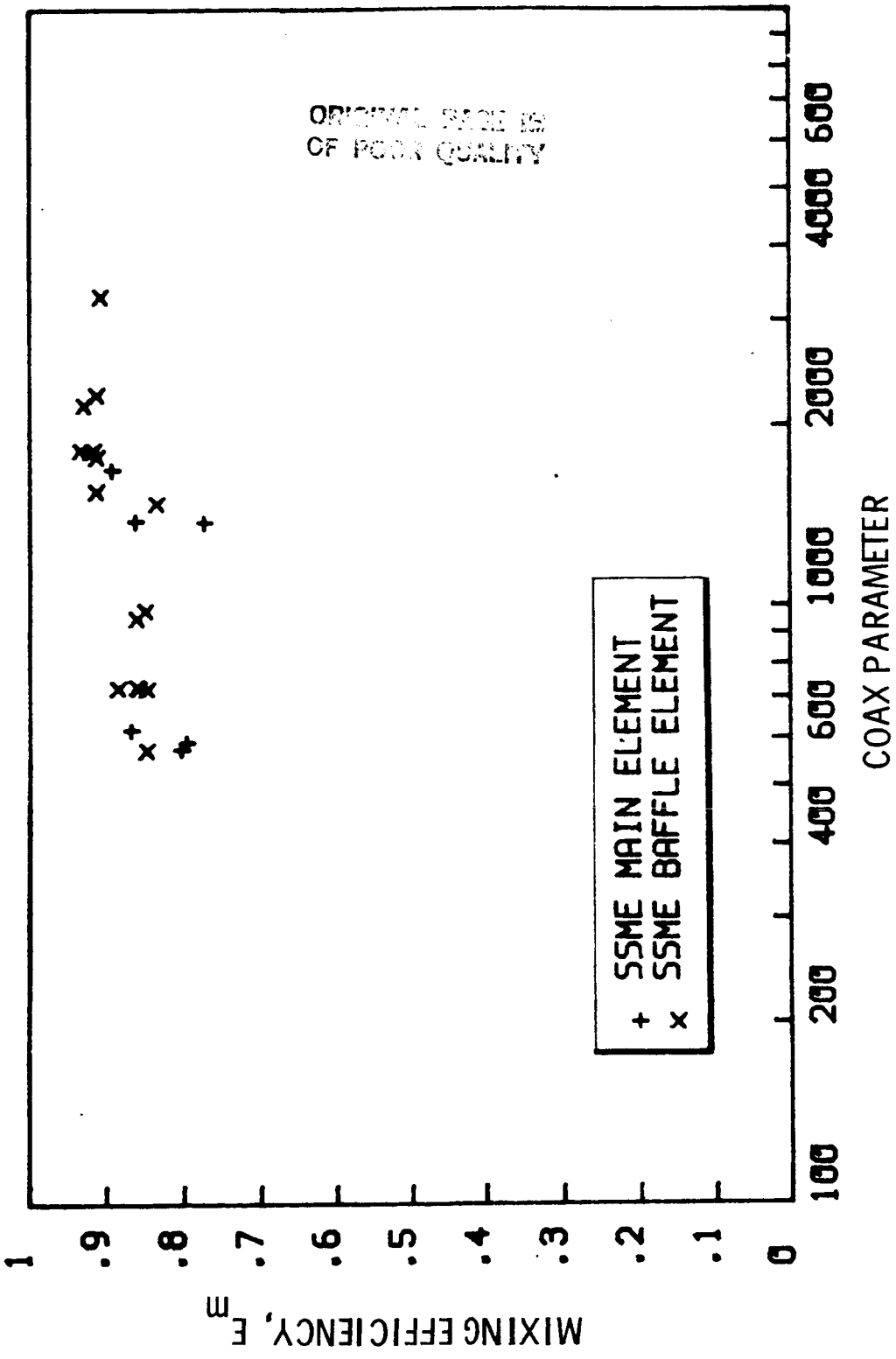

Figure 31. Mixing Efficiency for Coaxial Elements (IL PT 73-37) Depicting Falk and Burick Parameter Influence

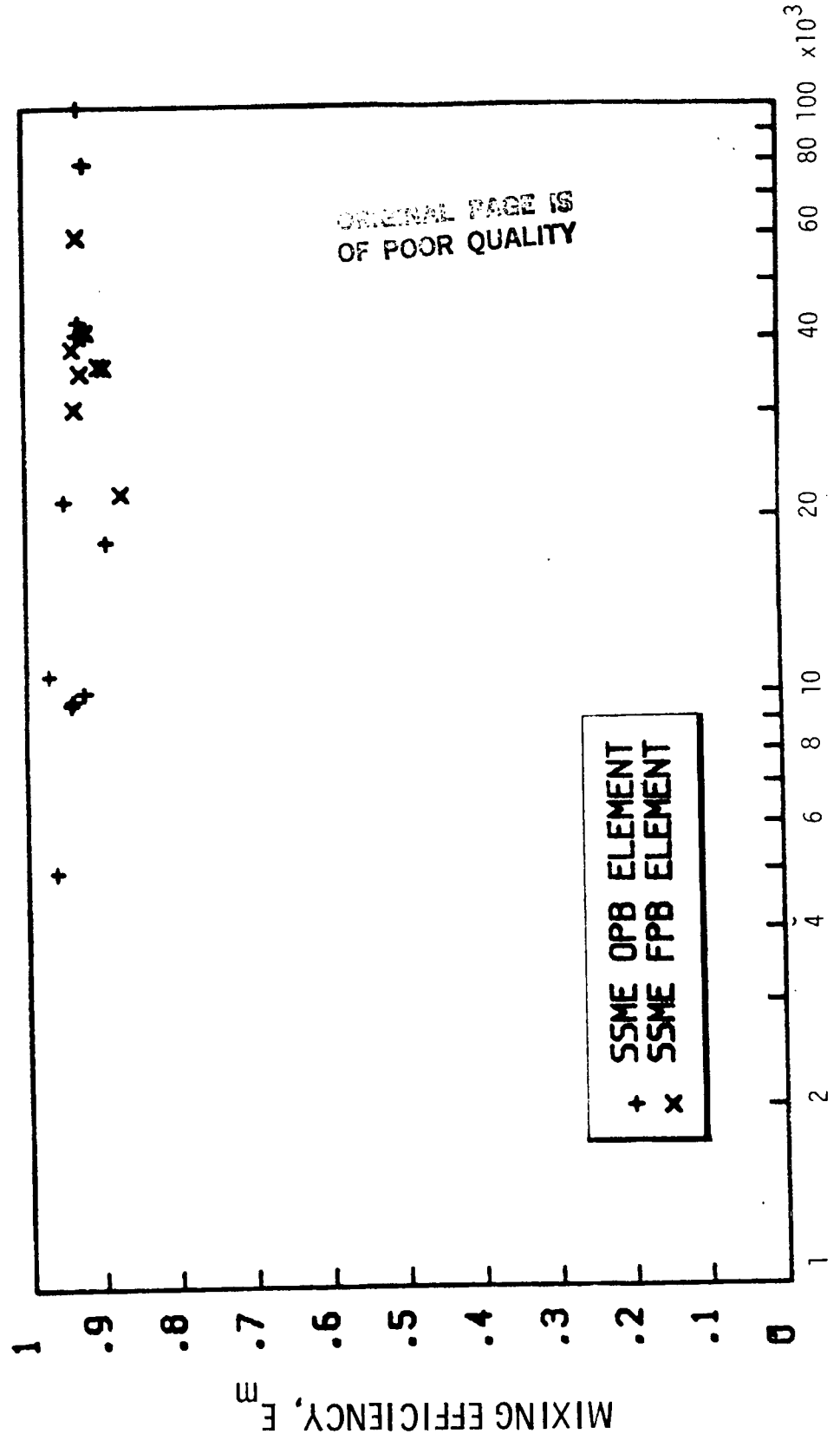

Figure 32. Mixing Efficiency for Coaxial Elements (IL PT 73-30) Depicting Falk and Burick Parameter Influence

COLD FLOW MIXING TESTS

A series of single element, cold flow, mixing tests were performed to (1) establish the validity of the correlating parameters as predictors of mixing efficiency, and (2) to define the mixing characteristics of particular LOX/hydrocarbon injector designs. These tests were performed in the Rocketdyne Engineering Development Laboratory and are described in detail herein.

Injector Elements

Test hardware for liquid/liquid and gas/liquid cold flow testing was designed and fabricated at Rocketdyne under Task II program objectives. A set of manifolds and replaceable single-element injector inserts were fabricated per Fig. A-1 (Appendix A). The physical data for each element, as well as the applications, operating ranges, and design rationale are presented in Table 7.

Specific selections and sizing of preburner element types were based on a subscale hot-fire evaluation program conducted by Rocketdyne under NASA contract NAS8-33243 (Ref. 32). A wide range of 2-inch diameter LOX/hydrocarbon preburner injectors were fabricated and hot-fire tested, which included (1) a fuel-rich LOX/methane coaxial element, (2) a fuel-rich LOX/RP-1 triplet, (3) a fuel-rich LOX/methane triplet, (4) a fuel-rich LOX/methane pentad, and (5) an oxidizer-rich LOX/methane pentad. Based upon those tests, several larger subscale preburners were selected for fabrication and delivered to NASA.

Main injector gas/liquid coaxial elements for LOX/methane and LOX/propane propellant combinations were derived from design criteria or analyses performed by Rocketdyne under NASA contract NAS8-33206. Under this program (Ref. 33), a high-performance LOX/methane main injector was designed, fabricated, and delivered to NASA for hot-fire evaluation.

The electro-deposited Nickel (EDNi) preburner triplet pattern was chosen because of Rocketdyne's on-going independent hot-fire research utilizing compact, high-element density injectors. The rationale for micro-orifice patterns is to achieve

TABLE 7. REPRESENTATIVE ELEMENTS CHOSEN FOR TESTING

	PATTERN	PROPELLANT	Pc (PSIA)	Tc (°R)	MR	ΔPO (PSI)	ΔPF (PSI)	INJECTOR ELEMENT SELECTION: ORIFICE DIA. (IN) OX	ORIFICE DIA. (IN) FUEL	ORIFICE LENGTH (IN) OX	ORIFICE LENGTH (IN) FUEL	IMPING'L ANGLE	VO FT/S	VF FT/S	FREE STREAM LENGTH (IN) OX	FREE STREAM LENGTH (IN) FUEL	REMARKS	COAXIAL ELEMENTS: OX POST RECESS (IN)	INNER TUBE I.D. (IN)	INNER TUBE O.D. (IN)	OUTER TUBE I.D. (IN)	LENGTH (IN) INNER TUBE	OUTER TUBE UNDISTURBED FLOW LGTH (IN)	INNER TUBE ORIFICE DIA (IN)
1	TRIPLET PB (FOF)	LOX/RP-1 (LIQ/LIQ)	3500	2100	.44	700	700	.0447	.055	.250 R	.239 S	60°	285	290	.250	.249	REF: RI/RD81-129 (NASA-33243)							
2	TRIPLET PB (FOF)	LOX/CH4 (GAS/LIQ)	2728	7100	.49	700	346	.045	.063	.300 R	.276 S	50°	151	402	.250	.275	REF: RI/RD81-129 (NASA-33243)							
3	PENTAD PB (FOF)	LOX/CH4 (GAS/LIQ)	1500	2100	.49	700	700	.0712	.0587	.174 S	.248 S	60°	544	544	.250	.289	REF: RI/RD81-129 (NASA-33243)							
4	TRIPLET PB (FOF)	LOX/CH4 (GAS/LIQ)	3500	2100	.44	600	850	.016	.027	.065 R	.062 R	60°	229	595	.098	.112	REF IPAD							
5	COAXIAL PB	LOX/CH4 (GAS/LIQ)	1500	2100	.49	700	700						54	634	-	-	REF: RI/RD81-129 (NASA-33243)	.2	.1955	.1955	.1935	2.3	.525	.1455 R
6	TRIPLET PB (FOF)	LOX/CH4 (GAS/LIQ)	1500	1400	.49	500	905	.015	.018		.040 R	60°	207	168	.25	.29	EL VERUM-MURFY							
7	COAXIAL PB	LOX/CH4 (GAS/LIQ)	1500	2100	.49	700	700						105	503	-	-	REF: RI/RD79-279 (NASA-33296)	.1	.182	.202	.247	2.53	.5	.086 R
8	COAXIAL PB	LOX/CH4 (GAS/LIQ)	1500	2100	.49	700	700				.035 R	60°	171	248	.25	.25	EL VERUM MURFY							
9	COAXIAL PB	LOX/CH4 (GAS/LIQ)	1500	2100	.49	700	700						104	600	-	-	SIMILAR TO ELEMENT #7	.23	.20	.23	.28	2.5	.5	.094 R

high performance in short distances and realize improved combustion gas spatial temperature uniformity across the preburner discharge.

The two liquid/liquid injector triplet elements were configured to obtain an Elverum-Morey factor of 0.66. The closeness of orifice diameter sizes at an Elverum-Morey of 0.66 products a generally high level of mixing efficiency.

Mixing Test Equipment, Procedures, and Data Reduction

The cold flow mixing tests were performed in the Atomization and Mixing tests facility of the Engineering Development Laboratory at Rocketdyne. The test apparatus consists of two separate units, one for testing liquid/liquid elements and one for testing gas/liquid elements. These apparatus and the associated test procedures are each described below for each type of test. The more general discussion of apparatus and procedures contained in a preceeding section of this report also applies to these tests. The data reduction and compilation techniques and software are presented in Appendix B.

Liquid-Liquid Mixing. The liquid-liquid mixing test facility utilizes a sample collection system consisting of a 13 by 20 sample grid of 0.318 cm square tubes as shown in Fig. 13a. This grid size thus provides resolution of the spray into 260 regions, and is a good compromise between the desired small sample size, and the practical flowrates in small tubes. This small grid size is designed espe- cially for single element tests. The sampling time is controlled by air actuated shutters that divert the flow away from this grid before and after the desired sampling period. Each of the samples is ducted to 50 milliliter graduated cylinders where the two liquids separate. The oxidizer simulant is colored to ensure readability (Fig. 13b). The quantities of each fluid are measured and subsequently input to the computer for data reduction.

Propellant simulant liquids used for these tests were 1-1-1 trichloroethane for the oxidizer simulant and water as the fuel simulant, providing a density ratio of:

$$\frac{\text{Density 1, 1, 1-trichloroethane}}{\text{Density water}} = \frac{82.6}{62.4} = 1.32$$

which is not too far from LOX/RP1 value of 1.42.

Gas-Liquid Mixing. The gas-liquid mixing measurement system has been utilized extensively at Rocketdyne for investigating hydrogen/liquid oxygen concentric elements (with the gas annulus surrounding the liquid core). The schematic of the process is shown in Fig. 14. The sample element is installed at the "head end" of a transparent, pressurized chamber, with a traversible probe mounted at the desired sampling plane. Water is used for the liquid oxygen simulant, and nitrogen gas is used to simulate the fuel. Gas density is controlled by tank back pressure. A "base bleed" gas is supplied through the injector face to minimize recirculation of droplets and partially simulate the axial gas flow present in a combustion chamber. A tracer gas (oxygen) is included in this base bleed flow to allow this local gas flow to be "calculated out" of the measured element gas flow in each sample.

The sample from the gas-liquid element flowfield is provided by the use of a sharp edge probe that is positioned in the desired sample area. The liquid spray in the sample zone is collected physically by the opening in this probe, and accumulated in a sample container over a measured time period. The gas flow flux in the sample zone is determined from the relationship between total and static pressure (corrected for the liquid in the two-phase flow). The gas measurement requires a second correction for the entrained "base bleed" flow, and the data for this correction is obtained from an "on-line" oxygen analyzer. A photograph of the test apparatus is presented as Fig. 33.

Each data point requires a sufficient time to stabilize the required readings. Concentric elements permit a reasonable assumption of circular symmetry, thus allowing a reduced number of required radial sample measurements. However, the more complex "fan" shapes of the gas-liquid triplets and pentads require careful study of the sample locations, and more numerous sample points are required to characterize these element types.

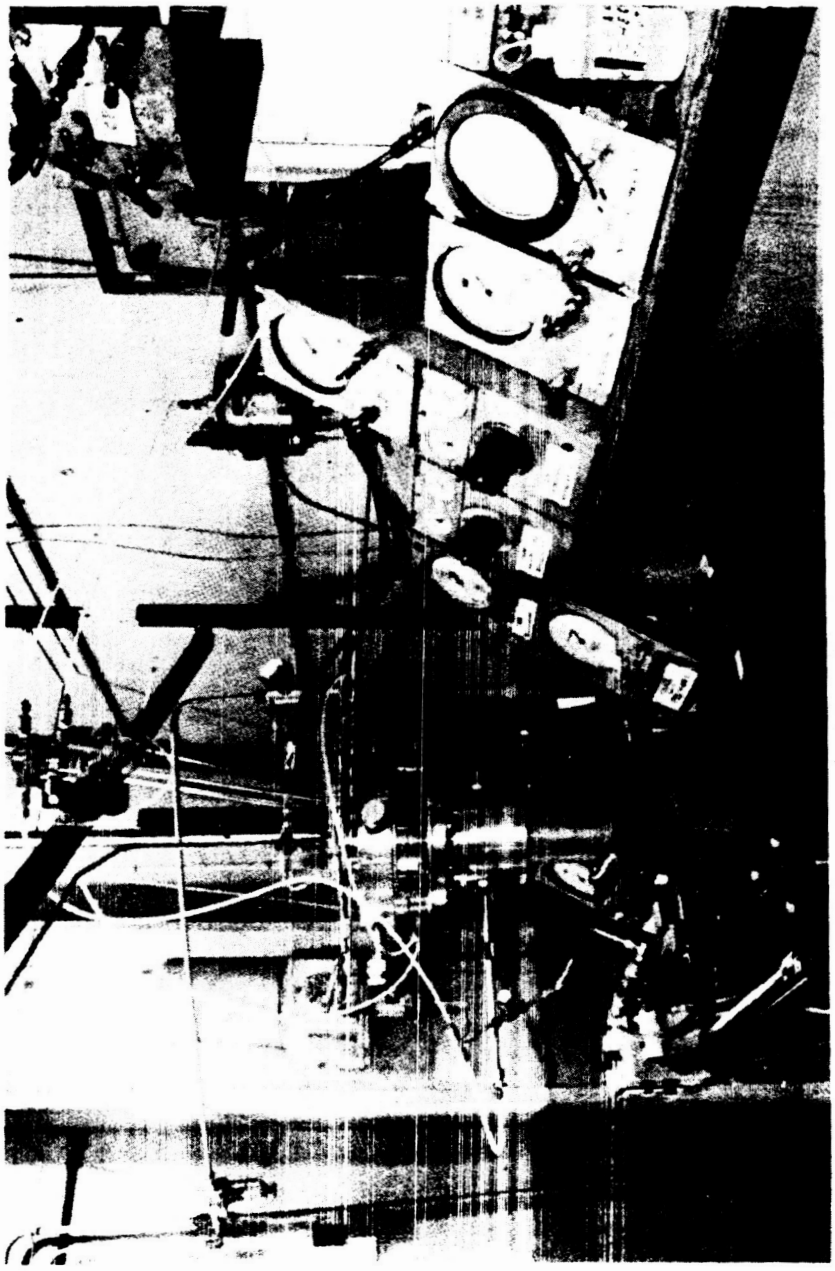

6AD42-9/28/82-C1B*

Figure 33. Gas/Liquid Mixing Test Apparatus

LIQUID-LIQUID MIXING TESTS

Test Results

Three different simulated injection elements were tested in the liquid-liquid mixing program. All of these elements were triplet configuration single-element models. Two elements (No. 1 and 6) were designed for preburner, or gas generator flowrates with "fuel-rich" design mixture ratios for low turbine inlet temperatures. Injector No. 1 was designed for a liquid oxygen/liquid RP1 gas generator, and injector No. 6 was designed for liquid oxygen/liquid propane reactants. The other element (injector No. 8) was designed as a main chamber element for a liquid oxygen/liquid RP1 reactant system. Detail dimensions of these elements are shown on Table 7.

A summary of the liquid/liquid mixing test conditions, correlating parameter values, and measured mixing efficiency is presented in Table 8. The nominal mixture ratio (NOM MR in the table) is the simulant's mixture ratio that was obtained when the simulant's injector pressure was set to provide a flow that would approximately match the momentum ratio of the real fluids at their design operating condition. Variations of approximately 20% on this mixture ratio also were tested. An attempt also was made to determine the effect of the grid location (i.e., collection distance) on measured mixing. The results for each element are discussed in detail in the following.

Triplet No. 1. Triplet No. 1 is a single element model of a fuel-rich gas generator injector for liquid oxygen and liquid RP-1, a kerosene-based liquid hydrocarbon fuel. This is a conventional triplet configuration with two fuel streams impinging on a central oxidizer stream. Fuel orifice diameters are .14 cm and they are angled inward at the traditional 30 degrees from axial. The oxidizer diameter is .116 cm and the centerline impingement distance is .64 cm from the injector face (further specifications are shown in Table 7).

Triplet No. 1 exhibited disappointing performance in the cold flow mixing tests. Mapping the mass distribution from the test results indicated significant

TABLE 8. LIQUID/LIQUID MIXING COLD FLOW TEST SUMMARY

ELEMENT	REMARKS	OXID SIM W KG/SEC	FU SIM KG/SEC	MIXTURE RATIO O/F	MOMENTUM RATIO	PENETRATION FACTOR	ELMERUM MOREY	VELOCITY RATIO	VEL HEAD RATIO	MIXING EFF (%)
TRIPLET #1 (F-O-F)	NOM MR .05 M	.0086	.028	.300	.183	2.066	2.460	.632	.531	64.57%
	+20% MR .05 M	.011	.03	.375	.287	1.649	1.565	.793	.834	66.49%
	-20% MR .05 M	.0069	.03	.230	.108	2.691	4.172	.486	.313	42.01%
	NOM MR 0.025 M	.0081	.030	.268	.147	2.307	3.059	.568	.427	50.11%
TRIPLET #6 (F-O-F)	NOM MR .05 M	.012	.048	.259	.242	1.795	1.212	.968	1.241	59.55
	+20% MR .05 M	.014	.045	.318	.364	1.465	.807	1.186	1.864	57.89%
	-20% MR .05 M	.011	.057	.188	.127	2.483	2.319	.700	.649	74.85%
TRIPLET #8 (O-F-O	NOM MR .05 M	.030	.0091	3.416	2.437	1.379	.977	.738	.721	93.59%
	+20% MR .05 M	.037	.0077	4.709	4.639	1.903	1.862	1.018	1.373	94.37%
	-20 MR .05 M	.029	.0095	3.033	1.922	1.220	.771	.655	.569	94.27%

maldistribution and nonsymmetry, indicating either a manufacturing or manifolding defect. The data should not be considered representative of triplets of this configuration, at these operating conditions. The data does demonstrate how cold flow measurement techniques can identify and quantify fabrication errors that may not be detected through normal quality control techniques.

One of the most arbitrary aspects of mixing assessment tests is the choice of the collection distance. In order to assess the importance of this choice, triplet No. 1 also was tested at a collection distance of 2 5 cm, that is, at half the previous collection distance. Flowrates were approximately the same in both tests. A 20% reduction in mixing efficiency was observed at the smaller collection distance. This one test of collection distance is insufficient to form any conclusions. However, it does indicate a need for further investigation.

Triplet No. 6. Triplet No. 6 is an element from a gas generator/preburner design for fuel rich operation with liquid oxygen and liquid propane. It is a single element model of a conventional triplet configuration utilizing two outer fuel streams impinging on a central oxidizer stream. The fuel orifice diameter is .2 cm, and the impingement angle is the traditional 30 degrees each side. The oxidizer orifice is .13 cm diameter and the centerline impingement distance is .64 cm.

The cold flow mixing test of this element indicated better symmetry than for triplet No. 1, although the mixing efficiency value was still relatively low (in the 60 to 70% range). The low mixing efficiency undoubtedly reflected the relatively large mismatch between oxidizer and fuel orifice diameters. The oxidizer orifice is too small relative to the two fuel holes (each one over double the area of the oxidizer orifice). Some minor skewing was evident in the mass distribution pattern, but it was felt that it was not particularly significant.

Figures 34 and 35 show the mass and mixture ratio contours of triplet No. 6 at two different operating conditions. Each figure set shows the front and back of the contour plot to improve the clarity. At the nominal mixture ratio this element shows evidence of the central oxidizer stream overpowering the fuel streams

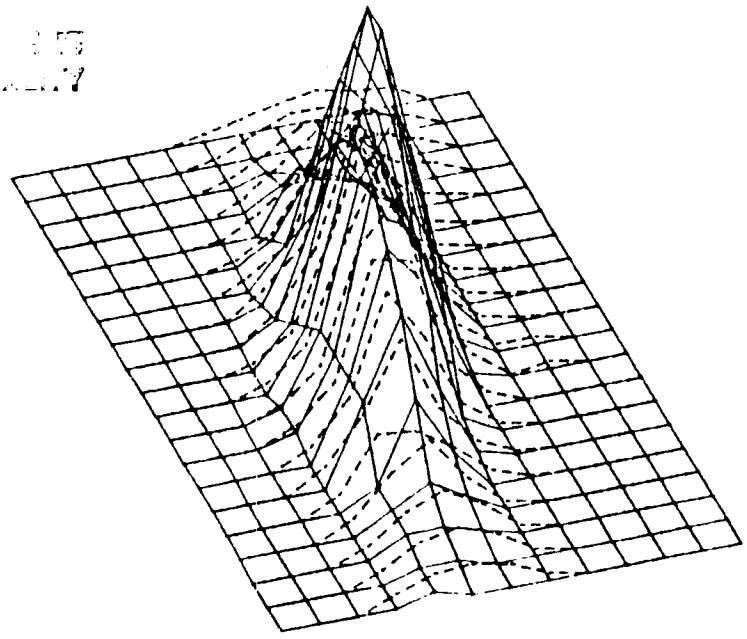

TRIPLET NO 6 NOM O/F 2IN DIST.
Oxidizer and Fuel Mass Flux (front side)
Mixture Ratio o/f .259262
Mixing Eff, Em .595469
Fuel: - - - -

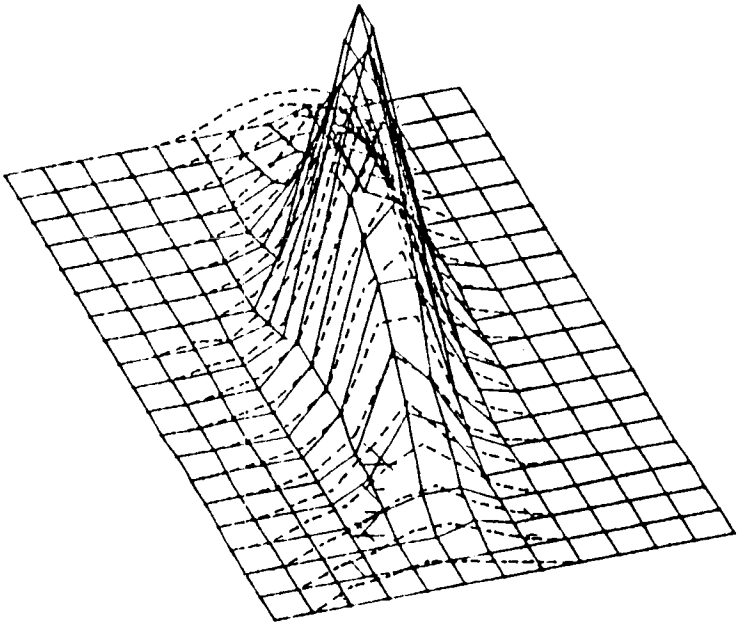

TRIPLET NO 6 NOM O/F 2IN DIST.
Oxidizer and Fuel Mass Flux (back side)
Mixture Ratio o/f .259262
Mixing Eff, Em .595469
Fuel: - - - -

Figure 34. Triplet #6 Mass Flux Distribution at Nominal Test Conditions

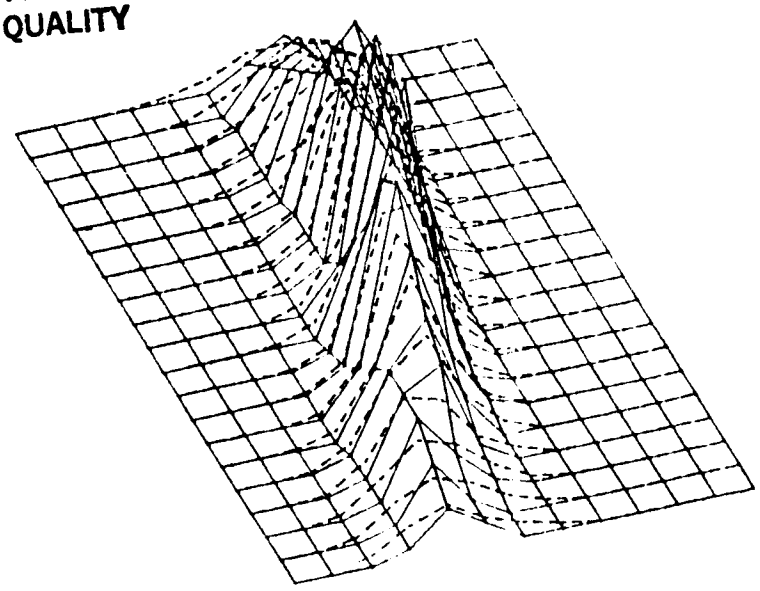

TRIPLET NO. 6, -20% O/F, 2-IN DIST.
Oxidizer and Fuel Mass Flux (front side)
Mixture Ratio o/f .187441
Mixing Eff, Em .748547
Fuel: - - - -

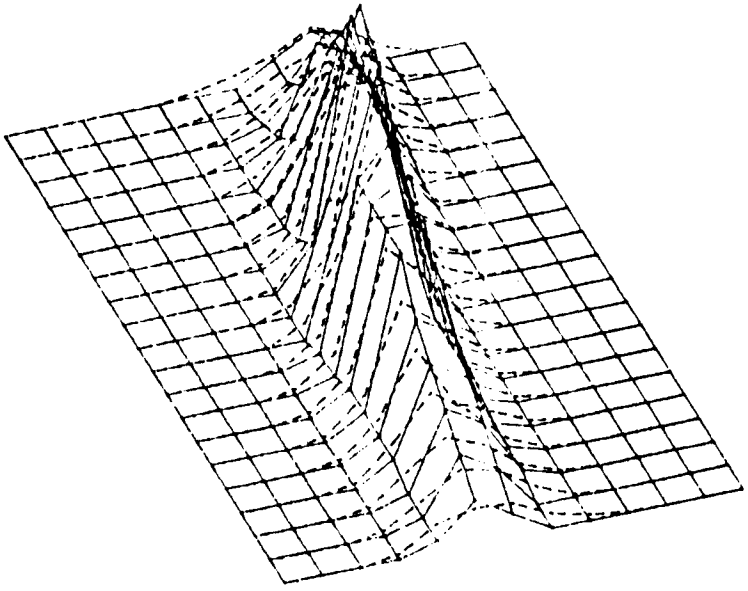

TRIPLET NO. 6, -20% O/F, 2-IN DIST.
Oxidizer and Fuel Mass Flux (back side)
Mixture Ratio o/f .187441
Mixing Eff, Em .748547
Fuel: - - - -

Figure 35. Triplet #6 Mass Flux Distributions at Below Nominal Mixture Ratio Test Conditions

producing a prominent central oxidizer, mass flux peak, and a relatively low mixing efficiency (.595). Reducing the mixture ratio by 20% results in better matching of the oxidizer and fuel mass flux distribution, as is evident in the improved mixing efficiency (.749). In the review of a new element design, these results would suggest a design change in the selected orifice diameters to optimize element performance at the design nominal mixture ratio.

Triplet No. 8. The third and last element to be tested with the liquid/liquid mixing system was triplet No. 8. Detail configuration is outlined in Table 7. The basic format is a triplet configuration geometrically similar to triplets No. 1 and 6. This unit, however, is what is generally referred to as a "reversed triplet". This description is applied to impinging elements where the two outer orifices are oxidizer streams impinging on the central fuel stream. This element is sized for main engine operating conditions with liquid oxygen and liquid RP1 propellant. The two oxidizer orifices are .165 cm diameter and the fuel orifice is .127 cm. The included angle is the traditional 30 degrees each side, with the impingement point at .64 cm from the injector face.

The "reverse" triplet, with nearly the same diameter for both oxidizer and fuel, demonstrated a high level of mixing efficiency, and an apparent low sensitivity to mixture ratio variations. A "reverse" triplet of similar configuration that was tested in an earlier IR&D test series (Ref. 5) indicated somewhat similar characteristics. The plots of mass distribution also reflect the good mixing efficiency in that the shape of the oxidizer and fuel mass distributions are very similar.

Figure 36 shows the mass and mixture ratio distribution plot for triplet No. 8. The oxidizer mass flux (solid line) and the fuel mass flux (dashed line) have similar shapes reflecting the high value of mixing efficiency (93.6%).

Liquid/Liquid Mixing Analysis of Results

The liquid/liquid test data have been plotted versus the most commonly accepted injector parameters to determine if significant correlation appears to exist. The most widely accepted parameter for liquid/liquid triplet elements is the

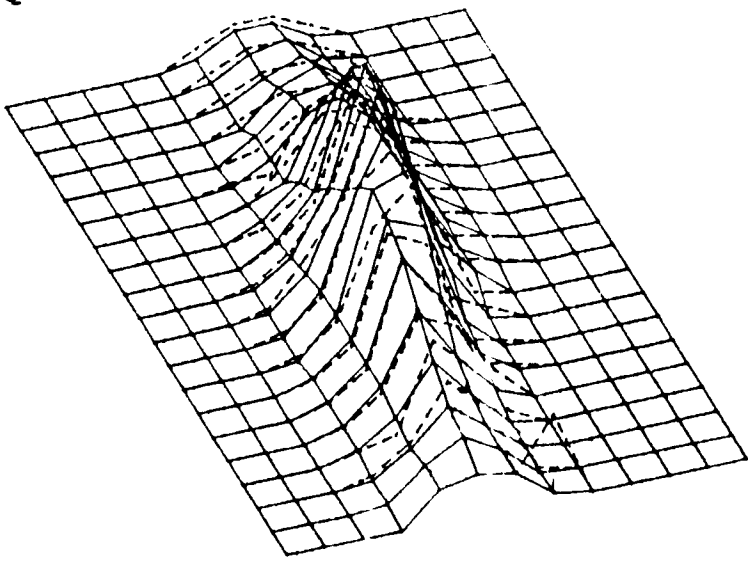

TRIPLET NO. 8, NOM O/F 2-IN DIST.
Oxidizer and Fuel Mass Flux (front side)
Mixture Ratio o/f 3.41978
Mixing Eff, Em .935961
Fuel: - - - -

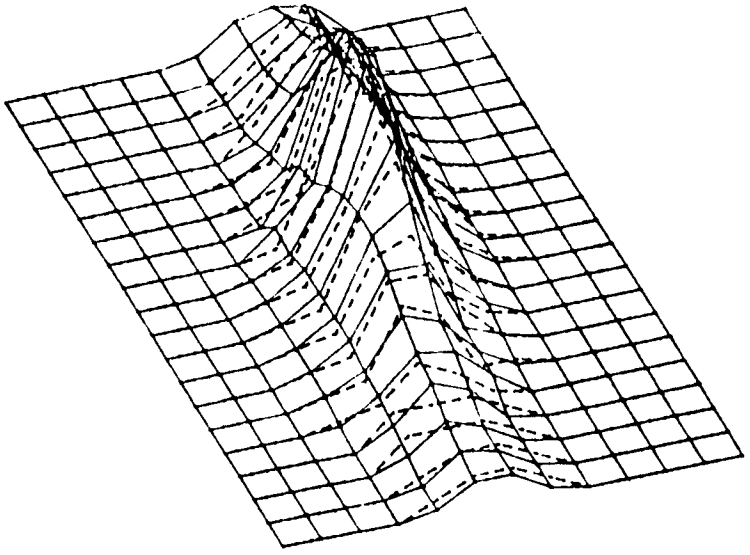

TRIPLET NO. 8, NOM O/F, 2-IN DIST.
Oxidizer and Fuel Mass Flux (back side)
Mixture Ratio o/f 3.41978
Mixing Eff, Em .935961
Fuel: - - - -

Figure 36. Triplet #8 Mass Flux Distribution at Nominal Test Conditions

Elverum-Morey parameter based on a diameter ratio modified momentum ratio. This parameter was generated by Elverum and Morey at JPL. Figure 37 shows the liquid/liquid mixing data plotted against this parameter. The purported optimum value for a triplet is .66, but this cannot be confirmed with the data obtained to date.

Also included in this series are plots of mixing efficiency as a function of mixture ratio, momentum ratio, velocity head ratio, and penetration parameter. None of these other parameters is purported to have a best value, with the exception of the penetration parameter. The penetration parameter is intended for use with two liquid streams impinging on a central gas stream, and a penetration parameter of 0.5 represents the optimum liquid penetration halfway into the central gas stream. The penetration parameter is not generally considered applicable for liquid-liquid impinging triplets.

The data plots for these parameters are displayed as Fig. 37 through 41. Although the data is very sparse, there is no obvious correlation between any of these parameters and mixing efficiency that applies to all of the three triplet elements.

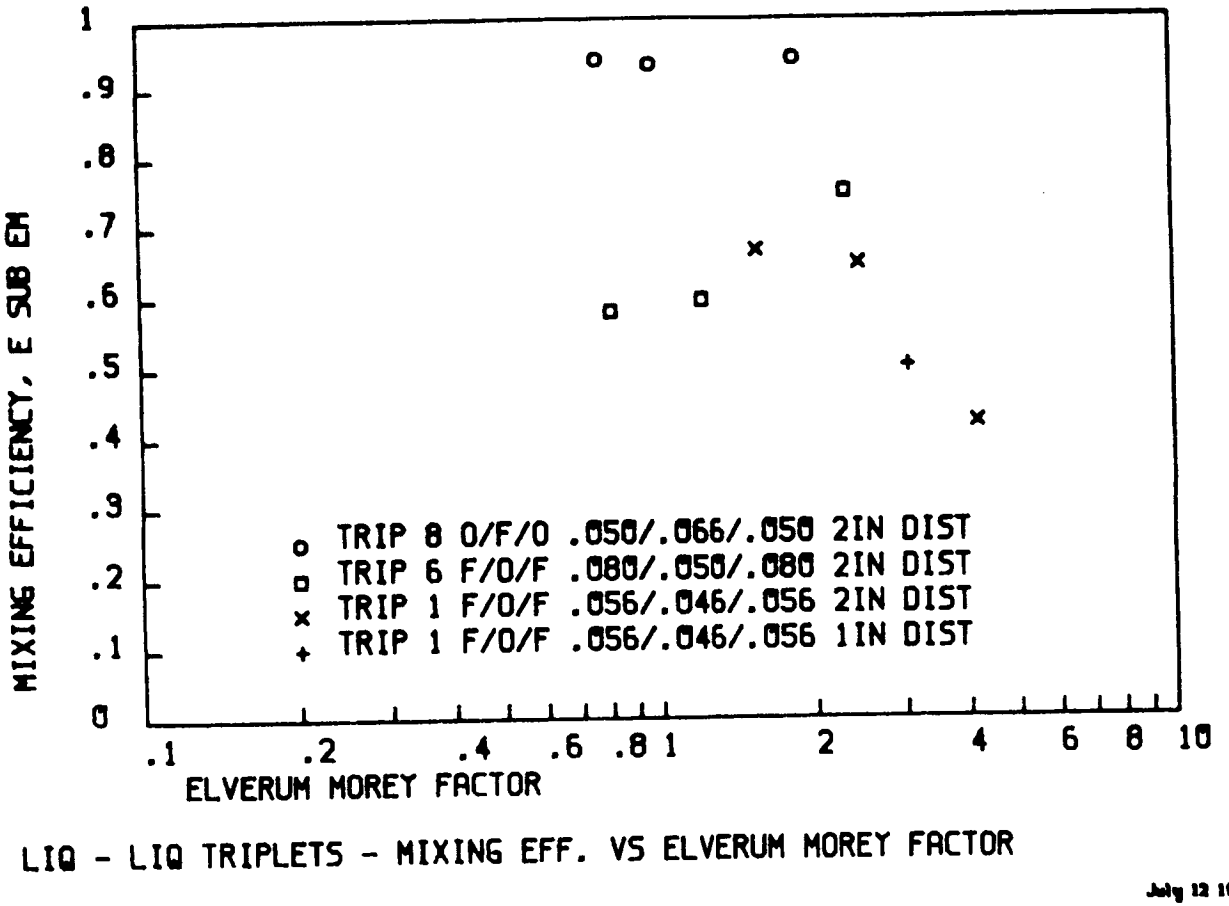

Figure 37. Liquid/Liquid Triplets - Mixing Efficiency vs Elverum Morey Factor

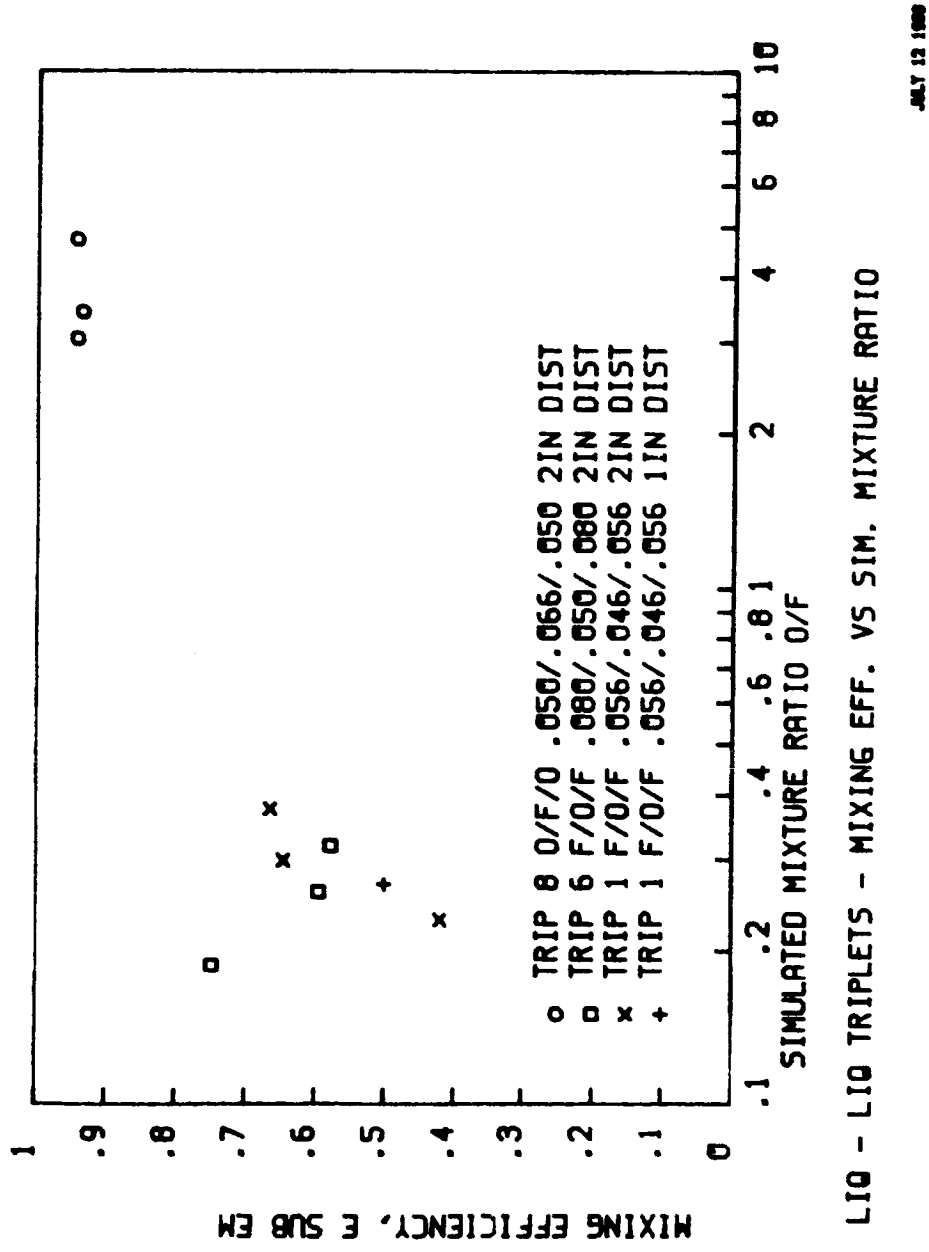

Figure 38. Liquid/Liquid Triplets - Mixing Efficiency vs Simulated Mixture Ratio

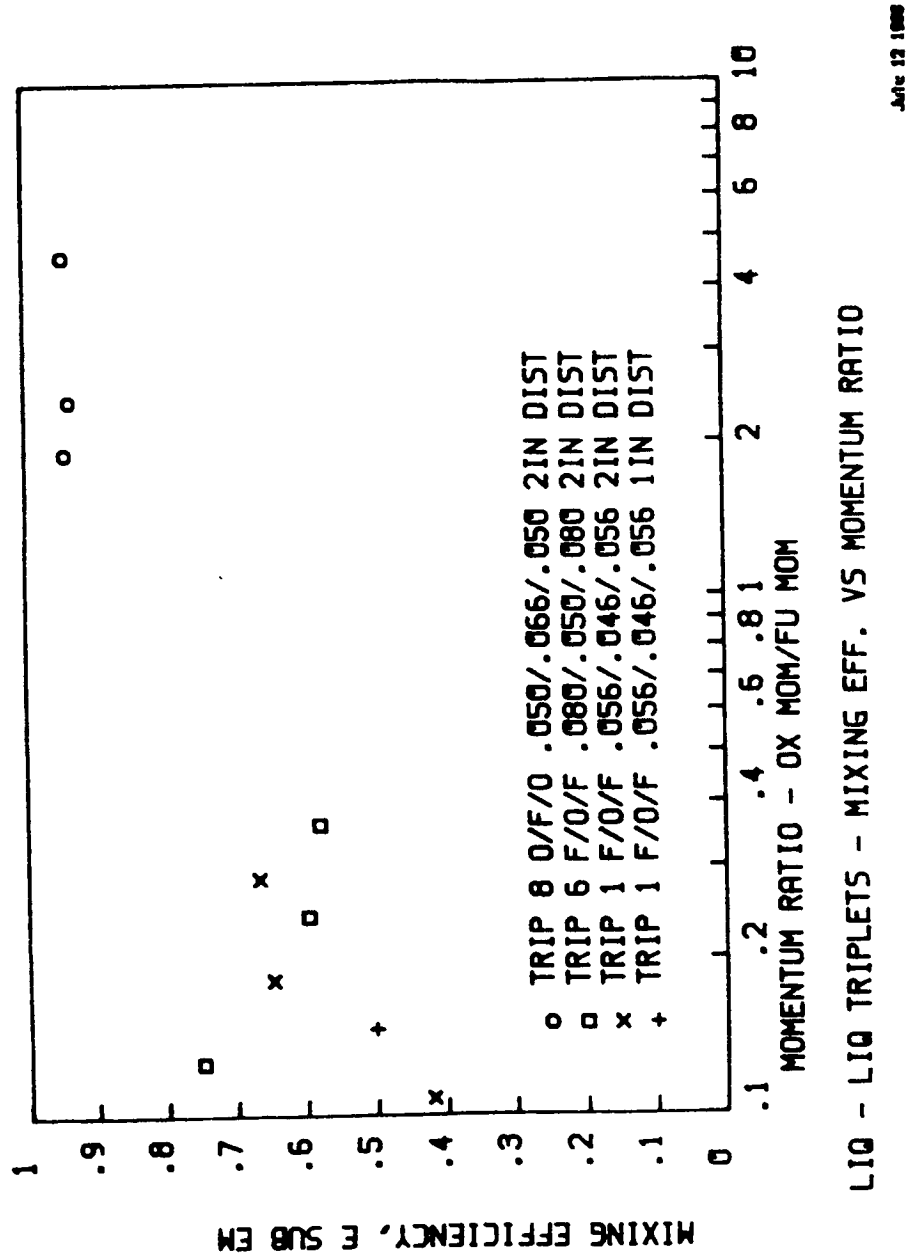

Figure 39. Liquid/Liquid Triplets - Mixing Efficiency vs Momentum Ratio

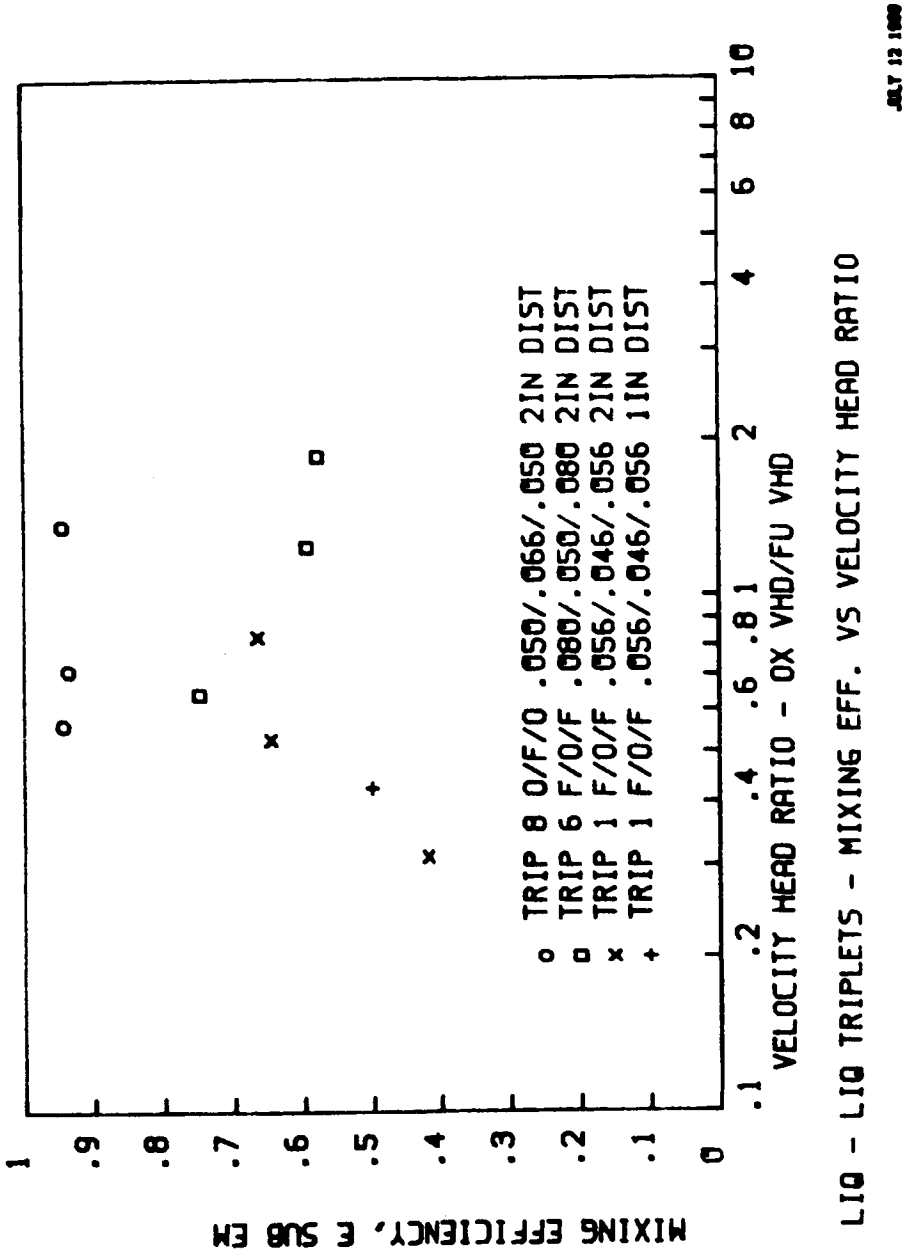

Figure 40. Liquid/Liquid Triplets - Mixing Efficiency vs Velocity Head Ratio

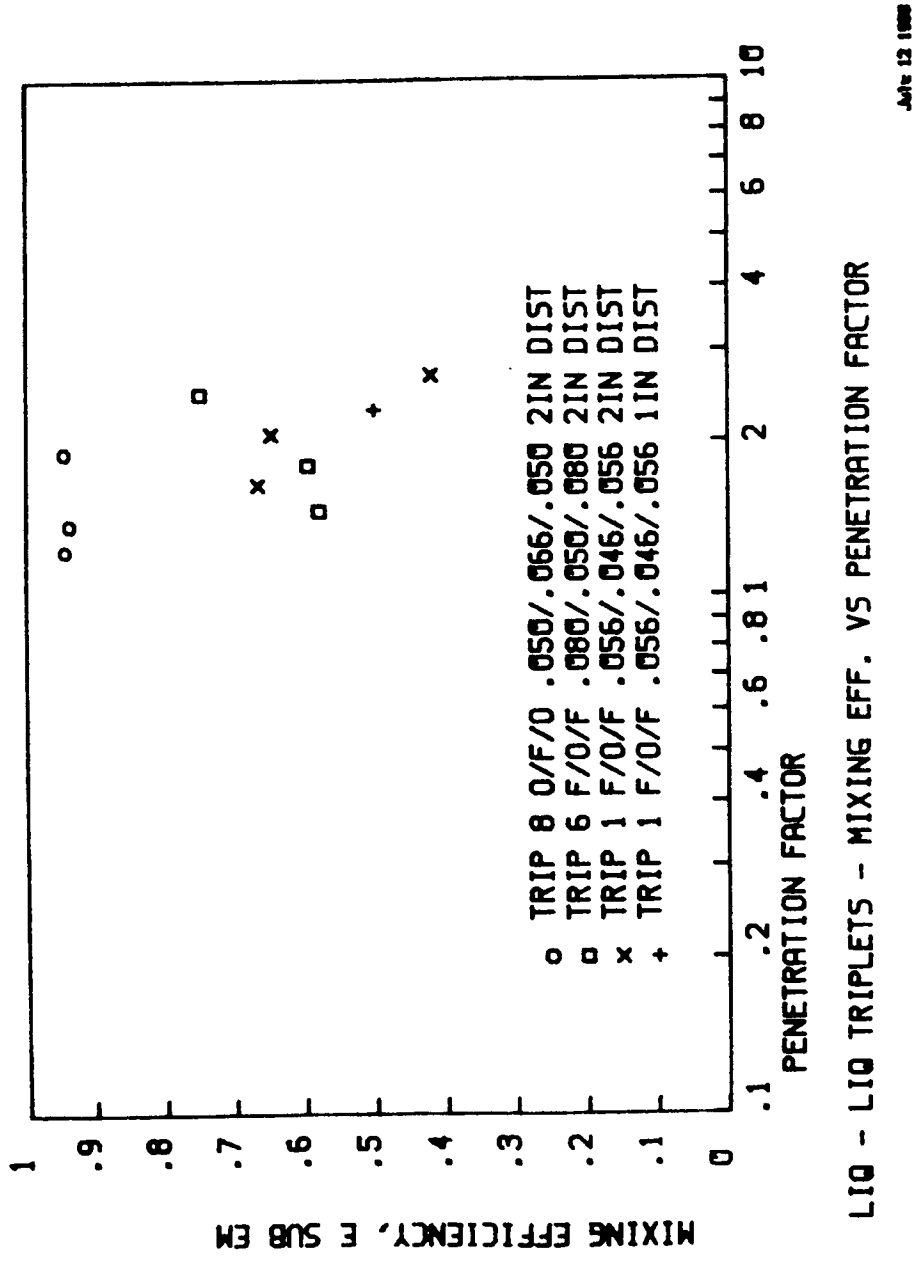

Figure 41. Liquid/Liquid Triplets - Mixing Efficiency vs Penetration Factor

GAS-LIQUID MIXING TESTS

Test Results

Three impinging elements and three coax (or concentric) elements were scheduled for the cold flow mixing tests. The impinging injectors (a pentad and two triplets) appeared to provide reasonable results. The coax element test activity was postponted, when relatively extensive testing of coax element 5 indicated serious problems. Operation at the simulated mixture ratio conditions indicated very little atomization or mixing of the liquid stream by the gas flow. This characteristic indicated problems in the assignment of equivalent flowrates for the test conditions. The test facility is not presently capable of matching the gas density of the hot-fire case, and is felt that matching either velocity ratio or momentum ratio was not truely equivalent for the coax element case. Some effort was expended in trying to establish a coax parameter, but indications were that the simulated operating points were not satisfactory. The coax element portion of this testing has been postponed until the high-pressure facility is available.

The three impinging elements were tested for a total of 12 useable tests (some additional tests were run to establish procedures). The parameters explored included mixture ratio simulations, two different sample distances, and two chamber pressures (changed gas density). Table 9 shows a detailed summary of element tests and test results, and the following section discusses the results obtained with each element.

Triplet No. 2. Triplet number 2 was conceived as a preburner injector for an engine using liquid oxygen and gaseous methane. The design mixture ratio was significantly fuel rich at .49, to provide combustion temperature suitable for turbine inlet conditions. This was a relatively conventional triplet configuration with a central liquid oxygen stream and two gaseous fuel streams (dimensional details are shown in Table 7).

The mixing efficiency of this element in cold flow testing was poor, with the distribution plots suggesting that the two fuel streams were overpowering the central

TABLE 9. GAS/LIQUID MIXING COLD FLOW SUMMARY

ELEMENT	REMARKS	BACK PRES. (kPa)	OXID SIM W (Kg/Sec)	FU SIM W (Kg/Sec)	MIXTURE RATIO (COLD FLOW) (Ox/Fu)	MIXTURE RATIO (HOT FIRE) (Ox/Fu)	MOMENTUM RATIO (Ox/Fu)	PENETRATION FACTOR (Out/In)	ELVERUM MOREY (Out/In)	VELOCITY RATIO (Gas/Liq)	VEL HEAD RATIO (Ox/Fu)	MIXING EFF
TRIPLET #2 (F-O-F)	NOM MOM RATIO, .025 M	271	.0150	.0039	3.882	.486	.181	2.078	1.985	21.417	.709	85.30%
	+20%MOM RATIO, .025 M	271	.0164	.0039	4.235	.530	.215	1.906	1.668	19.769	.844	88.20%
	-20%MOM RATIO, .025 M	271	.0132	.0039	3.412	.427	.149	2.305	2.533	24.476	.548	88.23%
	NOM MOM RATIO, .025 M	444	.0191	.0063	3.043	.489	.183	2.065	1.960	16.617	.718	82.[illegible]%
TRIPLET #4 (F-O-F)	NOM MOM RATIO, .025 M.	271	.0020	.0006	3.071	.384	.165	2.180	1.649	18.658	.937	88.73%
	+20%MOM RATIO, .025 M	271	.0021	.0006	3.357	.420	.197	1.994	1.381	17.100	1.119	79.6[illegible]%
	-20%MOM RATIO, .025 M	271	.0017	.0006	2.743	.343	.131	2.441	2.068	20.900	.746	85.[illegible]%
	+27%MOM RATIO, .025 M	271	.0017	.0005	3.063	.473	.209	1.935	1.300	14.765	1.188	79.2[illegible]%
PENTAD #2 (F-O-F)	NOM MOM RATIO, .025 M	271	.0232	.0059	3.922	.491	.123	1.746	[illegible]	30.574	.748	82.4[illegible]%
	+20%MOM RATIO, .025 M	271	.0255	.0059	4.308	.539	.154	1.590	5.343	27.846	.420	79.66%
	-20%MOM RATIO, .025 M	271	.0209	.0059	3.538	.443	.104	1.936	[illegible]	33.519	.283	90.10%
	NOM MOM RATIO, .05 M	271	.0232	.0059	3.923	.491	.128	1.746	6.09[illegible]	30.678	.348	85.23%
	NOM MOM RATIO, .05 M	444	.0295	.0105	2.805	.451	.109	1.903	[illegible].217	25.968	.292	81.[illegible]%
COAXIAL #5	NOM MOM RATIO, .05 M	271	.0154	.0050	3.054	.421	.038	N/A	N/A	81.130	.048	90.9[illegible]%
	-43% MR, .05M	271	.0087	.0050	1.730	.237	.012	N/A	N/A	143.240	.016	66.43%
	-50% MR, .05M	271	.0077	.0050	1.441	.193	.008	N/A	N/A	171.890	.011	71.94%
	-50% MR, .025M	271	.0073	.0059	1.441	.193	.008	N/A	N/A	171.890	.011	54.95%
	-62% MR, .05M	271	.0058	.0050	1.153	.152	.005	N/A	N/A	214.668	.007	70.89%
	-40% MR, .05M	444	.0092	.0050	1.838	.328	.023	N/A	N/A	81.340	.029	75.95%

liquid stream at all operating conditions. The mixing efficiency in the mid-60's does not necessarily reflect low C-star combustion efficiency, but significant macroscopic temperature striations would be expected in the combustion process. The mixing efficiency did not significantly change with mixture ratio, providing no significant clues for establishing parameters for element improvement. One test was performed at higher chamber pressure, producing only a slight change in mixing efficiency.

Pentad No. 3. Element No. 3 was a gas/liquid pentad (four-on-one) element designed for use in a liquid oxygen-gaseous methane preburner combustor, at the same basic operating conditions as the triplet element No. 2. Nominal mixture ratio was again .49 for fuel-rich turbine drive gases. A central oxidizer (liquid oxygen) stream is impinged by four gaseous fuel streams (dimensional detail is outlined in Table 7).

This element was tested over a mixture ratio range at the baseline test conditions of .025M distance from face to sample plane, and 173 kPa gage (25 psig) sample chamber pressure. Two additional tests were run to evaluate a more distant sample plane (.05M) and a higher chamber prssure (245 kPa gage). In general this element showed high levels of mixing efficiency, with the exception of the data taken at greater collection distance. The data taken at the greater distance seems to indicate greater over penetration of the gas streams further downstream in the chamber. This distance is greater than the anticipated flame front distance, and the data at the 2.5 cm plane is judged to be more representative, and was used for the majority of gas liquid testing with the impinging elements.

Triplet No. 4. Triplet No. 4 also was a preburner element design, differing primarily from element No. 2 by its physically smaller size. This element had been designed for a new fabrication process (electrical disposition) which permits low-cost replication of very small elements. This also was a relatively conventional triplet with a central oxidizer stream and two gaseous fuel streams. (Dimensional details ar given in Table 7).

This element indicated significantly better mixing efficiency than triplet No. 2 when tested over equivalent ranges. It is difficult to assess whether this higher performance should be attributed to its smaller scale, or to the fact that the diameter ratio results in higher oxidizer velocity at a given mixture ratio. The higher mixing efficiency quantitative data also is supported by the qualitative appearance of the mass distribution plot (Fig. 42), which shows the close agreement between fuel and oxidizer simulant mass flux profiles.

Coaxial Element Tests. Tentative testing with the coaxial (or concentric) elements was very discouraging, to the extent that these elements are being delayed to the second phase of testing in the higher pressure facility. The problems appeared to stem from the inability of the test equipment to simulate the high density of the gaseous fuel (methane) at high operating pressure. Both structural and supply system limitations of the gas liquid mixing facility made the simulation of gas density unattainable. Chamber pressure with this test position is limited to about 690 kPa, as compared to operating conditions in the 20.5 MPa range for the hot-fire design point.

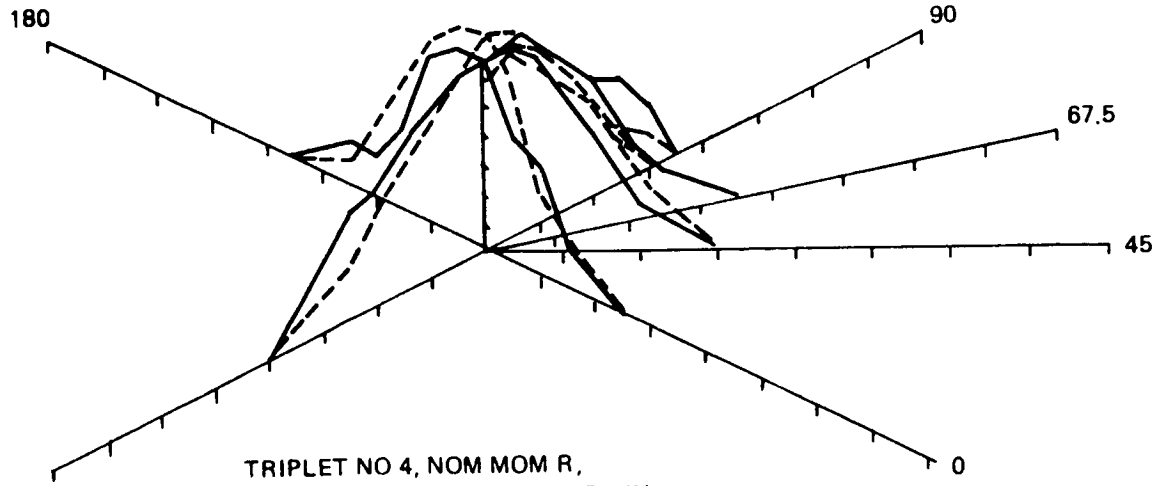

Figure 42. Triplet No. 4 NOM MOM R.

Attempting to simulate mixing conditions by velocity relationships or momentum relationships did not appear to provide the expected dispersal of the central liquid stream. The test results appeared to indicate a relatively solid central stream of liquid (Fig. 42), which overloaded the collection probe. Operating conditions were shifted in an effort to establish a rational parameter for simulation of the expected hot-fire case, but the results were inconclusive. Increasing the gaseous flowrate improved the liquid dispersion and atomization, but the parametric relationship between these test points and the hot-fire conditions were tenuous at best.

Gas-Liquid Mixing Analysis of Results

The gas liquid mixing data from the impinging elements has been plotted against the more common injection parameters, and the results are shown in Fig. 44 through 48. There is very little information available correlating the gas on liquid impinging elements with any flow parameters. The correlating parameters in general use are primarily either liquid/liquid parameters or, as in the case of the penetration parameter, designed for use with the liquid streams impinging on a central gas flow. None of the plots indicate any solid trends with any of the selected parameters. The mixture ratio plot (Fig. 44) verifies that these elements were designed for lower mixture ratios in the preburner or gas generator type operating range. The pentad, and smaller triplet were measurably above the regular triplet in mixing performance, but no pattern was evident in the data. The penetration parameter (nominally devised to describe the penetration of liquid streams into a central gaseous stream), Fig. 45, also failed to provide any useful trends when applied to the reverse case of gas streams penetrating liquid. The Elverum-Morey parameter (Fig. 46) also was disappointing, with each group of data seeming to start its own curve, with no interaction with the curves from the other elements.

The other parameters (momentum ratio and velocity head ratio, Fig 47 and 48), also show little tendency to provide a single orderly curve. The most likely conclusion from this is that the elements are too varied in geometry and design to produce a single curve. Serious parametric studies would require working with a

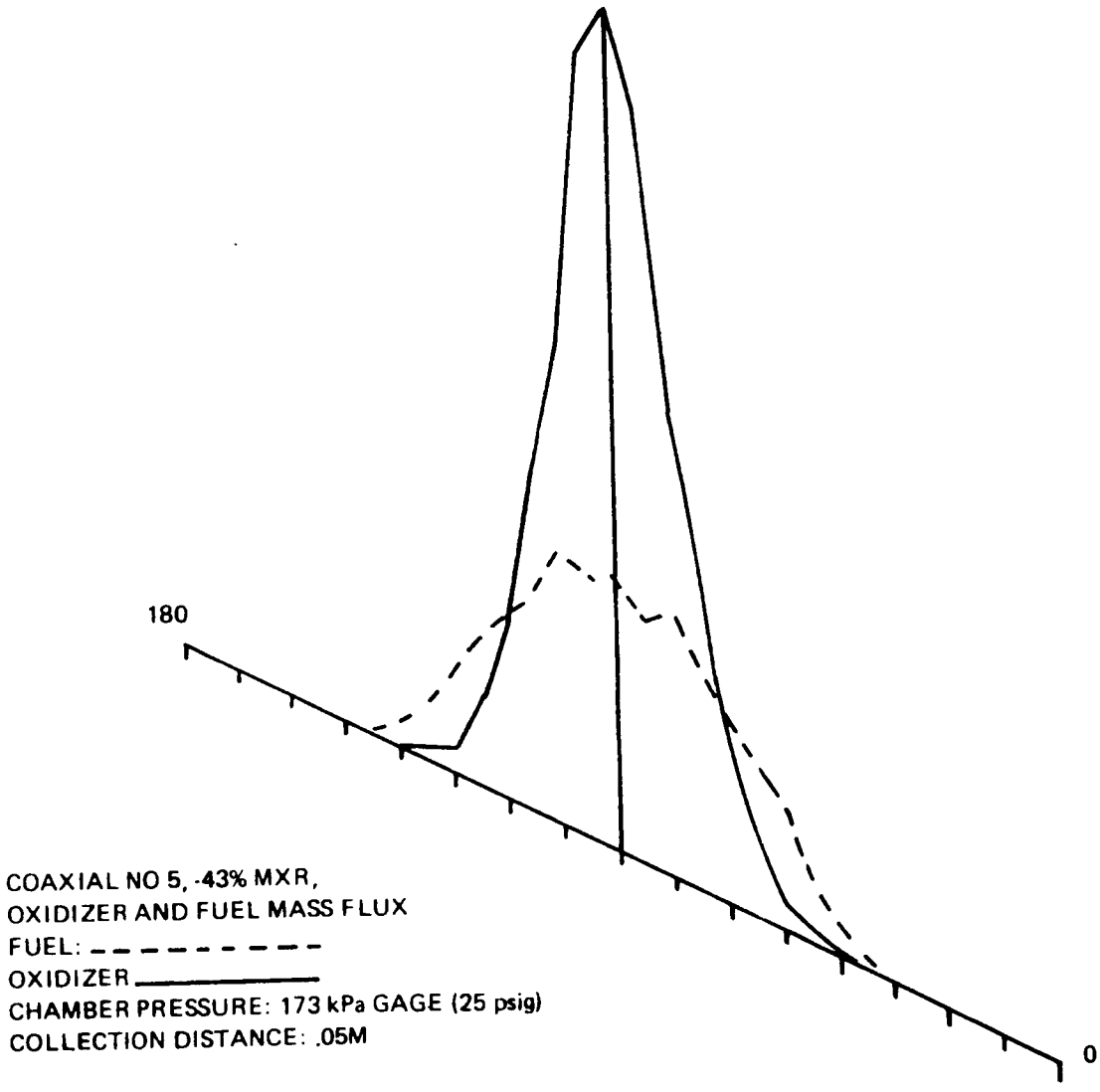

Figure 43. Coaxial No. 5 - 43% Mixture

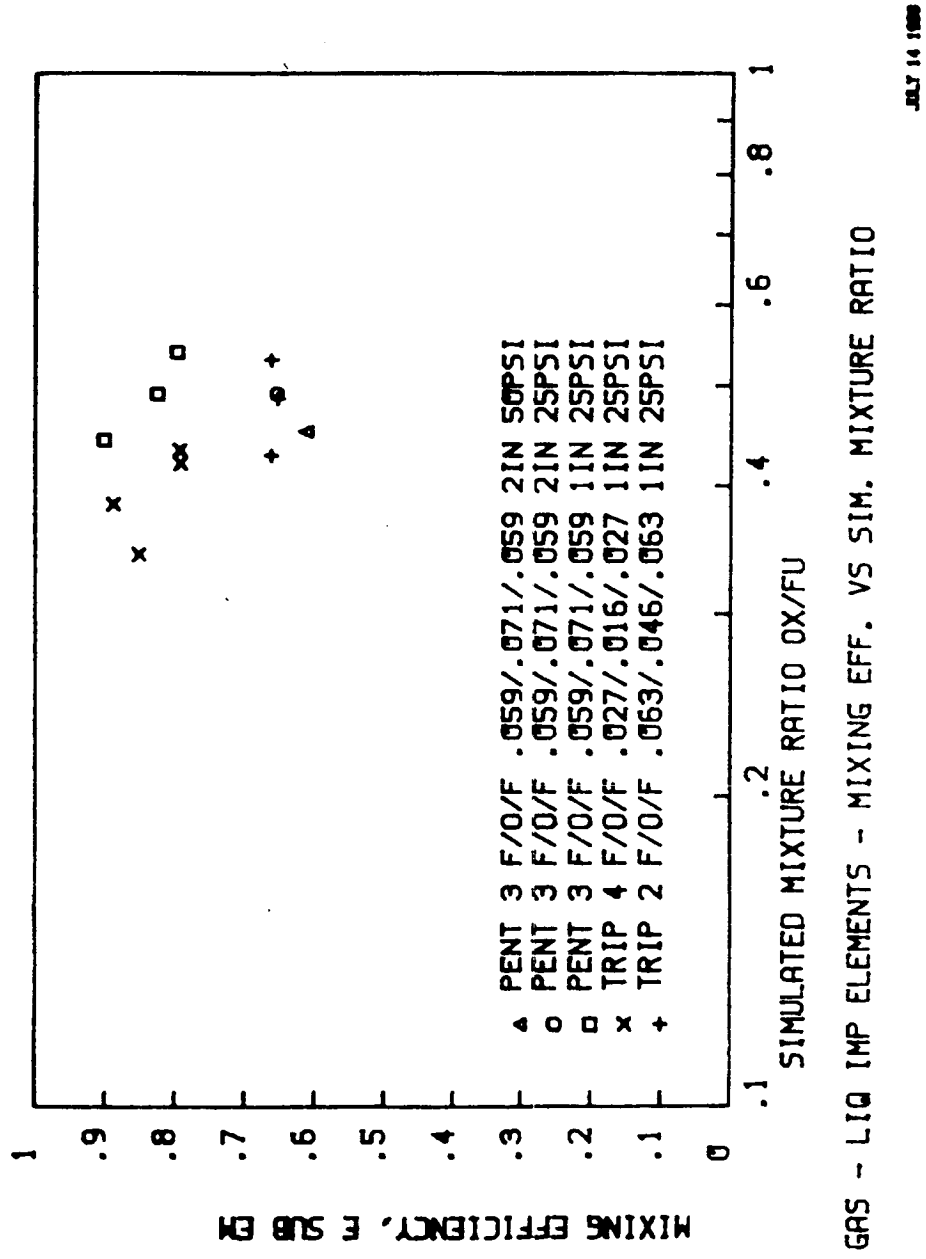

Figure 44. Gas/Liquid Impeller Elements - Mixing Efficiency vs Simulated Mixture Ratio

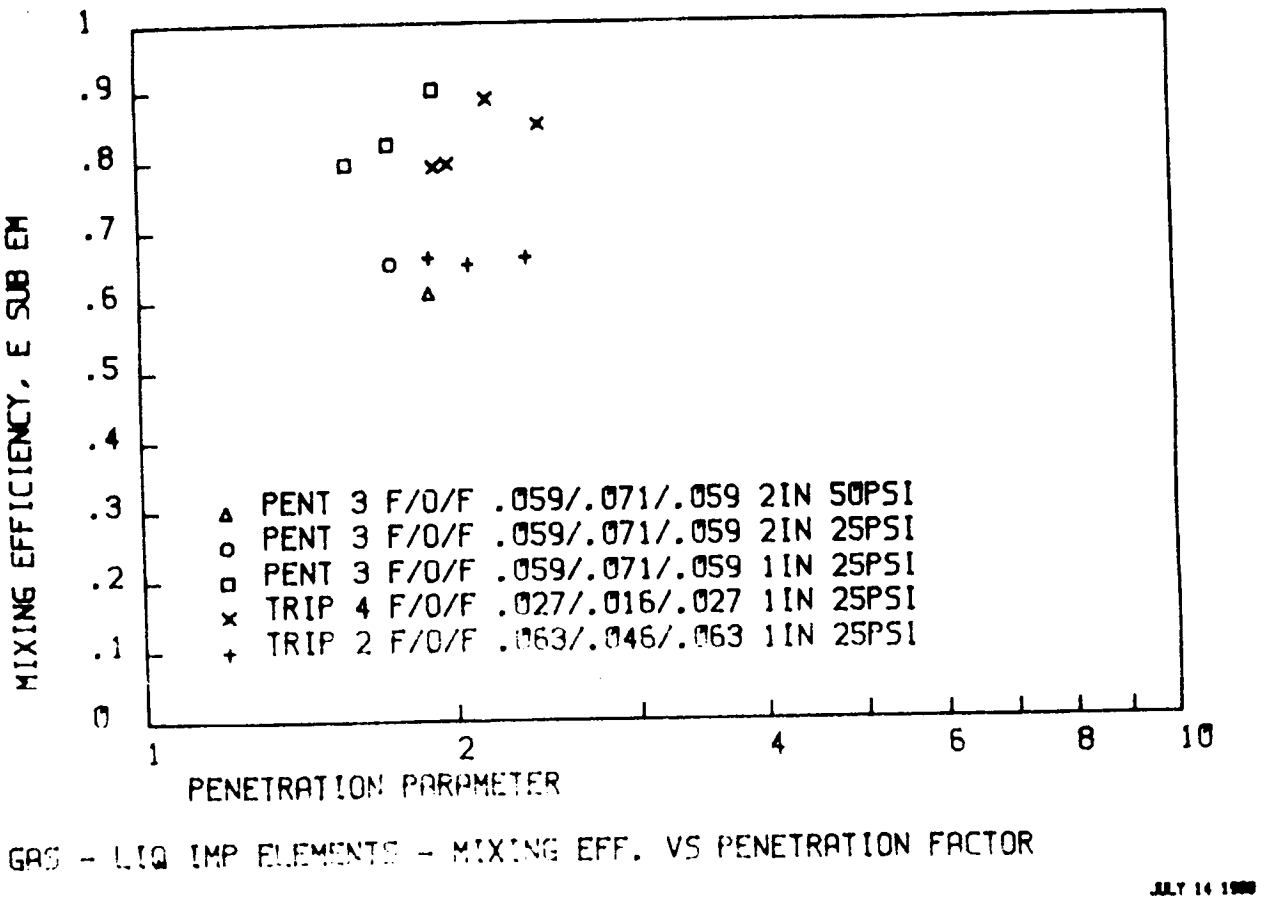

Figure 45. Gas/Liquid Impeller Elements - Mixing Efficiency vs Penetration Factor

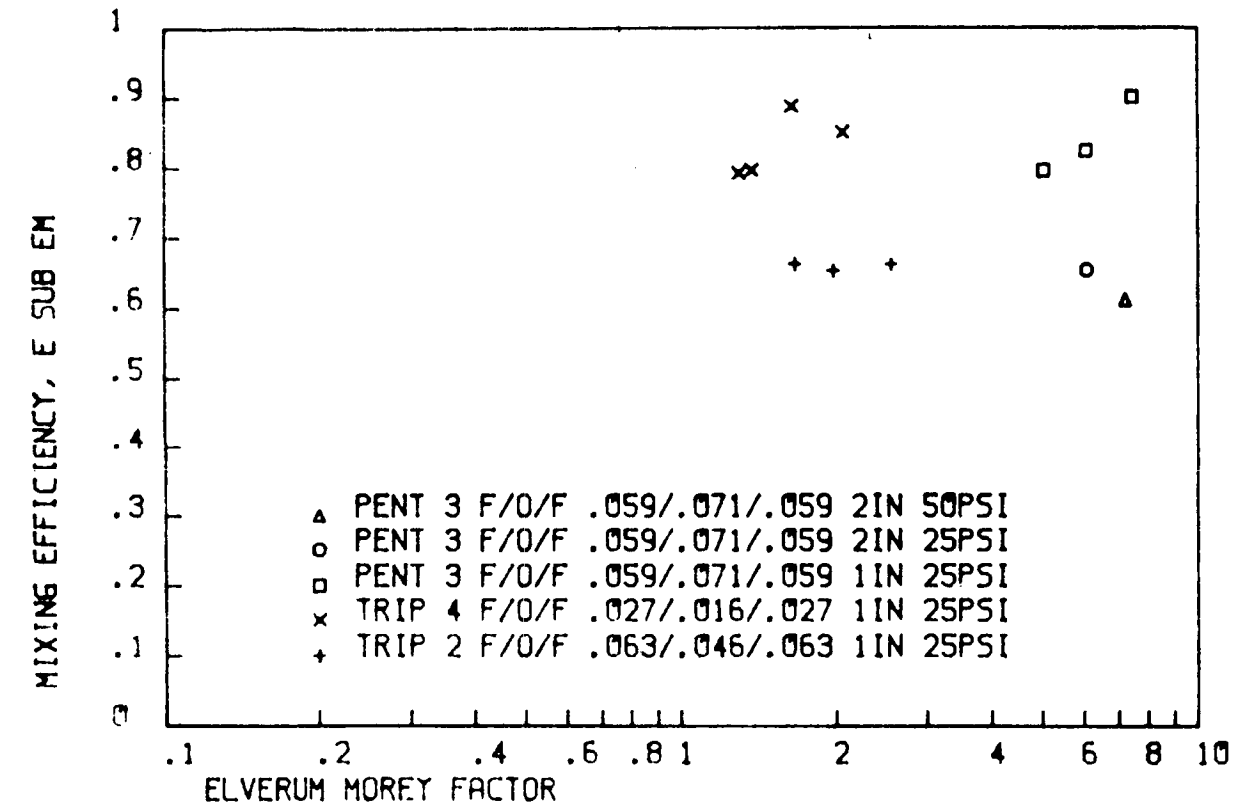

Figure 46. Gas/Liquid Impeller Elements - Mixing Efficiency vs Elverum Morey Factor

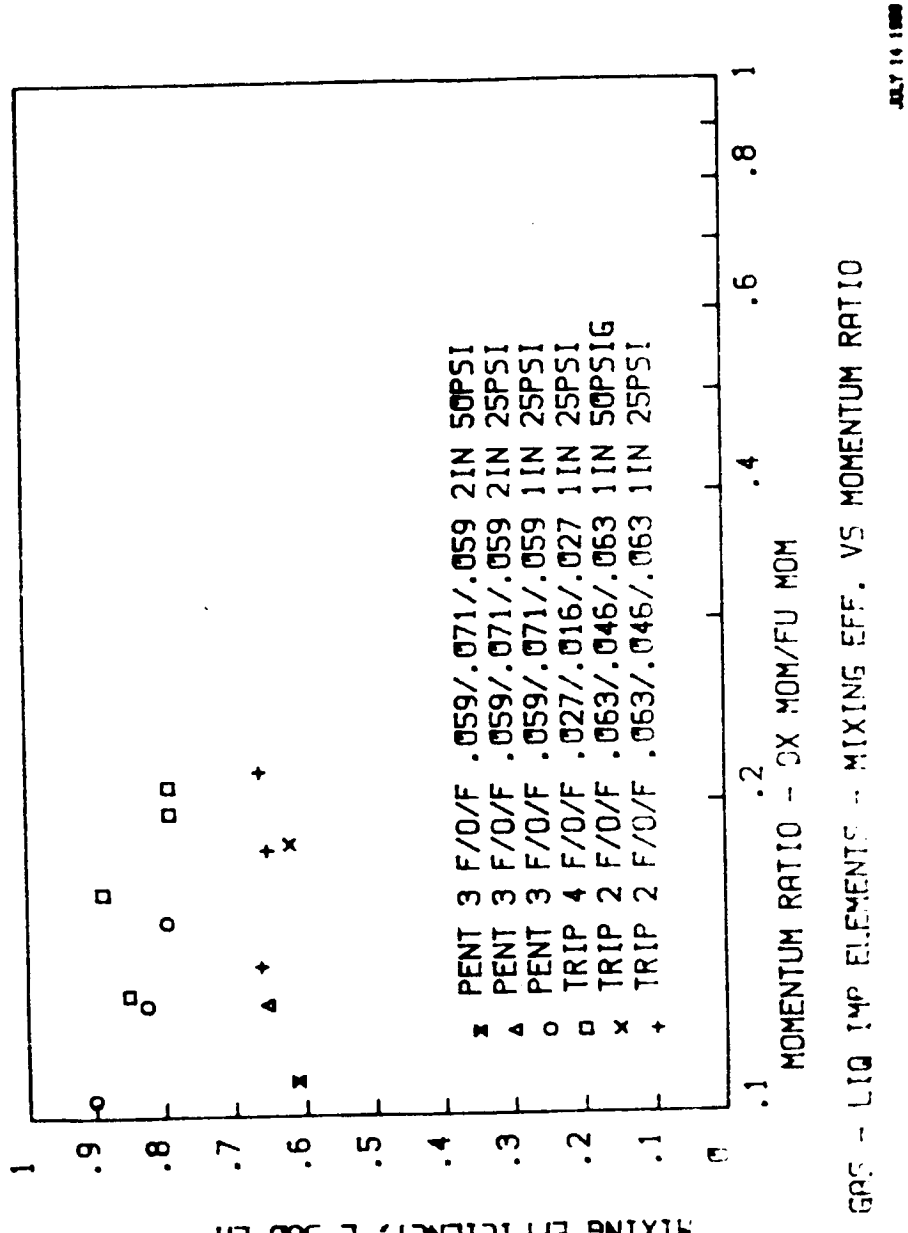

Figure 47. Gas/Liquid Impeller Elements - Mixing Efficiency vs Momentum Ratio

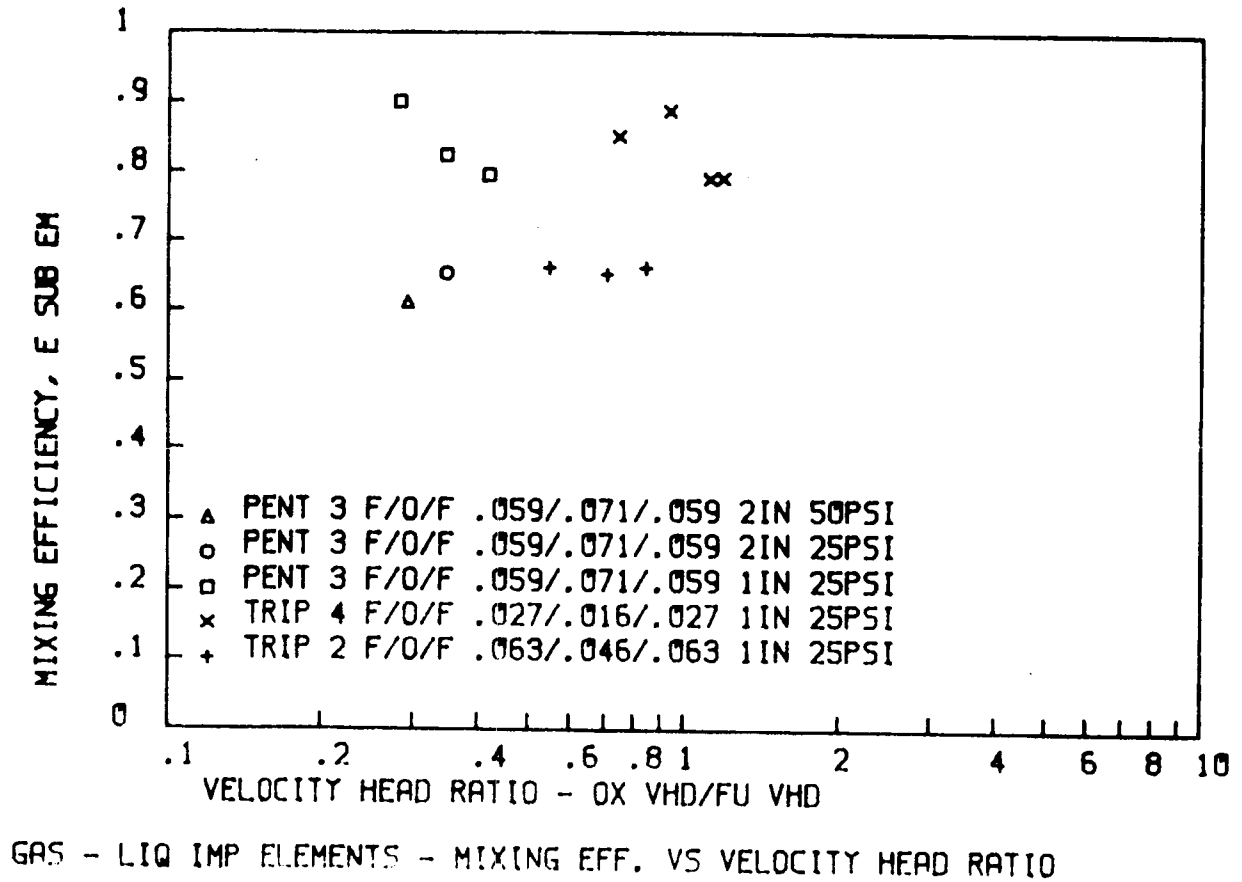

Figure 48. Gas/Liquid Impeller Elements - Mixing Efficiency vs Velocity Head Ratio

single family of elements, varying a minimum number of characteristics between elements. Minor manufacturing discrepancies appear to be capable of producing significant shifts in mixing characteristics.

The disappointing results of the coaxial (or concentric) elements resulted in reduced confidence for all the gas-liquid tests because of the inability to match reactant density values with the simulant fluids. The gas liquid mixing tests were hampered by facility limitations in simulating the gas injection density. Most of the elements selected for this test series were designed to operate with gaseous hydrocarbons at high chamber pressures. These gaseous hydrocarbons are many times denser than the hydrogen or hot hydrogen/oxygen combustion products, for which most previous data was obtained. The gas-liquid mixing chamber used in these tests was structurally limited to about 690 kPa (100 psig), and in most of these tests, the supply systems limited test operation below this value. With impinging element injectors, the most widely accepted correlation factors are based on the ratio of the stream momentums. With the diameter ratio fixed by common hardware matching momentums ratio is the most accepted method of simulation with fluid densities differing from the hot-fire conditions. In the liquid/liquid mixing tests, this was a minor correction, since the simulant density ratio was quite close to the reactant density ratio. For gas/liquid test this density ratio is significantly different.

The density of injected gaseous methane is on the order of 160-190 kg/M^3 (10 to 12 pounds per cubic foot) when the methane is employed as an engine coolant prior to injection. The maximum nitrogen gas density obtainable in the cold flow test apparatus is on the order of 9 kg/M^3 (.57 pounds per cubic foot), or a factor of 20 lower. Oxidizer to fuel density ratio for hot fire is typically 6 to one, while the lowest value obtainable in the available test hardware is 110 to one (the higher pressure test chamber now being pre- pared will be a significant improvement).

Matching the design point momentum ratio to simulate the reactive test conditions does not automatically match the other parameters. Those parameters that vary with the density ratio of the flowing fluids will end up with different values than for the hot-fire case. The various plots of mixing efficiency as a function of various parameters (Fig. 44 through 48) are plots of the cold flow parameters, using cold flow simulant mixture ratio, density ratio, etc.

MIXING TEST CONCLUSIONS

Both liquid-liquid, and gas-liquid, cold flow mixing tests were performed and the resultant data reduced for analysis. Three different triplet elements were tested in the liquid-liquid program. Two triplet elements, a pentad and a coaxial element, were tested in the gas-liquid portion of the evaluation. Two additional coaxial elements were scheduled for test, but the limitations of the test equipment has resulted in postponement of these tests, until a higher pressure facility, now being prepared, becomes available.

The liquid-liquid elements tested consisted of two elements sized for fuel-rich operation in gas generator or staged combustion preburner applications, and a "reverse" triplet sized for main chamber operating conditions. The two elements designed for low-mixture ratio exhibited depressed mixing efficiency due to the unbalance in flow and diameter ratio, while the reverse triplet indicated good mixing. Plotting the data from these three elements did not appear to support any continuous curve of mixing efficiency versus any of the accepted mixing parameters.

The gas-liquid mixing tests encompassed two triplets, and a pentad, impinging designs, and one coaxial injector. Three coaxial elements had been fabricated, but the results of the first coaxial element to be tested indicated the critical need for higher pressure testing. Therefore, the coax part of the program has been postponed until the high pressure facility is ready.

All three gas/liquid impinging pattern elements were sized for low-mixture preburner or gas generator operation with gaseous fuel and liquid oxygen. One of the triplets is a micro-orifice injector, which is characterized by a high-element density (elements per square inch) and small orifice sizes.

One of the goals of this program is to establish, or reinforce, injector correlations between mixing characteristics and injector design parameters. The primary benefit from this type of result would be to provide design guides for the selection and sizing of injector elements for new applications, and the ability to predict performance parameters of new designs prior to costly fabrication and test.

The results of the testing to date have not been particularly promising from this standpoint. These test results do not provide any high degree of correlation with any of the existing mixing parameters. Several factors undoubtedly led to this condition, and point out the difficulty in providing any sort of quantitative predictive parameter for a wide range of injection phenomena. Two of the elements tested had a significant unbalance in injection orifice diameters, as a result of operation at the extremes of mixture ratio associated with preburner and gas generator operating conditions. There also were some evidence of manufacturing or manifolding problems upsetting the symmetry of these elements.

To establish a proven injector mixing correlating design parameter requires a systematic program with duplicate configurations and redundant testing to overcome statistical spread in test results. In this manner, the random variation in geometry (e.g., misimpingement, smoothness of holes, hole entrance conditions) and flow conditions, which can be minimized but never eliminated, will be "averaged" out.

Mixing tests establish the degree of "mechanical" mixing (i.e., the mixing that occurs in the absence of combustion and combustion-induced gas motion). As such, they provide only a rough indication of the actual degree of mixing in an engine. Nevertheless, optimization of the mechanical mixing is a reasonable prerequisite for any injector design. Thus, mixing correlating parameters that can be utilized as design tools are an important technical need. The literature survey performed as a part of this effort demonstrates the lack of information regarding the mixing charactristics of, and the lack of verified mixing correlating parameters for, triplet, pentad, and coaxial elements. Thus, the need for a research program such as this is apparent.

The cold flow mixing testing has experienced a number of problems. Some of these are still being resolved and some serve as "lessons learned" and issues to be resolved in future testing. These problems and issues include (1) gas/liquid test collection efficiency deviations, (2) element imperfection effects (differences in mixing characteristics produced by "identically" constructed elements), (3) collection distance effects, (4) the need for high pressure testing, and (5) the lack, to date, of verification of the existence of, and the optimum values of mixing correlating parameters (especially for coaxial elements).

REFERENCES

1. Murthy, S.N.B.: "Turbulent Mixing In Nonreactive and Reactive Flows," Plenum Purdue University, W. Lafayette, IN, 1974
2. Evans, David D., Howard B. Stanford, Robert W. Riebling: "The Effect of Injector-Element Scale on the Mixing and Combustion of Nitrogen Tetroxide - Hydrazine Propellants," (Technical Report 32-1178), Jet Propulsion Laboratory, California Institute of Technology, Pasadena, CA 1 November 1967
3. Dickerson, R., K. Tate, N. Barsk: "Correlation of Spray Injector Parameters with Rocket Engine Performance," Rocketdyne, Canoga Park, CA, June 1968
4. Study of Droplet Effects on Steady-State Combustion (AFRPL-TR-66-152-VOL 1), Volume 1: Measured Spray Parameter Analysis and Performance Correlation, Rocketdyne, Canoga Park, CA, August 1966
5. Cheung, T.T., V. W. Jaqua: Cold Flow Investigation of Unlike Triplet Elements for Liquid Oxygen/Liquid Hydrocarbon Injectors (ITUR 80-9), 8 February 1980
6. Joshi, P., A. Jakubowski, J. Schetz: Effect of Injector Geometry on Penetration, Spread, and Structure of a Liquid Jet Injected Normal to a Supersonic Air Stream, Virginia Polytechnic Institute, September 1973
7. McHale, R. M.: Noncircular Orifice Holes and Advanced Fabrication Techniques for Liquid Rocket Injectors (NASA CR-R-9270), Rocketdyne, Canoga Park, CA, May 1974
8. Riebling, Robert W.: "Effect of Orifice Length-to-Diameter Ratio on Mixing in the Spray From a Pair of Unlike Impinging Jets," Journal of Spacecraft and Rockets Volume 7, No. 7, JPL, Pasadena, CA, July 1970
9. Riebling, Robert W.: "Criteria for Optimum Propellant Mixing in Impinging - Jet Injection Elements," Journal of Spacecraft and Rockets, Volume 4, No. 6, JPL, Pasadena, CA, June 1967
10. McFarland, B. L., V. Jaqua: Space Storable Thruster Investigation (NASA CR-7287, R-8415), Rocketdyne, Canoga Park, CA, 10 November 1971
11. Nagai, C. K., R. N. Gurnitz, S. D. Clapp: Cold Flow Optimization of Gaseous Oxygen/Gaseous Hydrogen Injectors for the Space Shuttle APS Thruster AIAA/SAE 7th Propulsion Joint Specialist Conference, Rocketdyne, Canoga Park, CA, June 1971

12. Hinde, P. T.: Basic Aspects of Gas - Mixing and Kinetics in Rocket Engine Combustion Chambers, Rocket Propulsion Establishment, Ministry of Technology, London, February 1979

13. Falk, A.Y.: Cold Flow Mixing Characteristics of the SSME Main and Baffle Elements, Rocketdyne Report No. PT73-37, Canoga Park, CA 14 February 1974

14. Paster, R. D.: Hydrogen - Oxygen APS Engines, Volume II: Low Pressure Thruster (NASA CR-120806, R-8837-2), Rocketdyne, Canoga Park, CA, February 1973

15. Nurick, W. H., R. M. McHale: Noncircular Orifice Holes and Advanced Fabrication Techniques for Liquid Rocket Injectors (NASA CR-108570, R-8224), Rocketdyne, Canoga Park, CA, 15 September 1970

16. Yost, M.: Preburner of Staged Combustion Rocket Engine, Rocketdyne, Canoga Park, CA, February 1978

17. Gill, G. S.: A Qualitative Technique for Concentric Tube Element Optimization, Utilizing the Factor (Dynamic Head Ratio - 1), Societe Europeenne de Propulsion, Vernon, France, January 1978

18. Dykema, Owen W.: Liquid Mixing of an Impinging Jet Using Immiscible Liquids (R.R. 60-28), Rocketdyne, Canoga Park, CA, 30 November 1960

19. Falk, A. Y., R. J. Burick: Injector Design Guidelines for Gas/Liquid Propellant Systems (NASA CR-120968, R-8973-3), Rocketdyne, Canoga Park, CA, May 1973

20. Buschulte, W.: Propellant Mixing By Injectors and its Efficiency Effect, 26th German Federal Republic, International Astronautical Congress of the International Astronautical Federation, 12 November 1975

21. Falk, A. Y.: Coaxial Spray Atomization in Accelerating Gas Stream (NASA CR-134825, R-9753), Rocketdyne, Canoga Park, CA, June 1975

22. Hoehn, F. W., J. H. Rupe, J. G. Sotter: Liquid-Phase Mixing of Bipropellant Doublets (Technical Report 32-1546), 15 February 1972

23. Trotter, C.: Swirling Hydrogen Jet Mixing With a Coaxial Airstream, Department of Chemical Engineering and Fuel Technology, Sheffield, England, August 1970

24. Nurick, W. H.: "Analysis of Sprays from Rocket Engine Injectors" Journal of Spacecraft and Rockets, Volume 8, No. 7, Rocketdyne, Canoga Park, CA, July 1971

25. Burick, R. J.: "Atomization and Mixing Characteristics of Gas/Liquid Coaxial Injector Elements," Journal of Spacecraft and Rockets, Volume 9, No. 5, Rocketdyne, Canoga Park, CA, May 1972

26. Fricke, Hans D., Charles J. Schorr: "Measurement of Gaseous Mixing Downstream of Coaxial And Adjacent Orifices," Journal of Spacecraft and Rockets, Volume 9, No. 8, Bell Aerospace Company, Buffalo, NY, August 1972

27. Falk, A. Y.: Space Storable Propellant Performance Gas/Liquid Like-Doublet Injector Characterization (NASA CR-120935, R-8973-1), Rocketdyne, Canoga Park, CA, October 1972

28. Analysis of Rocket Engine Injection/Combustion Processes Technical Proposal R-9668P-1, Advanced Programs, Rocketdyne, Canoga Park, CA 5 March 1975

29. Mehegan, P. F.: Two-Stage Bipropellant Injection System Studies (NASA CR-72303, R-7199), Rocketdyne, Canoga Park, CA, 30 August 1967

30. Jaqua, V., T. Yu: Coal Combustion For MHD Cold Flow Mixing Studies (ITR-76-011-C), Rocketdyne, Canoga Park, CA, 17 January 1977

31. Mehegan, Campbell, Scheverman: Investigation of Gas-Augmented Injectors (NASA CR-72703 R-8361), Rocketdyne, Canoga Park, CA, September 1970

32. Huebner, A. W.: High-Pressure LOX/Hydrocarbon Preburners and Gas Generators, (Final Report) Contract NAS8-332431, Rocketdyne, Canoga Park, CA, April 1981

33. Wheeler, D., and F. Kirby: High-Pressure LOX/Methane Injector Program (RI/RD79-278) Contract NAS8-33206

34. Nurick, W. H.: "Experimental Investigation of Combustor Effects on Rocket Thruster Chamber Performance," (RI/RD 9315), September 1973

APPENDIX A

The cold flow test hardware used in low-pressure mixing tests is presented here. Drawing 7R001670 depicts the gas/liquid and liquid/liquid element test specimens, as well as the necessary manifolds and mounting hardware.

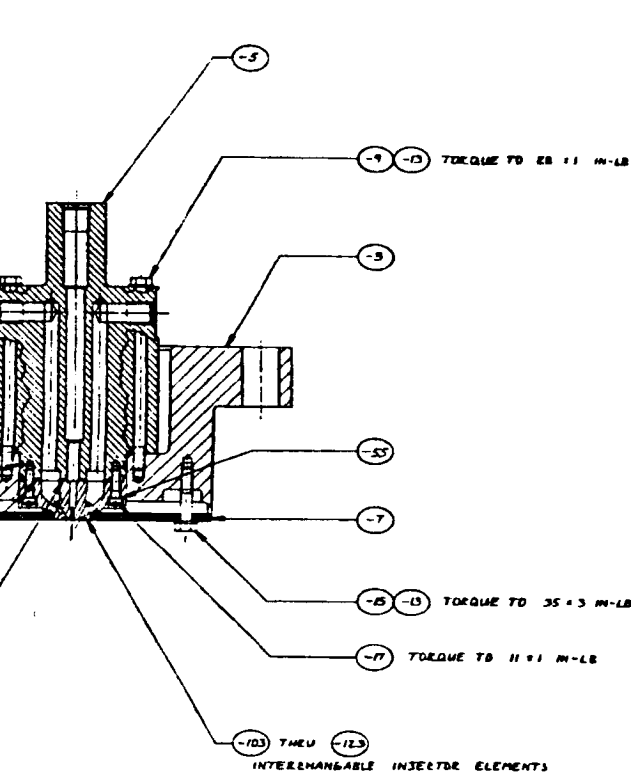

-1 ASSEMBLY
TOMIZATION APPARATUS

1	-129	COAX ELEMENT TUBE	CRES TUBE	300 SERIES	5
1	-127	COAX ELEMENT TUBE	CRES TUBE	300 SERIES	5
1	-125	COAX ELEMENT TUBE	CRES TUBE	300 SERIES	5
1	-123	COAX ELEMENT	ALUM.	6061-T6	5
1	-119	TRIPLET ELEMENT	〃	〃	〃
1	-117	COAX ELEMENT	〃	〃	5
1	-115	TRIPLET ELEMENT	〃	〃	〃
1	-113	COAX ELEMENT	〃	〃	5
1	-109	TRIPLET ELEMENT	〃	〃	〃
1	-107	PENTAD ELEMENT	〃	〃	〃
1	-105	TRIPLET ELEMENT	〃	〃	〃
1	-103	TRIPLET ELEMENT	ALUM.	6061-T6	〃

FOR INFORMATION

3	-57	O-RING SEAL	(6)	MS29512-06	5
16	-55	WASHER	CRES	MS9321-08	1.25
1	-53	BLEED PLATE	CRES	300 SERIES	2
1	-49	O-RING SEAL	BUNA-N	MS29513-155	2
1	-47	O-RING SEAL	BUNA-N	MS29513-[illegible]	2
1	-45	O-RING SEAL	(6)	[illegible]	2
1	-43	WASHER	CRES	MS9320-17	2
1	-39	NUT	CRES	RD114-1003-1012	2
6	-37	WASHER	CRES	MS9320-12	2
6	-35	BOLT	A-286	[illegible]	2
1	-33	BLEED MANIFOLD	CRES	[illegible]	2
1	-29	HOUSING	CRES	[illegible]	2
1	-27	CORE	CRES	MAKE FROM AMS-006-[illegible]	2.5
2	-25	O-RING SEAL	(6)	2-137 [illegible]	.2
2	-23	O-RING SEAL	(6)	2-[illegible]	.25
2	-19	O-RING SEAL	(6)	2-[illegible]	.2
16	-17	MACHINE SCREW	CRES	[illegible]	.25
6	-15	BOLT	A-286	[illegible]	1
14	-13	WASHER	CRES	MS9320-16	1
8	-9	BOLT	A-286	[illegible]	1
1	-7	BLEED PLATE	ALUMINUM	MAKE FROM AMS-[illegible]	1
1	-5	MANIFOLD	CRES	300 SERIES	1
1	-3	MOUNT	STL	MAKE FROM AMS-[illegible]	1
QUAN.	NO	DESCRIPTION	MATERIAL	SIZE/SPECIFICATION	WT

8. LUBRICATE FASTENERS EACH ASSY (MOLYKOTE PASTE OR EQUIV.)
(7) SEALING SURFACE MUST BE FREE OF ANY NICKS, SCRATCHES OR OTHER IMPERFECTIONS THAT WOULD IMPAIR THE SEALING FUNCTION
(6) REFER TO SPECIFIC TEST PLAN (ENG'G) FOR ACCEPTABLE SEAL MATERIAL/TEST FLUID COMPATIBILITY
5 HYDROSTATIC PRESSURE TEST -1 ASSY ONLY TO 1375 +15 -00 PSIG WITH FREON. HOLD FOR A DURATION OF 30 SEC. RELIEVE PRESSURE TO ZERO. REPEAT FOR A TOTAL OF 5 CYCLES.
4 ASSY -41 MAX OPERATING PRESSURE 100 PSIG (TANK)
3 ASSY -1 MAX OPERATING PRESSURE 915 PSIG., MAX TEMP 115°F (TANK)
2 IDENIFY PER RA0109-008
1 MACHINE PER RA0103-016

2	-11
1	-1
SH	ASSY

ACTED

TEST APPARATUS, MIXING AND ATOMIZATION TEST

E 02602 7R0016170

RI/RD83-170

A-2

2 FOLDOUT FRAME

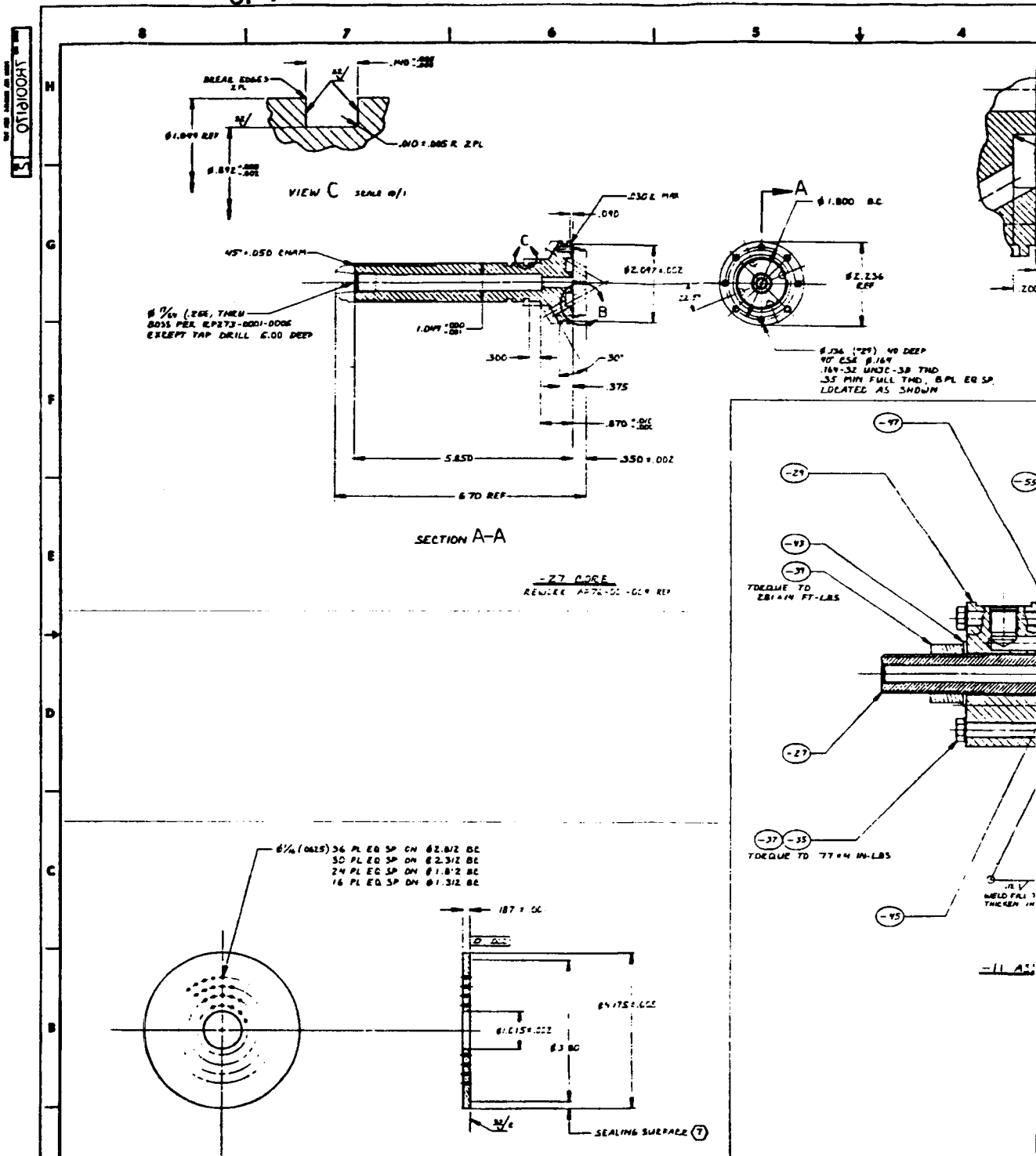

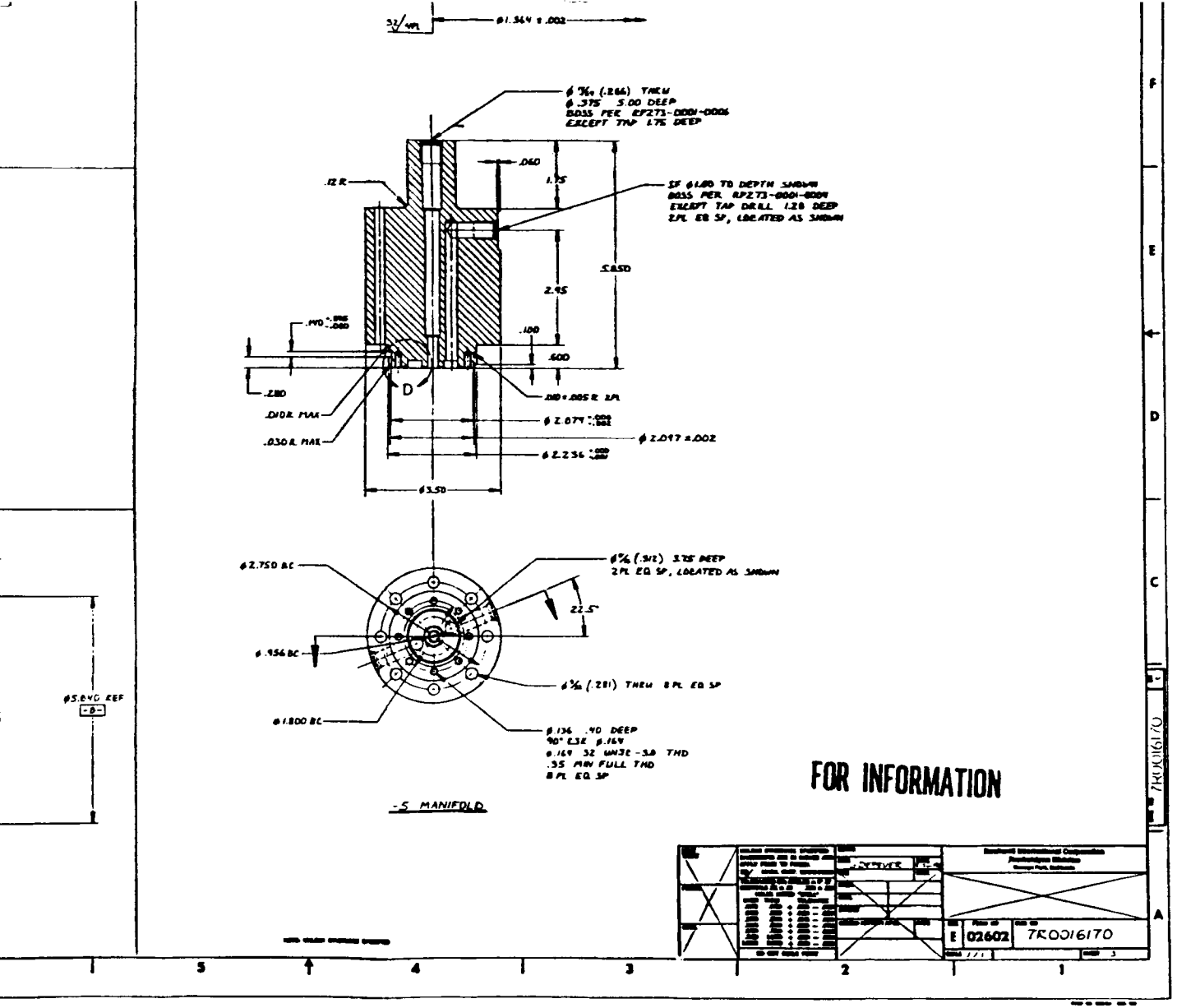
.12 R
.060
1.75
2.95
5.850
.100
.600
.140
.280
.010 R. MAX
.030 R. MAX
.010 ±.005 R. TYP.
D
ø3.50
ø2.750 BC
22.5°
ø.956 BC
ø1.800 BC
ø.136 .40 DEEP
90° E.S.E. ø.169
.169 32 UN3C-3B THD
.55 MIN FULL THD
8 PL EQ SP
-S MANIFOLD
FOR INFORMATION
E
02602
7R0016170

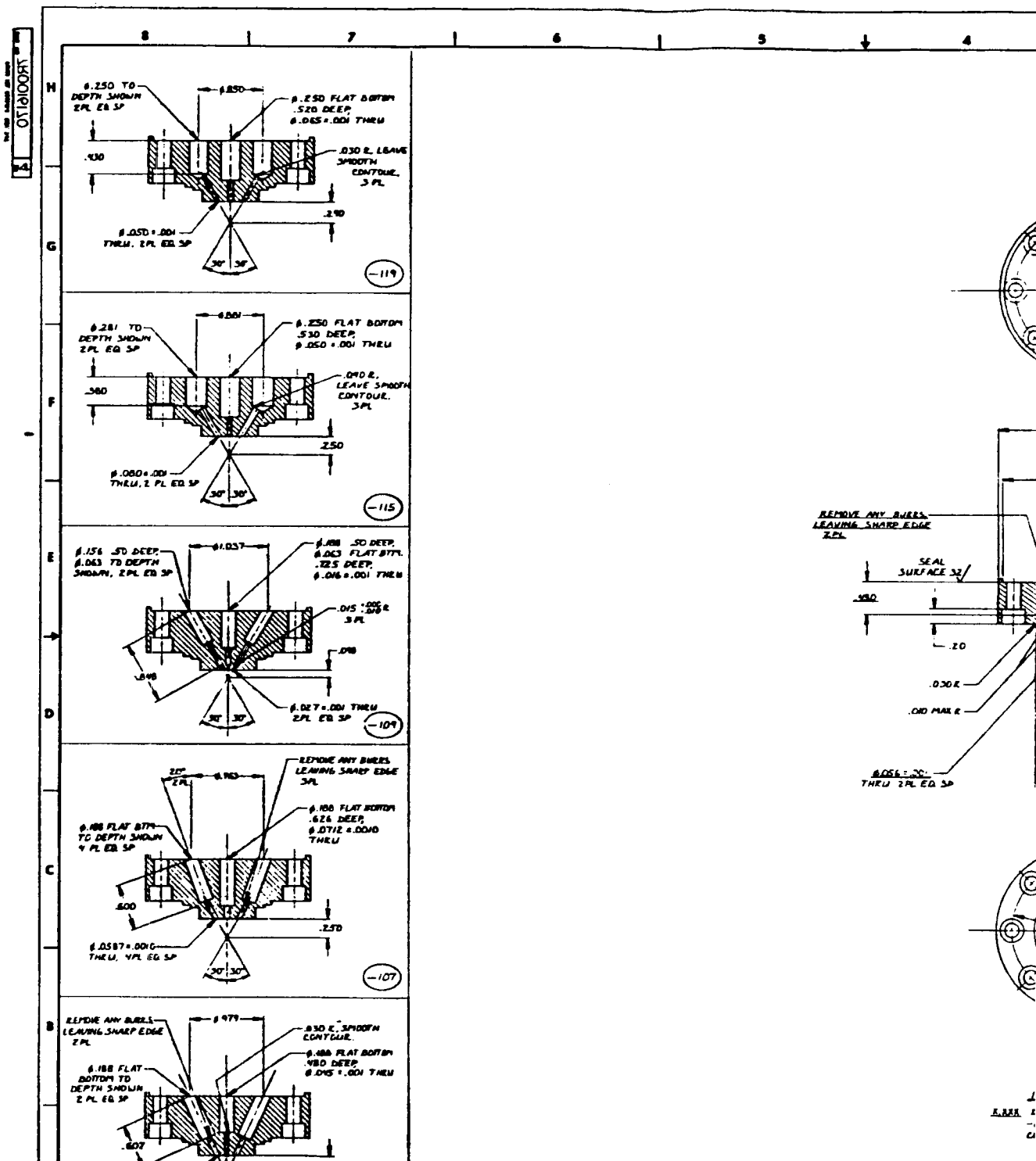

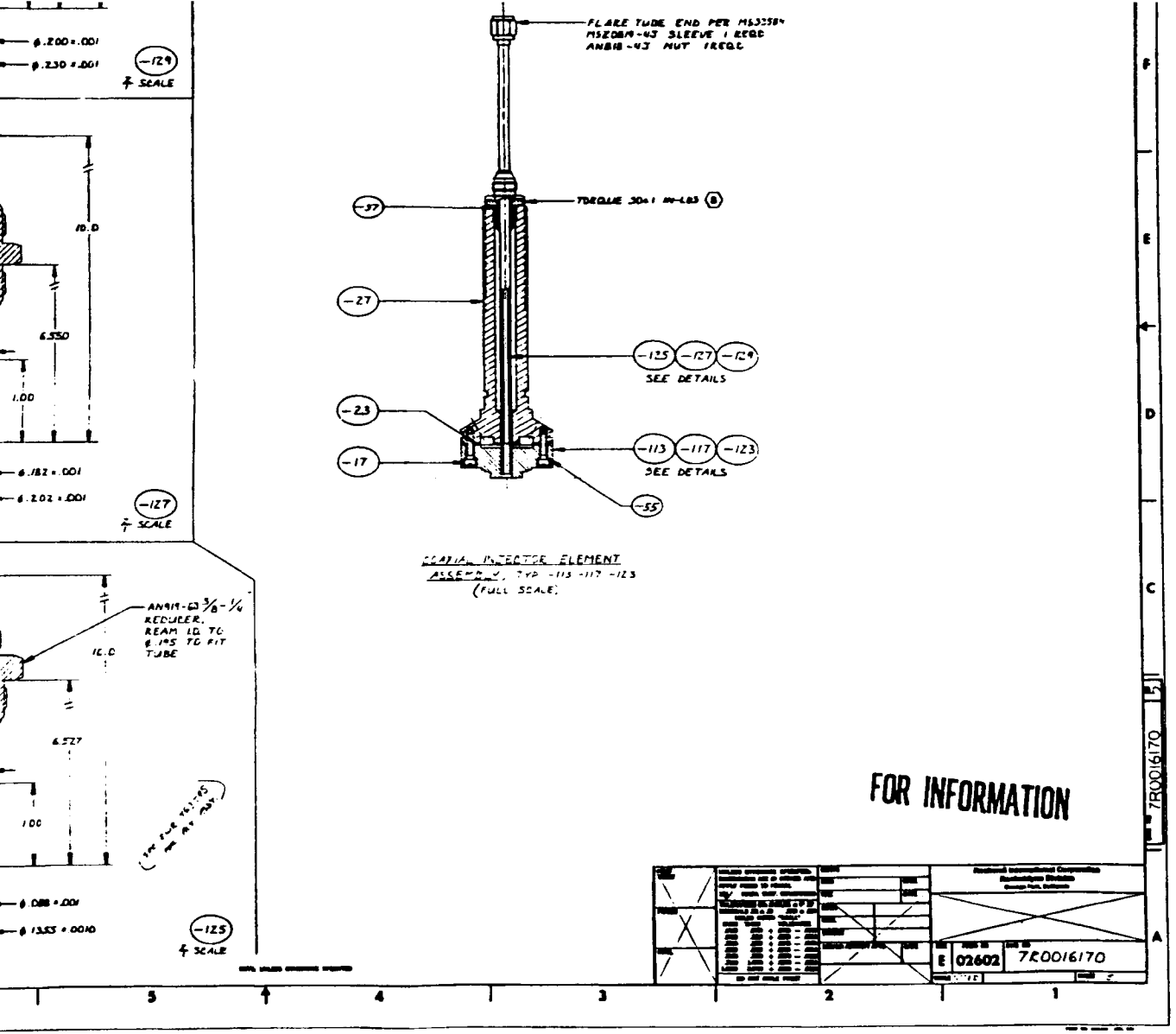

RI/RD83-170

A-6

APPENDIX B

This appendix describes the manner in which the raw test data is converted to the presented test results. The means by which mixing is measured (primarily mixing efficiency) are defined, and the manner and software by which these means are computed are described. The computer programs and examples of their input and output are presented. Data reduction methods for liquid/liquid and gas/liquid mixing tests are reported separately.

LIQUID-LIQUID DATA REDUCTION

The liquid-liquid mixing test data is hand recorded on a special form that aids in entering the information into microcomputer. The data for each sample tube is recorded in cubic centimeters as the total sample and the "Tric" sample level (the heavier trichloroethane settles to the bottom of the sample tube, and the coloring agent helps provide the demarcation line). A data file is typed into the microcomputer (Xerox 820) and saved on "floppy disk" for each of the test data sheets. This data file includes a text line describing and identifying the test, and several lines of overall test information with such things as pressures, flowrates, test times, element injection orifice diameters etc. The detail sample tube data is entered in a tabular format according to sample location as copied from the test data sheet. A sample of the test data sheet is presented as Fig. B-1.

The data reduction program was converted and updated from programs used in the past, and is configured to run in Micro soft BASIC on the Xerox 820 microcomputer (listing and sample data file are shown in Fig. B-2). This program converts the volumetric sample sizes in the input to equivalent propellant local flowrates in "stream tubes." This conversion is based on simulant and propellant densities. If the density ratio of the simulants is fairly close to the reactants, this correction factor is relatively small. The simulants, trichloroethane at 1320 Kg/M^3, and water at 1000 Kg/M^3, have a density ratio of 1.32 which is not too far from the "LOX" (at 1137 Kg/M^3) and RPI (at 800 Kg/M^3) ratio of 1.42. The liquid oxygen/liquid propane density ratio of 2.3 is further from the simulated value.

The most important factor in cold flow mixing data reduction is, of course, the determination of mixing effectiveness. The parameter that is generally accepted for this determination is the mixing efficiency, frequently referred to as "E sub M", the use of which was pioneered for rocket injectors by Jack Rupe at JPL. This mixing efficiency is computed by a mass weighted summation of all the samples, decrementing each sample as a function of its local oxidizer fraction related to the overall oxidizer fraction of the total sample.

The oxidizer fraction (oxidizer sample weight over the total sample weight) is used in place of the more usually referenced mixture ratio (oxidizer weight flow over fuel weight flow) because it is a more rational mathematic relationship, ranging from zero to one rather than zero to infinity. The computer program computes mixing efficiency based on the local oxidizer fraction and the local mass collected relative to the overall total collected oxidizer fraction and total mass collected.

The nominal form for computing mixing efficiency is:

$$E_m = 100 \left[1 - \left(\sum \left(M_{sb} \times \frac{0-0_{sb}}{0} \right) + \sum \left(M_{sa} \times \frac{0-0_{sa}}{0-1} \right) \right) \right]$$

where E_m = Mixing efficiency, Maximum = 100%

0 = Overall oxidizer fraction expressed as total oxidizer weight over total sample weight

M_{sb} = Mass fraction (total weight of local sample over total weight of all samples) subscript sb defines those samples with oxidizer fractions below the overall oxidizer fraction value

M_{sa} = Mass fractions of samples with local ox fractions above the overall value

0_{sb} = The sample oxidizer fraction value for those samples below the overall value

0_{sa} = The sample oxidizer fraction value for those samples above the overall value

The mixing efficiency of a set of samples, all at the same oxidizer fraction value, would be 100%, regardless of how the sample mass is distributed (so long as the mixture ratio is uniform). The opposite condition, where all the oxidizer (or oxidizer simulant) is in one set of samples and all the fuel in another set, will result in mixing efficiency of zero. Mixing efficiency values are much more sensitive than engine combustion efficiency, and it is not unusual that a mixing efficiency in the mid-80% range may indicate combustion C-star efficiencies that are much higher.

Frequently in evaluating mixing data, it is useful to utilize a simple stream tube analysis to predict mixing effects on measured combustion efficiency. The most common approach to this task is to assume that each sample represents a "tube" of the combustion process with little or no cross mixing between sample "stream tubes". Full-efficiency combustion is assumed for the mixed products within each "tube". The resulting C-star is multiplied by the total mass flow in the sample. These values are added, and the product is divided by the total mass flow of all the samples. The result is an approximation of the C-star resulting from the mixed flow. The form of this computation is:

$$C^*_{mix} = \frac{\left(M_{(1)}\ C^*_{theo(1)} + M_{(2)}\ C^*_{theo(2)} \quad M_{(n)}\ C^*_{(n)}\right)}{M_{tot}}$$

where

C^*_{mix}	=	Mixing Limited C-Star
$M_{(1)}$	=	Mass flow in respective samples
$C^*_{theo(1)}$	=	Theo C-star at local sample mixture ratio
M_{tot}	=	Total collected sample mass flow

The mixture limited C-star computations are generally very optimistic for operating conditions at non-stoichiometric mixture ratios. In these operating ranges, the low-mixture ratio "stream tubes" are balanced (and sometimes

overbalanced) by the high-mixture ratio samples. Two of the liquid/liquid elements tested in this program are designed for very low-mixture ratio operation in gas generator or preburner applications. The theoretical C-star curves in these low-mixture ratio regions cause very strange results for this type of computation, frequently predicting over 100% mixing limited C-star efficiency, even with poorly mixed elements. For this reason, the mixing limited C-star computations are not being utilized in this program.

The collection efficiency is the quantity of fluids collected divided by the quantity of flow through the injector during the test. Values far from one indicate some error or problem with the test procedure. For liquid/liquid tests, collection efficiency can be inferred from the test data in the following manner.

Collection efficiency is a method of cross checking the test sample against the theoretical sample element flow during the test period. With the liquid/liquid flow facility, any sample that escapes the collection grid can be inferred from the shape of the mass distribution plots. If the mass distribution plots show significant mass collected near the edge of the collection grid, this is strong evidence that measureable sample spray fell outside the sample grid. The quantitative measure of collection efficiency will assist in the decision of whether a rerun of the test with a repositioned element, is warranted. If the spray appears to have exceeded the collection grid, collection efficiency can be computed in the data reduction program by summing the collected samples and comparing to the computed value of total flow through the model element during the sample time. Generally this computed total flow is based on the calibration flow resistance of the element model and inlet pressure. For the liquid/liquid tests of this program, the collection efficiencies were very near to one.

DATE: 11-9-82
RUN #: +20% MR-MOM RAT
INJECTOR #: TRIPLET 1

PSID (WATER): 17 + 1 = 18
PSID (1,1,1,-TRIC): 36 + 3 = 39
TIME DURATION: 15 SEC
COLLECTION DISTANCE: 2"

	1	2	3	4	5	6	7	8	9	10	11	12	13
20					.25/4	.5/5	.25/3	0/1	0	0			
19					.25/4	.5/6	.5/4	0/1.5	0	0			
18					.25/3	1/7	.5/6	0/1.5	0/.5	0			
17					.25/3	1.5/9	1/8	0/2	0/.5	0			
16					.25/2.5	2/10	2/11	.25/3	0/1	0			
15					.25/2	2/11	2.5/16	.25/5	0/1	0/.25			
14					.25/2	2/11	4.5/24	1/7	.25/1.5	0/.25			
13					.25/2	2/11	6/31	2.5/11	.25/2	0/.25			
12					.25/2	2/11	7.5/36	3/16	.5/3	0/.5			
11					.25/2	2.5/10	8/34	5/20	.5/4	0/.5			
10					.25/2	2.5/9	8/28	5/20	1/5	0/.5			
9					.25/1.5	2.5/7	8/23	6/18	1.5/5	.25/1			
8					.25/1	2/5	7.5/19	6/14	1/4	0/1	0	0	
7					.0/.5	1/4	5/13	4/10	.5/2.5	0/.5	0	0	
6					0	.25/2.5	2.5/8	2/7	.25/1.5	0/.5	0	0	
5					0	0/1	1/5	1/6	.25/2.5	0/.5	0	0	
4					0	0/.5	.5/3	.5/5	.25/3	0/1	0	0	
3					0	0/0	0/1	.25/3.5	.25/3	0/2.5	0/.5	0	
2					0	0/0	0/.5	.25/2	.25/.25	0/2.5	0/1	0	
1					0	0/0	0/0	.25/1	0/1	0/1.5	0/1	0/.25	

Figure B-1. Liquid/Liquid Mixing Sample Data Sheet

```
1 REM PROGRAM CLDFLTC LIQ/LIQ COLD FLOW MIXING DATA REDUCT
2 REM UPDATED VERSION FEB 28 83
3 REM VERSION FOR TRIPLETS - NORMAL AND REVERSED
4 REM 3D DATA PLOT OR PLOT FILE OPTION
5 REM PROGRAM CLDFLTC II
7 REM WITH ROTATED DISPLAY AND PEN 1 FOR OX PEN 2 FOR FU
8 REM READ TEXT
9 REM READ INJ NO,RUN NO,TRIC DELP,H2O DELP,COLL TIME
10 DATA "TRIPLET NO 1 -+20%MXR - 2 IN"
11 DATA 1,1,39,18,15
12 DATA .056,.71,2,.0465,.614,1
110 DATA 0,0,0,0,.5,.5,.25,0,0,0,0,0,0
111 DATA 0,0,0,0,4,5,3,1,0,0,0,0,0
120 DATA 0,0,0,0,.25,.5,.5,0,0,0,0,0,0
121 DATA 0,0,0,0,4,6,4,1.5,0,0,0,0,0
130 DATA 0,0,0,0, .25,1,.5,0,0,0,0,0,0
131 DATA 0,0,0,0,3,7,6,1.5,.5,0,0,0,0
140 DATA 0,0,0,0,.25,1.5,1,0,0,0,0,0,0
141 DATA 0,0,0,0,3,9,8,2,.5,0,0,0,0
150 DATA 0,0,0,0,.25,2,2,.25,0,0,0,0,0
151 DATA 0,0,0,0,2.5,10,11,3,1,0,0,0,0
160 DATA 0,0,0,0,.25,2,2.5,.25,0,0,0,0,0
161 DATA 0,0,0,0,2,11,16,5,1,.25,0,0,0
170 DATA 0,0,0,0,.25,2,4.5,1,.25,0,0,0,0
171 DATA 0,0,0,0,2,11,24,7,1.5,.25,0,0,0
180 DATA 0,0,0,0,.25,2,6,2.5,.25,0,0,0,0
181 DATA 0,0,0,0,2,11,31,11,2,.25,0,0,0
190 DATA 0,0,0,0,.25,2,7.5,3,.5,0,0,0,0
191 DATA 0,0,0,0,2,11,36,16,3,.5,0,0,0
200 DATA 0,0,0,0,.25,2.5,8,5,.5,0,0,0,0
201 DATA 0,0,0,0,2,10,34,20,4,.5,0,0,0
210 DATA 0,0,0,0,.25,2.5,8,5,1,0,0,0,0
211 DATA 0,0,0,0,2,9,29,20,5,.5,0,0,0
220 DATA 0,0,0,0,.25,2.5,8,6,1.5,.25,0,0,0
221 DATA 0,0,0,0,1.5,7,23,18,5,1,0,0,0
230 DATA 0,0,0,0,.25,2,7.5,6,1,0,0,0,0
231 DATA 0,0,0,0,1,5,19,14,4,1,0,0,0
240 DATA 0,0,0,0,0,1,5,4,.5,0,0,0,0
241 DATA 0,0,0,0,.5,4,13,10,2.5,.5,0,0,0
250 DATA 0,0,0,0,0,.25,2.5,2,.25,0,0,0,0
251 DATA 0,0,0,0,0,2.5,9,7,1.5,.5,0,0,0
260 DATA 0,0,0,0,0,0,1,1,.25,0,0,0,0
261 DATA 0,0,0,0,0,1,5,6,2.5,.5,0,0,0
270 DATA 0,0,0,0,0,0,.5,.5,.25,0,0,0,0
271 DATA 0,0,0,0,0,.5,3,5,3,1,0,0,0
280 DATA 0,0,0,0,0,0,0,.25,.25,0,0,0,0
281 DATA 0,0,0,0,0,0,1,3.5,3,2.5,.5,0,0
290 DATA 0,0,0,0,0,0,0,.25,.25,0,0,0,0
291 DATA 0,0,0,0,0,0,.5,2,2.5,2.5,1,0,0
300 DATA 0,0,0,0,0,0,0,.25,0,0,0,0,0
301 DATA 0,0,0,0,0,0,0,1,1,1.5,1,.25,0
1000 REM COLD FLOW -BASIC VERSION OF CLDFLT
1020 REM WDOT IN LB MASS/SEC DENSITY IN LB/CU FT
1030 DIM TRIC(20,13)
1040 DIM OXSMP(20,13),TOT(20,13),H2O(20,13),OXFRSM(20,13)
```

Figure B-2. Liquid/Liquid Mixing Data Reduction Program

```
1050 DIM FUSMP(20,13),TOTP(20,13),XMR(20,13),DEC(20,13)
1060 DIM FUM(20,13),OXUM(20,13)
1070 DIM OFRTHE(10),CSTHE(10)
1080 DIM TMTHE(10)
1090 DIM SPIMPS(10),SPIMPF(10),CSTHES(10)
1100 DIM TOTS(20,13)
1102 PRINT"INPUT DATE AND TIME - ANY FORMAT"
1103 INPUT RT$
1110 PRINT"INPUT CODE FOR OUTPUT 0 SHORT, 1 DEI INP, 2 FULL OUTPUT"
1120 INPUT IPRT
1122 LPRINT"DATA REDUCTION RUN OF ";RT$
1130 REM ZERO OUT VARIABLES
1140 CSSUM=0
1150 DECSUM=0
1160 TOTPSM=0
1170 TOTOSM=0
1180 TOTFSM=0
1190 DENTRC=82.59
1200 DENWAT=62.27
1210 DENFU=5.7
1220 DENOX=71
1230 SAMPNO=260
1240 FUCOR=.0022*((DENFU/DENWAT)^.5)
1250 OXCOR=.0022*((DENTRC/DENWAT)*((DENOX/DENTRC)^.5))
1260 REM
1270 REM READ DATA
1280 READ TEXT$
1290 PRINT TEXT$
1300 LPRINT
1310 LPRINT TEXT$
1320 LPRINT
1330 READ INJ,ITEST,PITRIC,PIH2O
1340 REM INJ NO, TEST NO, INJET PR TRIC, H2O
1350 LPRINT"INJ ";INJ;" TEST NO. ";ITEST;" INJET PR TRIC ";PITRIC;" H2O ";PIH2O
1360 READ TIME
1370 READ DWAT,CDWAT,WATN,DTRIC,CDTRIC,TRICN
1380 REM DIA, CD, AND NO. OF WATER AND TRIC INJ ORIFICES
1390 LPRINT" OX DIA ";DTRIC;TRICN;" PLACES    FU DIA ";DWAT;WATN;" PLACES"
1400 LPRINT
1410 AREAFU=.7854*WATN*(DWAT^2)
1420 AREAOX=.7854*TRICN*(DTRIC^2)
1430 FOR KROW=1 TO 20
1440 FOR KCOL=1 TO 13
1450 READ TRIC(KROW,KCOL)
1460 IF TRIC(KROW,KCOL)<.0000001 THEN TRIC(KROW,KCOL)=.0000001
1470 NEXT
1480 FOR KCOL=1 TO 13
1490 READ TOT(KROW,KCOL)
1500 IF TOT(KROW,KCOL)<.0001 THEN TOT(KROW,KCOL)=.0001
1510 NEXT
1520 NEXT
1530 REM
1540 REM
1550 IF IPRT<2 THEN 1700
1560 REM DIAGNOSTIC PRINT OUT
```

Figure B-2. (Continued)

```
1570 LPRINT"INPUT DATA CC - TOT / TRIC"
1580 LPRINT
1590 FOR KROW=1 TO 20
1600 FOR KCOL=1 TO 13
1610 LPRINT USING"##.# ";TOT(KROW,KCOL);
1620 NEXT
1630 LPRINT
1640 FOR KCOL=1 TO 13
1650 LPRINT USING"##.# ";TRIC(KROW,KCOL);
1660 NEXT
1670 LPRINT
1680 LPRINT
1690 NEXT
1700 REM BYPASS W/O PRINT
1710 REM
1720 REM
1730 REM INITIALIZE MATRIX SIZE
1740 NROWS=1
1750 NROWE=20
1760 NCOLS=1
1770 NCOLE=13
1780 TOTPSM=0
1790 TOTTRC=0
1800 TOTSIM=0
1810 TOTOSM=0
1820 TOTFSM=0
1830 TOTWAT=0
1840 NMSAMP=0
1850 IF IPRT=2 THEN LPRINT
1860 IF IPRT=2 THEN LPRINT" MIXTURE RATIO"
1870 IF IPRT=2 THEN LPRINT
1880 FOR KROW=NROWS TO NROWE
1890 FOR KCOL=NCOLS TO NCOLE
1900 IF TOT(KROW,KCOL) < TRIC(KROW,KCOL) THEN TOT(KROW,KCOL)=.001+TRIC(KROW,KCOL)
1910 H2O(KROW,KCOL)=TOT(KROW,KCOL)-TRIC(KROW,KCOL)
1920 REM
1930 REM TEST FOR ZERO AMOUNTS
1940 IF TOT(KROW,KCOL)>.05 THEN NMSAMP=NMSAMP+1
1950 REM
1960 REM
1970 IF H2O(KROW,KCOL)=0 THEN 2000
1980 XMR(KROW,KCOL)=TRIC(KROW,KCOL)/H2O(KROW,KCOL)
1990 XMR(KROW,KCOL)=XMR(KROW,KCOL)*OXCOR/FUCOR
2000 REM
2010 IF IPRT=2 THEN LPRINT USING"##.## ";XMR(KROW,KCOL);
2020 OXSMP(KROW,KCOL)=OXCOR*TRIC(KROW,KCOL)
2030 FUSMP(KROW,KCOL)=FUCOR*H2O(KROW,KCOL)
2040 TOTP(KROW,KCOL)=OXSMP(KROW,KCOL)+FUSMP(KROW,KCOL)
2050 TOTS(KROW,KCOL)=TRIC(KROW,KCOL)+H2O(KROW,KCOL)
2060 FACTOR=1
2070 TOTP(KROW,KCOL)=TOTP(KROW,KCOL)*FACTOR
2080 TOTS(KROW,KCOL)=TOTS(KROW,KCOL)*FACTOR
2090 TOTOSM=TOTOSM+OXSMP(KROW,KCOL)
2100 TOTPSM=TOTPSM+TOTP(KROW,KCOL)
2110 TOTTRC=TOTTRC+TRIC(KROW,KCOL)
```

Figure B-2. (Continued)

```
2120 TOTSIM=TOTSIM+TOTS(KROW,KCOL)
2130 TOTFSM=TOTFSM+FUSMP(KROW,KCOL)
2140 TOTWAT=TOTWAT+H2O(KROW,KCOL)
2150 OXFRSM(KROW,KCOL)=OXSMP(KROW,KCOL)/TOTP(KROW,KCOL)
2160 NEXT
2170 IF IPRT=2 THEN LPRINT" "
2180 NEXT
2190 LPRINT
2200 REM
2210 REM 101 CONTINUE
2220 REM OVERALL SUMMATIONS
2230 XMROA=TOTOSM/TOTFSM
2240 OXFOA=TOTOSM/TOTPSM
2250 REM COPUTE FLOWRATES FROM INPUT PR,DIA,CD
2260 WWAT=CDWAT*SQR(DENWAT*PIH2O*(WATN^2)*(DWAT^4)/3.625)
2270 WTRC=CDTRIC*SQR(DENTRC*PITRIC*(TRICN^2)*(DTRIC^4)/3.625)
2280 WFUIN=WWAT*SQR(DENFU/DENWAT)
2290 WOXIN=WTRC*SQR(DENOX/DENTRC)
2300 WWATC=3.531E-05*TOTWAT*DENWAT/TIME
2310 WTRCC=3.531E-05*TOTTRC*DENTRC/TIME
2320 OFRIN=WOXIN/WFUIN
2330 OXFRIN=WOXIN/(WFUIN+WOXIN)
2340 OXTIN=TIME*WOXIN
2350 FUTIN=TIME*WFUIN
2360 OXCIEF=WTRCC/WTRC
2370 FUCIEF=WWATC/WWAT
2380 IPRINT" COLLECTED OX SIM ";TOTOSM;"  FUEI SIM ";TOTFSM
2390 IPRINT" COMPUTED OX SIM ";OXTIN;"  FUEI SIM ";FUTIN
2400 IPRINT" COMPUTED COLD FLOW O/F ";(WTRC/WWAT)
2410 LPRINT" COMPUTED SIMULATED O/F ";(WOXIN/WFUIN)
2420 IPRINT "COLL EFF OX ";OXCLEF;"  FU ";FUCIEF
2430 IPRINT" COLLECTED TRIC/WAT O/F ";(WTRCC/WWATC)
2440 IPRINT" COLLECTED SIMULATED O/F ";XMROA;"  OX FRACT ";OXFOA
2450 REM
2460 REM E SUB EM COMPUTATIONS
2470 TOTPST=0
2480 CSSUM=0
2490 DECSUM=0
2500 FOR KROW=NROWS TO NROWE
2510 PRINT"ROW ";KROW
2520 FOR KCOL=NCOLS TO NCOLE
2530 IF OXFRSM(KROW,KCOL) >= OXFOA THEN DECR=OXFRSM(KROW,KCOL)-OXFOA
2540 IF OXFRSM(KROW,KCOL) < OXFOA THEN DECR=OXFOA-OXFRSM(KROW,KCOL)
2550 DECRT=DECR*TOTP(KROW,KCOL)
2560 DECRT=DECRT/OXFOA
2570 DECSUM=DECSUM+DECRT
2580 TOTPST=TOTPST+TOTP(KROW,KCOL)
2590 REM
2600 REM MIXING LIMITED CSTAR
2610 REM INPUT MIX LIMIT CSTAR CALCS
2620 REM
2630 REM
2640 REM 331 CONTINUE
2650 NEXT KCOL
2660 NEXT KROW
```

Figure B-2. (Continued)

```
2670 ESUBM=(TOTPST-DECSUM)/TOTPST
2680 LPRINT"E SUB M EFF ";ESUBM
2690 CSTAR=CSSUM/TOTPST
2700 REM COMPUTE THEO CSTA[illegible] O/AIL OXRATIO
2710 REM COMPUTE CSTAR EFF
2720 REM INJECTOR PARAMETERS
2730 REM CONVENTIONAL TRIPLETS
2740 WOUT=WWATC
2750 WIN=WTRCC
2760 DENOUT=DENWAT
2770 DENIN=DENTRC
2780 AREAOT=AREAFU
2790 AREAIN=AREAOX
2800 DIAOUT=DWAT
2810 DIAIN=DTRIC
2820 LPRINT
2830 IF WATN>TRICN THEN 2950
2840 REM REVERSE TRIPLETS
2850 LPRINT"REVERSE (O-F-O) TRIPLET"
2860 WOUT=WTRCC
2870 WIN=WWATC
2880 DENOUT=DENTRC
2890 DENIN=DENWAT
2900 AREAOT=AREAOX
2910 AREAIN=AREAFU
2920 DIAOUT=DTRIC
2930 DIAIN=DWAT
2940 GOTO 2970
2950 REM
2960 LPRINT"NORMAL (F-O-F) TRIPLET"
2970 REM
2980 REM
2990 VELRAT=WTRCC*AREAFU*DENWAT/(WWATC*AREAOX*DENTRC)
2992 VELHDF=2.236*(WWATC^2)/(DENWAT*(AREAFU^2))
2994 VELHDO=2.236*(WTRCC^2)/(DENTRC*(AREAOX^2))
2996 VELHDR=VELHDO/VELHDF
3000 MOMRAT=WTRCC*VELRAT/WWATC
3010 REM ELV MOREY
3020 ELMRAT=(([illegible]OUT/[illegible])^.5)*([illegible])*((AREAIN/AREAOT)^1.75)
3030 REM PRINT OUT INJ PARAMETERS
3040 LPRINT
3050 LPRINT
3060 LPRINT"COLLECTED CONDITIONS- INJECTION PARAMETERS
3070 LPRINT
3080 LPRINT"MOMENTUM RATIO ";MOMRAT
3090 LPRINT"VEL RATIO ";VELRAT
3092 LPRINT" VEL HEAD OX SIDE ";VELHDO;" PSID"
3094 LPRINT" VEL HEAD FU SIDE ";VELHDF;" PSID"
3096 LPRINT"VEL HEAD RATIO ";VELHDR
3100 LPRINT"ELVERUM-MOREY FACTOR ";ELMRAT
3110 REM PENETRATION PARAMETER(30 DGREE ASSMED ANGL)
3120 PENT=1.25*SIN(30/57.3)*(WOUT/WIN)*((DENIN/DENOUT)^.5)*(DIAIN/DIAOUT)
3130 LPRINT"PENETRATION PARAMETER ";PENT
3140 LPRINT
3150 REM CALCULATE NORMALIZED MASS FLUX FU AN OX
```

Figure B-2. (Continued)

```
3160 FOR KROW=1 TO 20
3170 FOR KCOI=1 TO 13
3180 FUM(KROW,KCOL)=FUSMP(KROW,KCOL)*NMSAMP/TOTFSM
3190 OXUM(KROW,KCOL)=OXSMP(KROW,KCOL)*NMSAMP/TOTOSM
3200 NEXT KCOL
3210 NEXT KROW
3220 REM WRITE FILE FOR PLOT PROGRAM
3230 PRINT"IF YOU WANT O WRITE PLOT FILE INPUT Y"
3240 INPUT PL$
3250 IF PL$<>"Y" THEN 3440
3260 PRINT"INPUT DESIRED NAME OF PLOT FILE"
3270 INPUT PFIL$
3280 PFIL$=PFIL$+".BAS"
3290 OPEN"O",#1,PFIL$
3300 LN=10
3310 PRINT#1,LN;"DATA ";TEXT
3320 LN=LN+10
3330 PRINT#1,LN;"DATA ";XMROA
3340 LN=LN+10
3350 PRINT#1,LN;"DATA ";ESUBM
3360 FOR KROW=1 TO 20
3370 FOR KCOI=1 TO 13
3380 LN=LN+10
3390 PRINT#1,LN;"DATA ";
3400 WRITE#1,OXUM(KROW,KCOI),FUM(KROW,KCOI)
3410 NEXT
3420 NEXT
3430 CLOSE
3440 REM PLOT ROUTINE FOR MASS DIST
3450 PRINT"IF YOU WANT TO PLOT MASS DIST PLUG IN PLOTTER AND "
3460 PRINT"GET THE PEN AND PAPER READY THEN INPUT Y"
3470 INPUT PLOT$
3480 IF PLOT$<>"Y" THEN 4140
3490 LPRINT";:ICD C H A P1 U "
3500 XPO=1300
3510 YPO=300
3520 VSCALE=100
3530 LPRINT" 300,200 S12 PLOT OF OX AND FUEL MASS FLUX _ "
3540 LPRINT" 350,150 S12 ";TEXT$;"  "
3550 LPRINT" 350,100 S12 MIXTURE RATIO ";XMROA;"  "
3560 LPRINT" 350,50 S12 MIXING EFF - E SUB M ";ESUBM;" _ "
3570 REM PLOT FUEL DIST
3580 LPRINT" P2 "
3590 FOR KROW=1 TO 20
3600 XLPO=XPO-30*(KROW-1)
3610 YLPO=YPO+5*(KROW-1)
3620 FOR KCOI=1 TO 13
3630 KCO=KCOI-1
3640 IF KCO<1 THEN KCO=1
3650 XOFF=XLPO+30*(KCOI-1)
3660 YOFF=YLPO+15*(KCOI-1)
3670 XPI=INT(XOFF)
3680 YPI=INT(FUM(KROW,KCOL)*VSCALE+YOFF+.5)
3690 LPRINT" I0 "
3700 IF (FUM(KROW,KCOI)+FUM(KROW,KCO))<(OXUM(KROW,KCOI)+OXUM(KROW,KCO)) THEN LPRINT" I
```

Figure B-2. (Continued)

```
3710 LPRINT XPL;",";YPL;" D"
3720 NEXT
3730 LPRINT" U "
3740 LPRINT" I0 "
3750 NEXT
3760 REM PLOT OX DIST
3770 LPRINT" P3 "
3780 FOR KROW=1 TO 20
3790 XLPO=XPO-30*(KROW-1)
3800 YLPO=YPO+50*(KROW-1)
3810 FOR KCOL=1 TO 13
3820 KCO=KCOL-1
3830 IF KCO<1 THEN KCO=1
3840 XOFF=XLPO+80*(KCOL-1)
3850 YOFF=YLPO+15*(KCOL-1)
3860 XPL=INT(XOFF)
3870 YPL=INT(OXUM(KROW,KCOL)*VSCALE+YOFF+.5)
3880 LPRINT" I0 "
3890 IF (OXUM(KROW,KCOL)+OXUM(KROW,KCO)+.001)<(FUM(KROW,KCOL)+FUM(KROW,KCO)) THEN LPRI
3900 LPRINT XPL;",";YPL;" D"
3910 NEXT
3920 LPRINT" U "
3930 LPRINT" I0 "
3940 NEXT
3950 REM PLOT OX OTHER GRID
3960 FOR KCOL=1 TO 13
3970 XLPO=XPO+80*(KCOL-1)
3980 YLPO=YPO+15*(KCOL-1)
3990 FOR KROW=1 TO 20
4000 KRO=KROW-1
4010 IF KRO<1 THEN KRO=1
4020 XOFF=XLPO-30*(KROW-1)
4030 YOFF=YLPO+50*(KROW-1)
4040 XPL=INT(XOFF)
4050 YPL=INT(OXUM(KROW,KCOL)*VSCALE+YOFF+.5)
4060 LPRINT" I0 "
4070 IF (OXUM(KROW,KCOL)+OXUM(KRO,KCOL)+.001)<(FUM(KROW,KCOL)+FUM(KRO,KCOL)) THEN LPRI
4080 LPRINT XPL;",";YPL;" D "
4090 NEXT
4100 LPRINT" U "
4110 LPRINT" I0 "
4120 NEXT
4130 LPRINT" P0 200,0 0 "
4140 REm NO PLOT
4150 END
```

Figure B-2. (Concluded)

GAS-LIQUID DATA REDUCTION

The gas-liquid data reduction process is somewhat more complex than the techniques used for liquid-liquid data reduction. The fluid simulants cannot be collected and measured directly in a sample grid as they are in the liquid-liquid collection system since one component is a gas. The test procedure requires a probe that physically collects the liquid simulant (water), and senses the gaseous flow by total pressure, and gas sample measurements. A single gas liquid element flowing in a confined chamber induces very significant recirculation flow, which requires additional steps in the data acquisition and reduction.

The use of a so called "base bleed" flow from the injection face area around the element, is an aid in supressing the recirculation flow. However, this gas flow becomes a portion of the gas flow in the element sampling area, and must be identified and separated from the computed flow. In our test setup, we accomplish the identification of the "base bleed" flow flux by using gaseous nitrogen as the element flow, and air as the "base bleed" flow. The probe gas flow is then sampled for oxygen content. The quantity of oxygen indicates the amount of bleed flow entrained in the sample. The data indicates a surprising amount of entrained flow, often being as much or more than the primary element flow (even in high mass flux zones near the center of the element zone).

The test fixture allows probe movement along radial lines through the center of the sample chamber (a true rectangular coordinate system is not within the capabilities of the existing equipment), and the sample zone treatment in the data reduction program is based upon this radial system. The effective zone area is an annular arc section based on the probe radial distance from the center of the chamber, and the number of data "rays" indicated in the input data table. Figure B-3 shows this relationship for a case with eight rays assumed in the data acquisition. Frequently, in gas liquid testing, a limited number of actual sample "rays" are measured, and symmetry is assumed based on element type (anticipated shape of mass distribution). An extreme example of this technique is shown in Figure B-4. In this example, three actual "rays" have been measured, but an

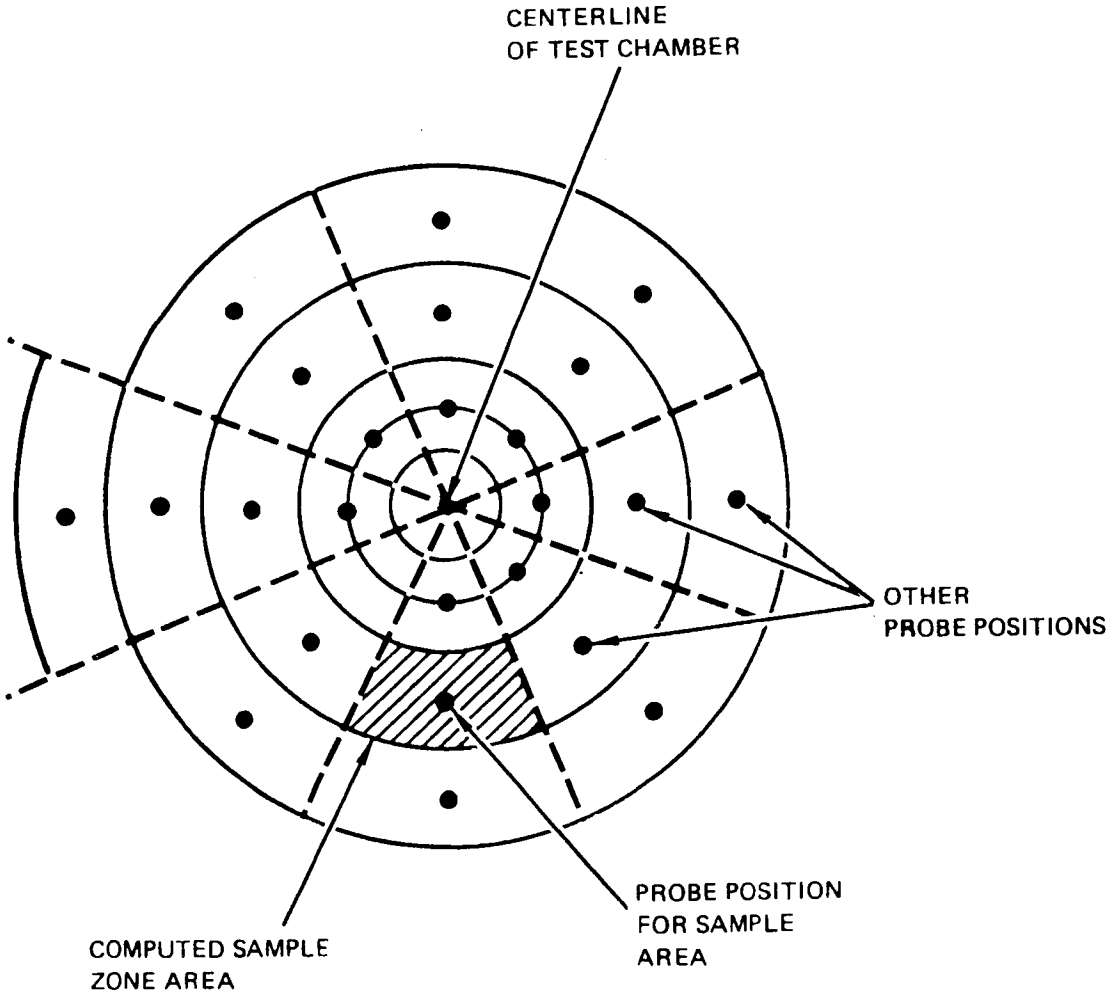

Figure B-3. Plan View of Probe Positions and Sample Areas for Eight Rays

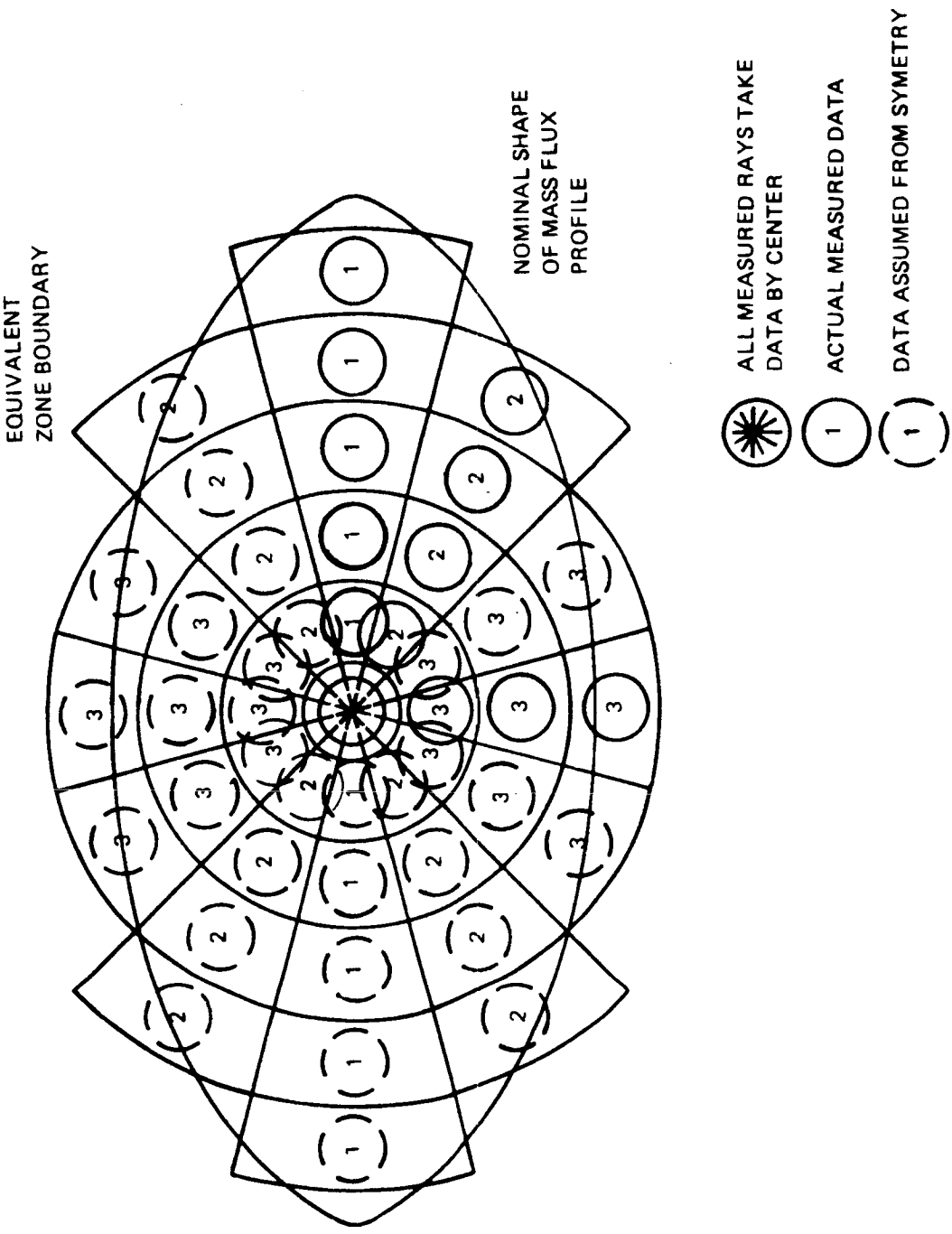

Figure B-4. Logic for Assumed Data Sample Zones for a Typical Element (Gas/Liquid Mixing Tests)

equivalent of 12 rays are being used in the data reduction. The lense shaped mass distribution of the triplet dictates the type of symmetry used to establish the imaginary rays.

The gas-liquid mixing data reduction program requires initial information on such items as the element configuration, flow rates, sampling time, radial spacing of the samples, and number of equivalent sampling rays. The individual probe sample point data is presented for each position, inputting the reference ray angle, the radial distance from the centerline, the dynamic pressure head reading, the amount of water collected during the sample time, and the percent of oxygen in the gases in the sample zone.

From this data, the computer program calculates the value of oxidizer and fuel simulant flow flux in the sample area. The computation of liquid mass flow is very straight forward. The collected liquid mass divided by the sample time, is further divided by the probe open area to derive the liquid mass flux. The gas flux computation is less simple. The total pressure reading of the probe is related to gas velocity, but corrections must be made for the impact pressure contribution of the liquid droplets in the stream. The liquid flowrate is basically known, as is the gas density. The program uses a closed form computation based on the apparent fluid density of a two-phase flow of the gas and liquid. A further correction is made for the amount of gas from the base bleed.

The two-phase flow correction, and the correction for entrained flow are rather large, and a potential source of error in this procedure. The entrained flow includes some recirculated element gases, as well as the "base bleed" flow, based on depressed oxygen content measured in zones well outside the element "spray pattern." To correct for this effect, a depressed oxygen percentage (lower than the nominal air value) is input based on this outer zone measurement. This becomes the reference value for corrective gas flow flux values in the spray.

One of the self-testing features of the data reduction procedure is the use of "collection efficiency." The program sums up the computed mass flux values times the respective sample areas, and compares this to the computed input flow values

for both the liquid and the gas. In many instances, collection efficiencies deviated significantly (by as much as 40%) from perfect collection efficiency. Since the probe measured areas do not overlap the entire sample zone (because of practical limits in the number of samples to be taken), some deviations between the computed total "collected" and the input values would be expected. However, the actual deviations in practice have been larger than anticipated, and several reviews of both the data acquisition procedures and data reduction procedures have been unable to resolve this. Since the liquid and gas flowrates are measured directly in these tests (using calibrated sonic orifices on the gas and a turbine meter on the liquid), it appears that some error in the test method exists. This problem still is being reviewed. Pending resolution of this problem, the error is assumed to be uniform across the entire sample area and the data is being "corrected" to the known flowrates.

The data reduction program uses the corrected sample values to compute the classic mixing efficiency (E sub M) in the same way as the liquid-liquid mixing data program, and also computes the injection parameters, such as Elverum-Morey, momentum ratio, velocity ratio, velocity head ratio and the penetration parameter. The local sample injected mass flux values also are recorded in a data file for a graphic display on the plotter. In the plotted data shown in this report, only the actual "rays" where data was taken are plotted. The imaginary rays used to account for the total flowfield are not displayed.

A listing of the gas/liquid data reduction program is shown in Fig. B-5.

```
1000 REM UPDATED VESION "CMXGLT" COLD MIX GAS LIQ TRIP
1010 REM APPEND DATA STARTING AT LINE 9000 WITH MERGE COMMAND
1020 REM UPDATED MAR 8 83
1030 REM INCLUDES CORR FOR OX READING WITH BASE BLEED
1040 REM WITH OX CONTENT ADJUSTED FOR RECYCLED GN2
1050 REM DATA REDUCTION PROGRAM FOR COLD FLOW LIQ MIXING VERSION WITH
1060 REM CORRECTION FACTOR FOR MIXED FLOW DENSITY AT PROBE
1070 PRINT"INPUT DAY AND TIME - ANY FORM"
1080 INPUT DAY$
1085 PRINT"TO SUPRESS ALL BUT SUMMARY PRINTOUT INPUT Y"
1090 INPUT TP$
1100 LPRINT"PROGRAM CMXGLT COLD FLOW MIXING DATA RED ";DAY$
1110 LPRINT
1120 DIM WLQS(40),WLQM(40),TS(40),PC(40),WGS(40),PRP(40)
1130 DIM WGSF(40),WLQF(40),NZ(40),ZONA(40),WLQZ(40),WGSZ(40),TEST(12)
1140 DIM OXPCTZ(40)
1150 DIM RAY(40),RAD(40)
1160 DIM CSTR(21)
1170 DIM RGSFLX(40),RLQFLX(40)
1180 REM
1190 REM C STAR DATA
1200 DATA 3000, 3140, 3290, 3440, 3600, 3770
1210 DATA 3950, 4130, 4300, 4470, 4650
1220 DATA 4900, 5200, 5700, 6170, 6280
1230 DATA 5950, 5400, 4600, 3550, 1300
1240 FOR I=1 TO 21
1250 READ CSTR(I)
1260 NEXT
2000 REM INPUT CONSTANTS
2010 CALIB=1
2020 GNDNA=.07274
2030 GFUDN=13.86
2040 PDIA=.125
2050 PAMB=13.6
2060 FLCD=.65
2070 LQDN=62.4
2080 LOXDN=71
2090 LQSC=.0022046 :REM CONV ML TO LBS
2100 REM INITIALIZE SUMMATION CONSTANTS
2110 WLQCT=0
2120 WGSCT=0
2130 WTLQM=0
2140 WTGSM=0
2150 EFMIX=1
2160 TEMFRC=0
2170 ARSUM=0
2180 DNGSM=0
2190 CSMTOT=0
2200 WTOTSM=0
2210 REM
3000 REM READ DATA
3010 READ TEST$
3020 READ DGSINJ,GSN,DLQINJ,LQN
3030 REM DIA GS INJ ORIF, NUMBER, DIA LQ INJ ORIF, NUMBER
3040 READ WGSIN,WLQIN
```

Figure B-5. Gas/Liquid Data Reduction Program

```
3050 REM INJECTED FLOWRATES LB/SEC
3060 READ NS,NRAY
3070 REM NO DATA POINTS, NO OF RAYS TESTED
3080 READ INPROB:REM INCREMENT BETWEEN PROBE RADIAL POS'N
3090 READ TTIME,PCHB: REM TEST TIME AND CHBR PR
3100 READ OXPB:REM OX PCT IN ENTRAINED CHAMBER GASES
3110 REM SUGGEST HIGHEST OX VALUE MEASURED AT EDGE OF FAN
3120 LPRINT
3130 LPRINT
3140 LPRINT TEST$
3150 LPRINT
3160 LPRINT"PERCENT OX ASSUMED IN RECIRC GAS ";OXPB
3165 LPRINT"TEST CHAMBER PRESSURE ";PCHB
3170 LPRINT
3180 LPRINT"INPUT DATA AND INITIAL COMPUTATIONS"
3190 LPRINT
3192 LPRINT"INJ ORIF DIA - GAS ";DGSINJ;GSN;" PLCS  - LIQ ";DLQINJ;LQN;"PLCS"
3194 LPRINT"INJECTED WT FLOWS ";WGSIN;"LB/SEC GAS - ";WLQIN;"LB/SEC LIQ"
3200 FOR N=1 TO NS
3210 REM READ LOOP
3220 READ NZ(N):REM ZONE NUMBER FOR REF
3230 READ RAY(N),RAD(N),PRP(N),WLQS(N),OXPCTZ(N)
3240 REM RAY ANGLE, RAD SAMP LOC, PROBE PRESS , LIQ COLL MI, PCT OX
3250 IF TP$="Y" THEN 3280
3260 LPRINT"ZONE";NZ(N),"RAY";RAY(N),"RAD";RAD(N),"PROBE PR";PRP(N),
3270 LPRINT"LIQ MI";WLQS(N),"PCT OX";OXPCTZ(N)
3280 REM BYPASS PRINT
3290 IF RAD(N)=0 THEN READ RAYMUL
3300 IF PRP(N)=0 THEN PRP(N)=.000001
3310 ZONA(N)=RAD(N)*.1*2*3.1417/NRAY
3320 IF RAD(N)<.0001 THEN ZONA(N)=.007854/NRAY
3330 ZONA(N)=ZONA(N)*(INPROB/.1)
3340 ZONA(N)=ZONA(N)*RAYMUL
3350 WLQM(N)=WLQIN
3360 WGS(N)=WGSIN
3370 TS(N)=TTIME
3380 PC(N)=PCHB
3390 WLQS(N)=WLQS(N)*LQSC/TS(N) :REM CORR SAMPLE FLOW
3400 IF WLQS(N)<.000001 THEN WLQS(N)=.000001
3410 ARSUM=ARSUM+ZONA(N)
3420 SAMPN=NS
3430 WTGSM=WTGSM+(WGS(N)/SAMPN)
3440 WTLQM=WTLQM+(WLQM(N)/SAMPN)
3450 NEXT N
4000 REM
4010 REM INITIAL MASS CALC LOOP
4020 FOR N=1 TO NS
4030 REM GAS MASS FLUX
4040 QPSF=PRP(N)*144
4050 GNDN=GNDNA*((PC(N)+PAMB)/14.7)
4060 DNGSM=DNGSM+(GNDN/SAMPN)
4070 WGSF(N)=((PRP(N)*GNDN/2.236)^.5)
4080 PRINT"Q ";QPSF;" PSF     FIRST WGAS ";WGSF(N);(WGSF(N)*144);"#/SEC/SQ FT"
4090 WGSF(N)=WGSF(N)*(WTGSM/WGS(N))
4100 REM LIQ MASS FLUX
```

Figure B-5. (Continued)

```
4110 PAREA=.7854*(PDIA^2)
4120 WLQF(N)=WLQS(N)/PAREA
4130 WLQFSF=WLQF(N)*144
4140 PRINT"WT LIQ FLOW PER SQ FT/SEC";WLQFSF
4150 WLQZ(N)=WLQF(N)*ZONA(N)
4160 WLQCT=WLQCT+WLQZ(N)
4170 REM CORRECTION FOR MIXED FLOW DENSITY AT PROBE
4180 CFSGS=WGSF(N)/GNDN
4190 CFSCOL=WLQF(N)/60
4200 CFST=CFSGS+CFSCOL
4210 WFST=WGSF(N)+WLQF(N)
4220 DNCOR=WFST/CFST
4230 VHDMFI=(2.236*(WFST^2)/DNCOR)
4240 VHDFR=PRP(N)/VHDMFI
4250 VHDEL=1-VHDFR
4260 VHDCR=VHDEL/3
4270 CORVHD=PRP(N)*(1-VHDCR)
4280 PRINT"CORRECTED VEL HEAD ";(CORVHD*144)
4290 WGSF(N)=(((CORVHD*GNDN)/2.236)^.5)
4300 PRINT"NEW GAS FLOW ";WGSF(N);(WGSF(N)*144);" #/SEC/SQ FT"
4310 WGSF(N)=WGSF(N)*(WTGSM/WGS(N))
4320 WGSZ(N)=WGSF(N)*ZONA(N)
4330 REM NEW CORRECTION FOR TWO PHASE FLOW
4340 A=1/(2*32.2*GNDN)
4350 B=(WLQFSF/64.4)*((1/LQDN)+(1/GNDN))
4360 C=((WLQFSF^2)/(64.4*LQDN))-QPSF
4370 X1=(-1*B)-((B^2)-4*A*C)^.5
4380 X1=X1/(2*A)
4390 X2=(-1*B)+((B^2)-4*A*C)^.5
4400 X2=X2/(2*A)
4410 PRINT"TWO SOLN ";X1;X2
4420 PRINT"GN DENSITY ";GNDN;" EQUIV VEL ";(X2/GNDN)
4430 REM REPLACE GAS FLOW WITH NEW CORR
4440 WGSF(N)=X2/144
4450 REM CORR FOR BLEED AIR
4460 WGSF(N)=WGSF(N)*(1-(GXPCTZ(N)/GXPB))
4470 WGSZ(N)=WGSF(N)*ZONA(N)
4480 PRINT "GN GAS FLUX =";WGSF(N);" GAS FLOW PER ZONE ";WGSZ(N)
4492 REM CORR FOR NEG GAS FLUX
4494 IF WGSF(N)<.000001 THEN WGSF(N)=.000001
4500 WGSCT=WGSCT+WGSZ(N)
4530 IF TP$="Y" THEN 4530
4510 LPRINT" ","GAS FLUX ";WGSF(N),"LIQ FLUX ";WLQF(N)
4520 PRINT
4530 REM BYPASS PRINT
4540 NEXT N
4550 REM COLLECTION EFF
4560 COLEFC=WLQCT/WTLQM
4570 COLEFG=WGSCT/WTGSM
4580 LPRINT
4590 LPRINT "COLLECTION EFF. LIQ=";COLEFC,"COLLECTION EFF. GS SIM=";COLEFG
4600 LPRINT
4610 REM OVERALL O/F
4620 RATIO=WTLQM/WTGSM
4630 LPRINT "OVERALL MIXTURE RATIO (O/F)=";RATIO
```

Figure B-5. (Continued)

```
4640 MEQCOR=((LOXDN/GFUDN)^.5)/((LQDN/GNDN)^.5):REM MOM RATIO CORR FOR EQ PROP
4650 EQRAT=RATIO*MEQCOR
4660 LPRINT"MOMENTUM EQUIVALENT MIXTURE RATIO (INJECTED) ";EQRAT
4670 LPRINT
4680 LPRINT "MEAN FLOW RATES:","GS SIM=";WTGSM,"LIQ=";WTLQM
4690 LPRINT
4700 WTOT=WTGSM+WTLQM
4710 FRACT=WTGSM/WTOT
4720 FLXCM=WTLQM/ARSUM
4730 FLXGSM=WTGSM/ARSUM
4740 REM
4750 IF TP$="Y" THEN 4800
4760 LPRINT
4770 LPRINT "RAY","RAD","AREA","WT FLOW","MIX RAT.","EQIV O/F","C STAR","GS FLUX","LIQ
4780 LPRINT"ANGLE"," IN.","SQ IN","TOTAL"," ","PROP."," FPS","FRACT.","FRACT"
4790 LPRINT
4800 REM BYPASS PRINT
5000 REM FINAL SUMMATION LOOP
5010 FOR N=1 TO NS
5020 REM CORRECT FOR COLL EFF
5030 WLQZ(N)=WLQZ(N)/COLEFC
5040 WGSZ(N)=WGSZ(N)/COLEFG
5050 WTOTL=WLQZ(N)+WGSZ(N)
5060 FRACTL=WGSZ(N)/WTOTL
5070 IF FRACTL <= FRACT THEN GOTO 5100
5080 DECR=(WTOTL/WTOT)*((FRACT-FRACTL)/(FRACT-1))
5090 GOTO 5120
5100 REM CONTINUE
5110 DECR=(WTOTL/WTOT)*((FRACT-FRACTL)/(FRACT))
5120 REM CONTINUE
5130 EFMIX=EFMIX-DECR
5140 REM NORMALIZED LOCAL MASS FLUX
5150 RLQFIX(N)=WLQZ(N)/(ZONA(N)*FLXCM)
5160 RGSFLX(N)=WGSZ(N)/(ZONA(N)*FLXGSM)
5170 RATL=WLQZ(N)/WGSZ(N)
5180 EQRTL=RATL*MEQCOR
5190 EQOFRC=EQRTL/(EQRTL+1)
5200 NRAT=INT(20*EQOFRC)
5210 DRAT=(20*EQOFRC)-NRAT
5220 CS1=CSTR(NRAT)
5230 CS2=CSTR(NRAT+1)
5240 DELCS=CS2-CS1
5250 CSANS=CS1+DRAT*DELCS
5260 IF TP$="Y" THEN 5280
5270 LPRINT RAY(N),RAD(N),ZONA(N),WTOTL,RATL,EQRTL,CSANS,RGSFIX(N),RLQFIX(N)
5280 REM BYPASS PRINT
5290 CSMTOT=CSMTOT+CSANS*WTOTL
5300 WTOTSM=WTOTSM+WTOTL
5310 NEXT N
5320 LPRINT
5322 LPRINT"COLLECTED MIXTURE RATIO ";WLQCT/WGSCT
5324 LPRINT"COMPUTED INJECTED O/F ";WTLQM/WTGSM
5330 LPRINT"MOMENTUM EQIVALENT MIXTURE RATIO (INJECTED)";EQRAT
5340 LPRINT "MIXING EFF.=";EFMIX
5350 CSTRM=CSMTOT/WTOTSM
```

Figure B-5. (Continued)

```
5360 LPRINT"MIXING LIMITED C STAR ";CSTRM;" FPS"
5370 REM O/ALL CSTAR
5380 EQFRC=EQRAT/(EQRAT+1)
5390 NRAT=INT(20*EQFRC)
5400 DRAT=(20*EQFRC)-NRAT
5410 CS1=CSTR(NRAT)
5420 CS2=CSTR(NRAT+1)
5430 DELCS=CS2-CS1
5440 CSTHEO=CS1+(DRAT*DELCS)
5450 LPRINT"THEO C STAR ";CSTHEO;" FPS"
5460 NCSTR=100*(CSTRM/CSTHEO)
5470 LPRINT"MIXING LIMITED C STAR EFF ";NCSTR
5480 LPRINT
5490 REM
6000 REM INJECTOR OPERATING CONDITIONS
6010 GSAREA=GSN*(DGSINJ^2)*.7854
6020 GSVEL=WTGSM*144/(DNGSM*GSAREA)
6030 CFCOI=WTLQM/60
6040 WTLQ=WTLQM
6050 DNLQ=LQDN
6060 LQAREA=LQN*(DLQINJ^2)*.7854
6070 LQVEL=WTLQ*144/(DNLQ*LQAREA)
6080 RATMOM=(LQVEL*WTLQ)/(GSVEL*WTGSM)
6090 AX=(WTGSM/WTLQ)^2
6100 BX=(DNLQ/DNGSM)
6110 CX=(LQAREA/GSAREA)^1.75
6120 ELMOR=AX*BX*CX
6130 VHDGS=3.625*(WTGSM^2)/(DNGSM*(GSN^2)*(DGSINJ^4))
6140 VHDLQ=3.625*(WTLQ^2)/(DNLQ*(LQN^3)*(DLQINJ^4))
6150 VHDR=VHDLQ/VHDGS
6152 REM PENETRATION PARAMETER FOR GAS-LIQ-GAS TRIP
6154 DIAOUT=DGSINJ
6156 DIAIN=DLQINJ
6158 DNOUT=DNGSM
6160 DNIN=DNLQ
6162 VELOUT=GSVEL
6164 VELIN=LQVEL
6166 PEN1=2.5*(DIAOUT/DIAIN)*((DNOUT/DNIN)^.5)
6170 PEN2=.5*(VELOUT/VELIN)
6172 REM .5 FOR 30 DEGREE ANGLE(SIN 30)
6180 PEN=PEN1*PEN2
6190 LPRINT "TRIPLET JET PENETRATION FACTOR=";PEN
6200 LPRINT
6210 LPRINT "MOMENTUM RATIO=";RATMOM,"ELVERUM-MOREY COEFF=";ELMOR
6220 LPRINT "INJECTION VEL - GS SIM=";GSVEL,"    LIQUID=";LQVEL
6230 LPRINT "VEL HEAD - GS=";VHDGS;" PSID - LQ=";VHDLQ;" PSID -VEL HEAD  RATIO=";VHDR
6240 LPRINT
6250 LPRINT
6260 LPRINT
6270 LPRINT
7000 REM
7010 REM FILE FOR PLOT
7020 PRINT"INPUT Y IF PLOT FILE IS DESIRED"
7030 INPUT FICOD$
7040 IF FICOD$<>"Y" THEN 8999
```

Figure B-5. (Continued)

```
7050 PRINT"INPUT DESIRED NAME OF FILE"
7060 INPUT NFI$
7070 NFI$=NFI$+".BAS"
7080 OPEN"O",#1,NFI$
7090 REM
7100 PRINT#1,"10 DATA ";CHR$(34);TEST$;CHR$(34)
7110 PRINT#1,"20 DATA ";EQRAT
7120 PRINT#1,"30 DATA ";EFMIX
7130 NSTRT=1
7150 FOR L=2 TO NS
7160 IF L=NS THEN L=L+1:GOTO 7180
7170 IF RAD(L)>.0001 THEN 7400
7180 REM LAST SET OF DATA
7190 PRINT#1,I*100;" REM DATA FOR RAY ",RAY(NSTRT)
7200 PRINT#1,(I*100+1);"DATA ";
7205 NDT=1+(L-NSTRT)
7210 WRITE#1,RAY(NSTRT),NDT
7230 FOR N=NSTRT TO L
7240 PRINT#1,(I*100+(2*N));"DATA ";
7250 IF N=L THEN 7280
7260 WRITE#1,RAD(N),RIQFIX(N)
7270 GOTO 7290
7280 WRITE#1,(RAD(N-1)+.1),0
7290 REM
7300 NEXT
7310 FOR N= NSTRT TO L
7320 PRINT#1,(I*100+50+(2*N));"DATA ";
7330 IF N=L THEN 7360
7340 WRITE#1,RAD(N),RGSFIX(N)
7350 GOTO 7370
7360 WRITE#1,(RAD(N-1)+.1),0
7370 REM
7380 NEXT
7390 NSTRT=I
7400 REM
7420 REM
7430 NEXT
7440 CLOSE(1)
7450 END
7460 REM
8999 REM LAST LINE BEFORE DATA
9000 DATA "TRIPLET NO 2, NOM MOM R, 50 PSIG, 1 IN"
9010 DATA .063, 2, .045, 1:REM GAS INJ ORIF DIA AND NO. LIQ ETC"
9020 DATA .0138, .042:REM GAS WT FLOW LIQ WT FLOW
9030 DATA 12, 8:REM NO OF DATA POINTS, NO OF RAYS
9035 DATA .1:REM INCREMENT BETWEEN SAMPLES
9040 DATA 60,50:REM TEST TIME IN SEC, TANK PRESS PSIG
9050 DATA 16.5 :REM PERCENT OX TO BE USED TO FACTOR OUT RECIRC GAS
9100 DATA 1
9110 DATA 0, 0, 2.85, 38, 16.5
9120 DATA 6
9130 DATA 2
9140 DATA 0, .1, 1.45, 30, 11
9150 DATA 3
9160 DATA 0, .2, .25, 8, 12.5
```

Figure B-5. (Continued)

```
9170 DATA 4
9180 DATA 0, .3, 0, 1, 14.5
9200 REM
9210 DATA 5
9220 DATA 90, 0, 2.7, 40, 11
9230 DATA 2
9240 DATA 6
9250 DATA 90, .1, 2.55, 40, 11
9260 DATA 7
9280 DATA 90, .2, 1.7, 36, 11.5
9290 DATA 8
9300 DATA 90, .3, .85, 32, 13
9310 DATA 9
9320 DATA 90, .4, .4, 31, 13.5
9340 DATA 10
9350 DATA 90, .5, .25, 26, 14.5
9360 DATA 11
9370 DATA 90, .6, .1, 21, 15
9380 DATA 12
9390 DATA 90, .7, .05, 8, 16
9400 DATA 13
9410 DATA 90, .8, 0, 5, 16
9999 END
```

Figure B-5. (Concluded)

☆U.S. GOVERNMENT PRINTING OFFICE 1983—746-070/67